

https://dspace.org/

Characterisation of rock mass rating (RMR) parameters by geostatistical analysis Orapa Mine Botswana

Kgomanyane, Joel Thabo

2019

https://hdl.handle.net/10539/29919

Kgomanyane, Joel Thabo. (2019). Characterisation of rock mass rating (RMR) parameters by geostatistical analysis Orapa Mine Botswana. University of the Witwatersrand, https://hdl.handle.net/10539/29919

Downloaded from a DSpace repository. https://dspace.org/



CHARACTERISATION OF ROCK MASS RATING (RMR) PARAMETERS BY GEOSTATISTICAL ANALYSIS AT ORAPA MINE, BOTSWANA

Student Name: **Joel Thabo Kgomanyane** (Cert. Sci. Nat.)

Student number: **672591**

Faculty of Engineering and the Built Environment,

University of the Witwatersrand, Johannesburg, South Africa

Supervisor: Prof C. E. Dohm

A research report submitted to the School of Mining, Faculty of Engineering and the Built Environment, University of the Witwatersrand, in fulfilment of the requirements for the degree of Master of Science in Mining Engineering.

Date: AUGUST 2019

DECLARATION

I declare that this report is my own, unaided work, except where otherwise referenced or acknowledged. It has not been submitted before for any other degree or examination at any other university. I have read the University Policy on Plagiarism and hereby confirm that no plagiarism exists in this report. I also confirm that there is no copying nor is there any copyright infringement. I willingly submit to any investigation in this regard by the School of Mining Engineering and I undertake to abide by the decision of any such investigation.



14 AUGUST 2019

Signature Date

ACKNOWLEDGEMENTS

This MSc research report is dedicated to my adorable family; my wife *Ponkie*, my three sons, *Teto, Letang* and *Tlotlo* for the endless support and encouragement they offered me throughout my years of study.

Special thanks go to Debswana MRM department for availing funds and the data for my research programme. Many thanks go to my manager, *Mr B. Rachere* for presenting the opportunity for me to complete my studies.

Finally yet importantly, special thanks go to my research supervisor, *Professor C. E. Dohm*, for providing her invaluable experience and knowledge in the field of geostatistics in Mineral Resource evaluation. Her guidance, challenges and support with the theoretical aspects of geostatistics assisted me in completing this research report.

Special thanks go to my MRM friends and colleagues for the encouragement to complete my MSc research.

ABSTRACT

The focus of this research project is on the application of geostatistics to evaluate the rock mass rating (RMR) parameters for Orapa AK1 kimberlite pipe. The RMR parameters evaluated are Uniaxial Compressive Strength (UCS), Fracture Frequency per Metre (FFPM), Rock Quality Designation (RQD) and Dry Density (DD). When applied appropriately, these RMR parameters have the potential to enhance and inform conventional geological models, blast designs and metallurgical plant performances. Compared with other assessment methods such as using the global mean of the RMR parameters, the geostatistical estimates resulted in a more accurate and robust assessment of the geotechnical variables studied herein.

Ordinary Kriging has been applied to estimate the RMR values at unsampled locations for the different rocktypes of the Orapa AK1 Kimberlite pipe. Variogram models were generated for the above RMR parameters within the different rocktypes both in the horizontal and vertical directions including an estimate for the nugget effect. The resulting block estimates were compared with sample data for all RMR parameters and bench plots for each rocktype were generated and analysed. Furthermore, geostatistics revealed that, RMR parameters have spatial correlation and these are strongly influenced by the geological environment of the AK1 Kimberlite at Orapa mine in Botswana.

It is concluded that the evaluation of the rock mass rating (RMR) parameters using geostatistics is an important future requirement for the success of any mining project. It is recommended that geological and geotechnical data processing and interpretation should be coupled with geostatistical modelling at project pre-feasibility studies to enhance the conventional methods used in geoscience mining projects. The geostatistical estimation approach provides a more reliable and accurate method (low kriging variance) by taking into account the spatial continuity of variables under study as compared to simple averaging of geotechnical parameters for a given volume of rock mass.

Table of Contents

DECLARATION i

ACKNOWLEDGEMENTS ii

ABSTRACT iii

LIST OF FIGURES viii

LIST OF TABLES xi

ABBREVIATIONS xii

1 INTRODUCTION 1

1.1 Research Motivation 2

1.2 Research Objectives 3

1.3 Applicability of Geostatistics to Rock Mass Rating Parameters 3

1.4 Chapter Overview 4

1.5 Research Achievement 5

2 STUDY AREA 7

2.1 Location of Orapa Mine 7

2.2 Orapa Resource Extension Project OREP Overview 7

2.3 Geology of the Study Area 9

2.3.1 Regional Geology 9

2.3.2 Internal Pipe Geology 12

3 Overview of Rock Mass Rating parameters 15

3.1 Uniaxial Compressive Strength (UCS) – MPa 16

3.2 Rock Quality Designation (RQD) - % 16

3.3 Fracture Frequency per metre (FFPM) – A qualitative assessment 16

3.4 Joint Conditions (JC) – A qualitative assessment 16

3.5 Water Condition (WC) 17

3.6 Density (g/cm^3) 17

4 GEOSTATISTICAL APPROACH 18

4.1 Literature Overview 18

4.2 Why Geostatistics? 21

4.3 Classical Statistics....22
5 RESEARCH METHODOLOGY....24
5.1 Review of Existing Relevant Datasets....24
5.2 Exploratory Data Analysis (EDA)....25
5.3 Variogram Modelling....25
5.4 Kriging Neighbourhood Optimisation....25
5.5 Estimation Validation Criteria....26
6 RMR DATA SELECTION AND VALIDATION....27
6.1 Uniaxial Compressive Strength (UCS)....27
6.1.1 Point Load Index – I_s....27
6.1.2 UCS Calculations....28
6.1.3 UCS Conversion Factors....28
6.2 Fracture Frequency per metre (FFPM)....29
6.2.1 Definition of FFPM....29
6.2.2 Calculation of FFPM....29
6.3 Rock Quality Designation (RQD)....30
6.3.1 Definition of RQD....30
6.3.2 Calculation of RQD....30
6.4 Dry Density (g/cm^3)....30
6.4.1 Definition of Dry Density....30
6.4.2 Calculation of Dry Density....30
6.5 Data Quality Checks – RMR Input Parameters....31
7 EXPLORATORY DATA ANALYSIS (EDA)....32
7.1 UCS (MPa) EDA for Orapa AK1 pipe rocktypes....33
7.1.1 UCS (MPa) Classical Statistics....33
7.1.2 UCS (MPa) Graphical Summary – Box Plots....34
7.1.3 UCS (MPa) Graphical Summary – Histogram Plots....39
7.2 FFPM EDA for Orapa AK1 pipe rocktypes....43
7.2.1 FFPM Classical Statistics....43
7.2.2 FFPM Graphical Summary – Box Plot....44

7.2.3 FFPM Graphical Summary – Histogram Plots 44
7.3 RQD (%) EDA for Orapa AK1 pipe rocktypes.....49
7.3.1 RQD (%) Classical Statistics 49
7.3.2 RQD (%) Graphical Summary - Box Plot 50
7.3.3 RQD (%) Graphical Summary - Histogram Plots.....50
7.4 Dry Density (g/cm^3) EDA for all Orapa AK1 rocktypes.....54
7.4.1 Dry Density (g/cm^3) Classical Statistics 54
7.4.2 Dry Density (g/cm^3) Box Plots 55
7.4.3 Dry Density (g/cm^3) Histogram Plots 56
8 GEOSTATISTICS.....61
8.1 Variogram Modelling 61
8.2 UCS - Variogram Models.....63
8.2.1 UCS Variogram Model Parameters Summary per rocktype 68
8.3 FFPM - Variogram Models 70
8.3.1 FFPM – Summary of Variogram Parameters.....79
8.4 RQD - Variogram Models 82
8.4.1 RQD – Summary of Variogram Parameters 90
8.5 Dry Density – Variograms 91
8.5.1 DD– Summary of Variogram Parameters.....99
9 KRIGING NEIGHBOURHOOD OPTIMISATION 101
9.1 Methodology.....101
9.2 Kriging of RMR parameters based on the KNA outcomes.....108
9.3 Summary of Neighbourhood Optimisation Results.....109
9.4 Estimation Validation.....111
9.4.1 Sample Averages versus Estimated Values.....111
9.4.2 Bench Plots.....111
10 DISCUSSION OF ESTIMATION RESULTS.....114
10.1 Sample Statistics versus Estimates – UCS.....115
10.2 Sample Statistics versus Estimates – FFPM 116
10.3 Sample Statistics versus Estimates – RQD.....117

10.4 Sample Statistics versus Estimates – Dry Density (DD) 119
10.5 Summary of Bench Plots Analysis.....120
11 CONCLUSIONS AND RECOMMENDATIONS.....127
REFERENCES 129
APPENDICES 132
Appendix 1 UCS Bench plots within the AK1 rocktypes.....133
Appendix 2 FFPM Bench plots within AK1 rocktypes 137
Appendix 3 RQD Bench plots within AK1 rocktypes 143
Appendix 4 Dry Density Bench plots within the AK1 rocktypes 149
Appendix 5 AK1 UCS sample data distribution 154
Appendix 6 AK1 FFPM sample data distribution 154
Appendix 7 AK1 RQD sample data distribution 155
Appendix 8 AK1 Dry Density sample data distribution.....155
Appendix 9 AK1 UCS variogram models 156
Appendix 10 AK1 FFPM variogram models.....163
Appendix 11 AK1 RQD variogram models.....176
Appendix 12 AK1 Dry Density variogram models 189

LIST OF FIGURES

Figure 1 Location Map of Botswana (insert) and Orapa AK1, Letlhakane and Damtshaa Mines (Letsatle et al., 2015) 1
Figure 2 Location Map for Orapa Kimberlite Cluster.....7
Figure 3 OREP Phase II diamond core drilling plan Orapa AK1 pit (Letsatle, et al., 2015) 8
Figure 4 Section view of Orapa AK1 mine, current Cut 3 and planned Cut 4 pit shells 9
Figure 5 Geology of the Orapa AK1 Kimberlite pipe (Sejoe, 2014) 12
Figure 6 A Typical Variogram Model showing the nugget, sill and range (adapted from Bohling, (2005)) 19
Figure 7 AK1 RMR Project in ISATIS^{TM} 2016.2 software 22
Figure 8 UCS Box plot, Summary Statistics & CDF – WRB 34
Figure 9 UCS Box plot, Summary Statistics & CDF – A3T.....35
Figure 10 UCS Box plot, Summary Statistics & CDF – SPK 36
Figure 11 UCS Box plot, Summary Statistics & CDF – SVK_U.....36
Figure 12 UCS Box plot, Summary Statistics & CDF – NPKD 37
Figure 13 UCS Box plot, Summary Statistics & CDF – NPK_GG.....37
Figure 14 UCS Box plot, Summary Statistics & CDF – MVK2_BBR 37
Figure 15 UCS histogram & statistics – SVK_M (left) and SVK_L (right) 39
Figure 16 UCS histogram & statistics – BBR (left) and DHB (right).....40
Figure 17 UCS histogram & statistics – NPK (left) and MVK2 (right) 41
Figure 18 UCS histogram & statistics – SDVK.....42
Figure 19 FFPM Box plot, Summary Statistics & CDF – WRB.....44
Figure 20 FFPM histogram – A3T 45
Figure 21 FFPM histograms – SVK_U (left) and SVK_M (right).....45
Figure 22 FFPM histograms – SVK_L (left) and SPK (right) 46
Figure 23 FFPM histograms – BBR (left) and DHB (right).....47
Figure 24 FFPM histograms – SDVK (left) and NPKD (right) 47
Figure 25 FFPM histograms – MVK2 (left) and NPK (right).....48
Figure 26 FFPM histograms – MVK2_BBR (left) and NPK_GG (right) 48
Figure 27 FFPM Box plot, Summary Statistics & CDF – WRB.....50
Figure 28 RQD (%) histograms – A3T (left) and SPK (right).....51
Figure 29 RQD (%) histogram – SVK_U 52
Figure 30 RQD (%) histograms – SVK_M (left) and SVK_L (right) 52
Figure 31 RQD (%) histograms – BBR (left) and DHB (right) 52

Figure 32 RQD (%) histograms – SDVK (left) and NPKD (right) 53
Figure 33 RQD (%) histograms – MVK2 (left) and NPK (right) 53
Figure 34 RQD (%) histograms – MVK2_BBR (left) and NPK_GG (right).....54
Figure 35 DD Box plot, Summary Statistics & CDF – A3T.....55
Figure 36 DD Box plot, Summary Statistics & CDF – WRB 55
Figure 37 DD Box plot, Summary Statistics & CDF – SVK_U 55
Figure 38 DD histograms – BBR (left) and DHB (right).....57
Figure 39 DD histograms – SVK_M (left) and SVK_L (right).....58
Figure 40 DD histograms – SDVK (left) and NPKD (right).....58
Figure 41 DD histograms – MVK2 (left) and NPK (right).....59
Figure 42 DD histograms – NPK_GG (left) and MVK2_BBR (right) 59
Figure 43 DD histogram – SPK.....60
Figure 44 FFPM Variograms Experimental (left) and Model (right) – DHB 62
Figure 45 UCS Variogram models – SVK_M (left) and SVK_L (right).....64
Figure 46 UCS Variogram models – BBR (left) and DHB (right) 66
Figure 47 UCS Variogram models – NPK (left) and MVK2 (right) 67
Figure 48 UCS Variogram model – SDVK.....68
Figure 49 FFPM variogram models – A3T (left) and SPK (right).....71
Figure 50 FFPM variogram models – BBR (left) and DHB (right) 73
Figure 51 FFPM variogram models – SVK_U (left) and SVK_M (right) 74
Figure 52 FFPM variogram models – SVK_L (left) and SDVK (right) 75
Figure 53 FFPM variogram models – NPK (left) and MVK2 (right) 76
Figure 54 FFPM variogram models – NPK_GG (left) and MVK2_BBR (right) 78
Figure 55 FFPM variogram model – NPKD.....79
Figure 56 RQD variogram models – A3T (left) and SPK (right) 84
Figure 57 RQD variogram models – BBR (left) and DHB (right) 85
Figure 58 RQD variogram models – SVK_U (left) and SVK_M (right) 86
Figure 59 RQD variogram models – SVK_L (left) and SDVK (right) 87
Figure 60 RQD variogram models – NPK (left) and MVK2 (right) 88
Figure 61 RQD variogram models – NPK_GG (left) and MVK2_BBR (right)89
Figure 62 RQD variogram model – NPKD.....90
Figure 63 DD variogram models – BBR (left) and DHB (right) 94
Figure 64 DD variogram models – SVK_M (left) & SVK_L (right).....95
Figure 65 DD variogram models – SDVK (left) and NPKD (right) 96
Figure 66 DD variogram models – NPK (left) and MVK2 (right).....97
Figure 67 DD variogram models – NPK_GG (left) and MVK2_BBR (right) ..98

Figure 68 DD variogram model – SPK 99
Figure 69 UCS Neighbourhood analysis results – SVK_M 104
Figure 70 RQD Neighbourhood analysis results – NPK 106
Figure 71 SDVK block model of UCS kriged blocks after the 1st pass.....108
Figure 72 SDVK block model of UCS kriged blocks after the 2nd pass.....109
Figure 73 UCS Bench plot for – MVK2.....112
Figure 74 UCS unpopulated (0%) block model for SDVK 114
Figure 75 UCS 100% populated blocks – UCS estimates for SDVK 115
Figure 76 UCS bench plots – BBR & SDVK.....121
Figure 77 FFPM bench plots – SDVK and MVK2.....122
Figure 78 RQD bench plots – DHB and NPK 123
Figure 79 DD bench plots – SVK_M and NPK.....125

LIST OF TABLES

Table 1 The Regional Stratigraphy of the area around Orapa AK1 Kimberlite pipe, (Basson, 2006) 11
Table 2 Summary of Orapa AK1 Kimberlite geology 14
Table 3 Summary of PLT, UCS and CF by rocktype. Adapted from (Clark and Barnett, 2015) 29
Table 4 UCS - Classical Statistics for Orapa AK1 pipe rocktypes 33
Table 5 FFPM - Classical Statistics for Orapa AK1 pipe rocktypes 43
Table 6 RQD (%) - Classical Statistics for Orapa AK1 pipe rocktypes 49
Table 7 DD (g/cm^3) Classical Statistics for Orapa AK1 pipe rocktypes 54
Table 8 UCS outlier capping for SDVK and MVK2 65
Table 9 UCS variogram models per rocktype 69
Table 10 FFPM Variogram Model Parameters Summary per rocktype 81
Table 11 RQD Variogram Model Parameters Summary per rocktype 91
Table 12 DD Variogram Model Parameters Summary per rocktype 100
Table 13 Summary UCS KNA results – SVK_M 105
Table 14 Summary RQD KNA results – NPK 107
Table 15 UCS, FFPM, RQD & DD Kriging Neighbourhood optimisation results 110
Table 16 UCS Sample versus block estimate statistics per rocktype 116
Table 17 FFPM Sample versus block estimate statistics per rocktype 117
Table 18 RQD Sample versus block estimate statistics per rocktype 118
Table 19 DD Sample versus block estimate statistics per rocktype 119

ABBREVIATIONS

CDF	Cumulative Distribution Function
CF	Correction Factor
COV	Coefficient of Variation
DCD	Diamond Core Drilling
DD	Dry Density
EDA	Exploratory Data Analysis
EOH	End of Hole
FF	Fracture Frequency
FFPM	Fracture Frequency per Metre
g/cm^3	grams per cubic centimetre
GEMS	3D geological modelling software owned by GEOVIA
ISATIS™	Statistical and Geostatistical software provided by Geovariances
ISRM	International Standards for Rock Mechanics
JC	Joint Condition
KNA	Kriging Neighbourhood Analysis
LogChief	MRM Database platform powered by Maxwell
LDD	Large Diameter Drilling
MA	Moving Average
MADA	Macro Diamond Analysis
mamsl	Metres above mean sea level
mbgl	metres below ground level
MiDA	Micro Diamond Analysis
MRM	Mineral Resource Management
MPa	Mega Pascal
ODS	Ore Dressing Studies
OKC	Orapa Kimberlite Cluster
OM1	Orapa Mine – Number One Plant
OM2	Orapa Mine – Number Two Plant
OREP	Orapa Resource Expansion Project
PLT	Pointload Testing
QKNA	Quantitative Kriging Neighbourhood Analysis
RMR	Rock Mass Rating
RQD	Rock Quality Designation
SOR	Slope of Regression
UCS	Uniaxial Compressive Strength
WC	Wet Condition
WD	Wet Density

1 INTRODUCTION

The Orapa AK1 diamond-bearing kimberlite pipe was discovered by De Beers' geologists in 1967 following a reconnaissance soil sampling for indicator minerals. The AK1 pipe is the world's largest diamond producing mine operating to date. The Orapa 2125A/K1 kimberlite pipe forms part of the Orapa Kimberlite Cluster (OKC) in the North Central District of Botswana. The AK1 kimberlite pipe is the largest (approximately 118Ha) of the known kimberlite pipes in the OKC area, highlighted in red ink on the insert map of Botswana in Figure 1 below. The AK1 consists of two distinct pipes that coalesce at the surface, the South pipe and the North pipe. The older pipe, AK1 North pipe, is cut and truncated by the younger AK1 South pipe, described in more detail under subsection 2.2.3 Internal Pipe Geology.

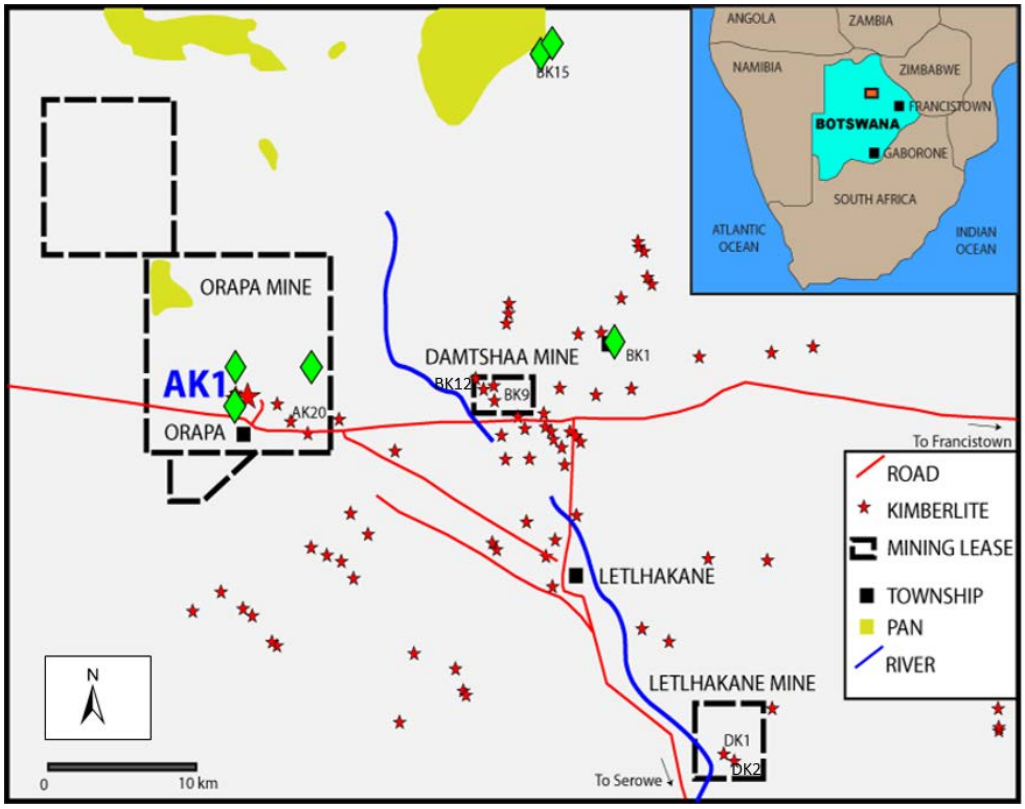


Figure 1 Location Map of Botswana (insert) and Orapa AK1, Letlhakane and Damtshaa Mines (Letsatle et al., 2015)

The Orapa mine, one of Debswana's flagship open pit mines is being operated by Debswana Diamond Company (including the Letlhakane, Damtshaa and Jwaneng mines), which is a 50/50 partnership between the Government of Botswana and De Beers Group. Furthermore, Anglo American plc owns 85% of De Beers Group (Anglo American PLC, 2016). Orapa mine was officially

brought into production on 1st July 1971 with an annual production call of 2.4 million carats (Gibson, 1984). The mine currently runs two on-site metallurgical diamond-processing plants (OM1 and OM2) with a combined annual production output of approximately 23 million carats.

1.1 Research Motivation

Currently Orapa mine (AK1) open pit is completing in 2018 the Cut 2 mining at 260 metres below ground level (mbgl). The mine is ramping up to implement Cut 3 pushback, which will be implemented to a depth of 450 mbgl. This will result in exposing deeper kimberlite ore with potential blasting and processing challenges. 3D geotechnical, geological, hydrogeological, structural and RMR models are required for the slope angle design process of Cut 3. There is a need to deliver the Cut 3 slope angle design well in time for business planning purposes. The author of this research report has been involved in the data collection processes for the Orapa Resource Expansion (OREP) programmes (Phase I & II) for the past 10 years summarised under subsection *2.3*. In evaluating the diamond value chain process during this time, the author of this research report found it fit to motivate and conduct a research on the use of geostatistical methods to estimate RMR parameters with the aim of enhancing diamond production at Orapa AK1 mine.

RMR Input parameters such as, hardness (UCS), ore fracture frequencies (FFPM), rock quality designation (RQD) and ore densities (g/cm^3) provide the required information for mine design and scheduling for both open pit and underground mining operations.

This design and optimisation of both mining methodologies and processing plant performance require an in depth understanding of the ore being mined. This orebody knowledge is dependent on reliable geoscientific information such as ore characterization, quantifiable data and predictive geoscientific models to support mining operations. The primary objective is to provide geoscientific input that reflect the inherent geological variability and affect the processing plants' performance. Ore (kimberlite) characterization is important in terms of addressing bottlenecks, which affect the entire value chain.

It has been postulated that incorporating the RMR parameters as input variables into the resource block model (50m x 50m x 15m); through the application of geostatistics to supplement the conventional geological models,

blasting designs and processing plant performance, would result in a more holistic approach and consequently improve mine planning optimisation and productivity.

The research topic was thus chosen to particularly demonstrate that RMR parameters have spatial distribution properties that allow for the application of geostatistics and specifically Ordinary Kriging as an estimation methodology. This scientific analytical tool can be applied to enhance knowledge and improve understanding of the spatial distributions of structural features and geotechnical environments, and eventually, can be applied to guide solutions to existing day to day challenges related to the diamond production pipeline.

The report seeks to demonstrate that geostatistics is a powerful technique that can be used to investigate and effectively address geoscience related problems. The resulting local block estimation methodology is based on information and available data generated by the on mine drilling programmes such as for the OREP.

1.2 Research Objectives

The main research objectives addressed by this report are highlighted below:

- To investigate the spatial distribution and spatial correlation of rock mass rating (RMR) parameters in 3D space within different rock masses.
- To demonstrate the suitability of using geostatistical estimation methods in the assessment of RMR parameters on different geological and or geotechnical domains.
- To apply these geostatistical methods in the analysis of RMR parameters within different geological and or geotechnical domains.
- To generate a 3D RMR model for the entire Orapa AK1 Kimberlite pipe for future business planning and decision-making.

1.3 Applicability of Geostatistics to Rock Mass Rating Parameters

In order to ensure the successful completion of this research study, the author expanded existing knowledge by undertaking a focused literature review on the concept of geostatistics and its applicability to RMR parameter data and used these reference papers as guidance in the research. Publications on the application of geostatistics to characterise geotechnical parameters per se are

scarce. Some authors have, however, used kriging techniques for estimating spatially distributed geotechnical variables, for example:

- Van De Wall and Ajalu, (1997) applied block kriging to produce reliable estimates for rock strength (hardness).
- Ordinary kriging was used to estimate rock quality designation (RQD) to characterise weathered zones, Ayalew et al., (2002).
- In a relatively recent publication, Egana and Ortiz, (2013) successfully applied geostatistics in the assessment of RMR uncertainty by using conditional gaussian simulation which is based on spatial correlation.

The evaluation of RMR parameters in this research study, refer to fracture frequencies (discontinuities), joint distribution (joint spacing), joint condition, intact rock strength and rock quality designation (RQD). These RMR parameters are a proxy to the behaviour of rock masses during and or post excavation processes.

1.4 Chapter Overview

Chapter 1 introduces the research study. Chapter 2 of the report discusses the background to the study area including the location and geological setting. The geological nomenclature of Orapa kimberlite is described in detail in this chapter with particular emphasis on the internal geological domains. This chapter further discusses a brief overview of Orapa Resource Expansion Project (OREP) and the objectives of the OREP programme.

The next chapter covers an overview of the Rock Mass Rating (RMR) input parameters. The RMR parameters discussed here include Uniaxial Compressive Strength, Rock Quality Designation, Fracture Frequency per Metre and dry density.

This is then followed by a literature review on geostatistics with particular reference to the variogram and its role in spatial estimation using ordinary kriging in Chapter 4. The choice of estimation software (ISATIS^{TM}) for geostatistical modelling , and JMP for classical statistics is contemplated both in terms of relevance and researchers ability to use the software to generate meaningful results are also given in this chapter.

Chapter 5 covers the research methodology followed and includes a review and compilation of the relevant and available geoscience data at Orapa mine. RMR parameter datasets have proved to be sparse, as over time not all

drilling programmes generated this type of data. Also included in this chapter is a literature review on variogram modelling, kriging neighbourhood optimisation and the estimation validation criteria for this project.

Chapter 6 addresses the data selection and validation for the individual RMR parameters considered in this research report. Thereafter in Chapter 7 the exploratory data analysis and classical statistics results of all RMR parameters including histograms and box plots and interpretations are detailed.

Variography analyses for each RMR parameter within all the rocktypes are detailed in Chapter 8. In Chapter 9 the kriging neighbourhood is optimised and Ordinary Kriging (OK) is used for local block estimation of all RMR parameters, this chapter also includes the estimation validation.

The estimation results are discussed in Chapter 10. This chapter also covers interpretation of bench plots for all the estimated RMR parameters and discussion of sample statistics versus local block estimates.

The final chapter, Chapter 11 reflects the conclusions and recommendations of this research project. Generation of bench plots for all the estimated RMR parameters and discussion of the same.

1.5 Research Achievement

The research objectives as set out in section 1.2 of this research report have been fully achieved as a result of the author putting in place a workable research methodology, to demonstrate knowledge and understanding of the RMR parameters and then incorporating this into the application of the geostatistical estimation process flow and the final results that were validated and debated with peers and others.

In summary, the AK1 RMR study has shown that massive and coherent rocktypes of the Orapa AK1 pipe such as NPK, SDVK, and MVK2 show an increase with depth of the UCS and Dry Density parameters. The brecciated rocktypes such as BBR, MVK2_BBR, SVK_M, and DHB have variable values for these two rocktypes. The FFPM parameter showed a decline with increase in depth for most rocktypes except for SPK and NPK_GG which were fairly consistent with increase in depth. RQD for most rocktypes is fairly consistent with increase in depth for most of the AK1 rocktypes.

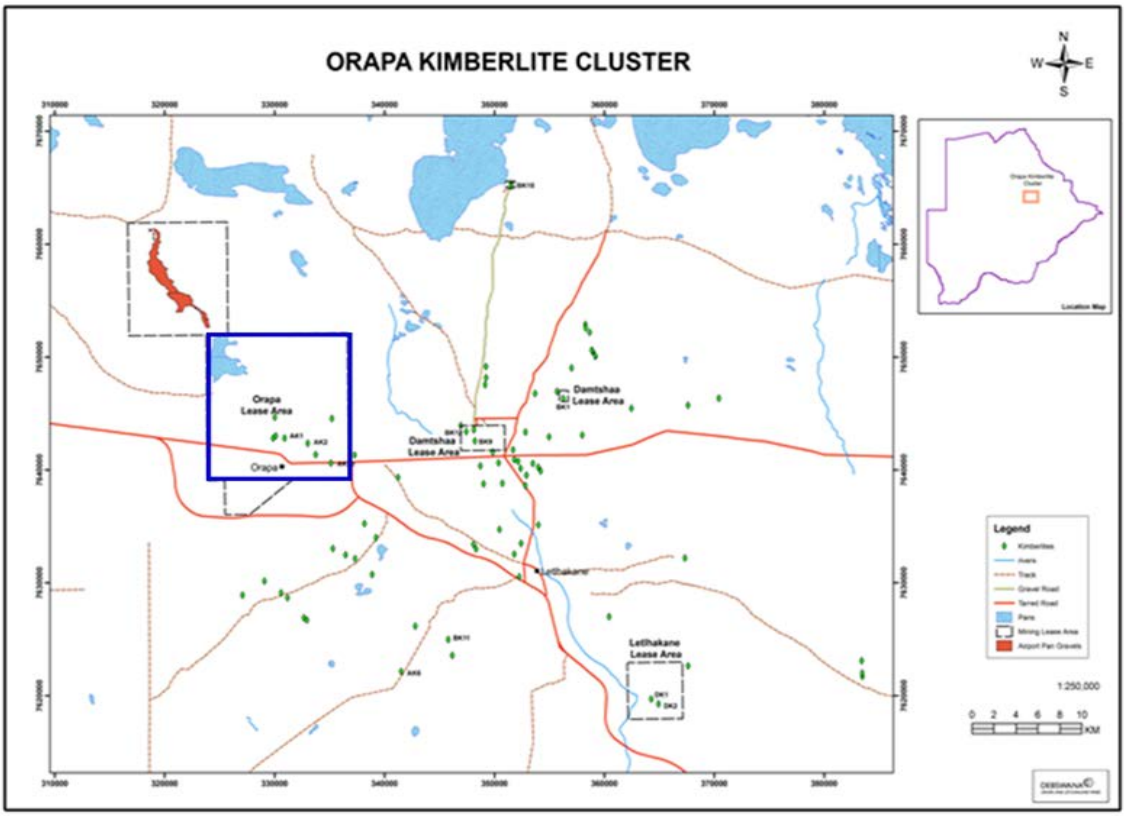
It is strongly recommended that all geological and geotechnical data analysis and interpretation for Orapa mine geoscience projects should be augmented

with geostatistical modelling at project pre-feasibility study phases to enhance the traditional methods used in geoscience mining projects.

2 STUDY AREA

2.1 Location of Orapa Mine

Orapa mine is located in one of Botswana's diamond mining districts. The area is accessible either by a 200km tarmac road from the town of Serowe in the South-Eastern direction, or a 300km road from Maun in the Western direction or another 200km tar road from the city of Francistown in the Eastern direction. The village of Letlhakane is the closest to the mine and the central sub-district focal point. Figure 2 below shows the geographic location of Orapa Kimberlite Cluster (OKC) in Botswana with Orapa Lease Area



highlighted in blue

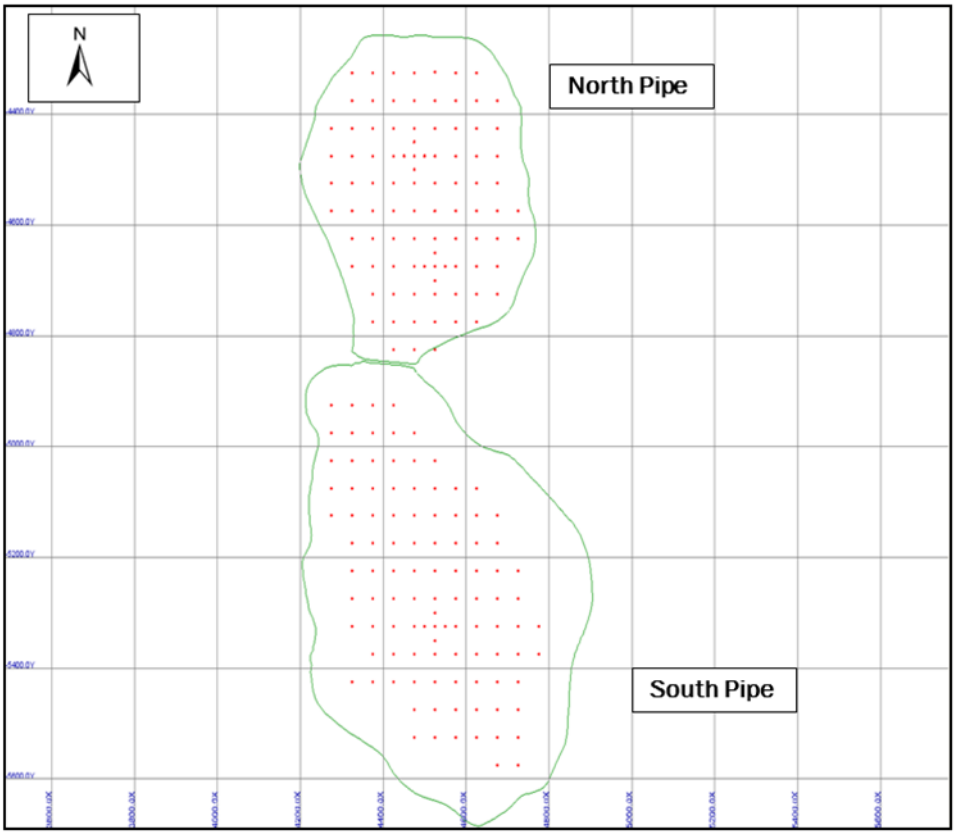
Figure 2 Location Map for Orapa Kimberlite Cluster

2.2 Orapa Resource Extension Project OREP Overview

OREP was conceived to convert and extend the Inferred Diamond Resources to Indicated Diamond Resources from 285 – 685 mbgl. The OREP programme was executed in two phases. Phase I focused on updating the geology, volume and density variables while Phase II addressed diamond grade and revenue estimation. The project sampling programme is based on Large Diameter

Drilling (LDD) and diamond core drilling (DCD) programmes. The LDD programme entailed drill chip sampling of 20 boreholes with an average depth of 500mbgl. Ultimately, the Orapa Resource Expansion Project in its entirety would deliver an integrated Diamond Resource model for the AK1 kimberlite in terms of geology, volume, grade and revenue estimates.

The OREP Phase II project has further been subdivided into two stages, with OREP Phase II Stage 1 having drilled 37 630 metres of core in the South pipe of the AK1 pit, while OREP Phase II Stage 2 covered 36 865 metres being drilled in the North pipe. Boreholes were drilled vertically from the pit bottom at a grid of 50m x 50m covering the entire Orapa AK1 kimberlite resource footprint. Figure 3 below illustrates OREP Phase II core drilling plan completed



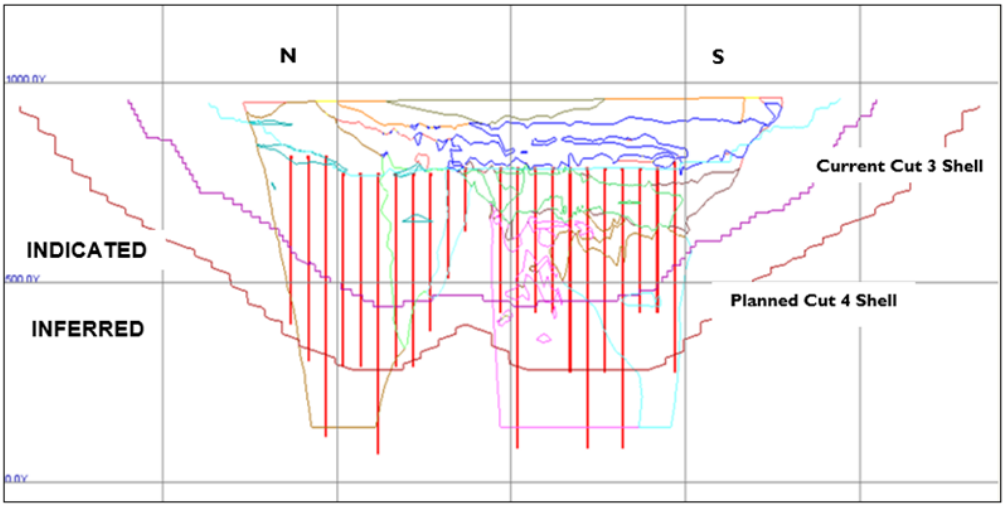
in 2014.

Figure 3 OREP Phase II diamond core drilling plan Orapa AK1 pit (Letsatle, et al., 2015)

In-pit cored boreholes were drilled to elevations of 550 mbgl (approximately 375m deep) while shallow boreholes (on the kimberlite pipe margin) were 150m deep below the mining surface. The boreholes were laid out in such a manner to provide information on the internal geology of the AK1 kimberlite

pipe, Ore Dressing Studies (ODS) and samples were collected for Micro Diamond Analyses (MiDA) to be used in grade estimation.

Furthermore, several deep boreholes (totalling 4000m) were planned to reach depths of 900mbgl to provide additional information on geology, volume and density to enhance the knowledge of the Inferred Diamond Resource to be



considered for the next mining cut (Orapa AK1 Cut 4, illustrated in Figure 4).

Figure 4 Section view of Orapa AK1 mine, current Cut 3 and planned Cut 4 pit shells

2.3 Geology of the Study Area

2.3.1 Regional Geology

The regional geology around Orapa Kimberlite Cluster (OKC) comprises of three major lithological packages; namely the Archaean Basement, the Karoo Supergroup (Ecca), the Stormberg Basalt and a thin cover of the Kalahari Sediments. These rocktypes have been described extensively by Basson (2006).

The Archaean Basement consists of the amphibolite bearing granite gneiss and tonalite. Some authors believe the basement granite is the SW part of the Zimbabwe Craton while others believe the suite forms the WNW extension of the Central Zone of the Limpopo Mobile Belt, (McCourt et al., 2004).

The Karoo Supergroup uncomformably overlies the Archaean basement and consists of six major stratigraphic formations, shown below in Table 1. These formations are; *Mea Formation*, which forms the base of the Karoo Supergroup, *Tlapana Formation*, where present, it overlies the Mea

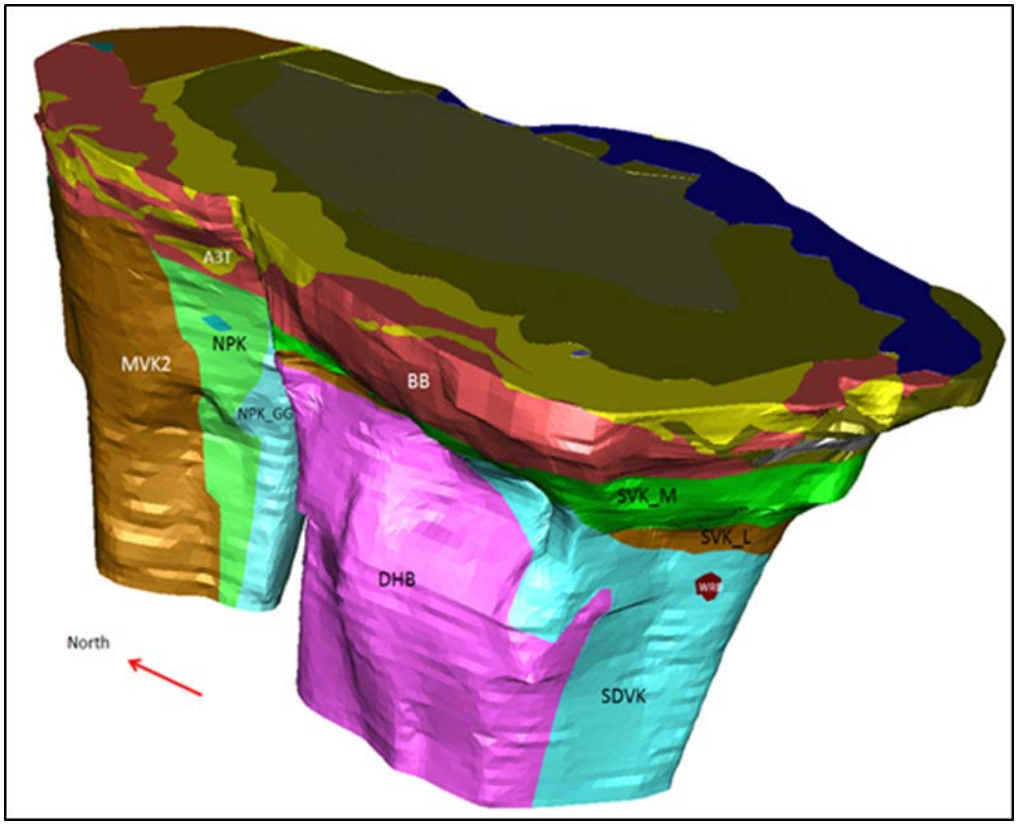
Formation, *Tlhabala Formation*, *Lekotsana Formation*, which has limited distribution in Orapa area, *Mosolotsane Formation* and *Ntane Formation.* Overlying the Karoo sedimentary sequence is the Stormberg Basalt sheets which are in turn overlain by the Recent Kalahari Sediments. The Kalahari Sediments around the Orapa area comprise of calcretes and silcretes, (Basson, 2006).

Table 1 The Regional Stratigraphy of the area around Orapa AK1 Kimberlite pipe, (Basson, 2006)

Depth below Surface (m)	Thickness (m)	Group	Formation	Description
0 - 10	10	**Kalahari Sediments**	Kalahari	Calcretes, silcretes, ferricretes, gravels and loose sand
5 - 110	110	**Stormberg**	Basalt	Basalt flows (10 - 15m thick), showing amygdaloidal bases, chilled top contacts and coarser grained gabbroic centers. Occasional discontinuous, often carbonaceous sandstone lenses (0.1 - 2m thick) between flows. Interflow zones are weathered, suggesting sub-aerial extrusion. The basal flow (e.g. Bobonong unit) contains olivine in both groundmass and as phenocryst, particularly at the base. Other flows higher in the sequence are olivine-free tholeites. Basalts are brecciated in the vicinity of the kimberlite
115 - 145	20 - 60	**Lebung**	Ntane	Massive fine grained to medium grained, orange-beige sandstone, with minor siltstone intercalations. Trough and planar cross-bedded
145 - 225	55 - 100		Mosolotsane	Intercalated reddish to medium-brown siltstones, mudstones and coarse grained to fine grained, massive, poorly cross-bedded to laminated sandstone
-	-		Lekotsana	(Limited distribution - It may not be present at Damtshaa). Medium grained micaceous sandstone, grading upwards into coarse grained sandstones, capped by a pebble conglomerate with siltstones at the top
225 - 315	90	**Beaufort**	Tlhabala	Grey to bluish grey massive mudstones, partly silty and variegated. Lenses rich in calcareous concretions and thin lenses of impure limestone. Minor sharp-based, upward-fining, micaceous sandstone lenses
315 - 355	40	**Ecca**	Tlapana	Laminated fine grained grey sandstone to siltstone, with carbonaceous lamellae, carbonaceous mudstone and coal units. Coal units/seams may be significantly thick (up to 15m)
355 - 455	15 - 20		Mea	Coarse grained, grey to beige arkosic sandstone. Appears porous in places - possible carbonate matrix/cement?
> 500m	N/A		Basement	Tonalitic to granodioritic, foliated to banded granite gneisses

2.3.2 Internal Pipe Geology

The classification and geological nomenclature used in this report is based on the geological model by Sejoe (2014) and the classification adopted during the OREP Phase I and Phase II core drilling programmes. The geology of Orapa Kimberlite pipe is illustrated in Figure 5. The geology of the AK1 kimberlite pipe comprises mainly of the Upper Sedimentary Crater deposits and the individual South and North Lobes with distinctly varying internal geological facies. It should be noted that most of these sedimentary deposits have been mined out and their nomenclature is not tied to any pipe (or lobe) in



particular. Table 2 summarises the geology of Orapa AK1 kimberlite pipe.

Figure 5 Geology of the Orapa AK1 Kimberlite pipe (Sejoe, 2014)

Details of all geological units appear in Table 2, and visible units in this view are: MVK2 – Massive Volcaniclastic Kimberlite; A3T – Bedded talus cone deposits; NPK – Northern Pyroclastic Kimberlite; BB – Basalt Breccia; NPK_GG – Northern Pyroclastic Kimberlite with Granite Gneiss; DHB – Deep Heterolytic Breccia; SVK_M – Southern Volcaniclastic Kimberlite (middle); SVK_L –

Southern Volcaniclastic Kimberlite (lower); and SDVK – Southern (dark) Volcaniclastic Kimberlite.

Table 2 Summary of Orapa AK1 Kimberlite geology

CODE	Occurrence	Geological Description
A3T/A3T FINE	Crater deposits	Bedded talus cone deposits
BBR	All pipes	Basalt Breccia
EBB	All pipes	Epiclastic Basalt Breccia
EGSST	All pipes	Epiclastic Grits, Shales and Sandstone
DFBB	All pipes	Debris Flow Basalt Breccia
DHB	AK1 - South pipe	Deep Heterolytic Breccia
SVK_U	AK1 - South pipe	Southern Volcaniclastic Kimberlite (upper)
SVK_M	AK1 - South pipe	Southern Volcaniclastic Kimberlite (middle)
SVK_L	AK1 - South pipe	Southern Volcaniclastic Kimberlite (lower)
SDVK	AK1 - South pipe	Southern (dark) Volcaniclastic Kimberlite
MVK2	AK1 - North pipe	Massive Volcaniclastic Kimberlite
NPK	AK1 - North pipe	Northern Pyroclastic Kimberlite
NPKD	AK1 - North pipe	Northern Pyroclastic Kimberlite (dark)
MVK2_BBR	AK1 - North pipe	Massive Volcaniclastic Kimberlite with basalt breccia
NPK_GG	AK1 - North pipe	Northern Pyroclastic Kimberlite with granite gneiss
WRB	AK1 - South pipe	Wall Rock Breccia

In summary, this chapter looked at the introduction to the study area, country rock and kimberlite geology of the area. It should be noted that the study focussed on the geostatistical evaluation of RMR parameters of Orapa AK1 kimberlite. So a thorough understanding of the internal geology of the AK1 pipe was very important in this research study. No evaluation of RMR parameters was undertaken for country rocks around the AK1 pipe as there was no available RMR data. Therefore, the scope of the research study was restricted to the kimberlite geology.

3 OVERVIEW OF ROCK MASS RATING PARAMETERS

The RMR parameters influence the geo-mechanical properties of rock masses and potentially the behaviour of the rocks. In the mining industry for example, the RMR parameters form an important input into geotechnical models for slope angle designs of open pits and underground mine designs. The RMR can also be used as a guideline for the selection of an appropriate excavation technique, rock reinforcement methods, and evaluation of landslide susceptibility of slopes to failure, (Ferrari et al., 2014).

The rock mass rating (RMR) system consists of weighted ratings assigned to each of the following parameters: uniaxial compressive strength (UCS), rock quality designation (RQD), fracture frequency (FF), Joint Condition (JC) and underground Water Condition (WC), (Bieniawski, 1989).

Different classification schemes are used to classify Rock properties, with the most commonly used methods for evaluating RMR parameters being the:

- Q-system (Barton et al., 1974)
- Rock Mass Rating (RMR) (Bieniawski, 1989)
- Mining Rock Mass Rating (MRMR) (Laubscher, 1990)
- Geological Strength Index (GSI) (Hoek, 1994)

The choice of preference on RMR engineering classification systems is however not the focus of this study.

The RMR classification system can be used as a guideline for the selection of an appropriate mining method, rock reinforcements and support system based on the evaluation of the RMR parameters. The resulting RMR values are based on the ratings assigned to various parameters ranging from 0 – 100 (Bieniawski, 1989): Uniaxial Compressive Strength (UCS), Rock Quality Designation (RQD), Fracture Frequencies per metre (FFPM), conditions of discontinuities and presence of water.

Other rock mass parameters that are useful for characterization are rock porosity and permeability. However, this research report only focusses on the geostatistical evaluation of the RMR parameters described in subsequent sections.

The classification of rock masses using the RMR characterization defines the geo-mechanical quality of the rock mass. For the sake of clarity, it is important to distinguish the difference between intact rock and rock mass properties.

Intact rock is defined as the rock material occurring between discontinuities while the rock mass comprises of the entire volume of rock and intact rock including discontinuities, (Egana and Ortiz, 2013).

3.1 Uniaxial Compressive Strength (UCS) – MPa

UCS is defined as the maximum stress that a sample of intact rock reaches before failure under uniaxial compression, (Egana and Ortiz, 2013). Basically, UCS is the maximum load that the intact rock specimen undergoes before failure. Intact rock strength can either be determined for rock specimen analysed in laboratories under controlled conditions or derived using calculations from point load index (point load testing). The UCS parameter is influenced by the mineralogy of the rock, degree of weathering, porosity and moisture content.

3.2 Rock Quality Designation (RQD) - %

The RQD parameter of a cored rock sample is the percentage of intact rock obtained by dividing the summed lengths of all core samples equal or greater than 10cm (4 inch) long by the total core recovery length. Core losses and crumbled core pieces (rubble) are zero rated – assumed to result from closely spaced fractures, shearing and faulting which directly affect the rock mass quality. An RQD of 100% indicates 100% core recovery suggesting that all cored samples are equal or greater than 10cm in length. RQD is a directionally dependent parameter and its value changes depending on the drillhole direction (orientation), (Hoek, 1994).

3.3 Fracture Frequency per metre (FFPM) – A qualitative assessment

The fracture frequency per metre (FFPM) measures the number of discontinuities per metre such as fractures, faults, shear zones etc. These variables are obtained by various geotechnical data collection processes such as scanline face mapping, downhole geophysics, geotechnical core logging.

3.4 Joint Conditions (JC) – A qualitative assessment

Joint condition refers to the surface characteristics of joints such as roughness, alteration, aperture and in-fill material (gouge) type and strength, (Bieniawski, 1989).

3.5 Water Condition (WC)

The presence of water under pressure in a rock mass affects its quality by reducing the rock strength. Hence this parameter should be considered under rock mass classification systems. General water conditions can be described as completely dry, damp, wet, dripping or flowing (Bieniawski, 1989).

3.6 Density (g/cm^3)

In simpler terms, density is the mass (m) of a substance divided by its volume (v). The units for measurement of density are g/cm^3, dry or wet density of a rock specimen and are measurable variables under controlled laboratory conditions.

It should be noted that in the determination of some of the RMR parameters considered in the preceding subsections there exists an element of subjectivity. These methods are usually determined using various geotechnical standards and methods and the parameters should be treated as having a degree of uncertainty. The classification system using the first five parameters allows for the characterization of a rock mass to be undertaken.

For this research study, it is highlighted that the available RMR data for geostatistical analysis included the following variables: Uniaxial Compressive Strength (UCS), Rock Quality Designation (RQD), Fracture Frequency per Metre (FFPM) and Dry Density (DD). The calculations for UCS, RQD, FFPM and density are described in more details in Chapter 6. All the data sets were derived by various methods as discussed in the subsections of this chapter and from the Orapa AK1 expansion projects, (OREP Phase I and II).

4 GEOSTATISTICAL APPROACH

4.1 Literature Overview

Geostatistical estimation refers to the estimation of a value of an attribute at a location at which it is unknown from the measured values of a number of known locations through a random function defining spatial correlation between values (the variogram or correlogram) – this methodology is known as Kriging. The mathematical technique to predict grades based on their spatial auto correlated point samples was developed by Georges Matheron, a French Mining Engineer, who developed the technique based on the work of the South African Mining Engineer, Daniel Krige, in the 1950s, (Krige, 1951); and named it Kriging in his honour, (Matheron, (1963), Brenning, (2013)).

To illustrate the Kriging concept, it is assumed that the grade value at an unsampled location, z(u), is related to a random variable, Z(u), characterised by a probability distribution. The goal of geostatistics is to predict the possible spatial distribution of an attribute. Two basic forms of prediction exist: estimation and simulation, (Zhang, 2011).

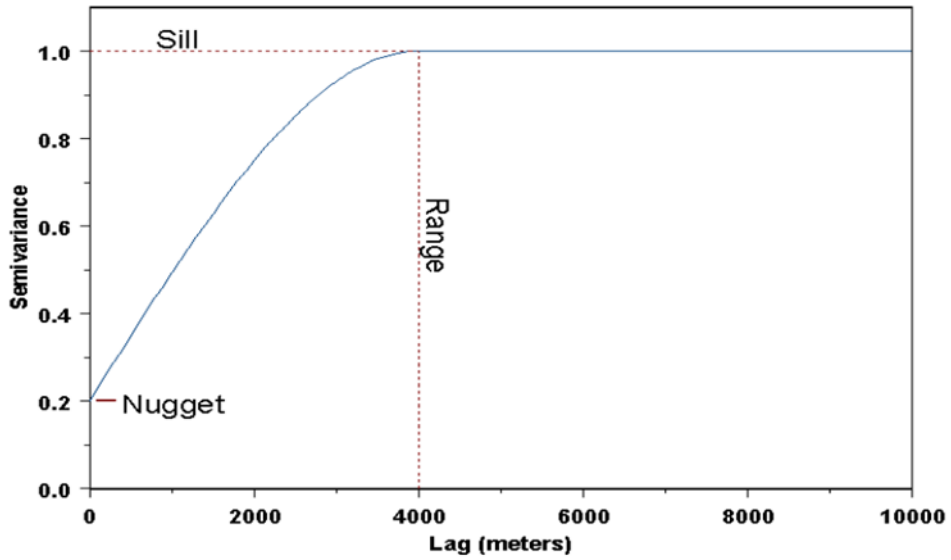
Estimation is thus undertaken by considering a linear estimator (Z*) that depends on the surrounding sample information. In Geostatistics, this estimator is called Kriging, which is a best linear unbiased estimator known as a "BLUE" estimator, (Isaaks and Srivastava, 1989).

Kriging estimation (Z^*_K) is therefore the best estimator in the least squares sense, in that it minimises the estimation variance error and this minimum error variance is called the kriging variance (σ^2_K). The estimation is based on the sample data and the variogram model that represents the spatial correlation of the samples, (Egana and Ortiz, 2013)

The kriging estimation technique is undertaken by relating random variables at distinct locations by means of a random function $\{Z(\mathbf{u}): \mathbf{u} \in D\}$, where D is the domain of interest. This random function is characterised by its statistical moments which must be inferred from sampled data, that is, values gathered at sample locations, $\{z(\mathbf{u}_\alpha), \alpha = 1, \ldots, n\}$. Therefore, the spatial distributions of actual values of the variable within a domain are interpreted as realisations of this random function. The geostatistical concept is based on estimating the expected value of the random variables at every location to obtain a local optimum estimate so as to characterise the uncertainty associated with

unsampled locations but preserving the spatial relationships between the locations (Bohling, 2005).

Geostatistics allows one to quantify the estimation uncertainty by using a variogram model, illustrated in Figure 6. The variogram model provides a measure of the spatial correlation between sample values. It is a tool that assists in obtaining sample weighting to ensure minimum estimation variance



in the estimate.

Figure 6 A Typical Variogram Model showing the nugget, sill and range (adapted from Bohling, (2005))

In theory, the four semi-variogram models used for spatial interpolation by kriging are the Spherical, Gaussian, Exponential and Power models. Matheron (1963) first defined the semi-variogram for geostatistical application. The Spherical model is the most commonly used variogram model and is mathematically described by the following formulae (Equation 1):

$$\gamma(h) = C_0 + C_1\left(\frac{3}{2}\frac{h}{a} - \frac{1}{2}\frac{h^3}{a^3}\right) \quad where\ h \leq a \qquad Eq\ 1$$

$$= C = C_0 + C_1 \qquad where\ h \geq a$$

Where:

$\gamma(h)$ = Semi-variogram model for the lag distance h

C_0 = Nugget effect

C_1 = Sill of the of the correlated component

$C = C_0 + C_1$ = the Total Sill of the semi-variogram

a = Range of influence of a sample

A variogram is characterized by the following components:

Sill: The semi-variance value at which the variogram levels off.

Range: The lag distance at which the variogram reaches the sill value and the spatial correlation between values disappears.

Nugget Effect: Representing the variability at distances smaller than the sample spacing including the measurement error.

The formula for the kriging estimator is given in Equation 2, and is a weighted sum of the data:

$$Z^*_{OK}(\boldsymbol{u_0}) = \sum_{\alpha=1}^{n(u)} \lambda_\alpha^{OK}(u) Z(\boldsymbol{u_\alpha}) \qquad Eq\ 2$$

Where:

$Z(\boldsymbol{u_\alpha})$ = the measured value at the location $\boldsymbol{u_\alpha}$

$\lambda^{OK}_{\boldsymbol{\alpha}}$ = the optimum weight for the measured value at the location $\boldsymbol{u_\alpha}$

$Z^*_{OK}(\boldsymbol{u_0})$ = the estimated value at location $\boldsymbol{u_o}$

$n(u)$ = the number of measured values considered in the estimation of $\boldsymbol{u_o}$ (Bohling, 2005).

The Covariance is a measure of the joint variability of two random variables. The sign of the covariance shows the tendency in the linear relationship between the variables. The covariance is used to calculate kriging variance. The distances between the unknown point at which there is need to make a prediction using the known points nearby. The covariogram is used for those distances to calculate the weight of each of the surrounding measured points. The variogram is inversely proportional to the covariogram.

The kriging variance can be computed using Equation 3 after the determination of kriging weights and the Lagrange parameter:

$$\sigma^2_{OK}(\boldsymbol{u_0}) = C(0) - \sum_{\alpha=1}^{n} \lambda_\alpha^{OK}(\boldsymbol{u}) C(\boldsymbol{u_\alpha}, \boldsymbol{u_0}) - \mu_{OK}(\boldsymbol{u_0}) \qquad Eq\ 3$$

Where:

$\sigma^2_{OK}(\boldsymbol{u_0})$ = kriging variance at location u_0

C(0) = spatial covariance of the population estimated and modelled from sample data.

$(\mathbf{u}_\alpha, \mathbf{u}_o)$ = covariance of the data located at u_α and u_0 the location of interest.

$\lambda_{\boldsymbol{\alpha}}^{OK}$ = optimum weight for sample $\boldsymbol{u_\alpha}$ that minimises the estimation error variance.

$\mu_{OK}\,(\boldsymbol{\mu_o})$ = the Lagrange multiplier of the estimate at $\boldsymbol{u_0}$

(Adapted from Bohling, 2005)

4.2 Why Geostatistics?

Classical statistics focuses on the analysis and interpretation of uncertainties caused by limited sampling data for a property under study. Geostatistics deviates from classical statistics in that it is not only tied to a population distribution that assumes that all samples of a population are normally distributed and independent of one another. Compared to classical statistics which focuses on the statistical distribution of a set of sampled data, geostatistics incorporates both statistical distribution of sample data and the spatial correlation among the sample data. Because of this difference, many geoscience problems are addressed effectively using geostatistical methods, (Zhang, 2011).

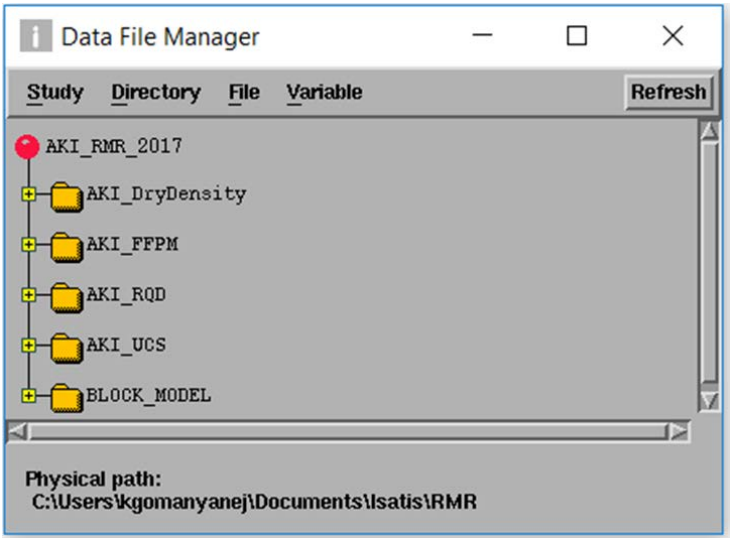
In geoscience, for example rock mechanics and rock properties do satisfy this assumption as these can have highly skewed distributions and can have spatial correlation properties. It has been observed that data values from locations that are closer together tend to be more similar than data values from locations that are further apart. Geotechnical variables such as RQD and fracture frequency tend to display directional behaviour depending on the direction of the drillhole or scanline survey, (Egana and Ortiz, 2013). The same directional behaviour is observed in other RMR input parameters.

Thus, the intention of this research study is to apply geostatistical analysis methodologies on rock mass rating (RMR) parameters and generate 3-D models for Orapa mine using available data from the Orapa Resource Expansion Project (OREP) datasets.

4.3 Classical Statistics

In this research study, classical statistical analyses were carried out firstly as a means of validating all parameter data sets and secondly in order to characterise the different datasets representing the various geotechnical domains.

A project (AK1_RMR_2017) was created in ISATIS^{TM} 2016.2 with sub directories representing all the input parameters to be analysed. All the data for the various input parameters were uploaded in these directories. Figure 7



illustrates the RMR project set up in ISATIS^{TM} 2016.2 software environment.

Figure 7 AK1 RMR Project in ISATIS^{TM} 2016.2 software

For better understanding of the various datasets of the RMR parameters, and to generate meaningful results, all the datasets were imported into ISATIS^{TM} 2016.2 software (Geovariances) for a first pass analysis and fine-tuning.

Basic statistical analyses were undertaken to determine various numerical values for all relevant statistics of the RMR parameters such as total number of samples, data population maximums, minimums, means, standard deviations and coefficient of variation for all sampled geotechnical domains.

In summary, this chapter looked at the various concepts and terminology pertaining to geostatistics. The chapter started with an overview of geostatistical estimation using variogram models and the kriging concept. The various characteristics of a variogram were illustrated and the development of kriging as a mathematical technique was also discussed. A comparison

between geostatistics and classical statistics was also elaborated. Estimation project set up and data import into ISATIS^{TM} software was discussed.

5 RESEARCH METHODOLOGY

The approach used on this study was to model the RMR input variables as consistent and discrete geotechnical units or domains. The RMR input variables were derived from OREP drilling programme for the Orapa AK1 Kimberlite pipe. The geological domains were expected to have similar geotechnical characteristics. For this study, the RMR input variables analysed (modelled) using statistics and geostatistics were: Uniaxial Compressive Strength (UCS MPa), Fracture Frequency per metre (FFPM), Rock Quality Designation (RQD %) and Dry Density (DD g/cm^3). Joint Condition and Water Condition were not considered in this study as the two are qualitative input parameters.

5.1 Review of Existing Relevant Datasets

Orapa Resource Expansion Projects (OREP) have generated an enormous amount of quality geoscience data sets on kimberlite core. The OREP programme was undertaken to upgrade the Orapa AK1 kimberlite pipe from an Inferred Diamond Resource to an Indicated level of confidence between 285 – 685 metres below ground level (mbgl), (Tait et al., 2009).

The OREP programme was executed in two phases; OREP Phase I which focused on geology, volume and density parameters while OREP Phase II focussed on defining grade and revenue (Letsatle et al., 2015).

Drill cores generated from these two programmes were logged geologically and geotechnically, generating good data packages, including density and structural data. It is these data sets that form the basis of this research study.

The review of data included data quality checks and validations to organise the data into a more usable format for this research. The basic checks comprised identifying duplicates and blanks.

The RMR parameter values: fracture frequency per metre (FFPM), joint distribution (joint spacing), intact rock strength and rock quality designation (RQD) were calculated using a recommended template for Orapa mine as per the International Society for Rock Mechanics (ISRM). De-surveying in GEMS^{TM} of the RMR parameter values to generate downhole 3-D positions, and lastly assigning geological codes based on the geological logging and interpretation, to each drillhole trace using GEOVIA GEMS^{TM} 6.8.1 software were carried out.

5.2 Exploratory Data Analysis (EDA)

Data analyses discussed and illustrated industry experts such as Dohm (2013a), Dohm (2013b); McKillup and Dyar (2010) formed the basis for the Exploratory Data Analysis (EDA) followed by and recorded in this research report. Classical statistics and histogram distributions or box plots as relevant were calculated, displayed and interpreted for each RMR input parameter. This allowed for validation on geological consistency, existence of structures and identification of trends in the rocktypes or domains.

5.3 Variogram Modelling

The spatial characteristics of the variables that is, the variography and covariance analyses, were determined within the different rock mechanics domains, which might be different from the geological domains. The so-called rock mechanics domains are simply rock masses with different mechanical properties (fracture frequencies, strength and weathering extent) which may not necessarily be geological domains.

The approach adopted in this study was to establish experimental variograms and produce fitted variogram models for all the lithological units. The downhole experimental variograms were used to model the nugget effect and the horizontal variograms were used to identify the existence of anisotropy and model the spatial continuity in the different directions.

Finally, the estimation of the various RMR input parameters were based on ordinary kriging techniques using the appropriate variogram models.

5.4 Kriging Neighbourhood Optimisation

An essential step in the estimation process has been the determination of the optimal kriging neighbourhood for each of the lithological units with respect to the modelled variograms and the sampling configurations as well as the block size. Kriging is commonly described as ‘minimum variance estimator’ provided the search neighbourhoods are properly defined (Vann et al., 2003).

The kriging weights are directly related to the variogram model, data geometry, block size and sample support involved in the kriging process. The choice of neighbourhoods is influenced by the slope of the variogram and the relative nugget effect (ratio of nugget variance to total variance). In the

kriging neighbourhood analysis the underlying assumption is that the variogram was modelled adequately and represents the domain of interest.

The process of optimum kriging neighbourhood entails adjusting the search radius so as to reach good regression statistics to reduce or eliminate conditional bias. Ordinary Kriging was applied to run different neighbourhood configurations from which the optimal kriging neighbourhoods were determined. The criteria used in this research report involved local block estimation of all RMR parameters using varying block size and the optimum number of pairs and assessing the following as illustrated by Vann et al., 2003:

- Maximum positive weight percentage
- Slope of regression of 'true' block grade on the 'estimated' block grade
- The percentage of blocks populated
- The weight of the mean for simple kriging
- The kriging standard deviation – a measure of estimation confidence.

5.5 Estimation Validation Criteria

The RMR parameter estimates were subjected to a validation criterion which allowed applying the following fundamental checks:

- Three-dimensional visualizing of the RMR samples and the estimates in the 2016.2 ISATIS^{TM} 3D viewer. All samples assigned a particular rock code must appear inside the blocks of the same rock type.
- Tabulation of RMR sample classical statistics with mean block estimates for all the estimated rock types.
- Choosing an optimal kriging neighbourhood (lowest kriging variance)
- Graphical comparison of de-clustered mean sample values with mean estimates of kriged 1st Pass, 2nd Pass.
- Moving Average (MA) and Final estimates (bench plots) where applicable, were carried out.

The research methodology chapter focussed on executional approach of the research study based on the available RMR data sets. This comprised of reviewing of all RMR data sets, exploratory data analysis (EDA), variogram modelling, kriging neighbourhood optimisation and estimation validation. These sub sections have been discussed in detail with the descriptions of the various steps undertaken in each sub section.

6 RMR DATA SELECTION AND VALIDATION

6.1 Uniaxial Compressive Strength (UCS)

6.1.1 Point Load Index – I_s

Point load testing provides measurements on rock strength, which is vital information for mine slope design and ore treatment purposes. The test measures the Point Load Index $I_{s(50)}$ of a rock specimen and their Strength Anisotropy Index (I_a), which is the ratio of Point Load Strengths in the directions that give the greatest and least values. The rock specimen is hydraulically loaded between spherically truncated, hardened, conical steel plates and fails by the development of tensile cracks parallel to the axis of loading. The maximum load, also known as the Failure Load, is the load that the specimen reaches under stress.

Brook (1985) proposed the analytical method of 'Size Correction' to a chosen standard core size. The point load index can be used to predict the rock specimen strength (Uniaxial Compressive Strength - UCS) using the industry formula for diametral tests as illustrated by Equation 4:

$$\boldsymbol{I_{s(50)} = {(f \times F)}/{D_e^2}} \qquad \boldsymbol{Eq\ 4}$$

Where

D_e = Equivalent Core Diameter (m)

I_s = Failure Pressure / D_e^2 = uncorrected pointload strength index (MPa)

F = Failure Pressure = Failure Load / Area of Platen

Area of Platen is assumed to be 0.001135 m^2

f = Size correction factor = $(D_e/50)^{0.45}$

A number of rock mechanics researchers such as Broch and Franklin (1972) have proposed the Index to strength conversion. They reported that for a 50mm diameter core the uniaxial strength is approximately equal to 24 times the point load index. These researchers also developed a size correction chart for different core diameters that could be used for UCS determination. According to the International Society for Rock Mechanics (ISRM), the UCS is approximately 20 to 25 times the index (I_s), (Ulusay, 2014).

6.1.2 UCS Calculations

It should be noted that in this research report the industry formula was applied to calculate the UCS by using the measured point load index values for both the Phase I and Phase II datasets.

The point load testing (PLT) machine provided calculated values for UCS, but to avoid possible errors from the machine calculations, these values were not used. The $I_{s(50)}$ for the entire data set were re-calculated from first principle using Equation 4.

For each individual rocktype in the Orapa AK1 kimberlite pipe, the PLT failure records were used to calculate the UCS using $I_{s(50)}$.

Applying this method (PLT records), the following rocktypes MVK2, SDVK, NPK, SVK_M, DHB, BBR, SVK_L, NPK_GG and MVK2_BBR were uniquely identified and their UCS Conversion Factors (CF) values are listed in Table 3. CF=24 is assumed where there is no Laboratory data available, as illustrated by Ulusay (2014), highlighted in Table 3.

6.1.3 UCS Conversion Factors

Typically, each individual UCS sample has an associated series of PLT values measured on the same or adjacent core samples, which can be averaged to calculate the conversion factor (CF). For similar geotechnical units, each UCS and associated $I_{s(50)}$ are plotted and the slope of best fit line is the CF of that unit. The CF value is a conversion factor to convert PLT values to uniaxial compressive strength (UCS) values, see Table 3.

An alternative method is to take the average UCS for each geological unit and divide it by average $I_{s(50)}$ for that rock unit and the result can be used as the CF, (Clark and Barnett, 2015).

Rock types without lab UCS data were assumed to have a CF = 24, based on typical practice when no data is available. Most rocktypes for Orapa AK1 have lab data available for CF determination.

Alternatively, a CF from a similar geotechnical domain or rock type can be used instead, this assumption may be better than using CF = 24, and more so, the risks associated with this method must be evaluated.

Table 3 Summary of PLT, UCS and CF by rocktype. Adapted from (Clark and Barnett, 2015)

Rocktype	PLT			UCS (Lab)			CF
	No. of samples	$I_{s(50)}$ Avg.	$I_{s(50)}$ Std. Dev	No. of samples	Avg. (MPa)	Std Dev. (MPa)	
MVK2	4150	1.58	0.95	12	30	4	19
SDVK	2025	2.05	1.30	10	51	15	25
NPK	1813	1.46	0.83	11	30	5	21
SVK_M	1739	1.54	1.98	15	21	3	14
DHB	852	2.90	2.87	**0**	-	-	**24**
BBR	606	5.79	2.65	13	74	24	13
SVK_L	587	3.22	2.84	7	32	7	10
SPK	138	1.99	2.47	**0**	-	-	**24**
NPK_GG	133	0.87	0.86	10	27	5	31
NPKD	111	1.89	0.62	**0**	-	-	**24**
MVK2_BBR	97	2.88	2.79	10	59	37	20

6.2 Fracture Frequency per metre (FFPM)

6.2.1 Definition of FFPM

Fracture frequency per metre (FFPM) is a qualitative assessment of a rock mass and is derived by determining the number of discontinuities along a defined line such as a scanline or a 1m long core string. This data is generated during a downhole geotechnical logging process.

6.2.2 Calculation of FFPM

The Debswana Resource MRM Evaluation procedure for visual core logging was followed. The FFPM parameter is determined by counting the number of fractures and dividing the sum by a specified length of core string. In this case a 3m core length was used. A point to note, is that geological contacts were not crossed. Thus the FFPM for all the rock types in the AK1 kimberlite were individually determined.

All the geotechnical logging data including FFPM is captured in the MRM *LogChief* database platform. The FFPM is calculated using the methodology described in the previous paragraph, in the database tables and is linked to the headers for every drillhole data. For this research report, the FFPM data for Orapa AK1 (OREP Phase I & II) was retrieved from the MRM *LogChief* database.

6.3 Rock Quality Designation (RQD)

6.3.1 Definition of RQD

RQD is also a calculated input parameter that is measured in percentages and is generated during the geotechnical core logging process. It is the total length of broken pieces of core 10cm in size or more divided by the total core recovery length, in this case 3m.

6.3.2 Calculation of RQD

This data has also been captured in the MRM *LogChief* database platform. The RQD parameter for each drillhole run is calculated by the methodology described above in the *LogChief* drillhole header tables. The RQD data is easily accessible and was extracted from the MRM geoscience database.

6.4 Dry Density (g/cm^3)

6.4.1 Definition of Dry Density

The dry density variable, measured in grams per cubic centimetre (g/cm^3), is basically the dry mass of a rock sample divided by its volume. The sampling for density for Orapa AK1 pipe followed the specified internal procedure for density sampling and testing. Density samples were taken every 15m (Orapa mine bench height) where a 20cm long drill core specimen was taken and dried for 24hrs in an oven before its volume measurement was determined.

6.4.2 Calculation of Dry Density

The dried density specimens were weighed on a calibrated digital scale, and the volume for the cylindrical drill core specimen was determined using the formula for the volume of a cylinder ($V = \pi \times r^2 \times h$). It is this dry mass and volume that was used to calculate the dry density parameter. All this data was also uploaded in the *LogChief* database platform and retrieved for analysis.

6.5 Data Quality Checks – RMR Input Parameters

Several aspects of the RMR input parameters were validated in order to check that the datasets were not erroneous. The basic checks included identifying duplicates and blanks, making sure sampling depths did not exceed end of hole (EOH) depths and making sure that the borehole collars plotted in the correct positions. To ensure that the samples had the correct lithological codes, the 2014 Geological model (Sejoe, 2014) was used for coding and de-surveying all the RMR input parameters. These basic checks were performed prior to loading all the datasets into GEOVIA GEMS^{TM} 6.8.1 software.

The focus of this chapter has been on the RMR data selected for geostatistical evaluation in the research study. Covering the definitions and methodology for calculating all the RMR parameters as well as dry density, as input into *LogChief,* for retrieval and final use in the RMR estimation process. The chapter concluded with data quality checks and validations conducted in the data capturing process. Furthermore, the software used for estimation was also highlighted.

7 EXPLORATORY DATA ANALYSIS (EDA)

Exploratory data analysis (EDA) were undertaken for all RMR input parameters on each kimberlite facies (rocktype) to better understand the statistical characteristics of the RMR data and dry density. This comprised the application of two descriptive methods the first being numerical (statistics) and the second being graphical (distributions).

EDA is carried out on data sets to get a feel and understanding of the statistical parameters that summarise the data such as the number of observations or samples, the minimum and maximum values for the variable being investigated and the mean, standard deviation and coefficient of variation. The difference between the maximum and minimum gives an idea of the range of the observations. The mean, median and mode tells the researcher where the most likely values lie within the statistical distribution. The variance is the average squared difference between the observations and the mean, and it provides a measure for the variability of observations around the mean. The variance is sensitive to the number of observations and becomes more reliable as the number of samples increases above 30. The standard deviation is the square root of the variance, the standard deviation provides an indication of the spread around the mean. The coefficient of variation (CoV) statistic which is the standard deviation divided by the mean can provide an indication of the spread of the data and the skewness of the frequency distribution of the data. As the CoV increases towards one and beyond the asymmetry of the distribution is accentuated. A CoV close to 0.33 is indicative of a symmetrical distribution.

Classical statistics are however not the only EDA technique, the graphical presentation or summary of the data is another powerful tool in understanding the statistical and distributional characteristics of the data under study. It is also useful for identifying outliers, (Dohm, 2013a). Classical statistical analyses were used firstly as a means of validating all the datasets and secondly to characterise the different data representing the various geotechnical domains.

To fine tune the data, the data sets were subjected to outlier analysis and where applicable these outliers were removed (masked out). The classical statistics results and interpretations of the RMR parameters are presented

and discussed in the next subsections. This is then followed by the graphical assessments of these parameters per rocktype.

Several rocktypes, had less than sixty (60) data points for some of the RMR parameters, this is considered too small a number to generate any meaningful histograms. In these cases, box plots would be a more appropriate to represent the distributional characteristics of the data. The whisker on the left of a box plot represent the scaled difference between the minimum value and the first quartile and right whisker, the scaled difference between the third quartile and the maximum value, (Dohm, 2013a). For the graphical analysis of the distributional characteristics of the RMR parameters below 60 observations Box plots and Cumulative Distribution Frequency (CDF) plots were generated. Where more than 60 observations were available classical statistics and histograms were generated in ISATIS^{TM} software. The EDA results and interpretations of all RMR parameters are discussed in the subsections below.

7.1 UCS (MPa) EDA for Orapa AK1 pipe rocktypes

7.1.1 UCS (MPa) Classical Statistics

The basic classical statistics for the UCS parameter for all the Orapa AK1 rocktypes are summarised in Table 4 below. It is clear from Table 4 that rocktypes A3T, WRB, NPKD and SVK_U have less than 30 UCS observations, and caution is needed when interpreting the statistics for these units, particularly for the standard deviation and consequently the CoV, as the variance is statistically not robust for less than 30 samples.

Table 4 UCS - Classical Statistics for Orapa AK1 pipe rocktypes

RMR parameter UCS (MPa)	Rocktype	Number of observations	Min	Max	Mean	Std Dev	CoV
	A3T	5	8.41	97.02	42.89	-	-
	WRB	2	32.73	44.78	38.75	-	-
	BBR	186	1.72	181.82	72.13	33.32	0.46
	DHB	368	4.20	439.50	63.83	66.44	1.04
	MVK2	1048	8.14	334.16	33.42	19.11	0.57
	MVK2_BBR	33	13.11	202.18	51.70	50.44	0.98
	NPK	564	2.81	188.40	35.37	19.13	0.54
	NPKD	27	18.67	78.95	45.61	13.58	0.30
	NPK_GG	57	4.63	262.96	29.67	33.98	0.84
	SPK	32	11.88	274.90	50.72	60.05	1.18
	SVK_U	22	7.48	154.42	42.26	39.76	0.94

	SVK_M	626	0.46	196.59	22.96	29.92	1.30
	SVK_L	176	2.25	104.01	31.30	26.03	0.83
	SDVK	561	1.97	338.13	50.17	30.99	0.62
	Total	3707					

The UCS for brecciated rocktypes such as DHB, NPK_GG MVK2_BBR and few layered units like SPK, SVK_U, SVK_M and SVK_L have relatively high CoV values indicative of widely dispersed values, which is to be expected from the breccias, because of their depositional nature. These units are mostly layered consisting of alternating country rock rich and poor zones. The massive rocktypes like NPK and MVK2 show low coefficient of variation which is consistent with the uniaxial strength characteristics of these rocktypes.

7.1.2 UCS (MPa) Graphical Summary – Box Plots

The UCS box plots, statistics and relative cumulative frequency plots are shown in Figures 8 to 14. The WRB and A3T box plot results (Figures 8 and 9) are not meaningful. There are very few samples obtained from both units (2 and 5 samples respectively), nonetheless a slightly positive skewness is observed in the A3T.

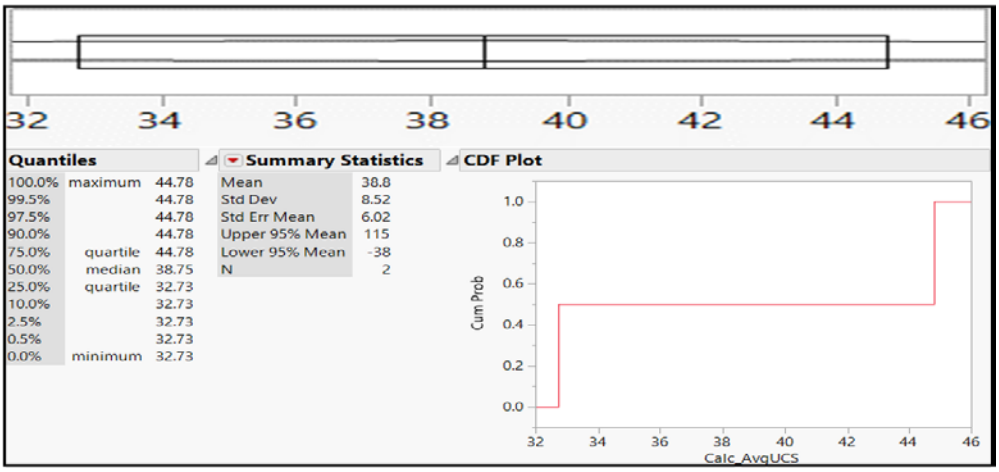
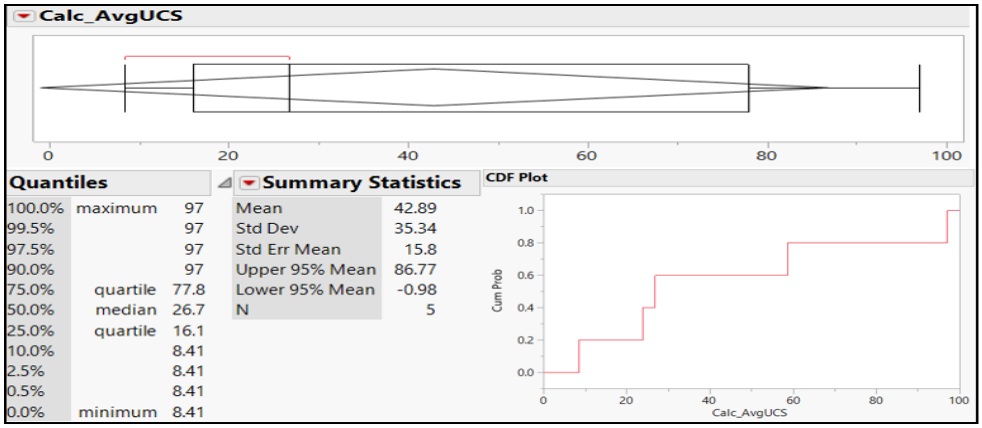


Figure 8 UCS Box plot, Summary Statistics & CDF – WRB

Figure 9 UCS Box plot, Summary Statistics & CDF – A3T



The UCS box plot interpretations can be summarised as follows:

The UCS parameter in the SPK, SVK_U, NPKD, MVK2_BBR and NPK_GG rocktypes are shown in Figures 10 to 14. All these rocktypes display positively skewed distributions, meaning there are many low values below the mean and a few high values above it.

The mean values are higher than the median values. The positive skewness is due to the variable nature of brecciated units. In all cases there is high probability (0.8) that a randomly chosen UCS sample from these rocktypes has a measurement of less than 50MPa. The box plot for the NPKD rocktype shown in Figure 12, however, reveals a more symmetrical distribution. The UCS box plot for the 33 observations for the MVK2_BBR rocktype shown in Figure 14, however, displays a highly positively skewed distribution.

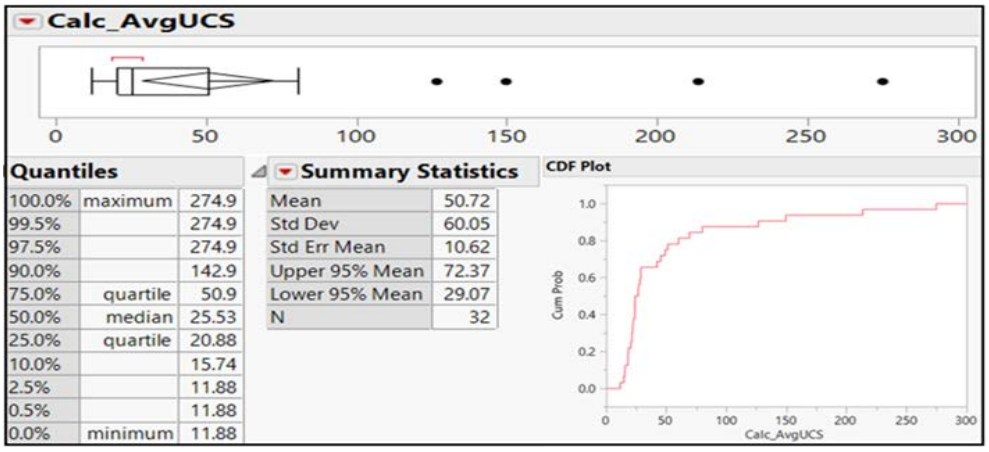


Figure 10 UCS Box plot, Summary Statistics & CDF – SPK

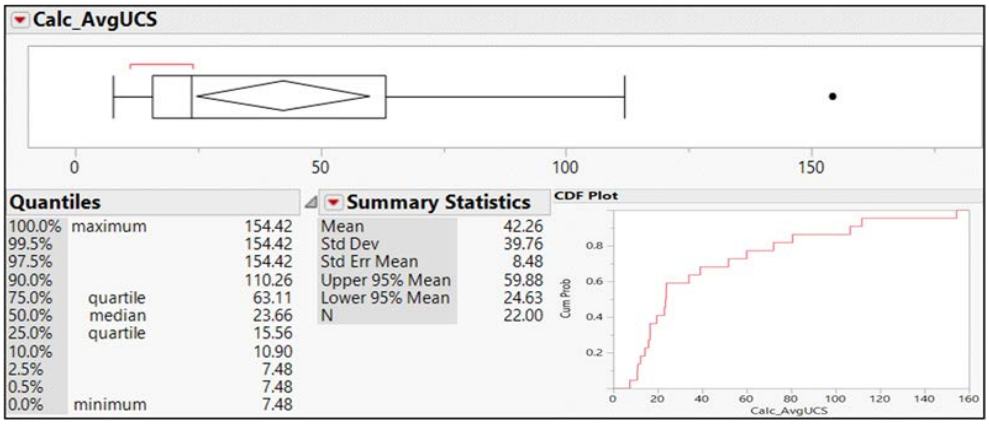


Figure 11 UCS Box plot, Summary Statistics & CDF – SVK_U

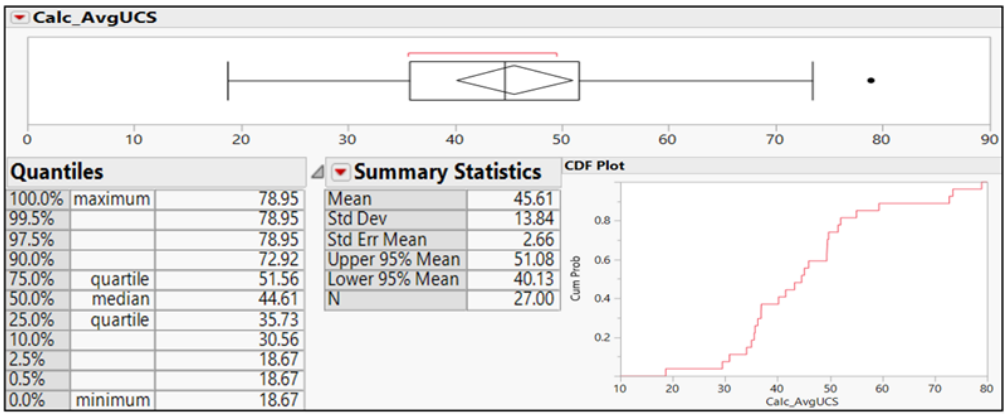


Figure 12 UCS Box plot, Summary Statistics & CDF – NPKD

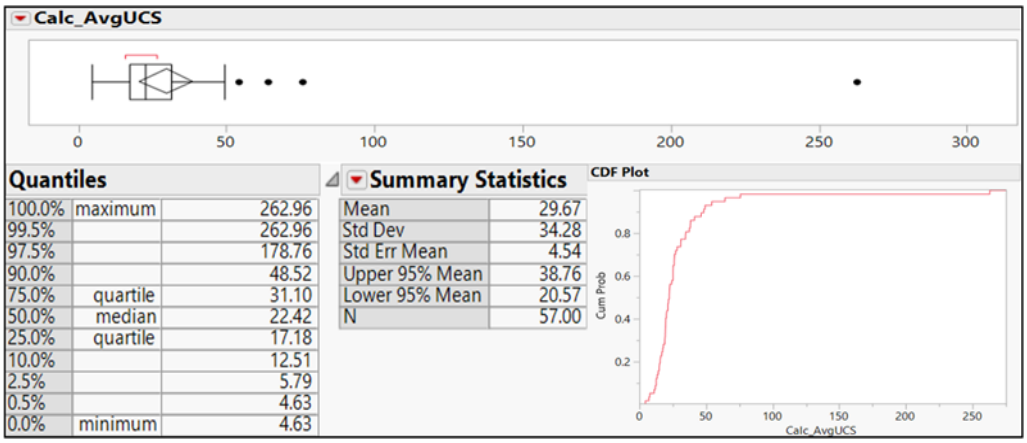


Figure 13 UCS Box plot, Summary Statistics & CDF – NPK_GG

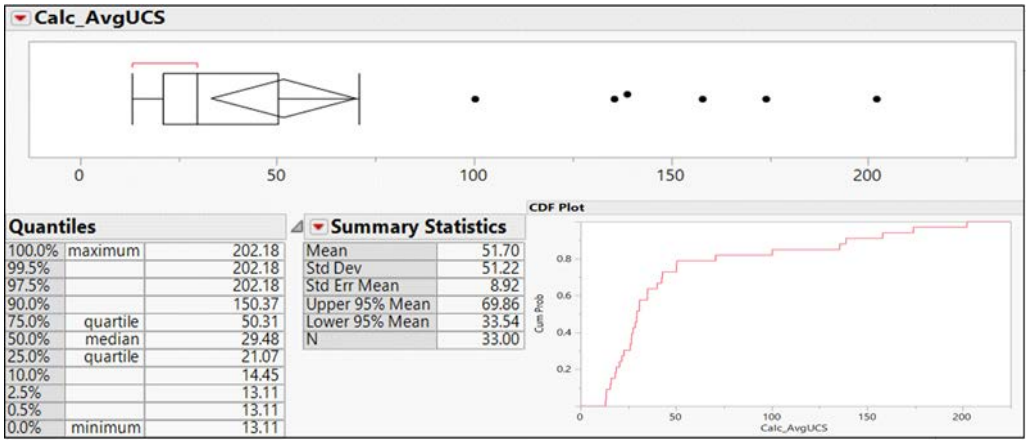
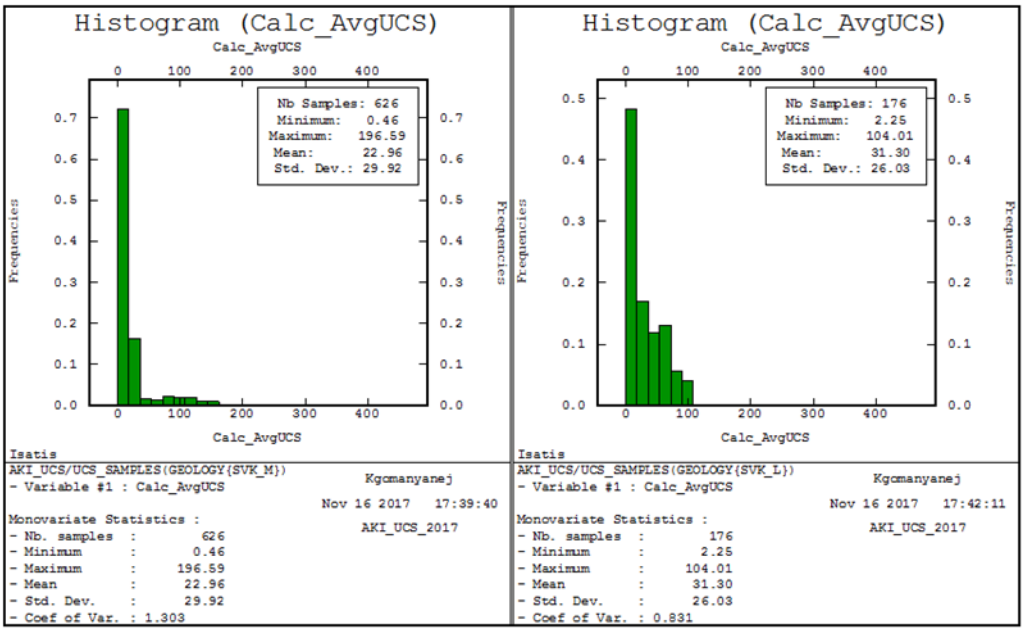


Figure 14 UCS Box plot, Summary Statistics & CDF – MVK2_BBR

7.1.3 UCS (MPa) Graphical Summary – Histogram Plots

The UCS classical statistics and histogram distributions for geological units with more than 60 observations appear in Figures 15 to 18. The histogram x-axis for all the units were set at a minimum of zero, maximum value of 450 MPa and 25 histogram classes to make the results comparable. The geological units represented here are SVK_M, SVK_L, BBR, DHB, NPK, MVK2 and SDVK. These are also the rocktypes which were subjected to variography analyses



and subsequent UCS local block estimation.

Figure 15 UCS histogram & statistics – SVK_M (left) and SVK_L (right)

The UCS histogram for the SVK_M rocktype shown in Figure 15 (left) is positively skewed and shows high variability in the data confirmed by the high coefficient of variation (COV).

This is expected from the SVK_M rocktype. This rocktype is layered and comprises of kimberlite rich and country rock rich portions; a mixture of soft and hard areas.

The UCS histogram for rocktype SVK_L shown in Figure 15 (right) is also asymmetric. The moderate to high coefficient of variation of 0.8 confirms the positive skewness and high UCS variability observed for this unit.

The SVK_L forms the base of the AK1 crater deposits. The geological makeup of the SVK_L rocktype is transitional between kimberlite rich portions (approximately 30%) and country rock dilution content.

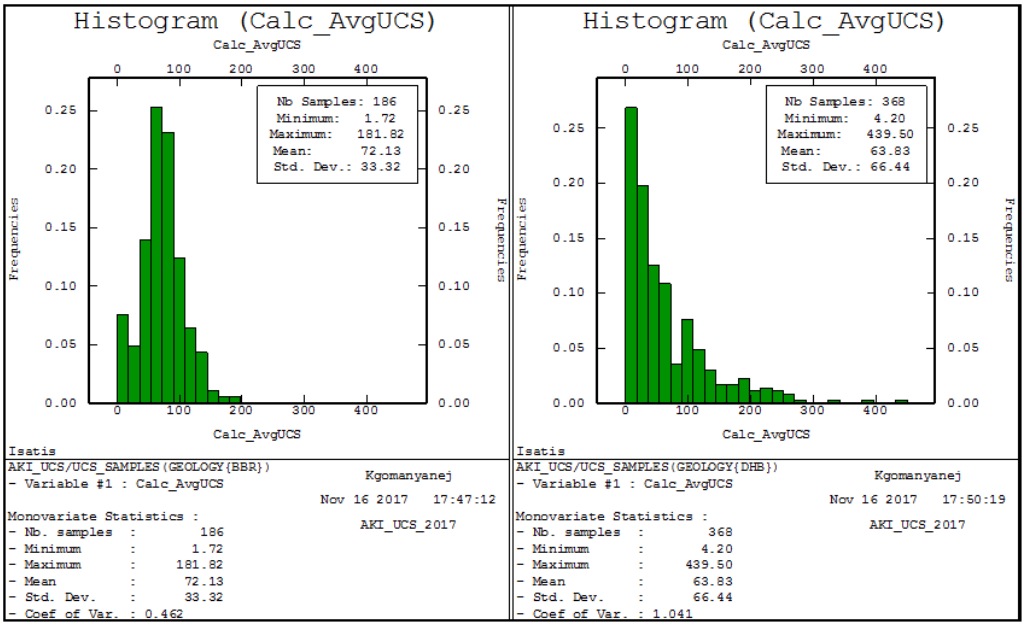


Figure 16 UCS histogram & statistics – BBR (left) and DHB (right)

The UCS histogram for rocktype BBR shown in Figure 16 (left) is near symmetrical. Most sample values are concentrated around the mean value. The mean and the median are expected to be similar. The low coefficient of variation of 0.46 confirms the relatively low UCS sample variability in the BBR rocktype. This is expected from the BBR; this rocktype is mostly basalt (90 - 100%) with very little kimberlite pockets. It is mainly clast supported.

The UCS histogram distribution for the DHB rocktype shown in Figure 16 (right), on the other hand, is an asymmetrical positively skewed distribution. The coefficient of variation on the UCS parameter is above 1. There is a large spread in the sample values and the mean value would be greater than the median value. This is expected for the DHB rocktype due to its morphological make up. The DHB rocktype comprises of various country rock xenoliths and soft kimberlite matrix between clasts.

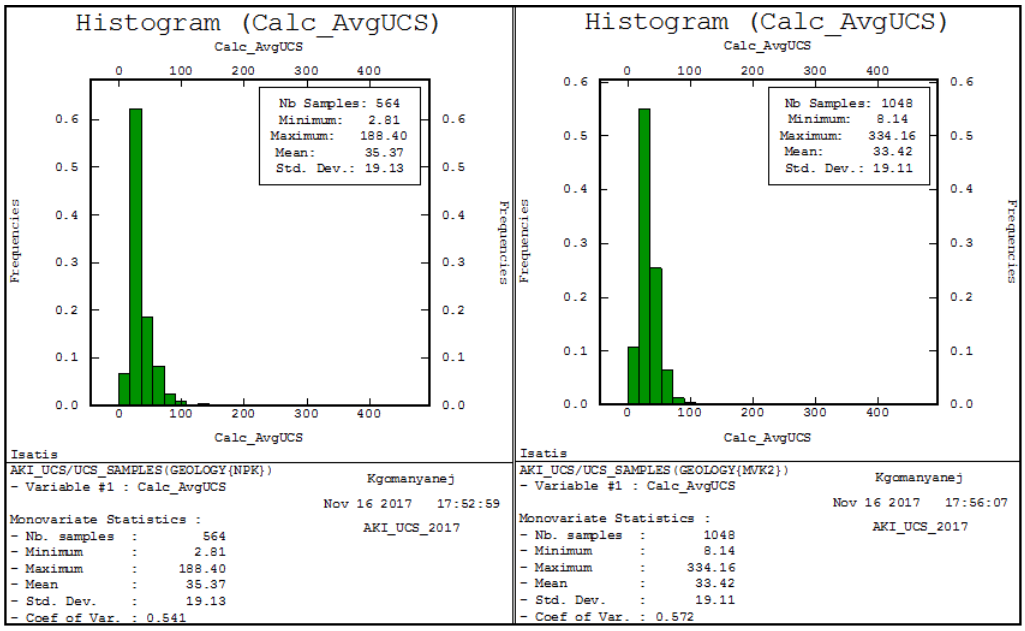


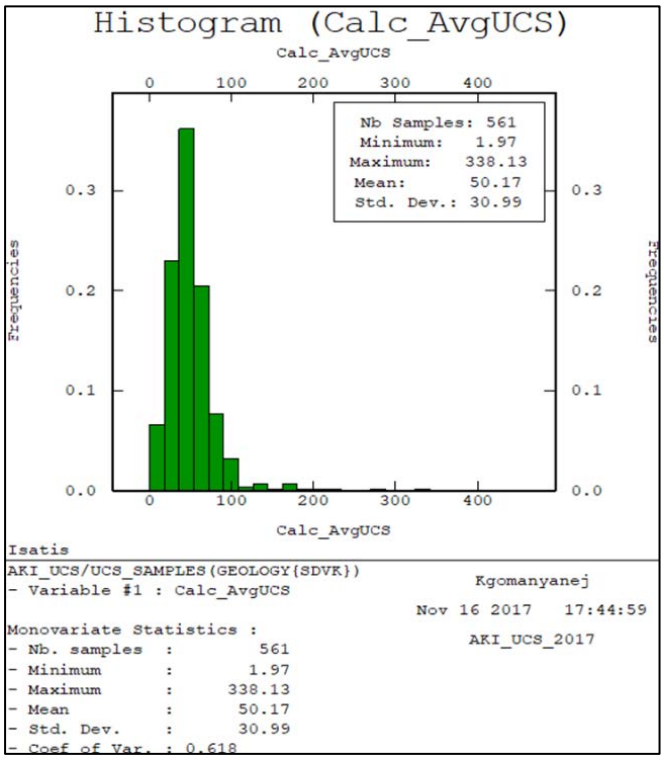
Figure 17 UCS histogram & statistics – NPK (left) and MVK2 (right)

The UCS histogram for the NPK rocktype shown in Figure 17 (left) shows a more bell-shaped, but non-symmetrical distribution. The coefficient of variation on the UCS parameter for the NPK rocktype is increasing compared to the other units. Most UCS values for the NPK rocktype are below 100MPa, with a few high values influencing the value of the variance and consequently the standard deviation and the CoV. However, the bulk of the distribution is clustered around the mean UCS value. This is expected of the NPK rocktype, it is massive, thickly bedded and consistent in composition and country rock xenolith size.

In the MVK2 rocktype shown in Figure 17 (right), a similar UCS distribution is observed. Whilst the UCS means and standard deviations for the two rocktypes are similar, the UCS CoV is slightly higher than that for the NPK rocktype and this is due to the very higher maximum value in the MVK2 rocktype.

The similarity in these distributions and statistics are expected as this unit is also a massive, thickly bedded and consistent in compositional make up and low in country rock dilution.

The UCS histogram for the SDVK rocktype shown in Figure 18 below reveals a similar shape clustered towards the left with a few high values to the right which were identified as possible outliers. The UCS coefficient of variation for the SDVK rocktype is slightly higher than for the NPK and MVK2 rocktypes. During variogram modelling, the outliers were masked out in order to produce a robust variogram for this rocktype. This is expected of this rocktype as it is massive, extremely thickly bedded, low in dilution content and



consistent in country rock clast size.

Figure 18 UCS histogram & statistics – SDVK

In summary, the UCS histograms for the layered crater deposits (SVK_M, SVK_L) and the brecciated DHB unit are asymmetrical with a tail to the right. The UCS values for these rocktypes show high sample variability supported by the high coefficient of variations observed. This is in line with the geological morphology of these rocktypes.

The massive rocktypes (SDVK, NPK, and MVK2) and the brecciated BBR unit show symmetrical distributions clustered on the left with a few high values in the right hand tail of the distributions.

The UCS histogram distributions for SDVK, NPK and MVK2 are in line with what is expected from massive rocktypes.

7.2 FFPM EDA for Orapa AK1 pipe rocktypes

7.2.1 FFPM Classical Statistics

The second RMR input parameter analysed is the fracture frequency per metre (FFPM). Similar to the UCS variable, EDA was also conducted on FFPM. The FFPM statistics for all the Orapa AK1 rocktypes are summarised in Table 5 below. It can be seen that overall there are significantly more observations for the FFPM parameter and with sufficient observations per rocktype, reliable interpretations are enabled. The WRB rocktype has 50 FFPM observations and therefore a box plot will be used in the distribution shape analysis to follow.

The CoV values are very high indicating that the FFPM parameter is quite variable for all the rocktypes.

Table 5 FFPM - Classical Statistics for Orapa AK1 pipe rocktypes

Fracture Frequency per metre FFPM	Rocktype	Number of observations	Min	Max	Mean	Std Dev	CoV
	A3T	109	0.00	6.32	0.74	1.02	1.38
	WRB	50	0.00	6.00	1.39	1.35	0.97
	BBR	2131	0.00	44.73	1.55	2.46	1.60
	DHB	4090	0.00	38.57	1.79	2.44	1.36
	MVK2	6975	0.00	10.00	0.34	0.64	1.89
	MVK2_BBR	641	0.00	6.00	0.92	0.99	1.08
	NPK	3314	0.00	7.33	0.26	0.49	1.93
	NPKD	227	0.00	10.00	0.32	0.85	2.68
	NPK_GG	664	0.00	5.00	0.47	0.67	1.42
	SPK	618	0.00	21.13	1.18	1.66	1.41
	SVK_U	212	0.00	13.33	1.33	1.68	1.27
	SVK_M	5438	0.00	40.00	1.03	1.46	1.42
	SVK_L	1547	0.00	18.18	1.25	1.65	1.32
	SDVK	3427	0.00	12.67	0.53	0.86	1.63
	Total	**29443**					

Most massive rocktypes such as NPKD, MVK2, NPK, SDVK and BBR show extremely high COVs for the FFPM parameter, which is opposite of the UCS parameter, where the CoV values were more moderate.

This phenomenon is directly related to the strength of these rocktypes, the higher the number of fractures the lower the strength. The FFPM for layered rocktypes i.e. A3T, SVK_U, SVK_L, SPK and the breccias such as DHB, NPK_GG and MVK2_BBR are more variable, as to be expected for these rock types.

7.2.2 FFPM Graphical Summary – Box Plot

The only rocktype with less than 60 FFPM observations is WRB. This rocktype has not been subjected to histogram analysis. Instead, a box plot and a CDF graph were generated, and the results are illustrated in Figure 19. The FFPM has a positive skew distribution.

The WRB rocktype is a brecciated type of deposit hence the variability in the FFPM measurements. The unit is mainly wall rock breccia of varying clast size with notable kimberlite matrix between country rock xenoliths.

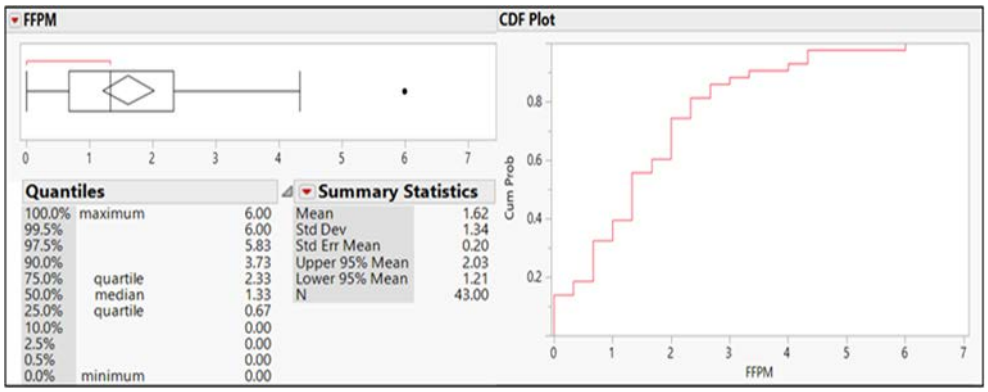


Figure 19 FFPM Box plot, Summary Statistics & CDF – WRB

7.2.3 FFPM Graphical Summary – Histogram Plots

FFPM histograms for all AK1 rocktypes with more than 60 observations were generated for the relevant kimberlite facies. These are illustrated in Figures 20 to 26 and the statistical interpretations follow thereafter. For comparability, the criteria used to generate these histograms was to set the x-axis to a minimum of zero, maximum value was set at 45 and number of histogram classes at 25.

Figure 20 represents the FFPM histogram for the A3T rocktype. The histogram distribution for this parameter is positively skewed but with a short tail. Most FFPM values are clustered around the minimum value. The A3T rocktype is a thinly layered crater deposit with minimal clast size variability, mainly fine grained.

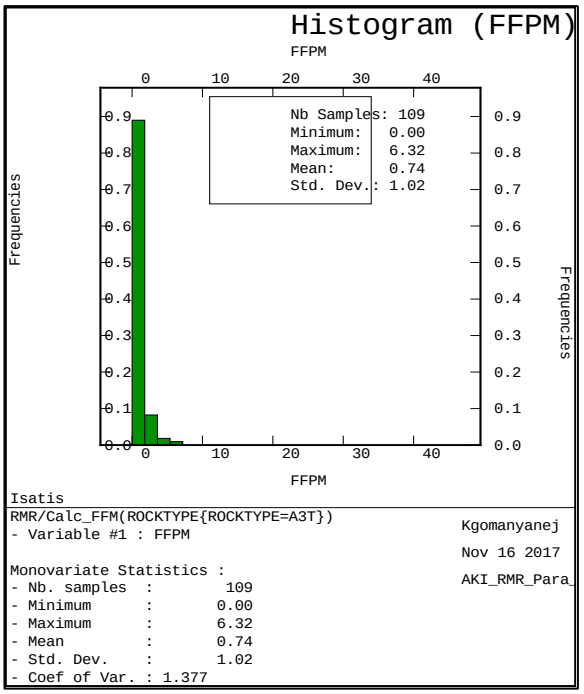
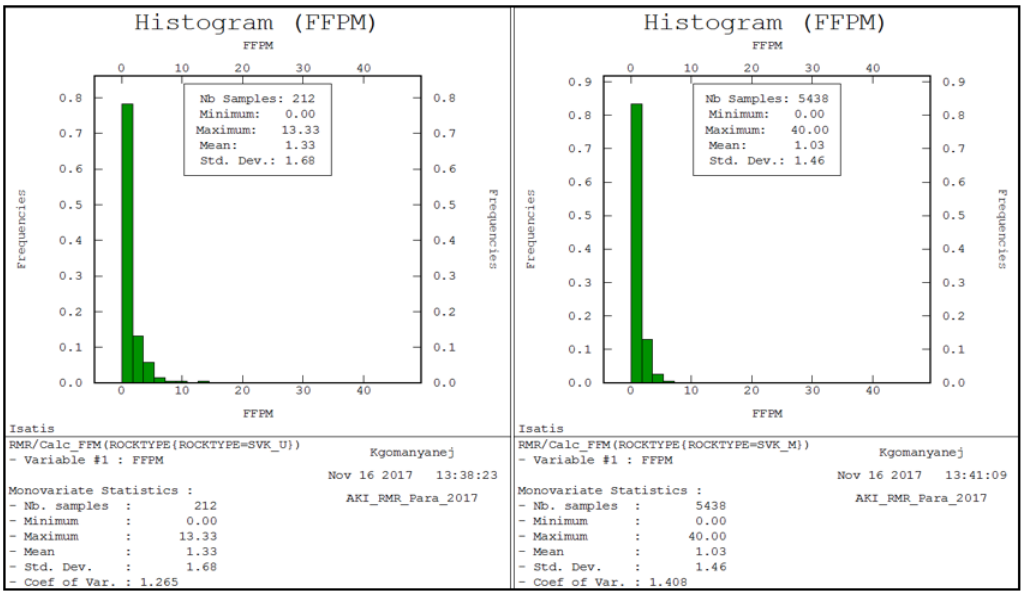


Figure 20 FFPM histogram – A3T

The histograms displayed in Figure 21 represent FFPM distributions for the SVK_U and SVK_M rocktypes. The SVK_U histogram has most FFPM values clustered towards the minimum but with positive skewness. The histogram for this rocktype has few outliers with a lower maximum.

The FFPM histogram for the SVK_M is also positively skewed but with a larger maximum compared to the SVK_U histogram. Most FFPM values on the



histogram for this rocktype are also clustered towards the minimum.

Figure 21 FFPM histograms – SVK_U (left) and SVK_M (right)

Figure 22 illustrates FFPM histogram distributions for the SVK_L and SPK rocktypes. The FFPM histogram for the SVK_L is positively skewed with notable outliers. Most FFPM values are clustered towards the low end but with moderate FFPM maximum value. The FFPM histogram for the SPK rocktype is similar to that of SVK_L. These rocktypes extend laterally and are highly variable in the vertical extent.

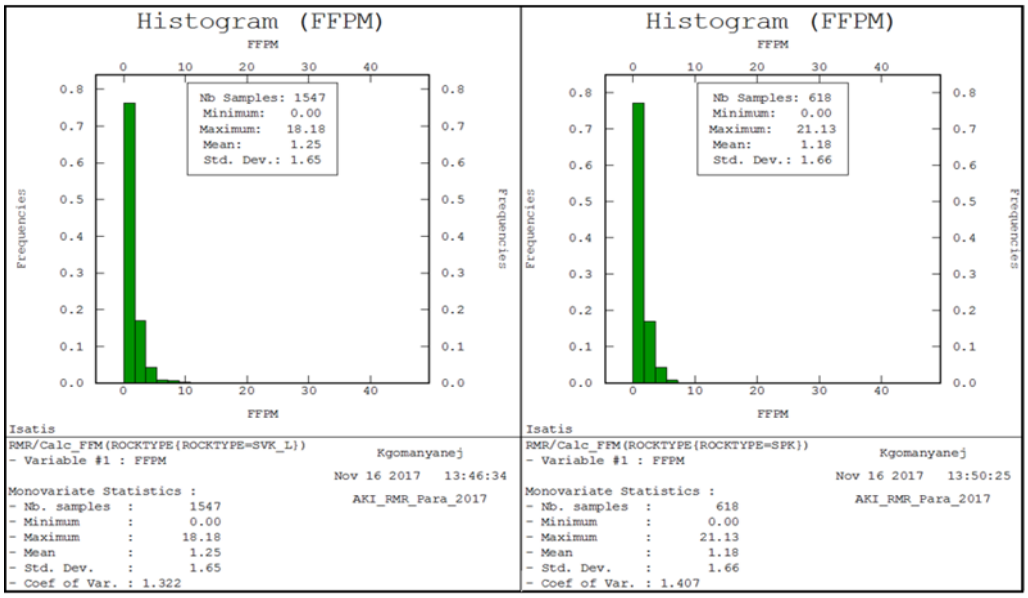


Figure 22 FFPM histograms – SVK_L (left) and SPK (right)

Figure 23 represents FFPM histogram distributions for the BBR and DHB rocktypes. The FFPM histogram is positively skewed with the highest maximum. Most FFPM values are also clustered around the minimum value. The FFPM histogram for the DHB rocktype has similar characteristics as the FFPM histogram for the BBR. However, the latter has a slightly lower maximum as compared to the former. The two rocktypes occur at the upper elevations of the AK1 kimberlite where the units are exposed to weathering and continuous fracturing due to mining activities.

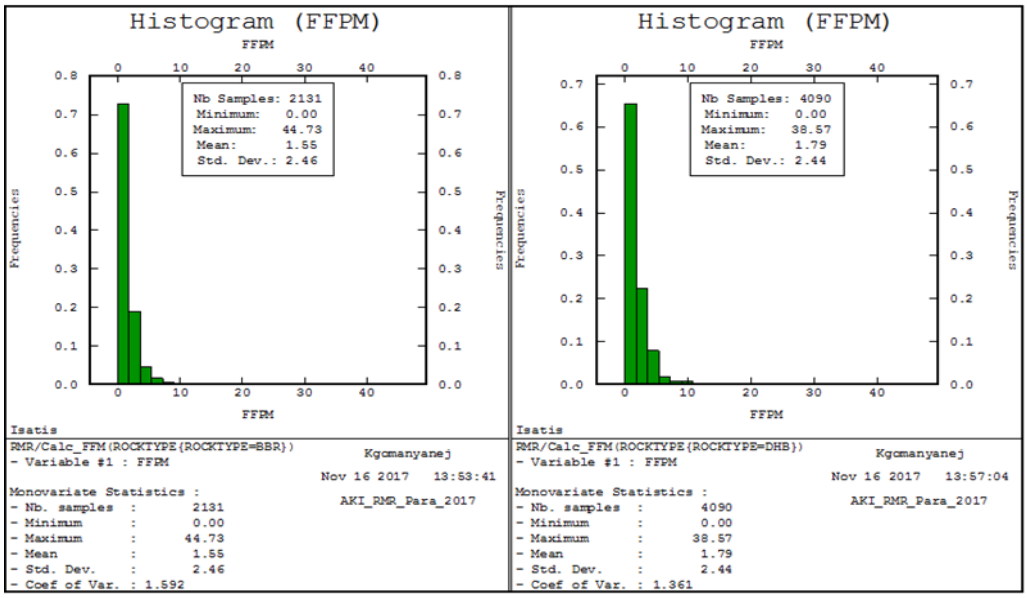


Figure 23 FFPM histograms – BBR (left) and DHB (right)

The FFPM histograms for SDVK and NPKD rocktypes are represented by Figure 24. The histogram for rocktype SDVK is positively skewed with a shorter tail. Most FFPM values are clustered around the minimum value and the maximum is lower compared to other rocktypes. The histogram for the NPKD rocktype is similar to that of SDVK, however, the FFPM maximum is the third lowest. This is expected of the two rocktypes due to their geological morphology (massive and coherent in nature).

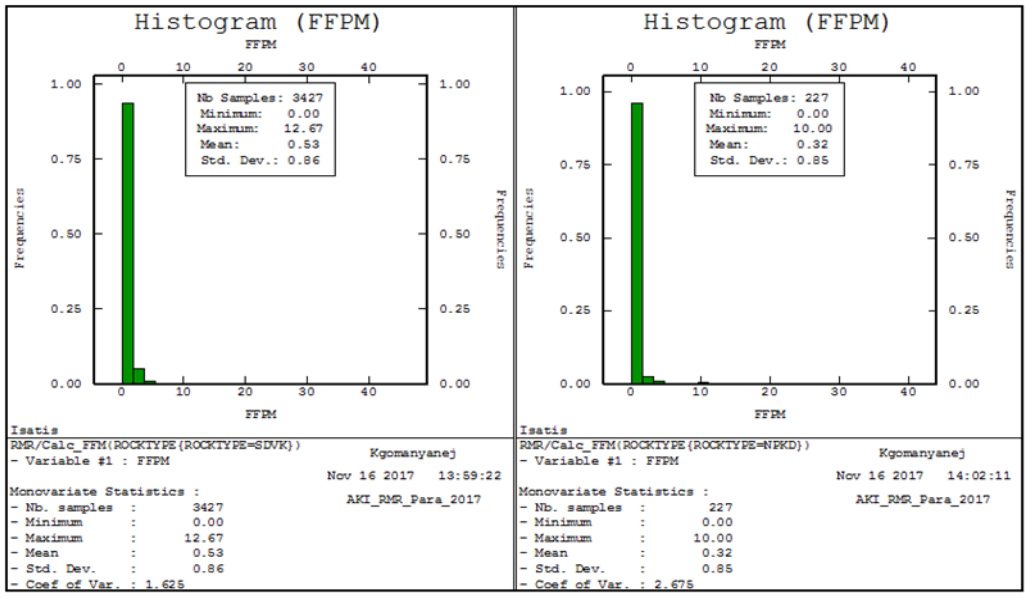


Figure 24 FFPM histograms – SDVK (left) and NPKD (right)

The FFPM histograms for MVK2 and NPK are represented in Figure 25. For these two histograms, the FFPM values are clustered around the minimum

value (>95%) and the maximums are second lowest for the FFPM. The two histograms are positively skew but with shorter tails than the previous rocktypes. This is expected of these two rocktypes; they are massive and extensively consistent.

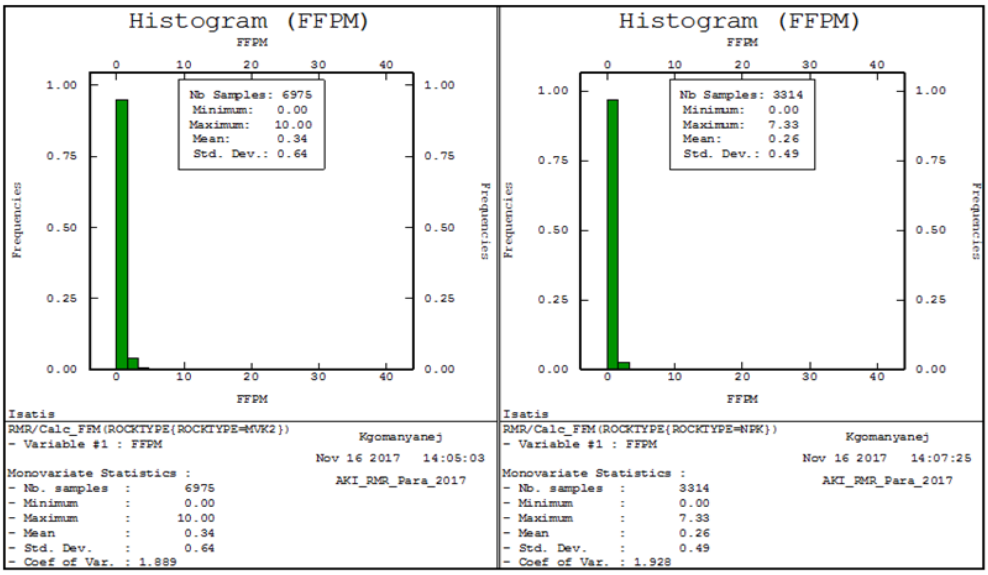


Figure 25 FFPM histograms – MVK2 (left) and NPK (right)

The FFPM histograms for MVK2 and NPK_GG are presented in Figure 26. The FFPM histograms are both positively skewed with values clustered around the minimum. The histograms for these two rocktypes have the lowest maximums with much shorter tails.

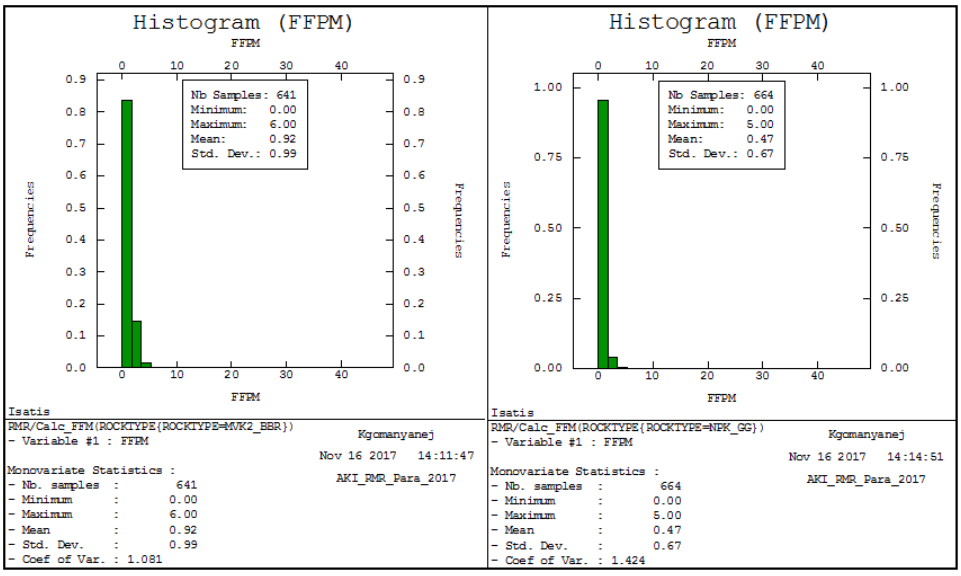


Figure 26 FFPM histograms – MVK2_BBR (left) and NPK_GG (right)

The common distributional characteristics of the FFPM parameter is the positive skewness, seen in all rocktypes. The FFPM values in the majority of

the cases cluster in the range 10 to 15 FFPM. In these cases the tails of the distributions are relatively short. For the distributions where the maximum FFPM values are above 15 FFPM, the tails of the distributions are much longer. The high fracture frequency per metre observed on the BBR, DHB, SPK, SVK_M and SVK_L is brought about by the fact that these rocktypes are brecciated and exposed at the mining surface. These rocktypes are exposed to heavy fracturing due to mining activities as well as weathering.

7.3 RQD (%) EDA for Orapa AK1 pipe rocktypes

7.3.1 RQD (%) Classical Statistics

Summary statistics for RQD appear in Table 6. It is again clear that the smaller (by volume) rocktypes like SVK_U, WRB and SPK, have fewer RQD% samples.

Table 6 RQD (%) - Classical Statistics for Orapa AK1 pipe rocktypes

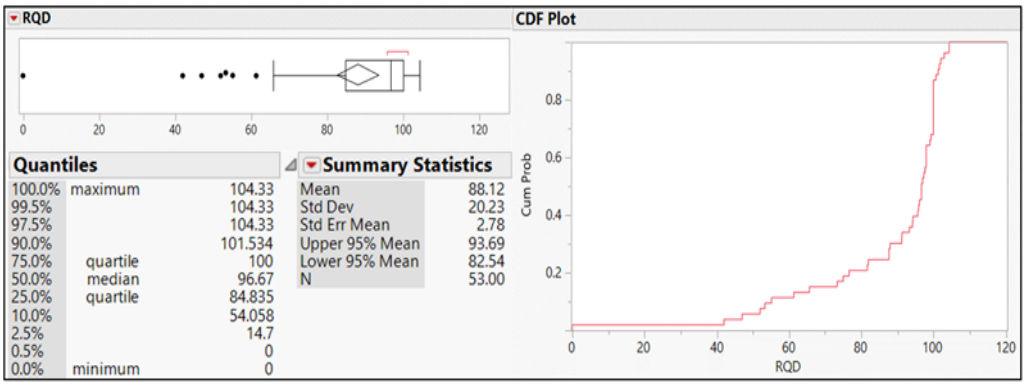
RMR Parameter RQD (%)	Rocktype	Number of observations	Min	Max	Mean	Std Dev	CoV
	A3T	108	0.00	104.67	80.07	26.36	0.33
	WRB	53	0.00	104.33	88.12	20.04	0.23
	BBR	2227	0.00	120.00	86.37	22.39	0.26
	DHB	4533	0.00	119.00	88.26	18.72	0.21
	MVK2	8387	0.00	120.49	96.96	8.66	0.09
	MVK2_BBR	607	0.00	115.56	93.51	14.39	0.15
	NPK	4576	0.00	120.00	96.10	12.12	0.12
	NPKD	220	0.00	110.00	97.71	8.42	0.09
	NPK_GG	857	0.00	110.67	90.51	16.89	0.19
	SPK	616	0.00	112.67	92.09	14.92	0.16
	SVK_U	275	0.00	102.67	82.65	24.82	0.30
	SVK_M	6472	0.00	119.17	93.28	13.15	0.14
	SVK_L	1618	0.00	120.00	92.85	13.46	0.15
	SDVK	4273	0.00	114.67	96.16	10.52	0.11
	Total	34822					

The RQD CoV results show an almost similar trend as for the UCS. Whilst the breccia RQD CoV values are higher and indicative of greater dispersion, these values are relatively low and indicate little variability. The A3T rocktype has the highest RQD CoV, however a CoV of 0.33 is indicative of a normal distribution. Massive rocktypes like SDVK, NPK, MVK2 and NPKD show low CoV values which suggested that the RQD values are less dispersed and cluster around the means.

The coefficient of variation on the RQD parameter for the brecciated units is relatively high compared to other rocktypes. The massive units (SDVK, NPKD, MVK2 and NPK) show normal histogram distributions and again the RQD coefficient of variation for these rocktypes is lower suggesting lower sample variability within these rocktypes.

7.3.2 RQD (%) Graphical Summary - Box Plot

The third rock mass rating input parameter analysed is the RQD %. Only the WRB rocktype had less than 60 RQD observations; the boxplot and related information for this unit appear in Figure 27. The RQD boxplot for the WRB rocktype shows a negatively skewed distribution, as expected and also highlighted by several low values outside the box which could be possible outliers. There is a large spread in the RQD measurements, and most values



are concentrated towards the upper end, above 95%.

Figure 27 FFPM Box plot, Summary Statistics & CDF – WRB

7.3.3 RQD (%) Graphical Summary - Histogram Plots

The RQD histograms for all other rocktypes in the AK1 kimberlite pipe were generated. The distributions were standardised and constructed such that the x-axis minimum was set to zero, maximum at 125% and the number of classes were set at 25 for consistency and realistic comparison. The resulting frequency distributions are illustrated in Figures 28 to 34.

Scrutinising these Figures the unique characteristic of the RQD (%) distributions for all the AK1 rocktypes is that they are asymmetrical and negatively skewed in shape. RQD values vary between 0% and 100% and the averages values are in a narrow band between about 80% and 95 %

The RQD histogram distributions for the layered crater deposits and brecciated units show an opposite behaviour compared to the FFPM parameter. The distributions are negatively skewed with longer tails as opposed to positively skewed distributions and none of the distributions are normal. The FFPM is the inverse of the RQD hence the opposite behaviour on the histogram distributions for the two parameters.

There is a close similarity between the RQD histograms for SVK_M and SVK_L as well as between the BBR and DHB rocktypes. In terms of RQD, the two pairs should be treated as similar geotechnical domains.

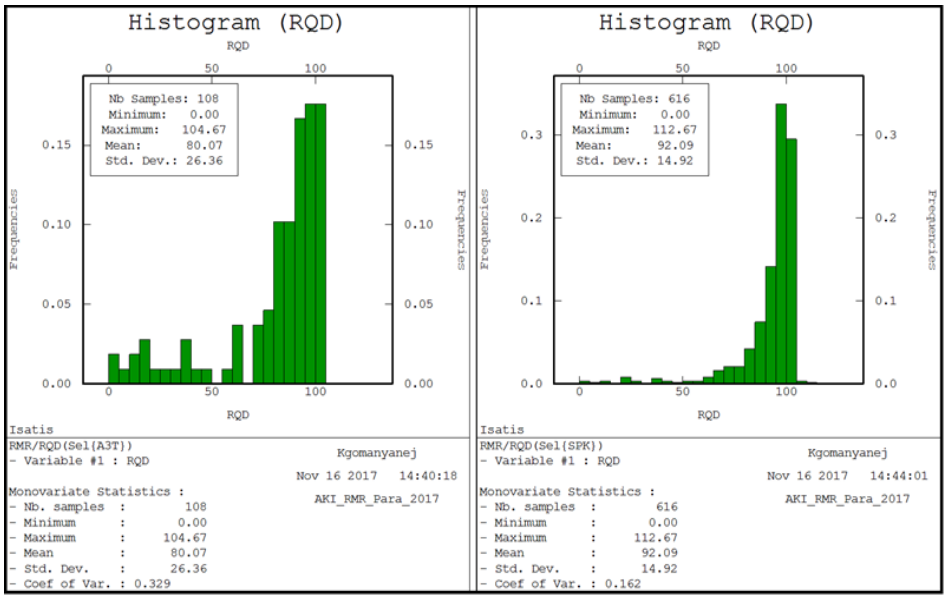


Figure 28 RQD (%) histograms – A3T (left) and SPK (right)

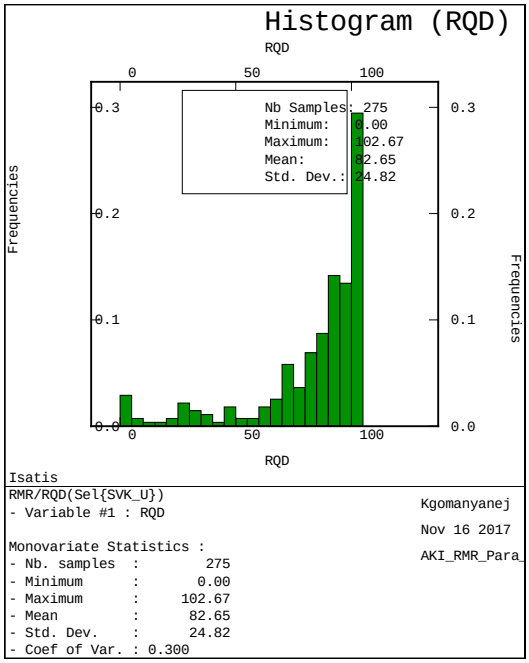


Figure 29 RQD (%) histogram – SVK_U

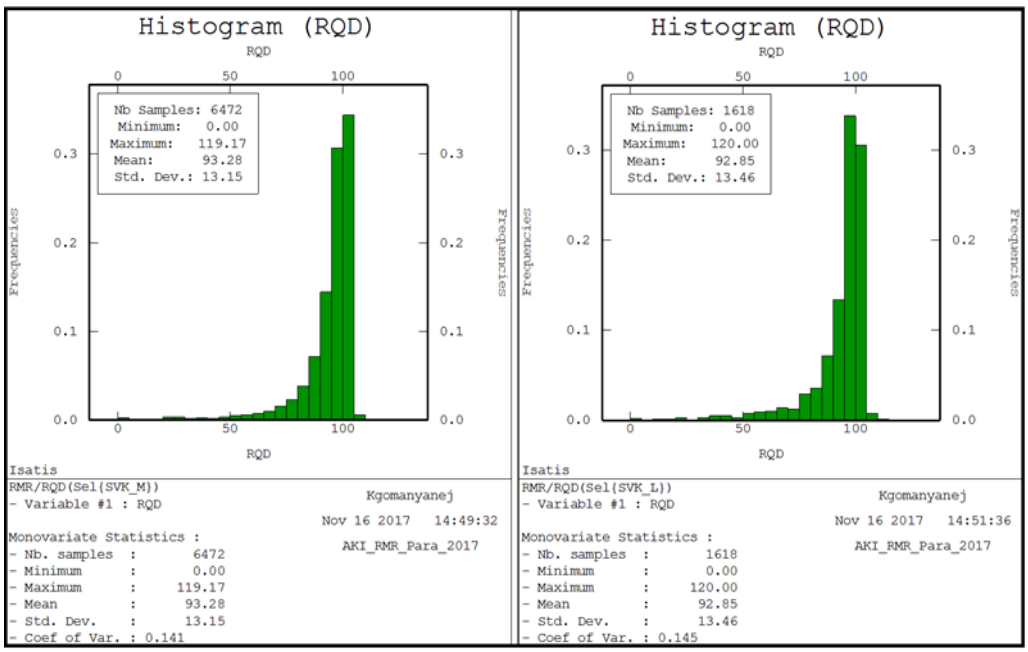


Figure 30 RQD (%) histograms – SVK_M (left) and SVK_L (right)

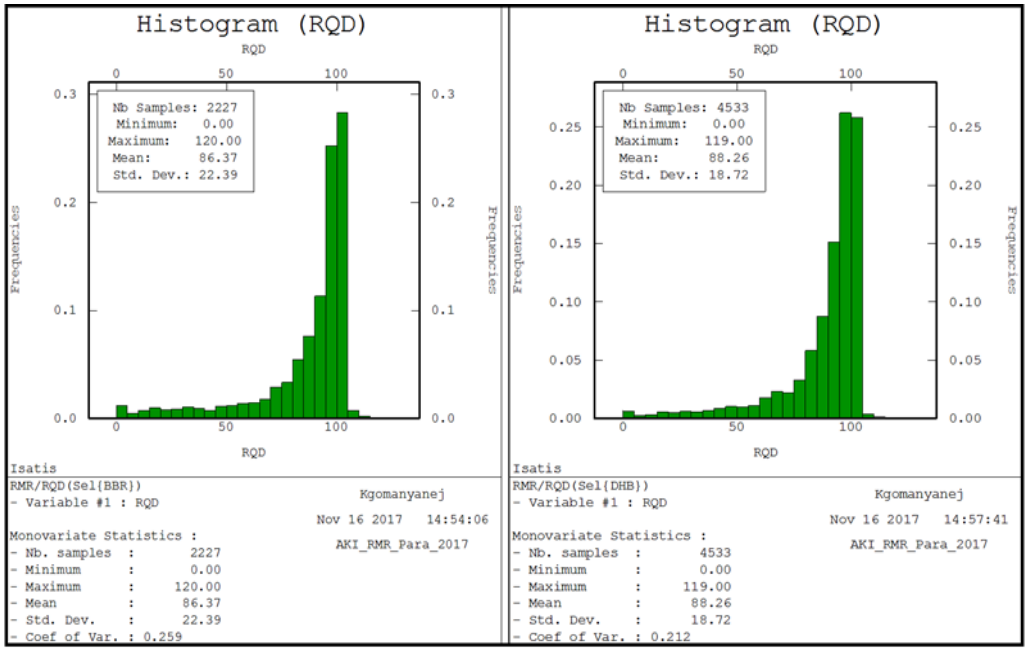


Figure 31 RQD (%) histograms – BBR (left) and DHB (right)

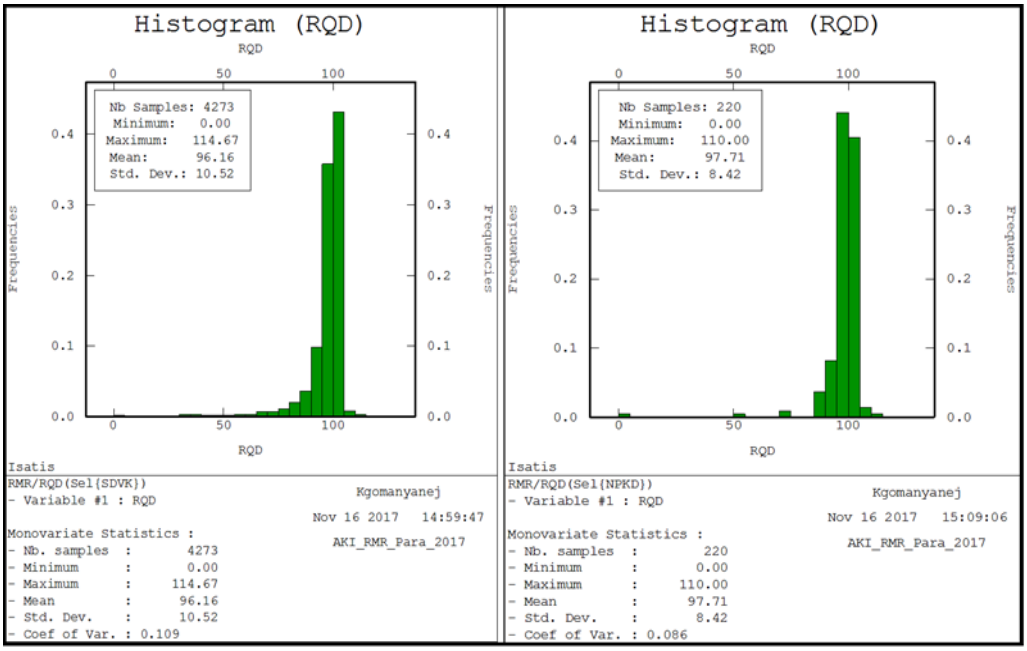


Figure 32 RQD (%) histograms – SDVK (left) and NPKD (right)

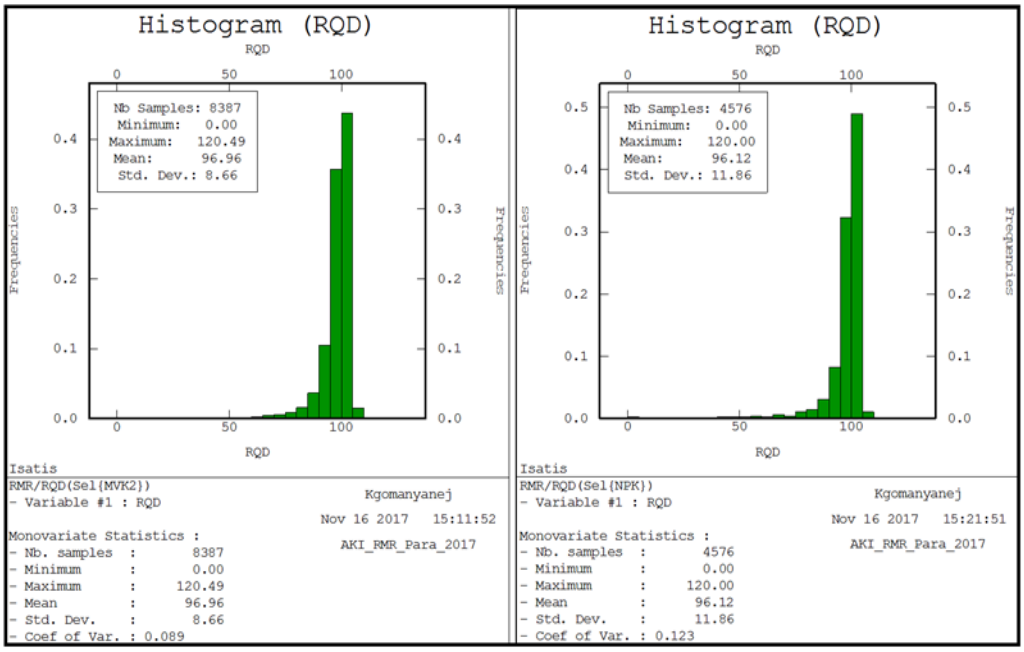


Figure 33 RQD (%) histograms – MVK2 (left) and NPK (right)

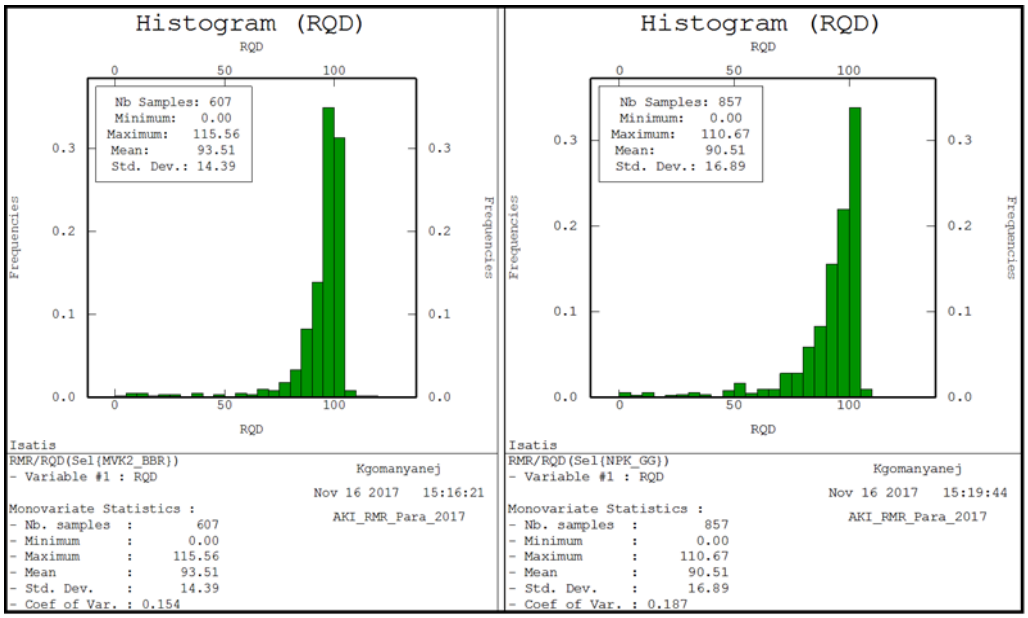


Figure 34 RQD (%) histograms – MVK2_BBR (left) and NPK_GG (right)

7.4 Dry Density (g/cm^3) EDA for all Orapa AK1 rocktypes

7.4.1 Dry Density (g/cm^3) Classical Statistics

Dry Density (DD) measurements were obtained following an in-house MRM procedure. This variable was analysed to supplement the RMR parameters. The DD statistics are summarised in Table 7 followed by an interpretation thereof.

Table 7 DD (g/cm^3) Classical Statistics for Orapa AK1 pipe rocktypes

	Rocktype	Number of observations	Min	Max	Mean	Std Dev	CoV
Dry Density (g/m^3)	A3T	18	2.09	2.67	2.35	0.16	0.07
	WRB	13	2.23	2.39	2.30	0.06	0.02
	BBR	657	1.92	2.88	2.56	0.15	0.06
	DHB	1270	1.56	2.88	2.31	0.18	0.08
	MVK2	3864	2.1	2.91	2.45	0.08	0.03
	MVK2_BBR	217	2.18	2.89	2.50	0.16	0.06
	NPK	1777	2.07	2.83	2.28	0.08	0.04
	NPKD	95	2.3	2.64	2.46	0.06	0.02
	NPK_GG	213	2.01	2.89	2.21	0.14	0.06
	SPK	166	1.98	2.83	2.37	0.17	0.07
	SVK_U	28	1.92	2.86	2.47	0.23	0.09
	SVK_M	1888	1.99	2.91	2.31	0.17	0.07
	SVK_L	579	1.98	2.87	2.40	0.19	0.08
	SDVK	1656	1.98	3.00	2.43	0.12	0.05
	Total	12441					

In general the CoV values for all the rocktypes are very low COV, which means that the dry density within the individual rocktypes do not vary much, which is true for kimberlite density. This behaviour is brought about by the sensitivity of dry density which requires high accuracy. It also indicates that within any specific rocktype the dry density values are fairly similar.

7.4.2 Dry Density (g/cm^3) Box Plots

Dry density (DD) boxplots were generated for three of the rocktypes in the AK1 kimberlite pipe with less than 60 Dry Density data entries. These comprise of the A3T, WRB and SVK_U rocktypes, with their boxplots, summary statistics and CDF graphs being illustrated in Figures 35 to 37.

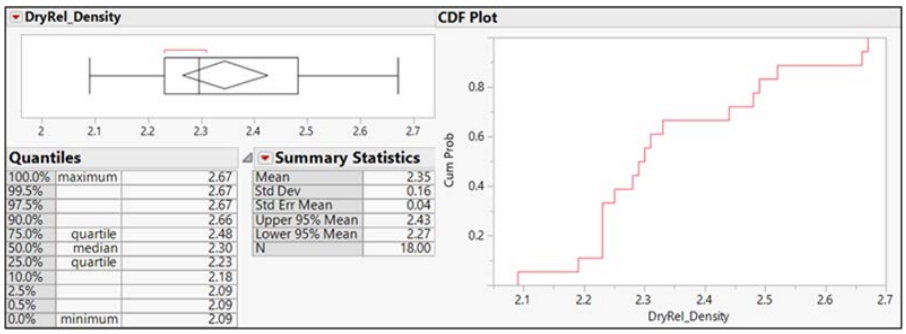


Figure 35 DD Box plot, Summary Statistics & CDF – A3T

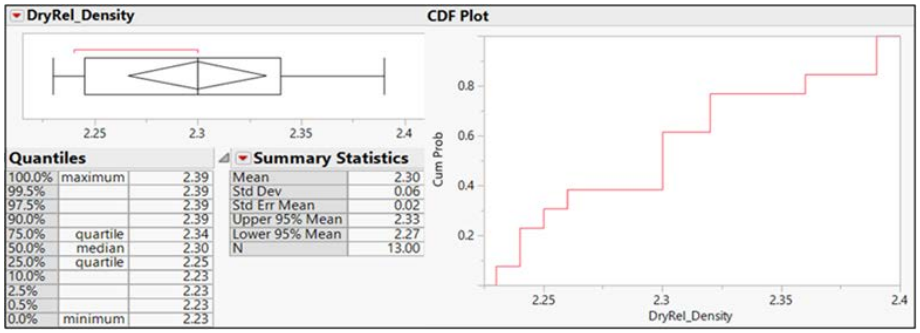


Figure 36 DD Box plot, Summary Statistics & CDF – WRB

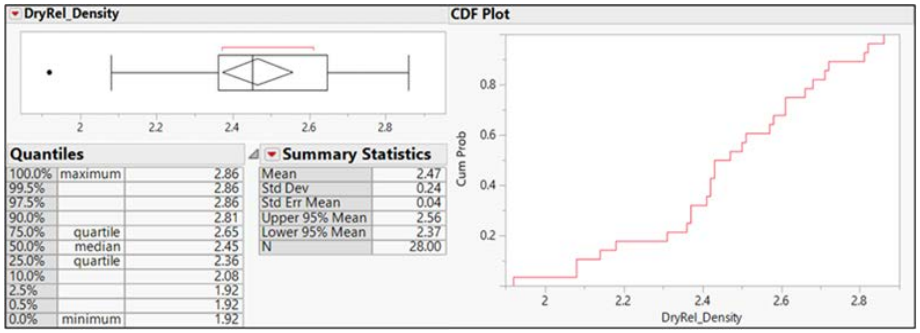


Figure 37 DD Box plot, Summary Statistics & CDF – SVK_U

In summary, the dry density input parameter, for rocktype A3T shows a positively skewed distribution with the mean value slightly bigger than the median value. The dry density distributions for the SVK_U and the WRB rocktypes display a more symmetrical nature.

The average of the Dry Density measurements for these rocktypes are very close to their median values. The DD for rocktype WRB has the lowest standard deviation i.e. the lowest sample variability. Due to the low number of observations these three rocktypes (A3T, WRB and SVK_U) were not subjected to any variography analysis and average values for the Dry Density are more appropriate estimates at unsampled areas of these rocktypes.

7.4.3 Dry Density (g/cm^3) Histogram Plots

As for the other RMR parameters the histograms were generated in such a way as to ensure comparability between the results of the different rocktypes. As such the x-axis minimum was set at 1.5 and the maximum at 3.5.

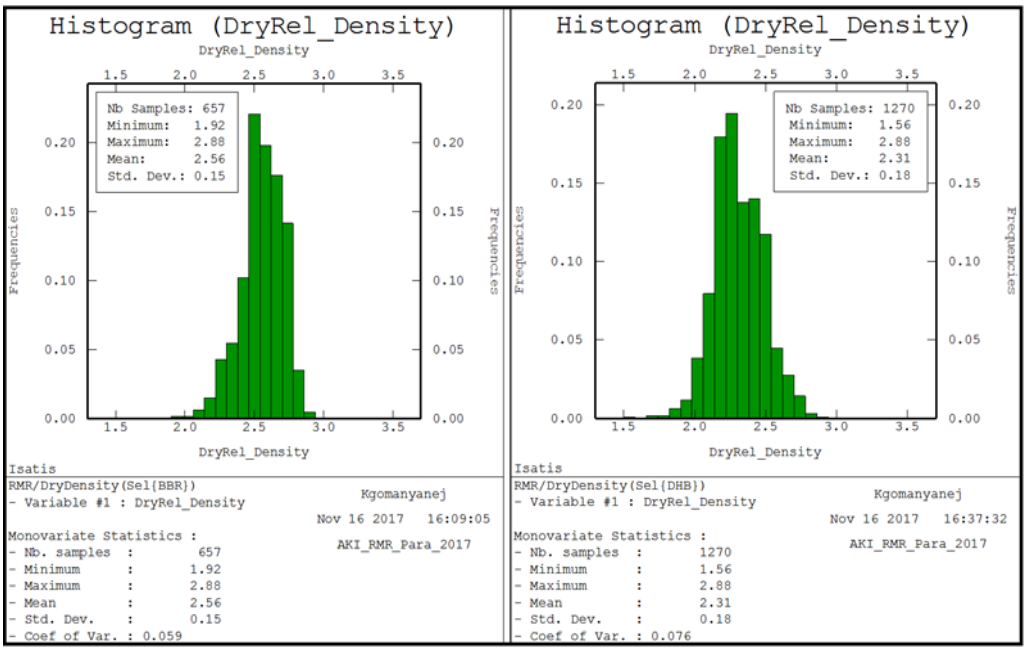
The dry density histograms were created for all rocktypes for which n > 60 observations was met as before. The distributions for the rocktypes that met the n > 60 observations criteria are represented in Figures 38 to 43.

In summary, the dry density (DD) histograms for the majority of the brecciated rocktypes and massive rocktypes show normal (symmetrical) distributions. This behaviour is noticeable on the BBR, DHB and MVK2_BBR representing the AK1 breccias. The dry density histogram distributions show high coefficient of variation suggesting high sample variability within these rocktypes.

In the massive rocktypes such as the SDVK, NPKD, NPK and MVK2, the DD (g/cm^3) has the lowest coefficient of variation. DD variability within these rocktypes is low. The dry density in the layered crater deposits (SPK, SVK_M, SVK_L and NPK_GG) show positively skewed histogram distributions. The slightly higher DD coefficient of variation implies that variability amongst their sample values are higher.

A point to note is the bimodality displayed by dry density histograms for SVK_M, NPK_GG and MVK2_BBR rocktypes. This behaviour is peculiar with these rocktypes and is due to the presence of kimberlite rich and country rock xenolith poor zones or vice versa. This is mainly attributed to the rocktype morphology of the breccias.

The Dry Density determination was undertaken using the calliper method. The method is not entirely accurate, errors may arise due to incorrect measurements or due to the shape of the 'cylinder' being analysed. This could have attributed to some of the strange behaviours in the dry density



histograms.

Figure 38 DD histograms – BBR (left) and DHB (right)

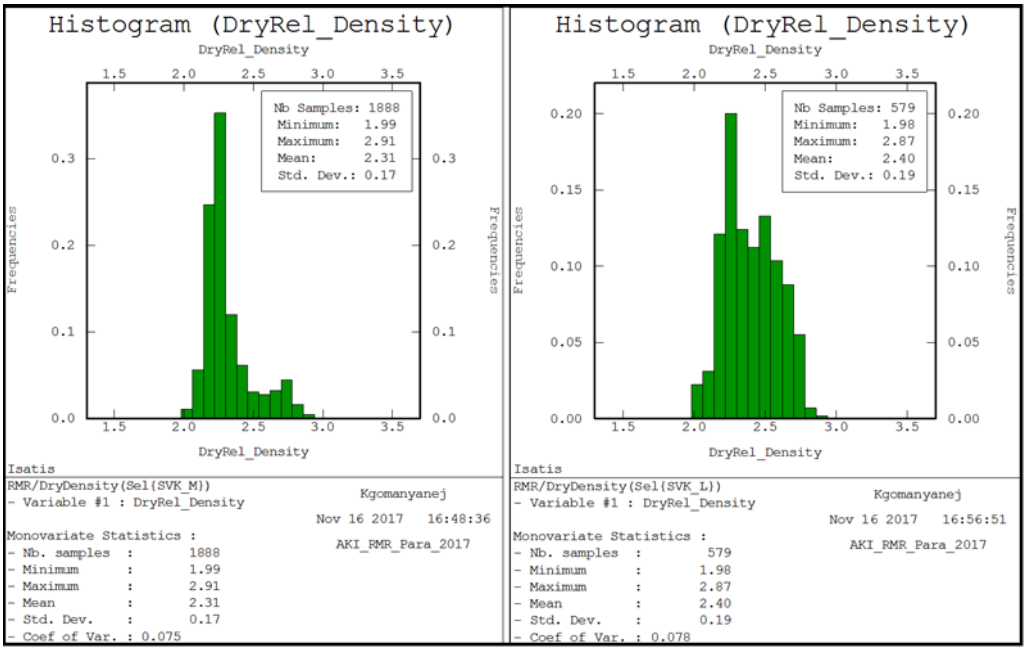


Figure 39 DD histograms – SVK_M (left) and SVK_L (right)

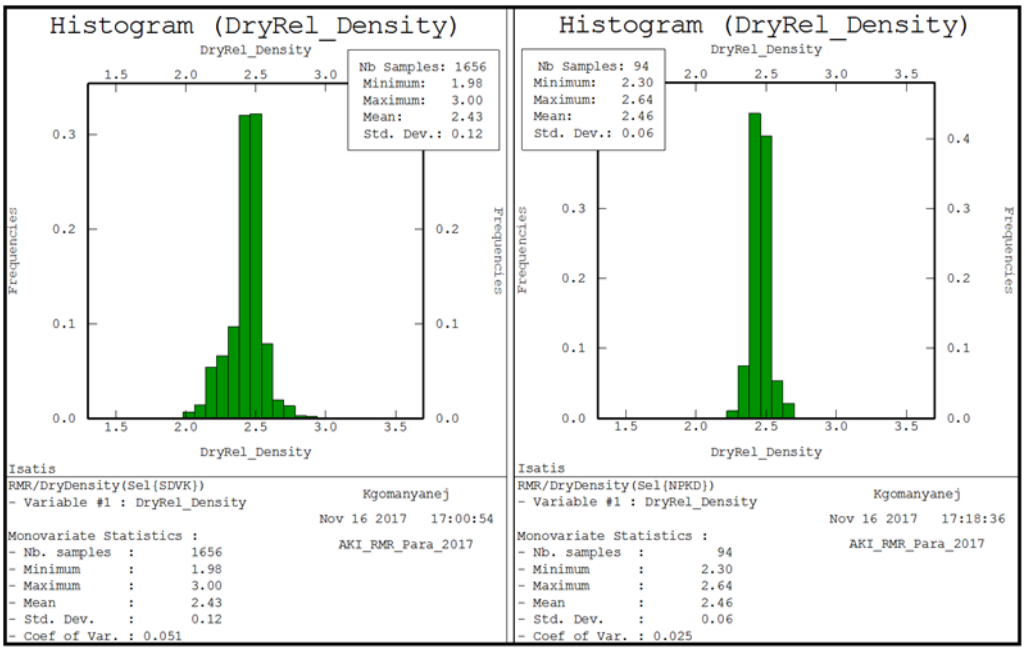


Figure 40 DD histograms – SDVK (left) and NPKD (right)

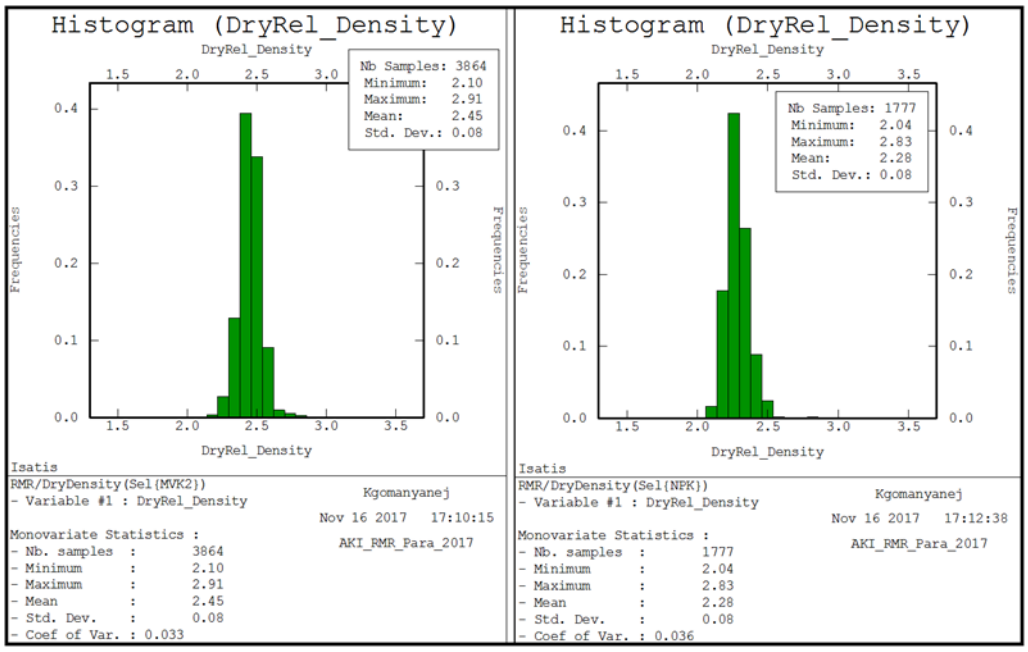


Figure 41 DD histograms – MVK2 (left) and NPK (right)

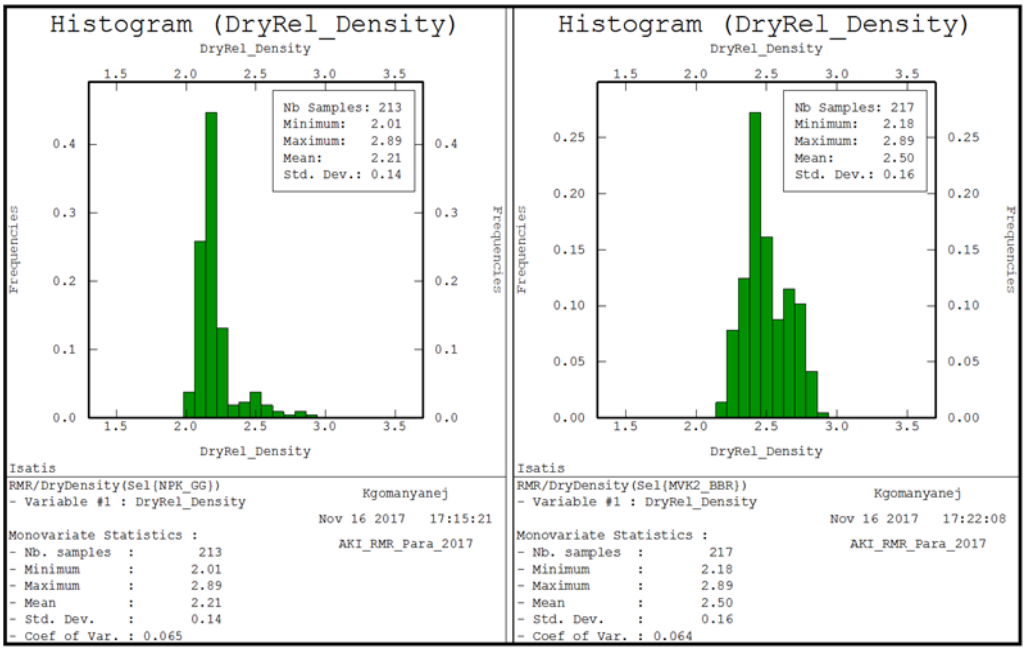


Figure 42 DD histograms – NPK_GG (left) and MVK2_BBR (right)

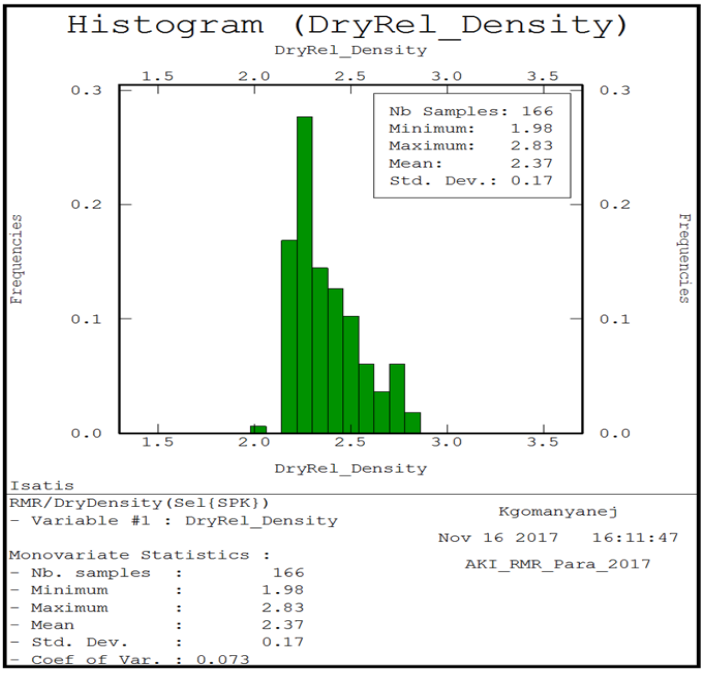


Figure 43 DD histogram – SPK

Classical statistics and graphical summaries in the form of box plots, histograms and cumulative distributions of the all the RMR input parameters including DD were analysed and discussed in this chapter. Interpretations of the distributional behaviours of these parameters were also undertaken in this section.

8 GEOSTATISTICS

8.1 Variogram Modelling

Using ISATIS^{TM} 2016.2 (Geovariances) software, directional variograms for all rocktypes with n > 60 data entries were generated for all the RMR input parameters in the horizontal and vertical planes. The approach adopted in this research study was to calculate experimental variograms and then fit variogram models to that in all the rocktypes.

An example of an experimental variogram and variogram model on the FFPM parameter for rocktype DHB is illustrated in Figure 44.

In these and all variograms to follow *D-90* depicts a search radius in the vertical direction while *N0* is the horizontal direction. The dotted line at the middle of the variogram is the experimental variance for the parameter being analysed. The letter *U* denotes the range in the horizontal plane (x-direction), *V* is the range in the y – direction of the ellipsoid while *W* is the range in the z-direction of the search ellipsoid.

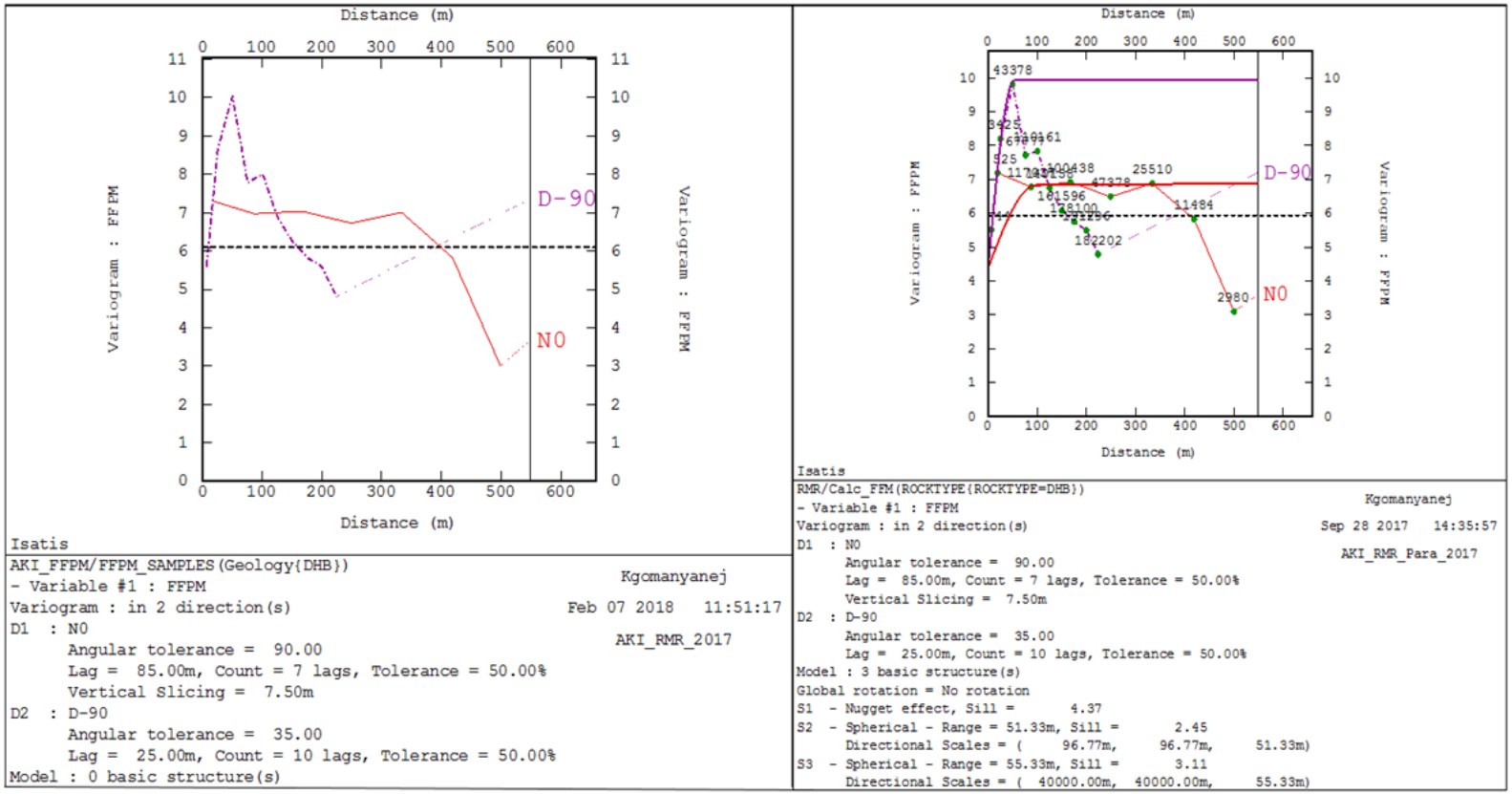


Figure 44 FFPM Variograms Experimental (left) and Model (right) – DHB

8.2 UCS - Variogram Models

Variogram models for calculated UCS data were generated for each rocktype having sample population greater than 60 entries. This was only possible for seven (7) out of fourteen (14) facies represented in the samples, namely BBR, DHB, SVK_M, SVK_L, SDVK, NPK and MVK2. For the rocktypes with n < 60, the mean of samples obtained from these facies was applied as the estimate for UCS in the rocktype.

The modelled UCS variograms for the various rocktypes are illustrated and discussed below. The modelled variogram parameters for the UCS variable for the relevant rocktypes are summarised in Table 9, at the end of this subsection.

The SVK_M unit consists of portions with dissimilar basalt dilution content. A zonal anisotropic variogram was modelled, see Figure 45 (left). In the vertical direction the UCS variogram sill has been modelled below the experimental variance. The nugget effect is relatively low and ties in with the shape of the histogram where the majority of the data fell within the first two classes and it is expected that close spaced data would behave similarly.

The horizontal UCS variogram(N0) has been modelled above the experimental variance. There is high correlation on the samples in the horizontal direction supported by a longer range in this direction. This ties in well with the nature of SVK_M. The rocktype is layered and extends laterally in the AK1 kimberlite.

The UCS variogram for SVK_L unit depicts a geometric anisotropic structure with a longer horizontal range than the vertical, see Figure 45 (right). Both variogram structures (horizontal and vertical) have been modelled to the experimental variogram sill. The horizontal variogram has a longer range than the vertical structure due to similar reasons as illustrated for the SVK_M rocktype. The UCS variogram for the SVK_L rocktype has a relatively high nugget effect (> 50% of the total sill).

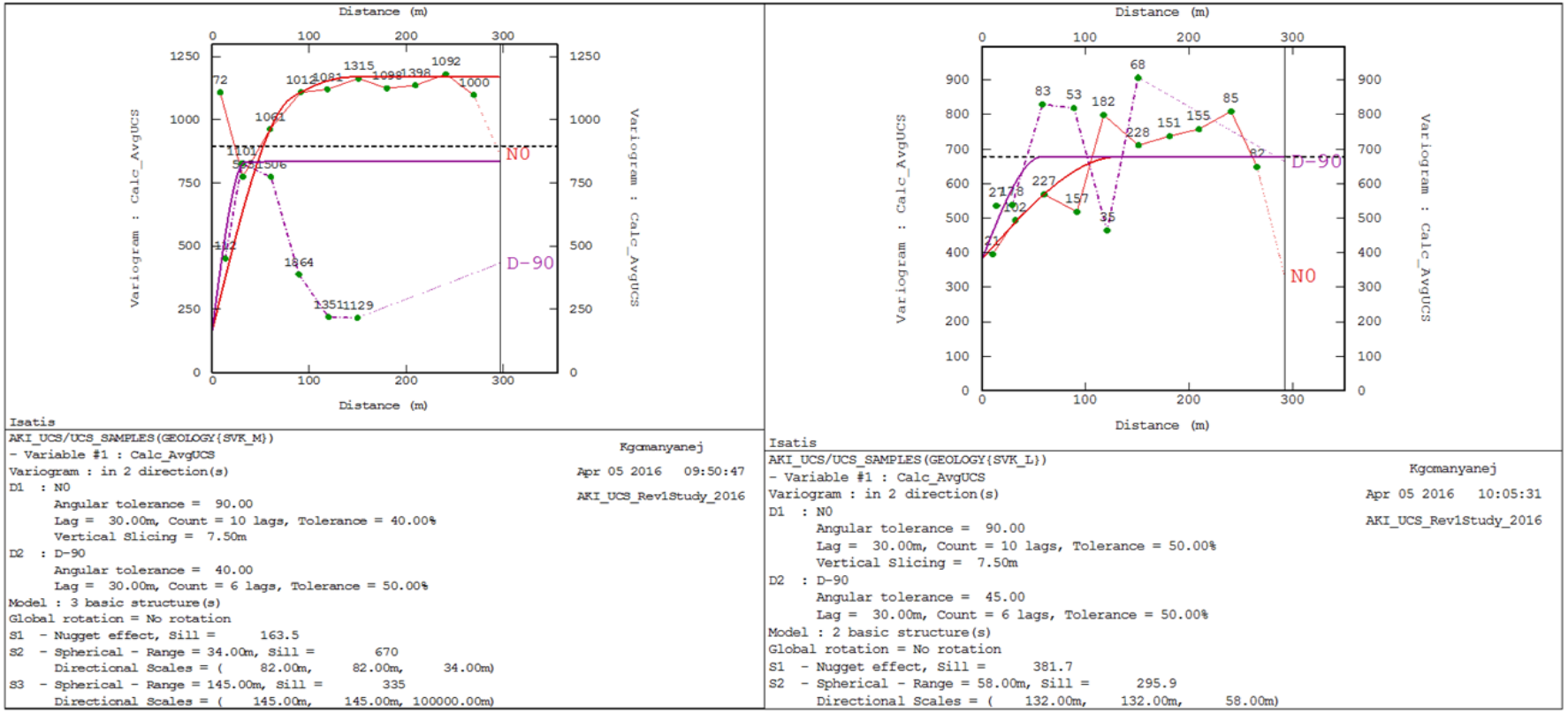


Figure 45 UCS Variogram models – SVK_M (left) and SVK_L (right)

The UCS variogram for the BBR rocktype, shown in Figure 46 (left), highlights zonal anisotropy with almost similar ranges in both the horizontal and vertical directions. The nugget effect for this rocktype is high which is in agreement with the UCS histogram for the BBR.

Figure 46 (right) depicts the UCS variogram in the DHB rocktype. It shows geometric anisotropy with a longer range in the horizontal than the vertical direction, which is due to the lateral extent of the DHB rocktype. Both directions have been modelled below the experimental variance. The UCS nugget effect is also high as is the norm with breccias the nugget effect in the BBR is 43% and for the DHB is at 48% of the respective modelled sills.

The NPK rocktype is massive and extensive in the vertical direction within the AK1 North pipe. Figure 47 (left) illustrates the UCS variogram. It exhibits geometric anisotropy with the vertical range longer than the horizontal range. The UCS spatial correlation is thus vertically higher than horizontally in this rocktype. The variogram sill has been modelled to the experimental semi-variance.

The UCS variogram for the MVK2 rocktype, shown in Figure 47 (right), also exhibits a similar geometric anisotropy. The correlation is more pronounced in the vertical direction. The experimental variogram model has been generated by capping (masking) outliers, shown in Table 8 and as such, the model is considered to be robust. The process of masking outliers involved the commonly used 1.5 x IQR tests for all the parameters. The tests were not validated by a different method, as this was assumed to be adequate.

Table 8 UCS outlier capping for SDVK and MVK2

Lithology Code	No. of samples	No. of Outliers	No. of samples outliers removed
SDVK	561	2	559
MVK2	1048	1	1047
Total		**3**	

The UCS variogram for the SDVK rocktype depicts zonal anisotropic nature i.e. different sills in the different directions, with a slightly longer range in the horizontal direction than the vertical see Figure 48. The modelled variogram has been generated by ignoring outliers in order to get a robust model. The SDVK unit is a relatively massive rocktype and extends both laterally as well as vertically.

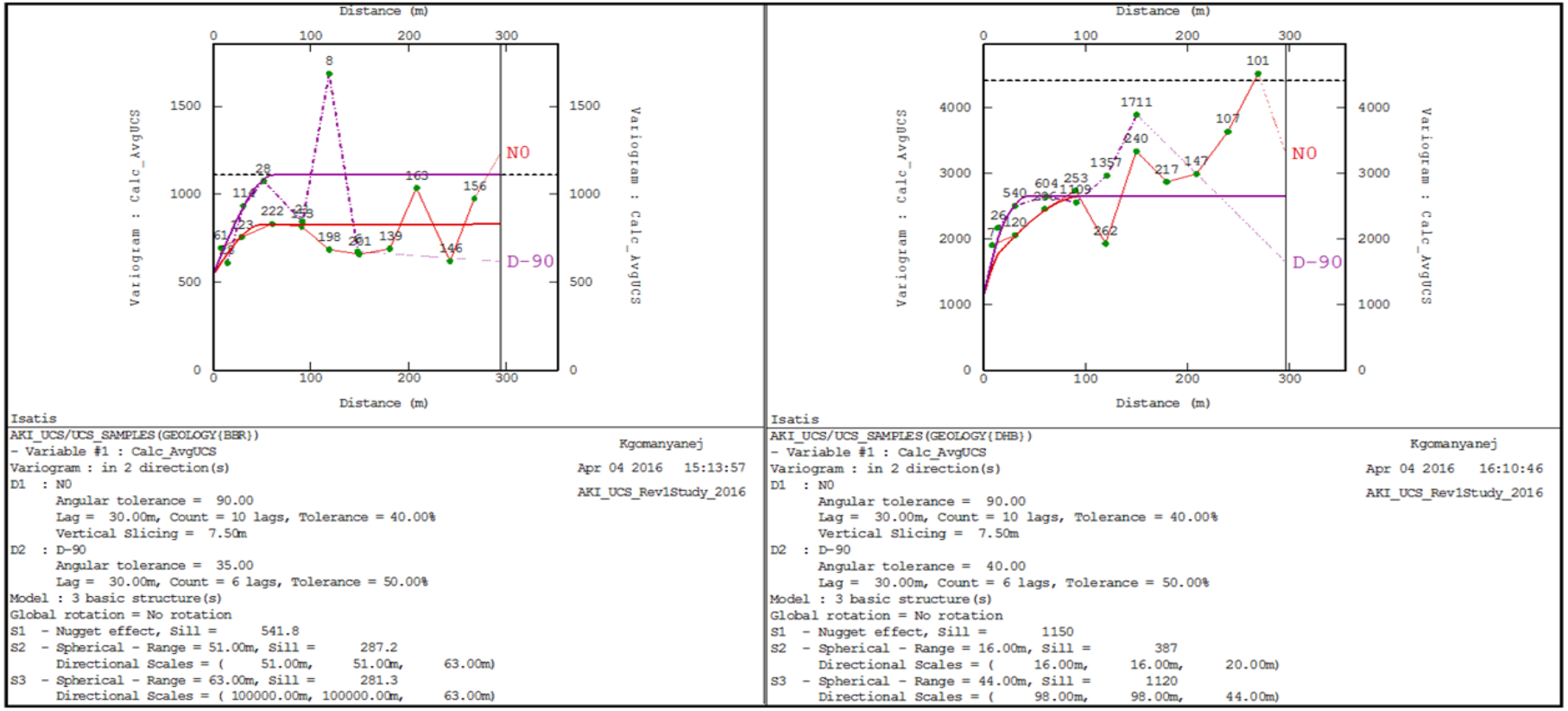


Figure 46 UCS Variogram models – BBR (left) and DHB (right)

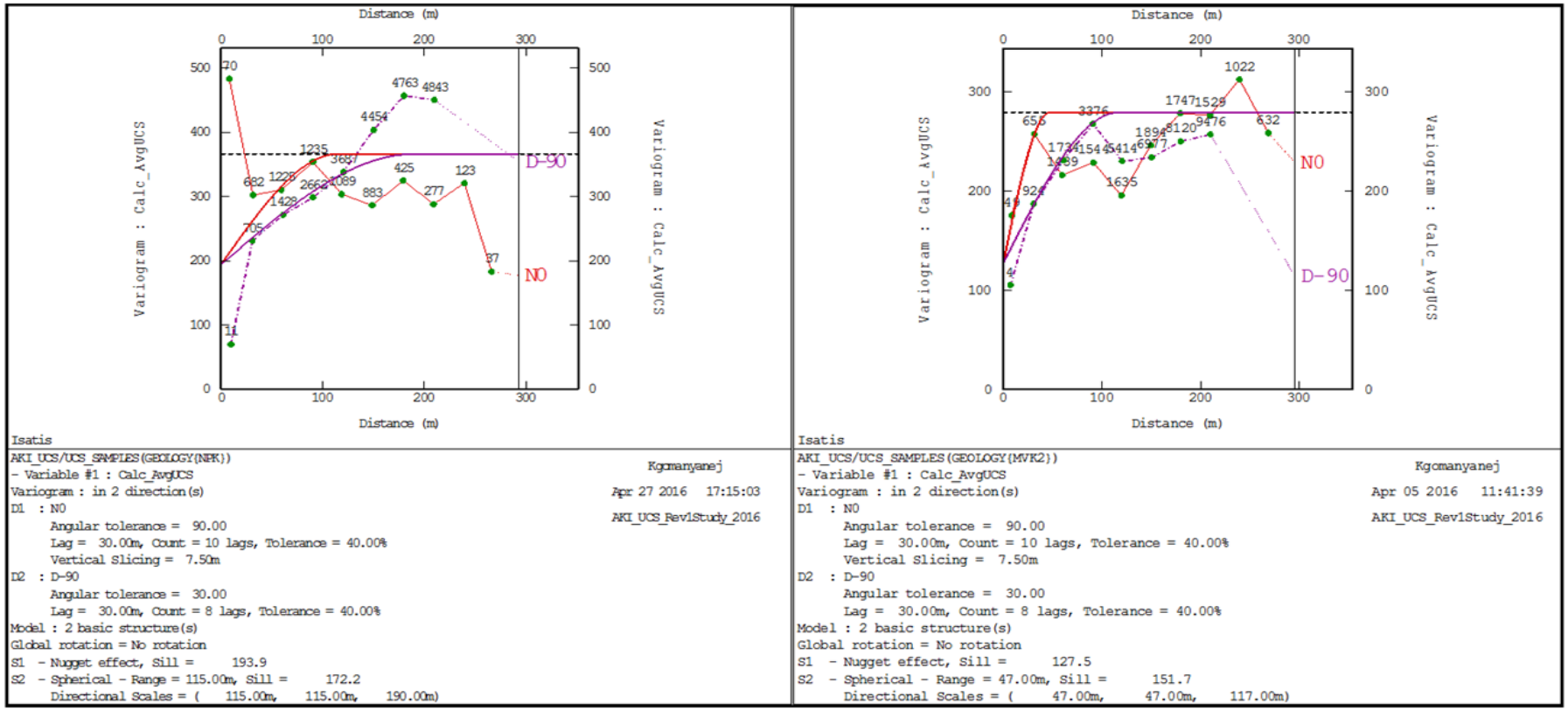


Figure 47 UCS Variogram models – NPK (left) and MVK2 (right)

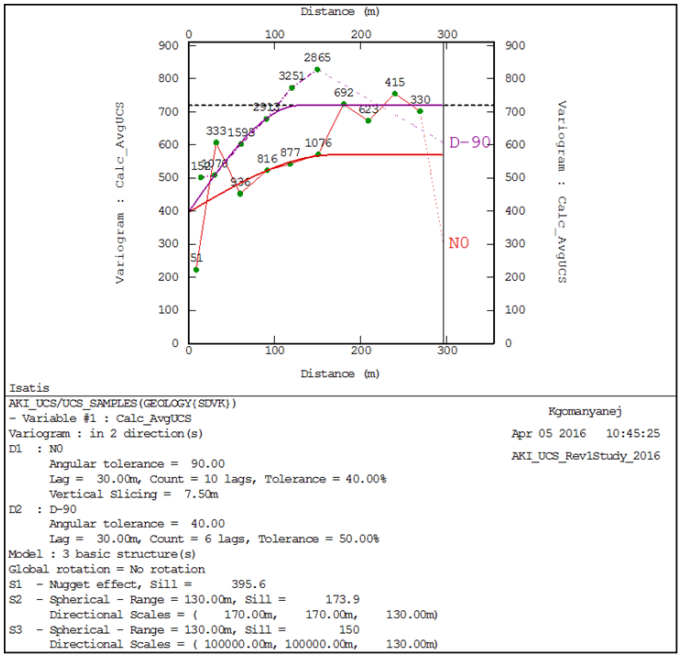


Figure 48 UCS Variogram model – SDVK

8.2.1 UCS Variogram Model Parameters Summary per rocktype

The summarised UCS variograms models are represented in Table 9. All the UCS variogram models for the rocktypes listed are double structured spherical models and are anisotropic.

Variogram Parameters								
Geological Unit	Type	Variance	Type	Sill	% Sill	Range (U)	Range (V)	Range (W)
BBR	Anisotropic	1110.29	Nugget	541.80	49%			
			Spherical	287.20	26%	51	51	63
			Spherical	281.30	25%	100000	100000	63
DHB	Anisotropic	4414.50	Nugget	1150.00	26%			
			Spherical	387.20	9%	16	16	20
			Spherical	1120.00	25%	98	98	44
MVK2	Anisotropic	279.21	Nugget	127.50	46%			
			Spherical	151.70	54%	47	47	117
NPK	Anisotropic	366.06	Nugget	193.90	53%			
			Spherical	172.20	47%	115	115	190
SDVK	Anisotropic	719.13	Nugget	395.60	55%			
			Spherical	173.90	24%	170	170	130
			Spherical	150.00	21%	100000	100000	130
SVK_L	Anisotropic	677.34	Nugget	381.70	56%			
			Spherical	295.90	44%	132	132	58
SVK_M	Anisotropic	895.20	Nugget	163.50	18%			
			Spherical	670.00	75%	82	82	34
			Spherical	335.00	37%	145	145	100000

Table 9 UCS variogram models per rocktype

*Note U and V are horizontal ranges and W is the vertical range

8.3 FFPM - Variogram Models

The same approach as in the previous section for the UCS parameter, was applied to generate variogram models for the FFPM RMR parameter for all the rocktypes. A nugget effect was modelled in all cases and either two or three spherical structures were modelled as relevant. The variogram parameters for the FFPM parameter are summarised in Table 10 (at the end of this subsection).

The FFPM experimental variograms and fitted models for the A3T and SPK rocktypes appear in Figure 49. Due to the small number of samples, a decision was taken to model FFPM parameter in these two rocktypes, based on the omnidirectional (isotropic behaviour) experimental variograms in order to have robust models. For both models, the variograms were modelled to the experimental variance. The FFPM in the SPK unit has a longer range compared to that in the A3T unit.

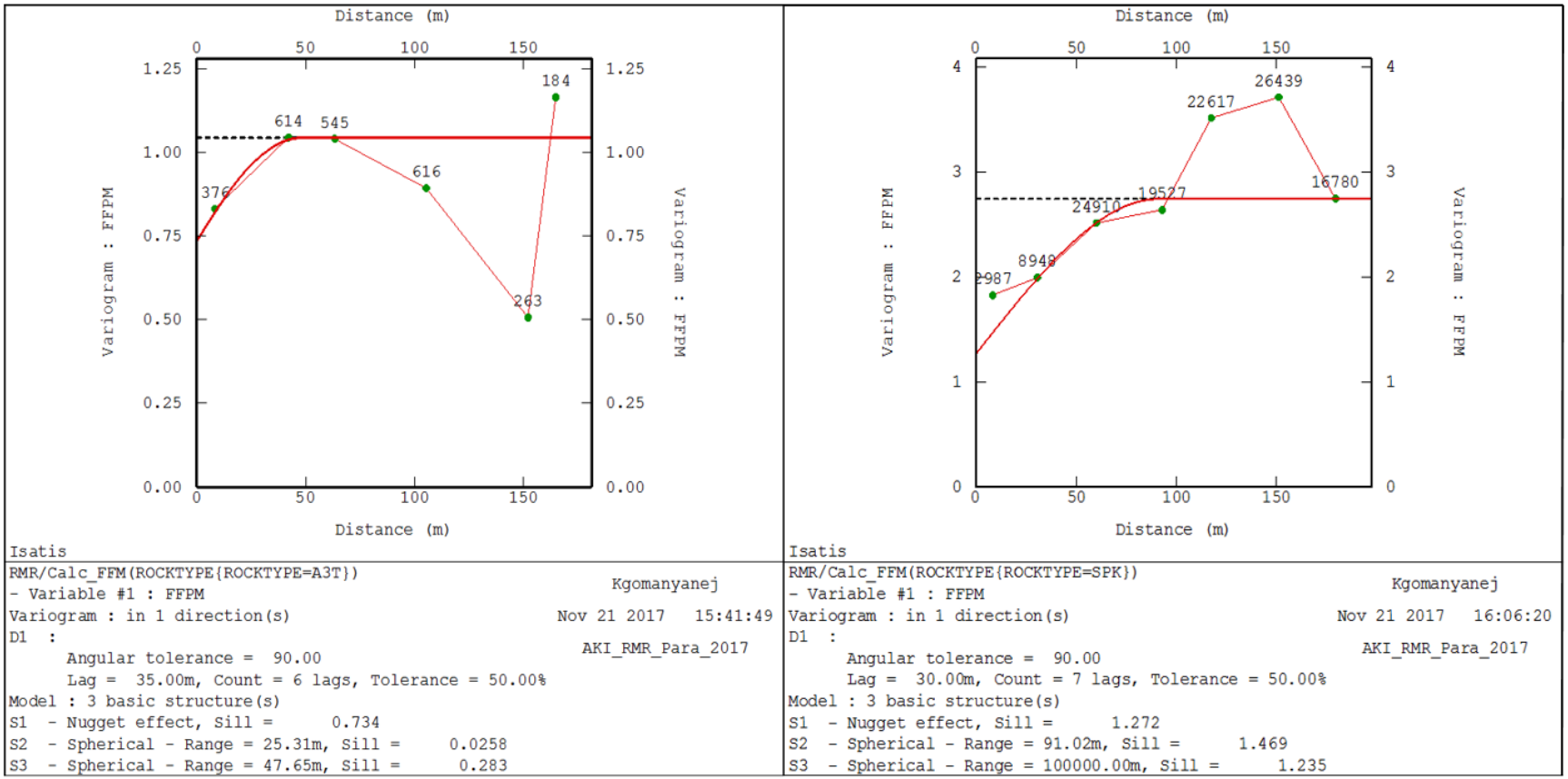


Figure 49 FFPM variogram models – A3T (left) and SPK (right)

Figure 50 illustrates modelled FFPM variograms for rocktypes BBR and DHB. Both variograms for the two rocktypes display zonal anisotropic behaviour due to their varying composition (brecciated units). The FFPM variogram for two rocktypes have the highest nugget effect as compared to the rest of other models on the FFPM parameter. Again, the FFPM models for these two rocktypes (BBR and DHB) show a shorter range in the vertical direction as compared to a longer range in the horizontal direction.

Modelled FFPM variograms for SVK_U and SVK_M are shown in Figure 51. The FFPM variogram model on the SVK_U show a geometric anisotropy while the SVK_M depicts a zonal anisotropy. Once again, the FFPM models for the two rocktypes show a longer range in the horizontal direction. The nugget effect on the FFPM model for the SVK_U rocktype is similar to SVK_L model which is discussed below. The SVK_U and SVK_M discussed above also form the crater deposits (layered facies) of the AK1 pipe.

Modelled FFPM variograms for rocktypes SVK_L and SDVK are represented by Figure 52. The FFPM models for these two rocktypes show a shorter range in the vertical direction as compared to a longer range in the horizontal. The FFPM variogram for the SVK_L rocktype is fixed at the experimental variance (zonal anisotropy). On the other hand, the FFPM variogram for the SDVK rocktype is fixed on the experimental variance only in the horizontal direction (geometric anisotropy). The FFPM model for the SDVK rocktype has a fairly lower nugget effect (massive in nature).

FFPM variogram models for the NPK and MVK2 rocktypes are illustrated in Figure 53. The FFPM model for the NPK rocktype shows a zonal anisotropy with the horizontal fixed at the experimental variance. The FFPM model for the MVK2 rocktype displays a geometric anisotropic behaviour. Both models for the two rocktypes show a longer range in the horizontal than the vertical. Both rocktypes are massive units with a longer horizontal extent compared to the vertical. The FFPM model for the NPK rocktype has the lowest nugget effect (0.10) compared to all AK1 rocktypes.

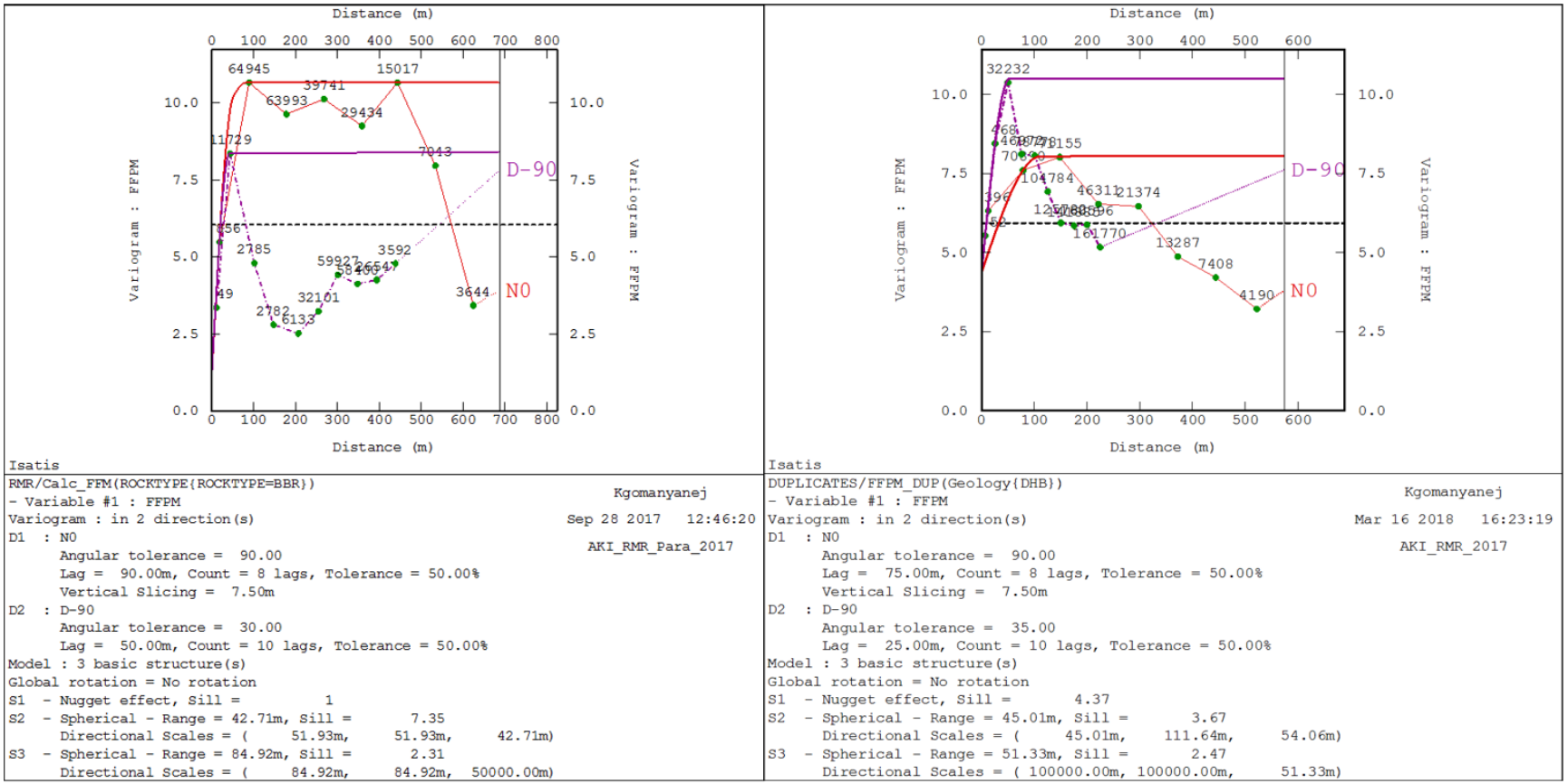


Figure 50 FFPM variogram models – BBR (left) and DHB (right)

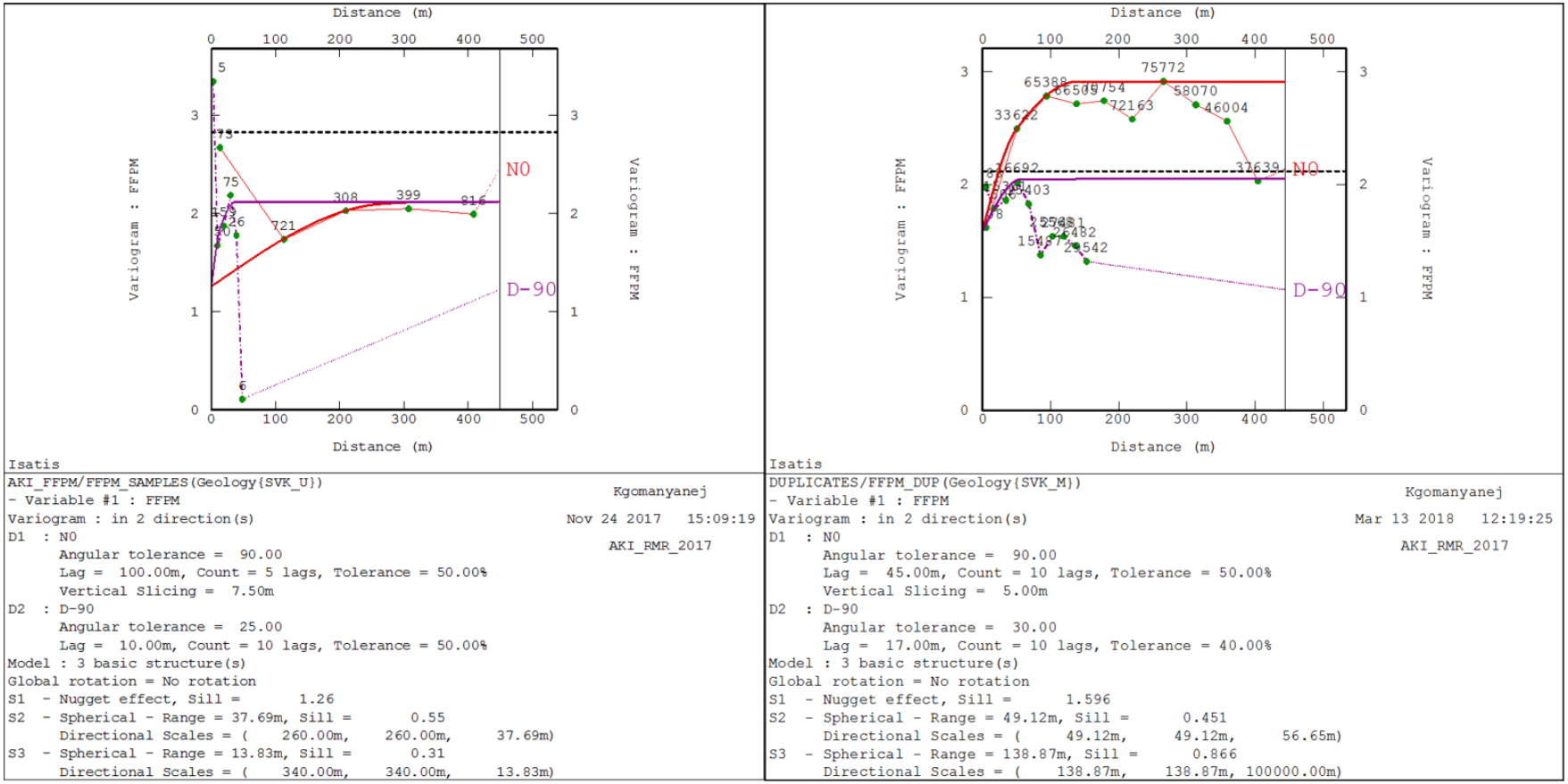


Figure 51 FFPM variogram models – SVK_U (left) and SVK_M (right)

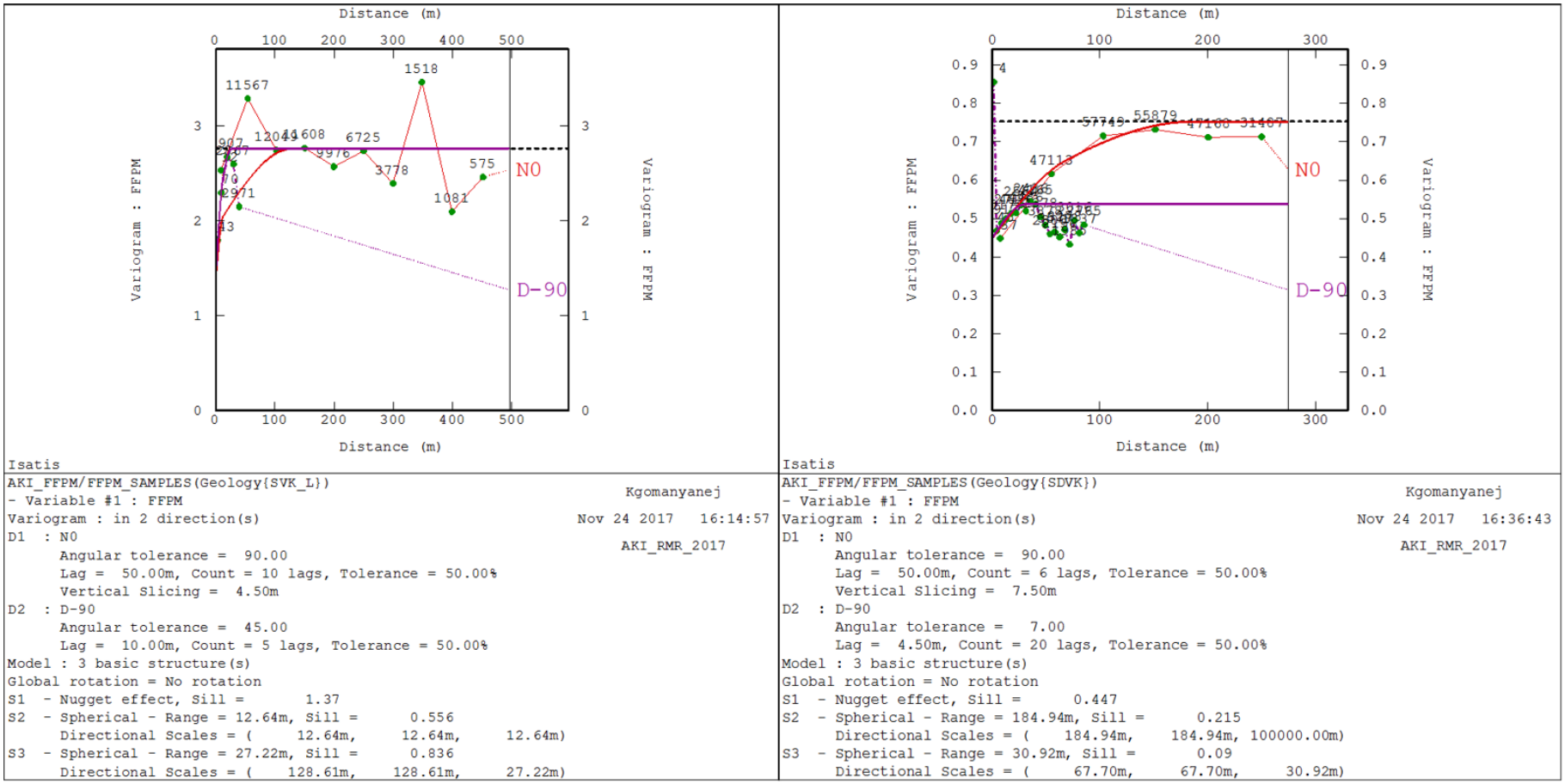


Figure 52 FFPM variogram models – SVK_L (left) and SDVK (right)

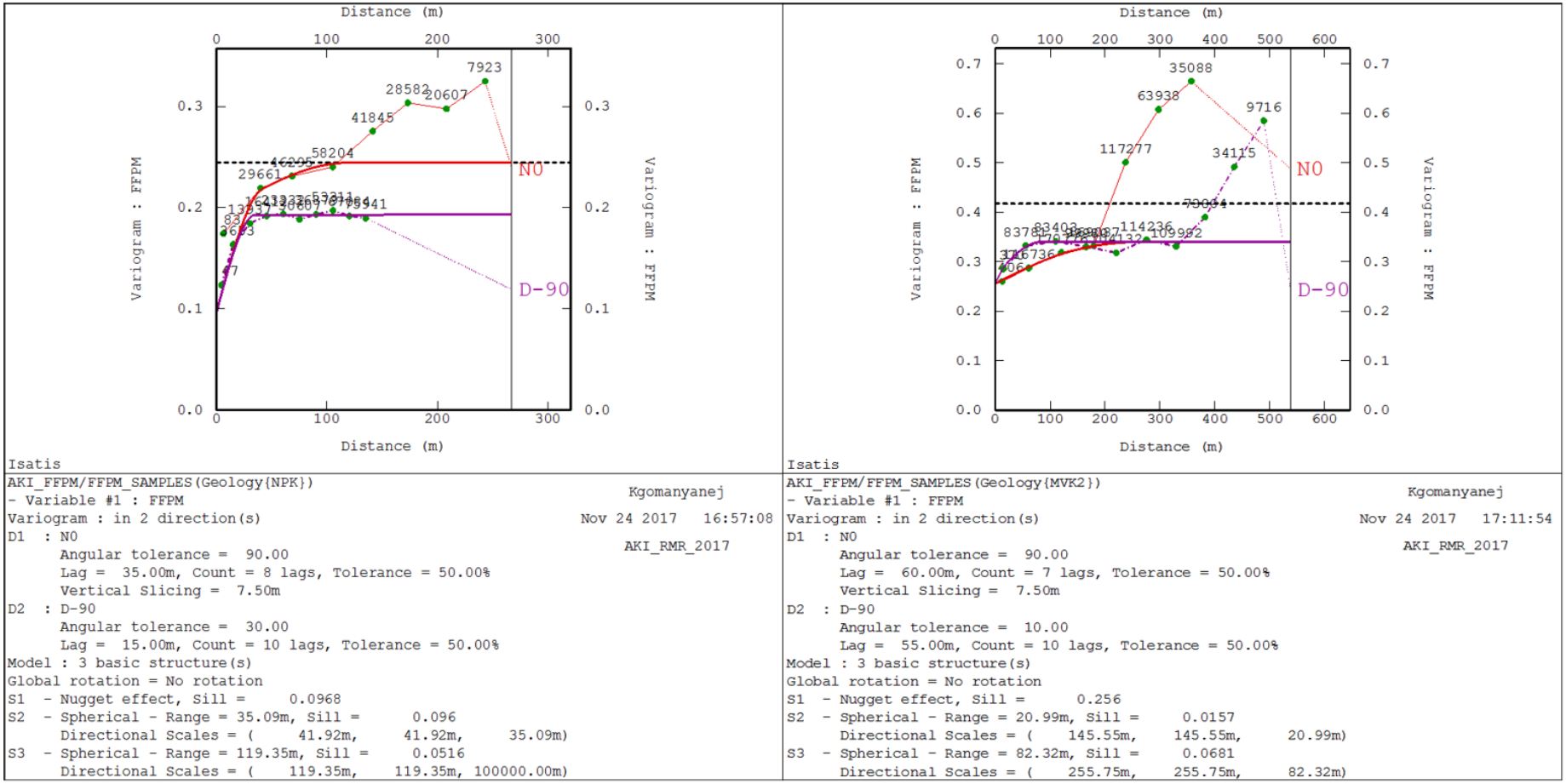


Figure 53 FFPM variogram models – NPK (left) and MVK2 (right)

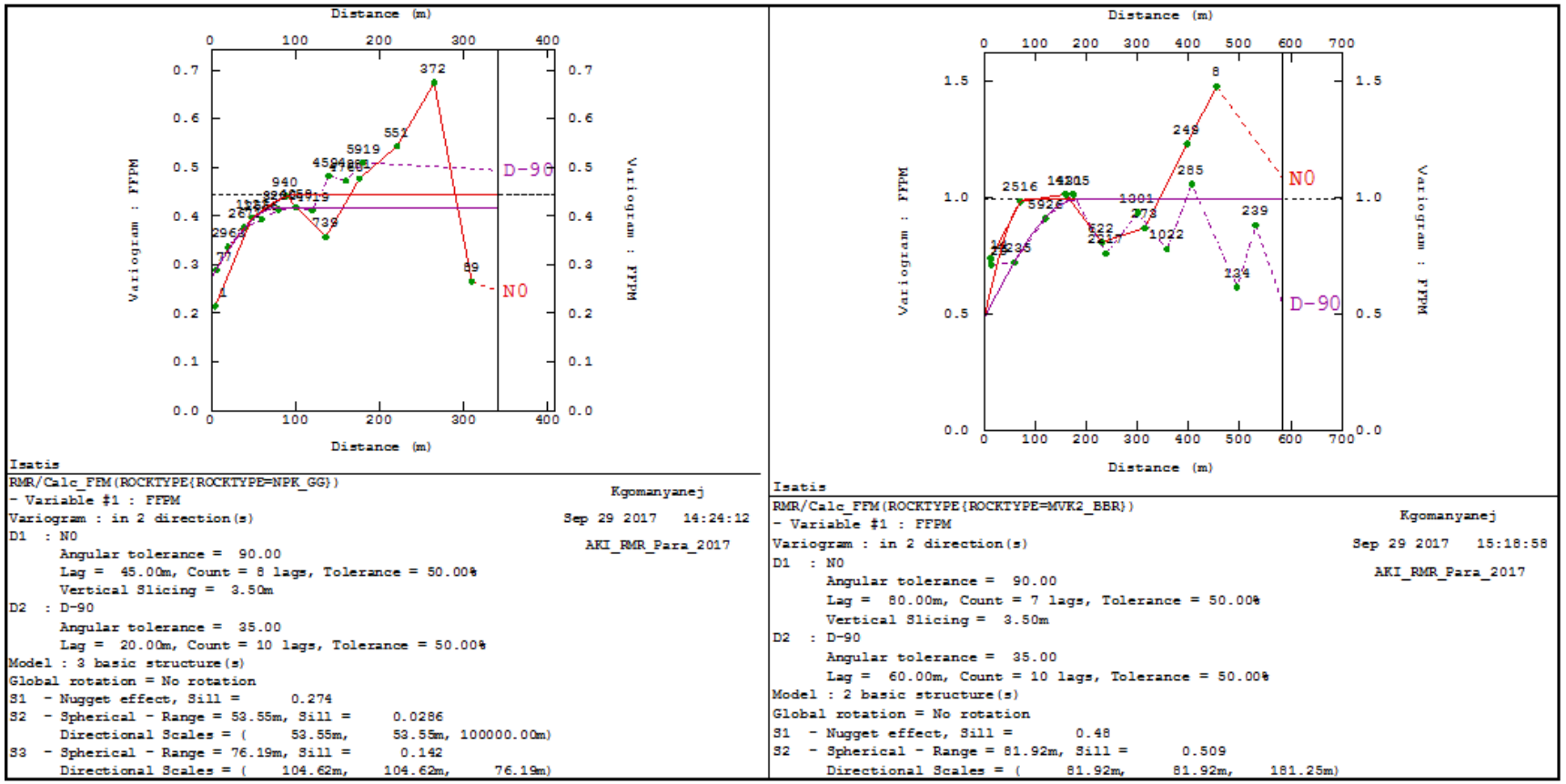
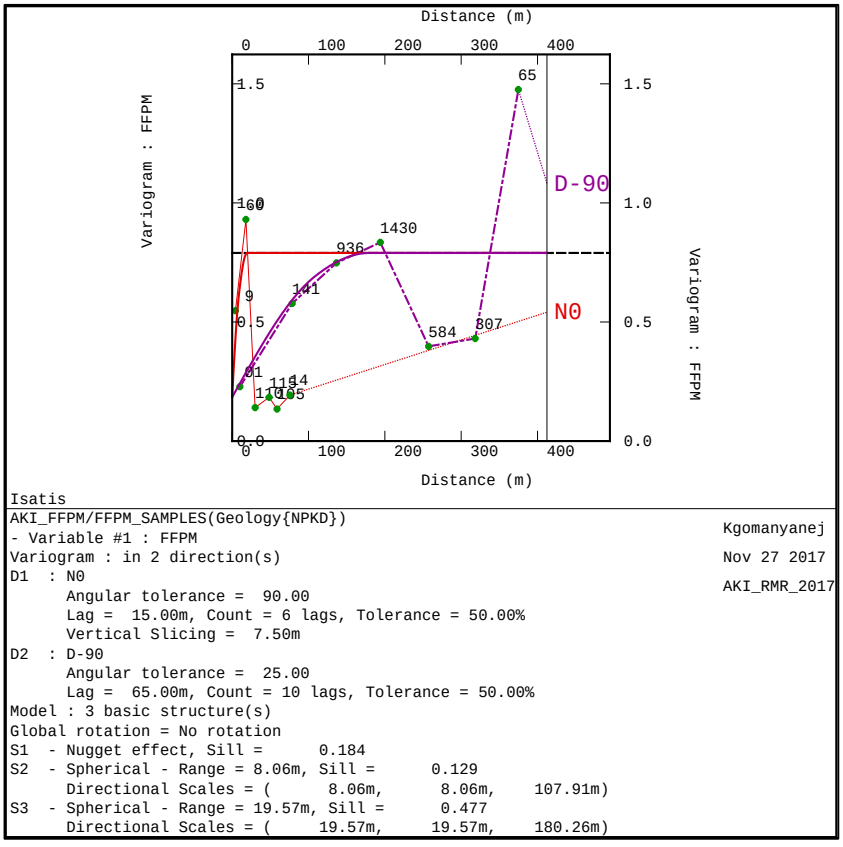


Figure 54 FFPM variogram models – NPK_GG (left) and MVK2_BBR (right)

The FFPM variogram models for NPK_GG and MVK2_BBR are illustrated in Figure 54. The FFPM model for rocktype NPK_GG shows zonal anisotropic behaviour with the horizontal fixed at the experimental variance longer than the vertical range. The FFPM model for the MVK2_BBR rocktype shows geometric anisotropic behaviour and the vertical is longer than the horizontal range. These rocktypes are brecciated derivatives of the NPK and MVK2 rocktypes.

The FFPM variogram model for NPKD is shown below in Figure 55. The model for this rocktype is characterised by geometric anisotropy (modelled at the experimental variance) on both directions. The horizontal range is much shorter than the vertical range. The FFPM model for this rocktype has the



second lowest nugget effect at 0.18.

Figure 55 FFPM variogram model – NPKD

8.3.1 FFPM – Summary of Variogram Parameters

All the variogram models for the FFPM are double structured spherical models and are anisotropic except for SPK and A3T that are isotropic. The summarised variogram parameters for the FFPM are represented in Table 10.

Table 10 FFPM Variogram Model Parameters Summary per rocktype

Variogram Parameters						
Geological Unit	Structure Type	Sill	% Sill	Range (U)	Range (V)	Range (W)
BBR	Nugget	1.00	17%			
	Spherical	7.92	131%	66.58	66.58	54.76
	Spherical	1.96	32%	97.11	97.11	100000
DHB	Nugget	4.37	74%			
	Spherical	2.57	45%	96.77	96.77	51.33
	Spherical	3.32	53%	40000	400000	55.33
MVK2	Nugget	0.26	62%			
	Spherical	0.02	4%	145.55	145.55	20.99
	Spherical	0.07	17%	255.75	255.75	82.32
MVK2_BBR	Nugget	0.48	48%			
	Spherical	0.51	52%	91.92	91.92	181.25
NPK	Nugget	0.10	40%			
	Spherical	0.10	40%	41.92	41.92	35.09
	Spherical	0.05	22%	119.35	119.35	100000
NPK_GG	Nugget	0.27	62%			
	Spherical	0.03	7%	53.55	53.55	100000
	Spherical	0.14	32%	104.62	104.62	76.19
NPKD	Nugget	0.18	25%			
	Spherical	0.13	18%	8.06	8.06	107.91
	Spherical	0.48	65%	19.57	19.57	180.26
SDVK	Nugget	0.45	61%			
	Spherical	0.22	29%	184.94	184.94	100000
	Spherical	0.09	12%	67.7	67.7	30.92
SVK_U	Nugget	1.26	45%			
	Spherical	0.55	20%	260	260	37.69
	Spherical	0.31	11%	340	340	13.83
SVK_M	Nugget	1.60	63%			
	Spherical	0.45	29%	49.12	49.12	56.65
	Spherical	0.87	45%	138.87	138.87	100000
SVK_L	Nugget	1.37	50%			
	Spherical	0.56	20%	12.64	12.64	12.64
	Spherical	0.84	31%	128.61	128.61	27.22
SPK	Nugget	1.34	55%			
	Spherical	1.5	3%	91.02		
	Spherical	1.3	46%	100000		
A3T	Nugget	0.754	71%			
	Spherical	0.0301	3%	16.35		
	Spherical	0.294	28%	37.71		

8.4 RQD - Variogram Models

A variography analysis to capture the spatial variability of the rock quality designation (RQD) parameter was conducted in a similar manner as for the RMR input parameters discussed in the preceding subsections of Section 8. As before, experimental variograms for RQD were generated for all rocktypes in the AK1 kimberlite with sufficient data. This step was followed by variogram modelling. Resultant models all had a random component represented by the nugget effect and included either two or three spherical structures. The RQD variogram models are discussed in the subsequent paragraphs, with the summary of the variogram parameters shown in Table 11.

The RQD variogram models for rocktypes A3T and SPK are illustrated in Figure 56. Omnidirectional variograms have been modelled for these two rocktypes due to insufficient samples for robust anisotropy identification. The RQD variogram model for A3T has been modelled at the experimental variance but has a shorter range compared to the SPK rocktype. The RQD variogram model for the A3T rocktype displays a higher nugget effect. The RQD model for rocktype A3T has the highest experimental variance.

The RQD fitted variogram models for the brecciated BBR and DHB rocktypes are illustrated in Figure 57. The RQD model for the BBR rocktype depicts a zonal anisotropy with the vertical fixed below the experimental variance. The horizontal range is longer than the vertical and the latter has been modelled above the experimental variance. The RQD variogram model for the DHB rocktype shows geometric anisotropy but both structures have been modelled above the experimental variance. The ranges for this model on the DHB rocktype are almost similar in both directions, that is, correlation of samples was realised for shorter distance in both directions

The fitted RQD variogram models for the layered units (SVK_U and SVK_M) are illustrated in Figure 58. As a norm the RQD variogram models for these two rocktypes are more pronounced in the horizontal direction as compared to the vertical. The RQD variogram model for the SVK_U rocktype has been fixed at the experimental variance (geometric anisotropic behaviour). The RQD variogram model in the SVK_M unit displays a geometric anisotropic behaviour but both the horizontal and the vertical directions have been modelled below the experimental variance. The SVK_M has the longest horizontal range at 379.67m.

The fitted RQD variogram models for rocktypes SVK_L and SDVK are illustrated in Figure 59. The RQD model for the SVK_L rocktype displays a zonal anisotropic behaviour with the horizontal range slightly longer than the vertical. The vertical structure has been fixed on the experimental variance while the horizontal is fixed above it. The RQD variogram model for the SDVK rocktype shows a geometric anisotropic behaviour and the horizontal range again is much longer the vertical. Both structures for the RQD model for the SDVK have been fixed at the experimental variance. The RQD model for this rocktype has the second longest horizontal range at 275.86m.

The RQD variograms model for the NPK and MVK2 are illustrated in Figure 60. The RQD model for the NPK rocktype displays a zonal anisotropic behaviour with the horizontal and vertical modelled below the experimental variance. The horizontal and vertical range are almost similar in length in both directions. The RQD model for the MVK2 rocktype displays a much longer horizontal range than the vertical but with a geometric anisotropic behaviour. Both structures have been modelled below the experimental variance. The RQD model for the MVK2 rocktype has the third lowest nugget effect at 34.89m.

The fitted RQD variogram models for NPK_GG and MVK2_BBR are shown in Figure 61. Both models for these two rocktypes display a geometric anisotropy and are fixed at the experimental variance. The RQD variogram model for the NPK_GG unit shows a slightly longer range in vertical direction. The RQD model for the MVK2_BBR unit shows a longer range in the horizontal direction but a shorter range in the vertical direction. This is expected of this unit, a behaviour associated with the layered units. The model for the MVK2_BBR has the lowest nugget effect.

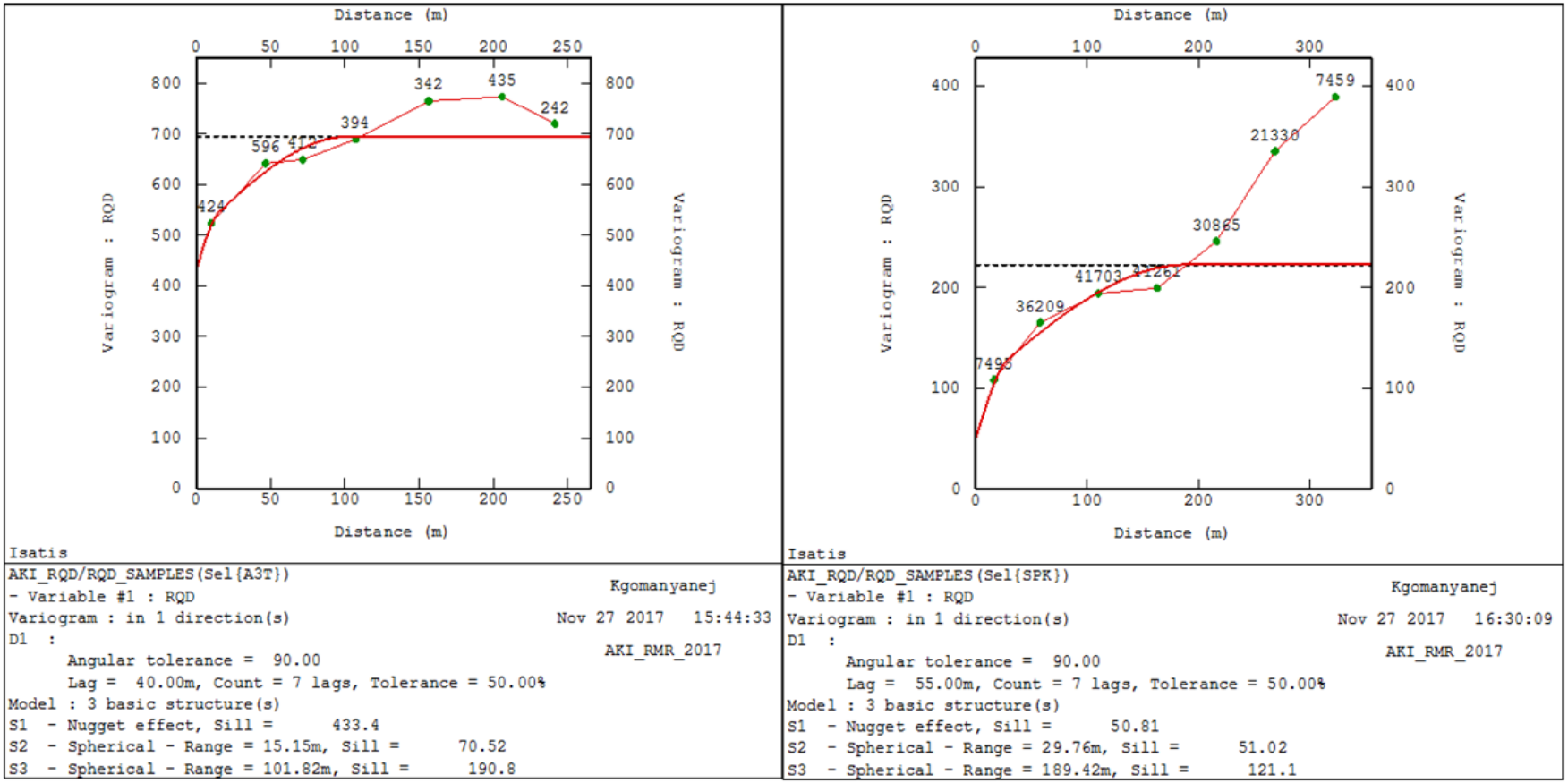


Figure 56 RQD variogram models – A3T (left) and SPK (right)

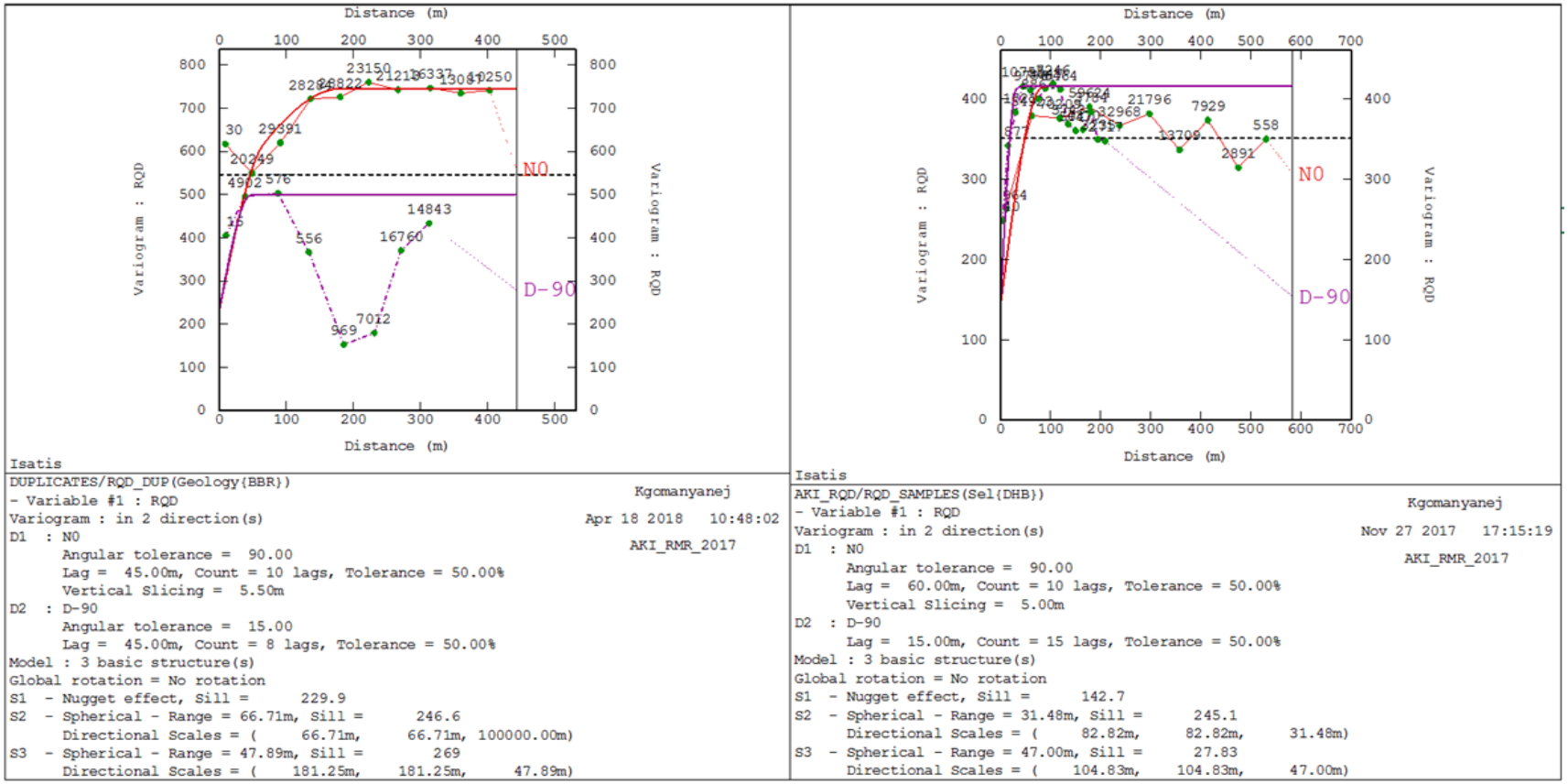


Figure 57 RQD variogram models – BBR (left) and DHB (right)

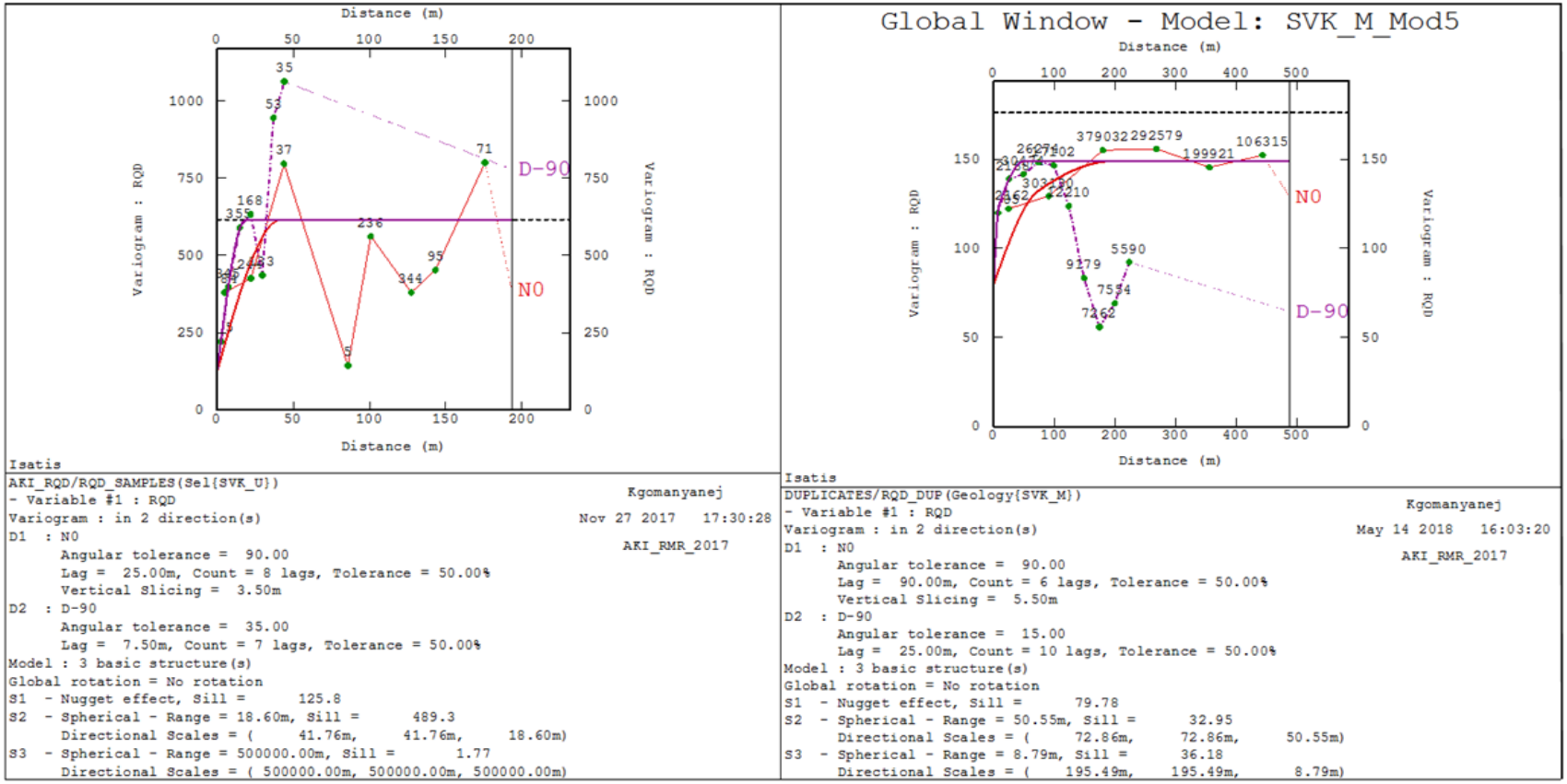


Figure 58 RQD variogram models – SVK_U (left) and SVK_M (right)

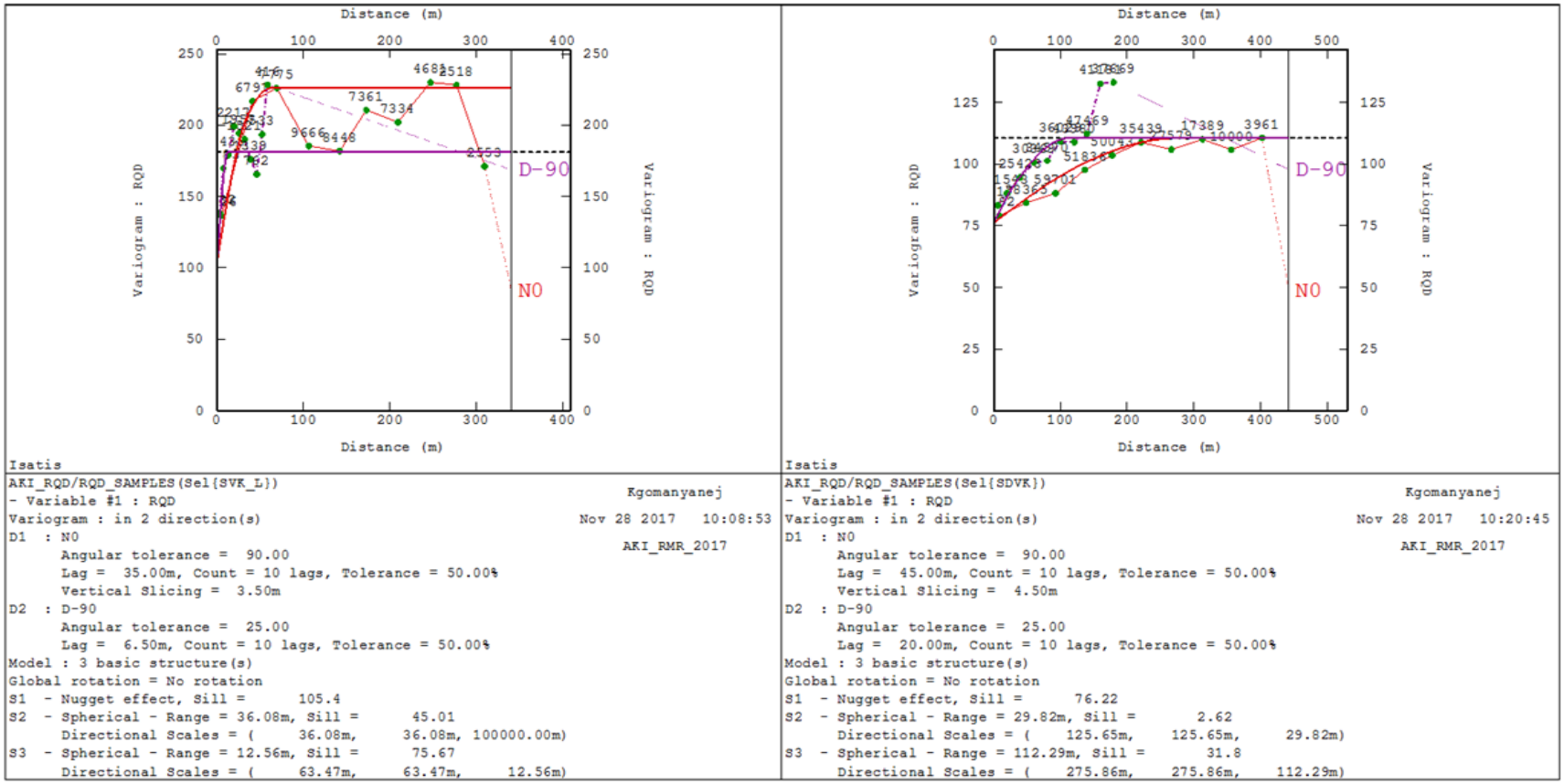


Figure 59 RQD variogram models – SVK_L (left) and SDVK (right)

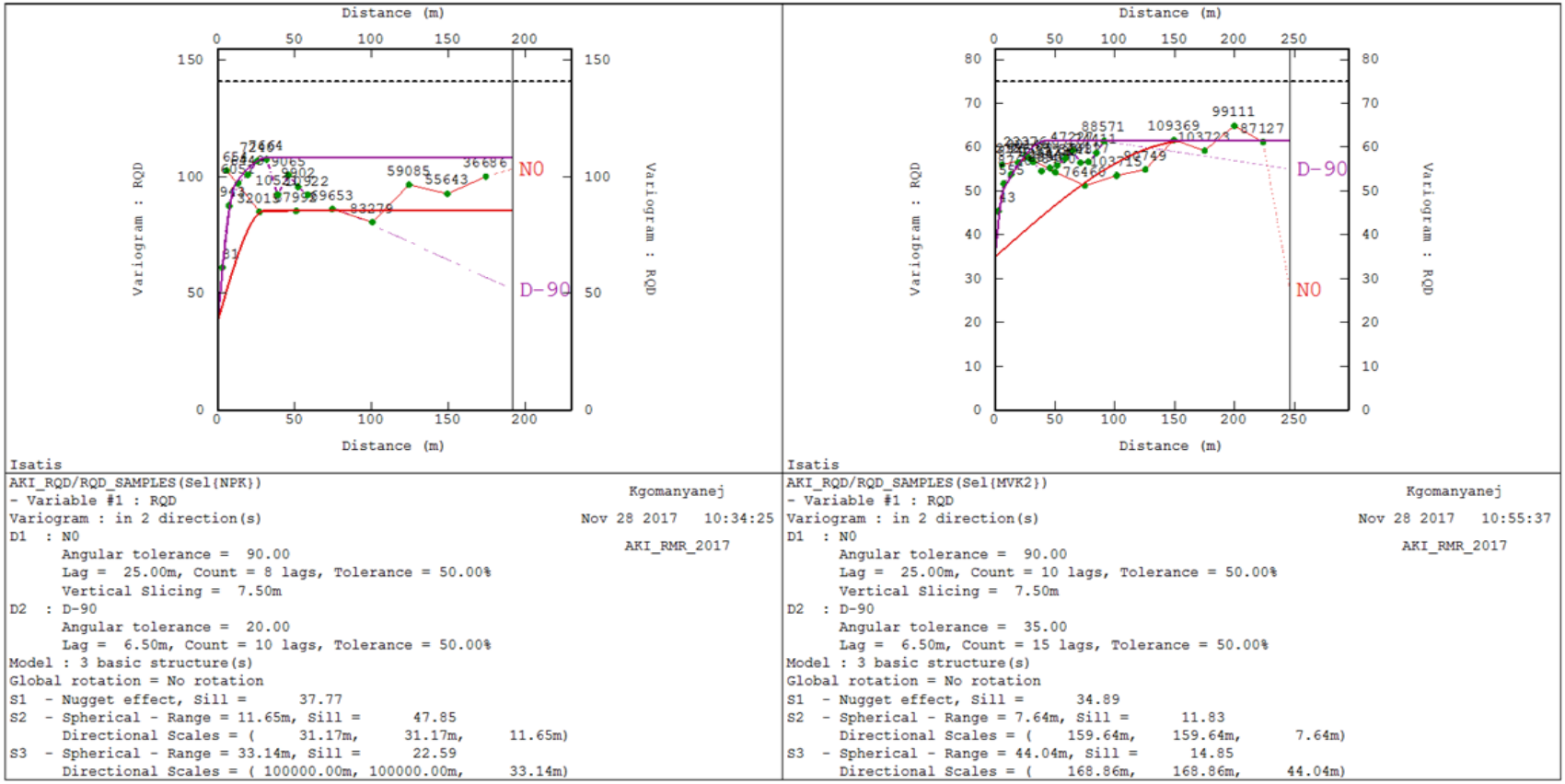


Figure 60 RQD variogram models – NPK (left) and MVK2 (right)

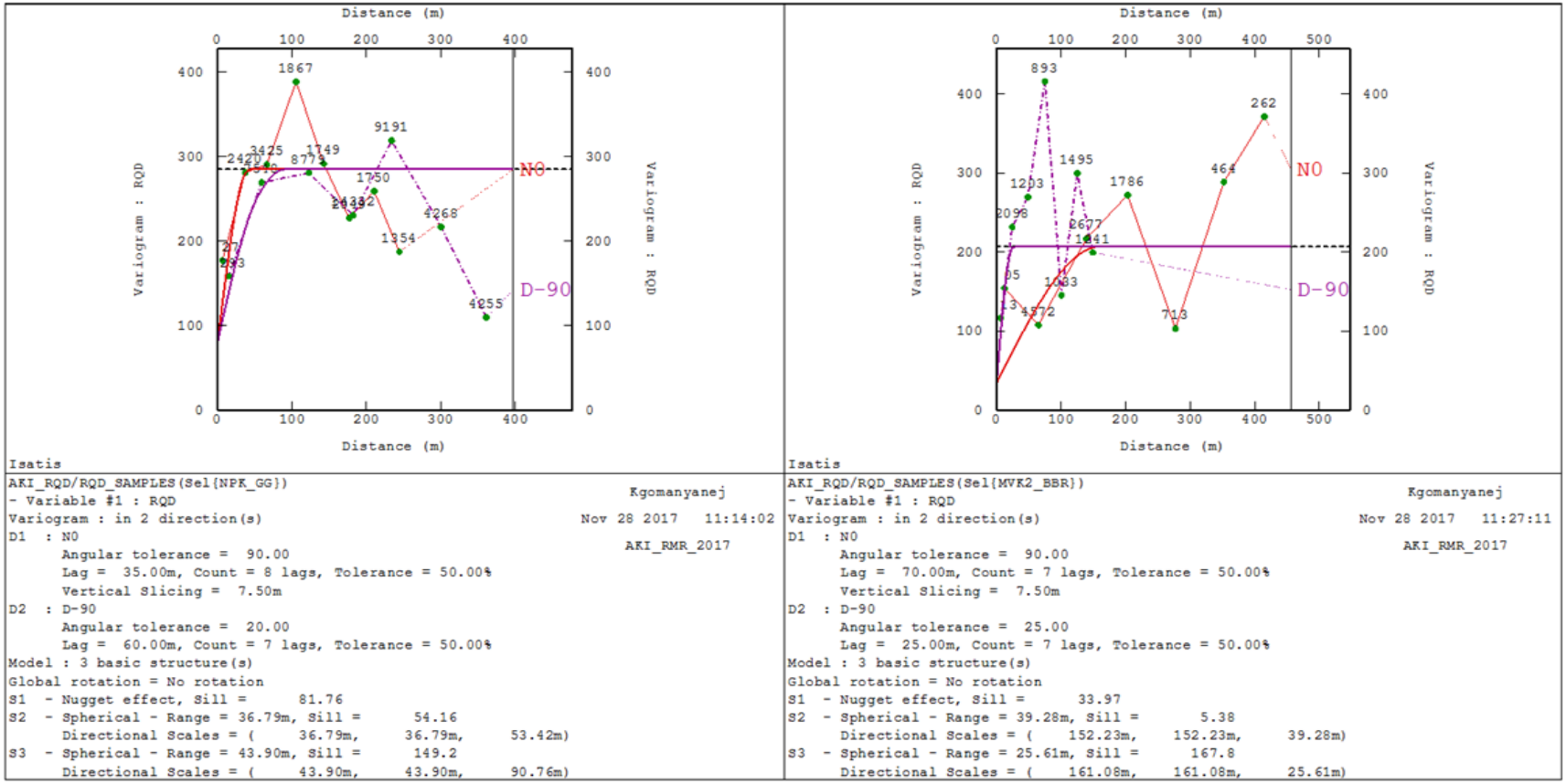
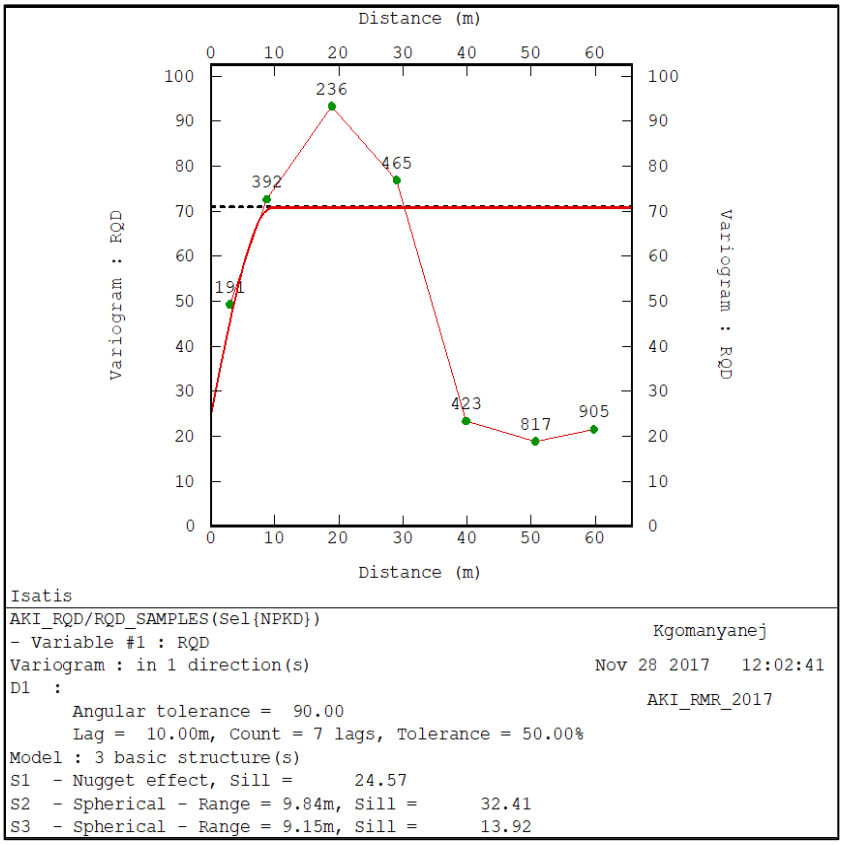


Figure 61 RQD variogram models – NPK_GG (left) and MVK2_BBR (right)

The last variogram model for the RQD parameter to be discussed, is for the NPKD rocktype, and is shown in Figure 62. The fitted RQD variogram model for this rocktype shows isotropic behaviour and it has been modelled at the experimental variance. This omnidirectional modelling approach has been adopted due to 'insufficient' number of measurement readings obtained from



this rocktype.

Figure 62 RQD variogram model – NPKD

8.4.1 RQD – Summary of Variogram Parameters

A summary of variogram parameters for RQD are presented in Table 11. All the variogram models are double structured spherical models and anisotropic except for the three rocktypes NPKD, A3T and SPK which are omnidirectional.

Table 11 RQD Variogram Model Parameters Summary per rocktype

Variogram Parameters						
Geological Unit	Structure Type	Sill	% Sill	Range (U)	Range (V)	Range (W)
BBR	Nugget	229.90	36%			
	Spherical	246.60	95%	66.71	66.71	100000
	Spherical	249.00	64%	181.25	181.25	47.89
DHB	Nugget	142.70	41%			
	Spherical	245.10	70%	82.82	82.82	31.48
	Spherical	27.83	8%	104.83	104.83	47
MVK2	Nugget	34.89	47%			
	Spherical	11.83	16%	159.64	159.64	7.64
	Spherical	14.85	20%	168.86	168.86	44.04
MVK2_BBR	Nugget	33.97	16%			
	Spherical	5.38	3%	152.23	152.23	39.28
	Spherical	167.80	81%	161.08	161.08	25.61
NPK	Nugget	37.77	27%			
	Spherical	47.85	34%	31.17	31.17	11.65
	Spherical	22.59	16%	100000	100000	33.14
NPK_GG	Nugget	81.76	29%			
	Spherical	54.16	19%	36.79	36.79	53.42
	Spherical	149.20	52%	43.9	43.9	90.76
NPKD	Nugget	24.57	35%			
	Spherical	32.41	46%			
	Spherical	13.92	20%	9.84	9.15	
SDVK	Nugget	76.22	69%			
	Spherical	2.62	2%	125.65	125.65	29.82
	Spherical	31.80	29%	275.86	275.86	112.29
SVK_U	Nugget	125.80	20%			
	Spherical	489.30	79%	41.76	41.76	18.6
	Spherical	1.77	0%	500000	500000	500000
SVK-M	Nugget	88.26	54%			
	Spherical	21.98	16%	39.66	39.66	8.81
	Spherical	29.20	30%	195.91	195.91	27.52
SVK_L	Nugget	105.40	58%			
	Spherical	45.01	25%	36.08	36.08	1000000
	Spherical	75.67	42%	63.47	63.47	12,56
SPK	Nugget	50.81	23%			
	Spherical	51.02	23%			
	Spherical	121.10	54%	29.76	189.42	
A3T	Nugget	433.4	62%			
	Spherical	70.52	10%			
	Spherical	190.8	27%	15.15	101.82	

8.5 Dry Density – Variograms

Similarly as for the other RMR input parameters discussed in the previous sections, variogram modelling for dry density (DD) was achieved following the same process, whereby firstly, experimental variograms for all rocktypes were

generated. Fitted variogram models were therefore constructed from the latter representing all rocktypes in the AK1 kimberlite. The variogram modelling was undertaken with a nugget effect and two or three spherical structures were observed. The dry density variogram models are discussed in the next subsections and Table 12 summarises the variogram parameters.

The fitted dry density variogram models for rocktypes BBR and DHB are illustrated in Figure 63. The model for the BBR rocktype has been fitted at the experimental variance (geometric anisotropy). Sample correlation is more pronounced in the horizontal direction than the vertical. The dry density model for the DHB rocktype also displays a geometric anisotropic behaviour. The variogram model for this rocktype has been fitted at the experimental variance and again sample correlation is more evident in the horizontal direction than the vertical direction.

Modelled dry density variograms for SVK_M and SVK_L are presented in Figure 64. The dry density variogram model for the SVK_M rocktype has been modelled at the experimental variance indicating a geometric anisotropic behaviour. For this variogram model on the SVK_M rocktype, the vertical continuity is longer than the horizontal. Therefore sample correlation is more evident in the vertical direction than the horizontal. The SVK_L variogram model also displays geometric anisotropic behaviour. The variogram has been modelled at the experimental variance for both structures. For the SVK_L rocktype, the opposite is true, that is, sample correlation has been more pronounced in the horizontal than in the vertical direction.

The dry density variogram models for rocktypes SDVK and NPKD are represented in Figure 65. The dry density variogram for SDVK rocktype shows zonal anisotropy with different sills on both structures. For this model on the SDVK rocktype, the longer horizontal structure has been modelled at the experimental variance while the vertical structure has been modelled below it. The horizontal structure shows more sample correlation than the vertical (longer range in the horizontal direction). The dry density variogram model for the NPKD rocktype shows a geometric anisotropic behaviour, both structures have been modelled at the experimental variance. The horizontal range is slightly longer than the vertical range. The dry density model for the NPKD rocktype has the lowest nugget of all rocktypes in the AK1 kimberlite pipe.

Figure 66 illustrates variogram models for rocktypes the NPK and MVK2. The dry density variogram model for the NPK rocktype has been modelled (both

directions) far below the experimental variance but displaying geometric anisotropic behaviour. The horizontal direction on this model shows a more pronounced sample correlation than the vertical (longer horizontal range). The dry density variogram model for the MVK2 rocktype shows a geometric anisotropic behaviour, both structures have been modelled far below the experimental variance. For this model on the MVK2 rocktype, the vertical range is longer than the horizontal.

Figure 67 shows dry density variogram models for rocktypes. NPK_GG and MVK2_BBR The dry density variogram model for NPK_GG displays geometric anisotropic behaviour with both structures having been modelled far below the experimental variance. The horizontal range on this model for the NPK_GG rocktype is longer than the vertical range. The dry density variogram model for the MVK2_BBR also shows geometric anisotropy but both structures have been modelled at the experimental variance. The horizontal range on the MVK2_BBR dry density model is much larger than the vertical range, so sample correlation is more pronounced in the horizontal direction than the vertical.

Figure 68 illustrates the dry density model for the SPK rocktype. The fitted dry density variogram model for this rocktype shows isotropic behaviour and it has been modelled to the experimental variance. This omnidirectional modelling approach has been adopted due to the insufficient number of measurement readings obtained from the SPK rocktype.

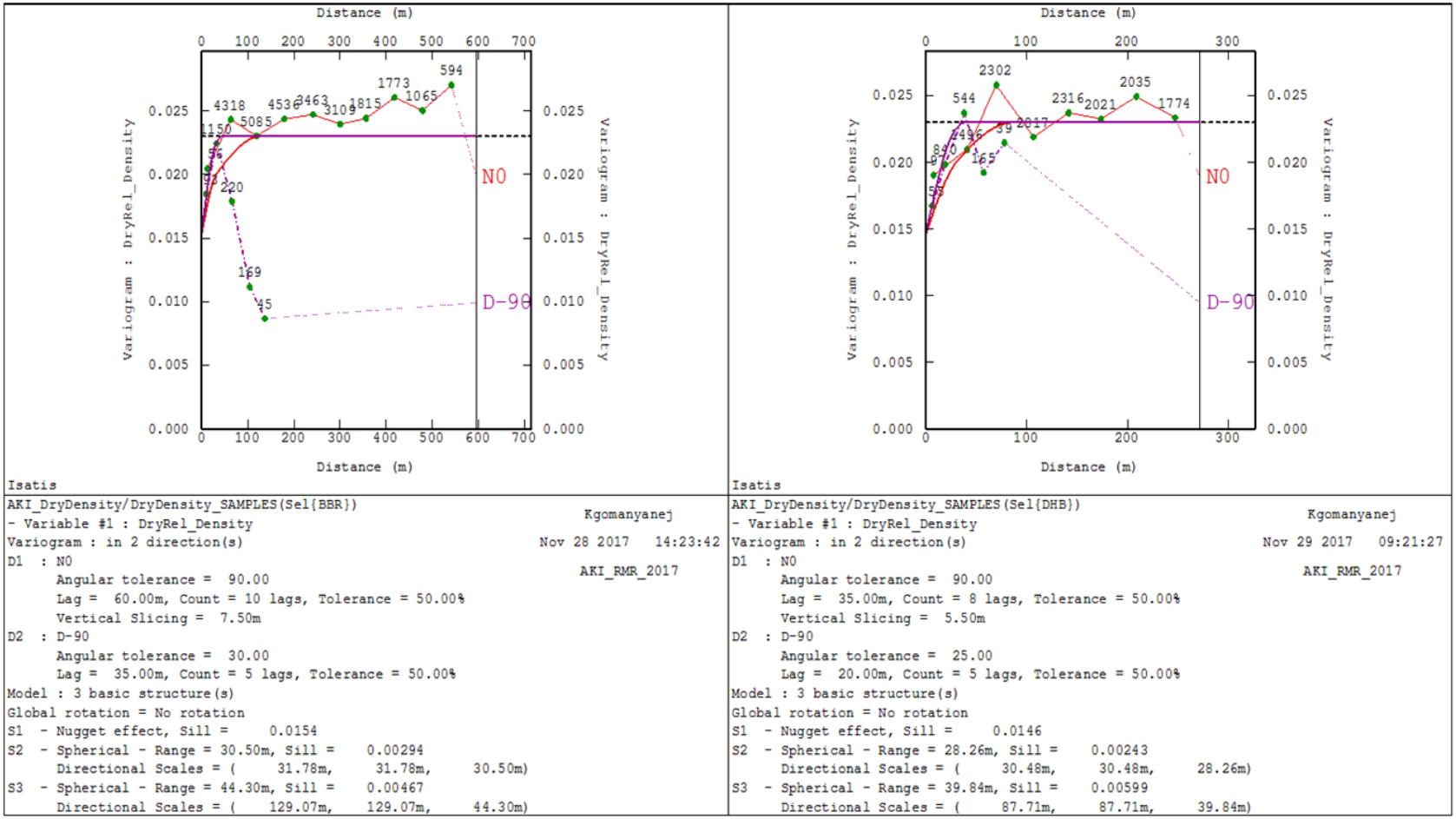


Figure 63 DD variogram models – BBR (left) and DHB (right)

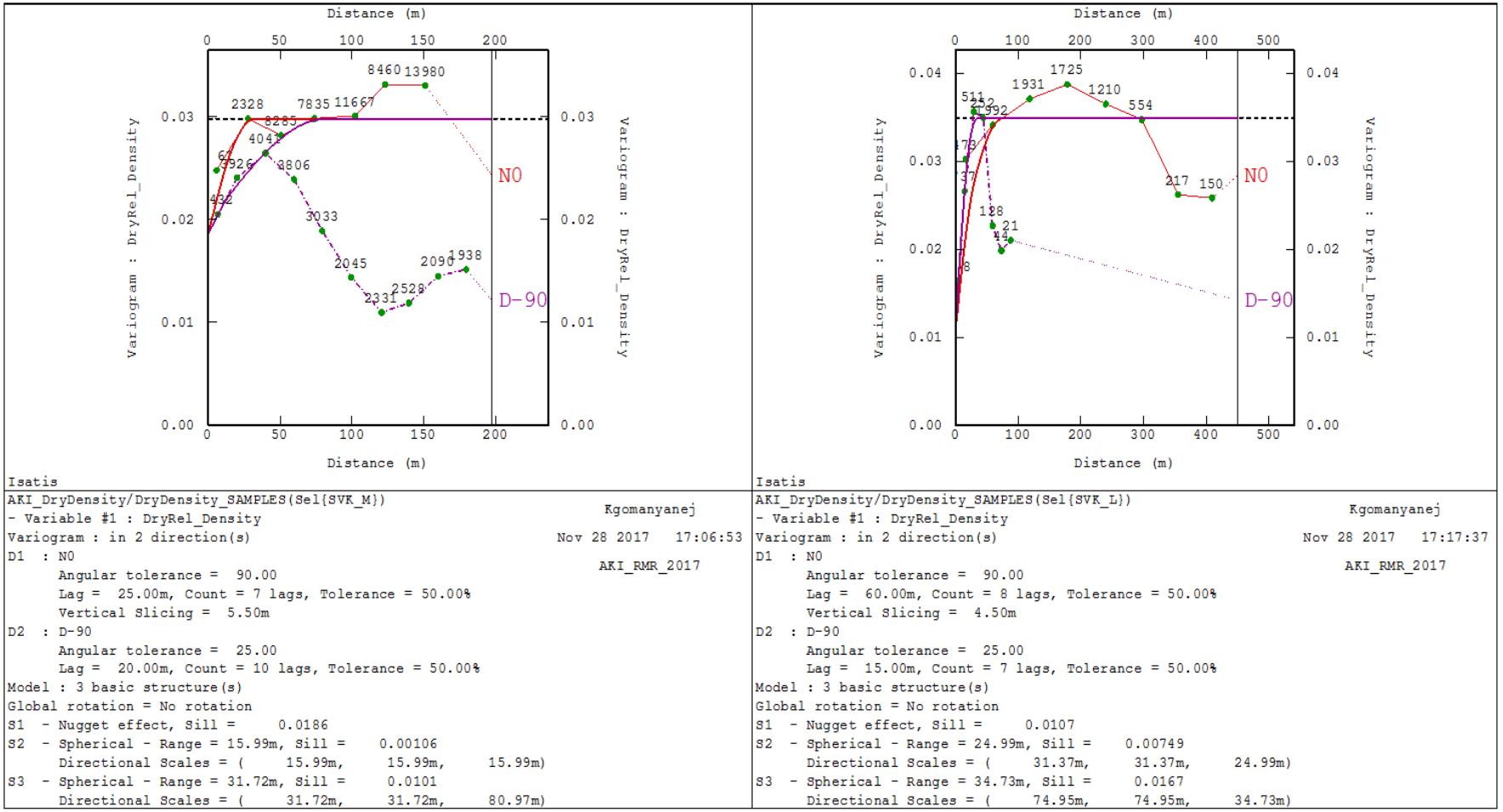


Figure 64 DD variogram models – SVK_M (left) & SVK_L (right)

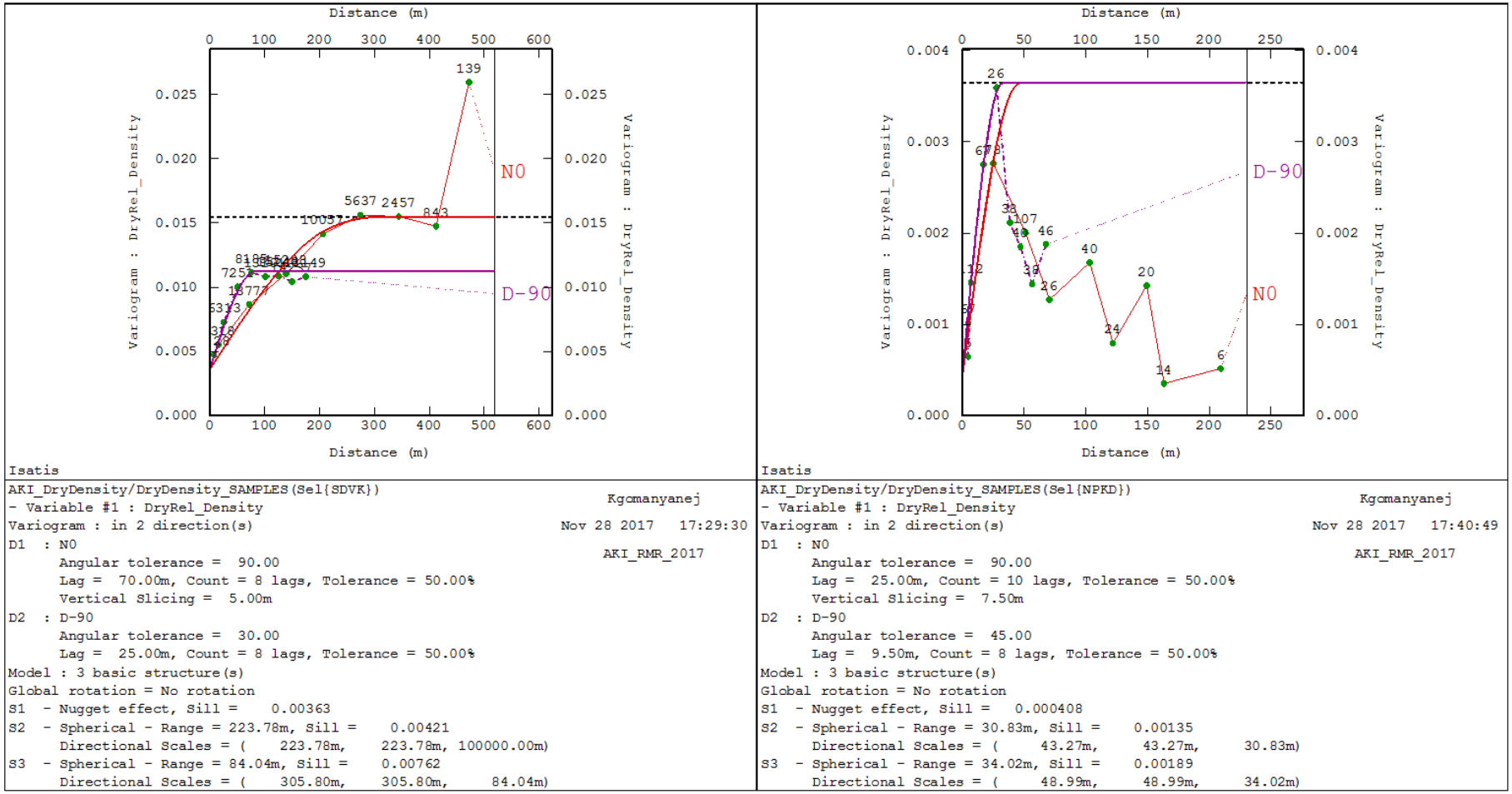


Figure 65 DD variogram models – SDVK (left) and NPKD (right)

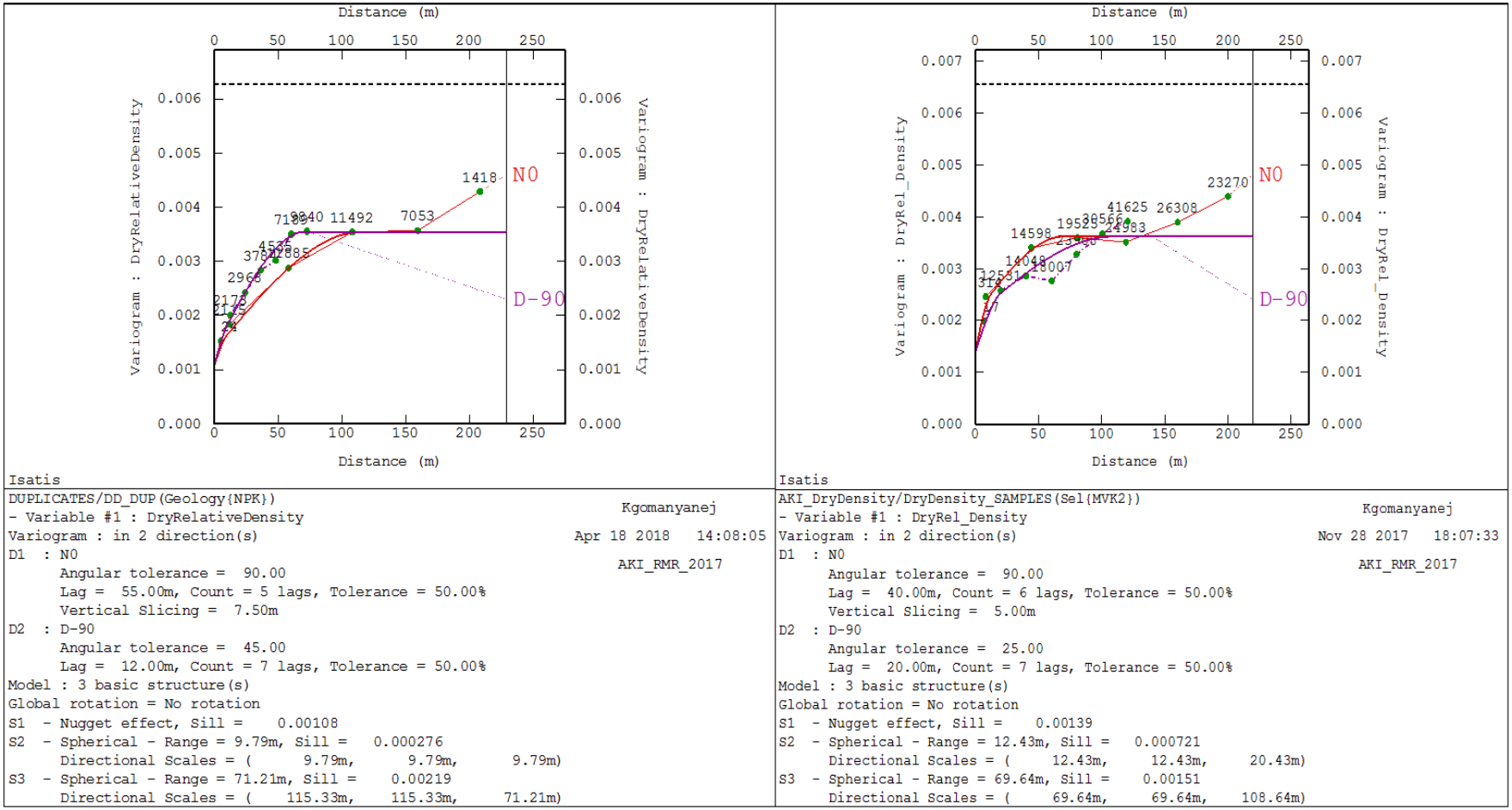


Figure 66 DD variogram models – NPK (left) and MVK2 (right)

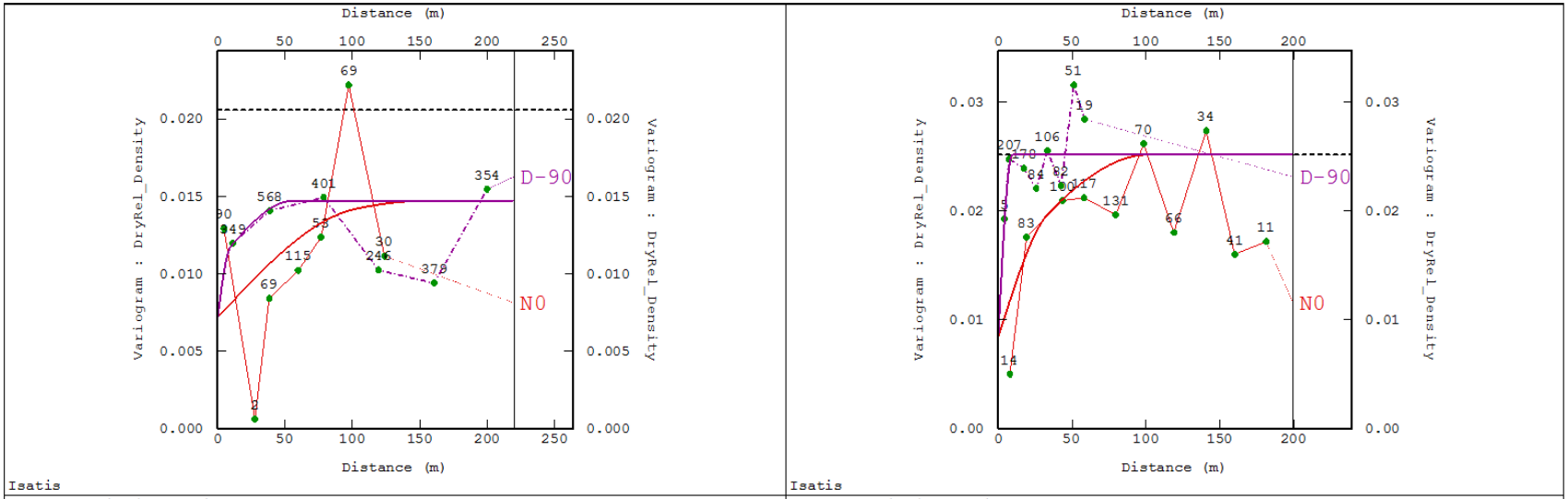


Figure 67 DD variogram models – NPK_GG (left) and MVK2_BBR (right)

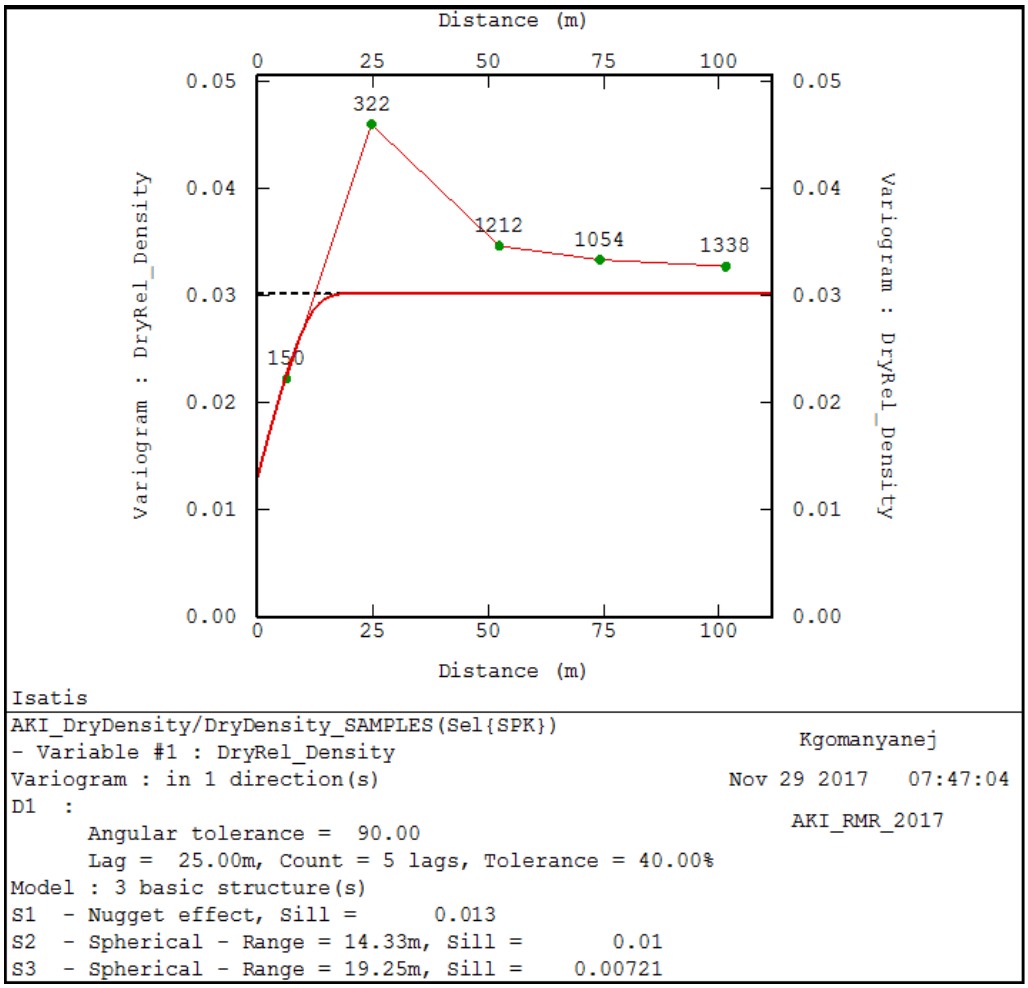


Figure 68 DD variogram model – SPK

8.5.1 DD– Summary of Variogram Parameters

The dry density variogram parameters are summarised in Table 12. The variogram models for all the rocktypes are double structured and anisotropic except the model for SPK which is isotropic. All the variograms have been modelled with a nugget effect.

Table 12 DD Variogram Model Parameters Summary per rocktype

Variogram Parameters							
Geological Unit	Structure Type	Type	Sill	% Sill	Range (U)	Range (V)	Range (W)
BBR	Anisotropic	Nugget	0.0154	67%			
		Spherical	0.0029	13%	31.78	31.78	30.5
		Spherical	0.0047	20%	129.07	129.07	44.3
DHB	Anisotropic	Nugget	0.0146	63%			
		Spherical	0.0024	11%	30.48	30.48	28.26
		Spherical	0.0060	26%	87.71	87.71	39.84
MVK2	Anisotropic	Nugget	0.00139	21%			
		Spherical	0.00072	11%	12.43	12.43	20.43
		Spherical	0.00151	23%	69.64	69.64	108.64
MVK2_BBR	Anisotropic	Nugget	0.0084	34%			
		Spherical	0.0104	42%	101.66	101.66	9.23
		Spherical	0.0064	26%	34.65	34.65	9.97
NPK	Anisotropic	Nugget	0.00108	19%			
		Spherical	0.00028	4%	9.79	9.79	9.79
		Spherical	0.00219	2%	115.33	115.33	71.21
NPKD	Anisotropic	Nugget	0.00041	11%			
		Spherical	0.00135	37%	43.27	43.27	30.83
		Spherical	0.00189	52%	48.99	48.99	34.02
NPK_GG	Anisotropic	Nugget	0.00719	33%			
		Spherical	0.00355	16%	152.96	152.96	9.51
		Spherical	0.00398	18%	101.42	101.42	56.13
SDVK	Anisotropic	Nugget	0.00363	24%			
		Spherical	0.00421	28%	223.78	223.78	100000
		Spherical	0.00762	50%	305.8	305.8	84.04
SVK_M	Anisotropic	Nugget	0.0186	62%			
		Spherical	0.0011	4%	15.99	15.99	15.99
		Spherical	0.0101	34%	31.72	31.72	80.97
SVK_L	Anisotropic	Nugget	0.0107	31%			
		Spherical	0.0075	21%	31.37	31.37	24.99
		Spherical	0.0167	48%	74.95	74.95	34.73
SPK	Isotropic	Nugget	0.0130	43%			
		Spherical	0.0100	33%			
		Spherical	0.0072	24%	14.33	19.25	

In this chapter the variogram models of the RMR parameters including DD for all the AK1 rock were established. The variogram results have been interpreted and elaborated on for each RMR parameter. Summaries of the variogram models for each RMR parameter presented in Tables 9 to 12, the latter containing the dry density variogram models. The variogram models for each RMR parameter are as expected and are aligned to the AK1 pipe geology as interpreted.

9 KRIGING NEIGHBOURHOOD OPTIMISATION

9.1 Methodology

To reduce conditional bias, it is essential to determine the optimum kriging parameters to be used in the estimation process. These parameters are chosen by the resource estimator. It is therefore essential to carry out a Kriging Neighbourhood Analysis (KNA) and identify the optimal kriging neighbourhood for each of the RMR parameters based on their modelled variograms within each of the lithological units. The optimum kriging neighbourhood is defined by the search volume with the best slope of regression i.e. closest to 1 (Rivoirard, 1987). The chosen search volume can have a significant impact on the quality and outcome of the kriging estimate. Kriging is commonly described as 'minimum variance estimator' but only when the neighbourhoods are properly defined. The process of assessing a kriging neighbourhood is called Quantitative Kriging Neighbourhood Analysis (QKNA) (Vann et al., 2003).

Decisions on the kriging neighbourhoods are risky because the kriging weights; assigned to the samples values; are directly related to what is known as the kriging neighbourhood and this is a function of the variogram model, data geometry (block size and shape and the sample support), search volumes and directions as well the number of samples considered in the kriging estimation process. To reduce or eliminate conditional bias the KNA involves adjusting the kriging neighbourhood parameters with the aim to achieve slope of regression (SOR) values close to 1. It is assumed that the variogram is correctly modelled, representative of the domain of interest (intrinsic stationarity i.e. variance of the difference is the same between any two points in the same direction and at the distance apart), and the relationship between true values and estimated values is linear (Vann et al., 2003), (Dohm, 2013b).

Orapa is a well-established mine with fixed mining blocks thus there was no point in optimising the block size as recommended by Vann et al. (2003). The Orapa AK1 Block Model extends to 1200m below surface and all the blocks within the AK1 pipe geometry, were populated with estimates to this depth. The resource estimation methodology is Ordinary Kriging into a resource model with a fixed block size of 50m x 50m x 15m. The block discretization applied is 10 x 10 x 3, thus sub-dividing the blocks into 5m x 5m x 5m cubes in

the kriging process. The discretization of the blocks are used to calculate the average point to block values from the variogram for each sample and establish right hand side of the kriging equations of any local block estimate.

It was thus natural to use Ordinary Kriging for the local estimation of the RMR parameters investigated in this research report. In all cases, the relevant variogram models were applied to the RMR parameters and the specific rocktype. Other predefined kriging parameters applied to all rock-types were the minimum number of samples to be used for an estimate which was set to three (3), the number of angular sectors to be used was set at four (4) and the maximum number of samples per sector to ten (10). Therefore the maximum number of samples was implicitly set at forty (40).

Before completion of KNA, the de-clustering process was undertaken. The most common method applied in geostatistics is cell de-clustering (Isaaks and Srivastava, 1989). The cell de-clustering method overlays the data into a regular grid and assigning cell weights. The weights assigned by cell de-clustering are sensitive to the cell size. The cell sizes were set at minimums of 10m and maximums of 100m for x, y and z directions. A specific cell size will result in a unique set of weights. Therefore, the cell size was configured such that it minimized or maximized the de-clustered sample mean.

Therefore, for the optimisation of the Kriging Neighbourhood in this research, only the search volumes were varied to obtain the best (close to 1) slope of regression of true grade on estimated grade. The slope of regression (SOR) is a measure of conditional bias and the neighbourhood parameters that would achieve a high slope of regression would minimise the conditional bias (Vann et al., 2003). In the assessment of the RMR kriging neighbourhood attention thus focussed on the slope of regression, the proportion of blocks estimated within a search volume, the maximum percentage negative weights, the maximum positive weight, and the average number of samples used for the estimate. Other measures considered were less important in the assessment; these are all presented in the KNA results tables.

In all cases, a First Pass estimate (P1_Est) was utilised and the neighbourhoods were optimized such that the variogram ranges were not exceeded and the negative weights were kept to below 5%. A Second Pass estimate (P2_Est) was run, where there was still a chance to extend the neighbourhoods but not exceeding the modelled variogram ranges.

The process outlined above was repeated for all the rocktypes where local estimation was going to be carried out and for the four parameters (UCS, FFPM, RQD and Dry Density). Figures 69 and 70 show examples of neighbourhood optimisation for UCS and RQD parameters respectively. Examples of the KNA results for the UCS (SVK_M) and RQD (NPK) are illustrated in Tables 13 and 14 respectively.

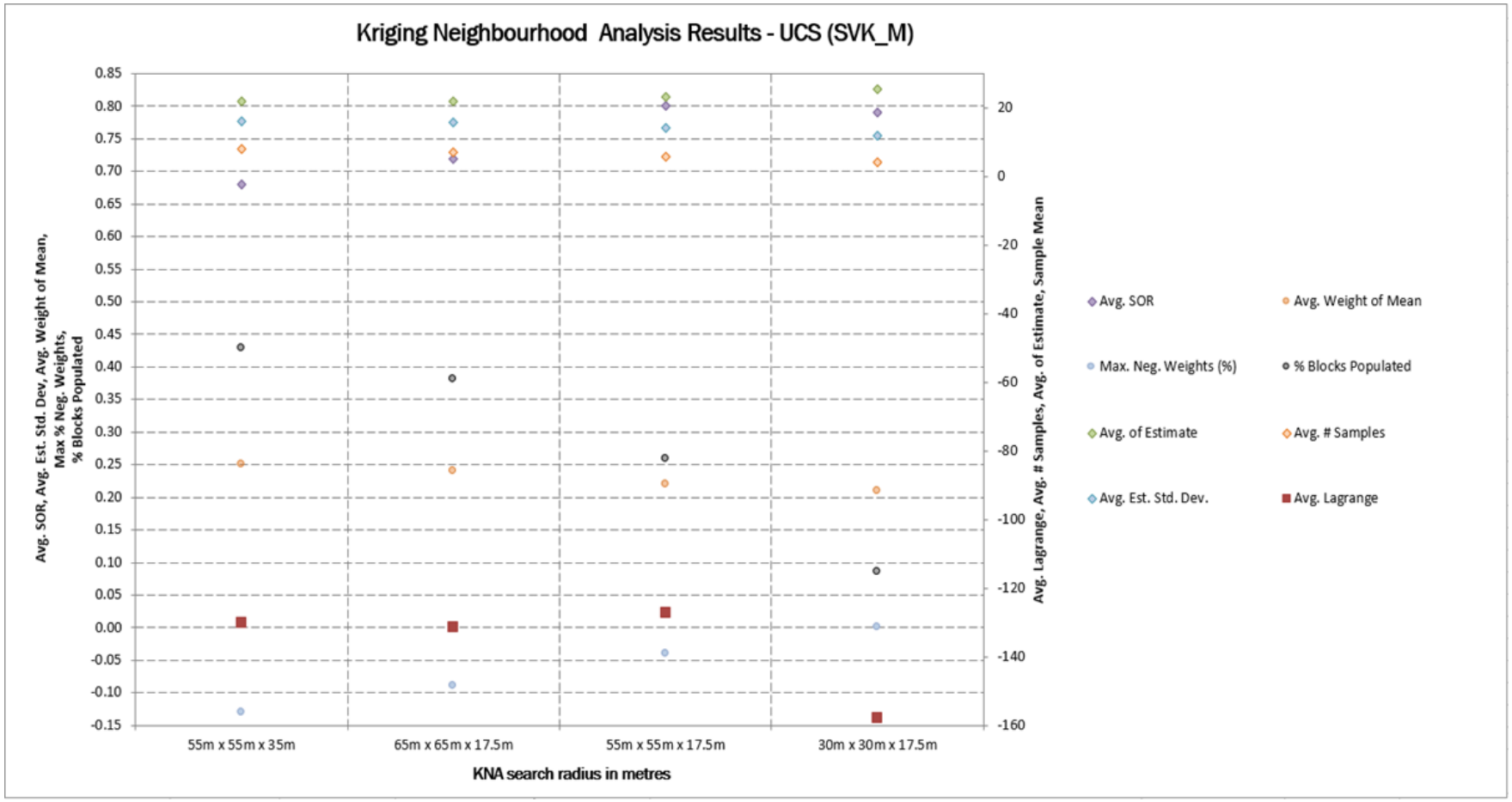


Figure 69 UCS Neighbourhood analysis results – SVK_M

Table 13 shows the UCS KNA results for (SVK_M) and have been used to identify of the optimal search volume.

Using the P1_Est_SVK_M (30m x 30m x 17.5m) search volume, only 8.5% of the blocks were estimated, which is a poor performance, but it had no negative weights and an acceptable SOR of 0.79. The highest SOR was obtained for the 55m x 55m x 17.5m search volume. P2_Est_SVK_M (55m x 55m x 17.5m) show reasonably informed blocks, second lowest standard deviation and the highest slope of regression at 0.80, 4 % negative weights, which is acceptable .On increasing the search radius to 65m, the negative weights increased to 9%, which is unacceptable (beyond the 5% cut-off).

The remaining search volumes shown in Table 13 have lower slopes of regression, increased negative weights percentages. Consequently, there was no point in increasing the search radius as the 'estimated' values have been increasingly varying from the 'true' UCS values. Therefore the search volumes highlighted in green and yellow, have been selected as optimal and appropriate for first and second pass estimation of the UCS of the SVK_M rocktype. The same approach has been applied to all the other RMR input parameters and associated rocktypes.

Table 13 Summary UCS KNA results – SVK_M

Search Radii in m	55 x 55 x 35	65 x 65 x 17.5	55 x 55 x 17.5	30 x 30 x 17.5
Total # of Blocks	1,816	1,816	1,816	1,816
# Blocks Populated	778	691	471	155
Max Pos. Weights	1.13	1.09	1.04	1.00
Avg. of Estimate	22.02	22.03	23.33	25.35
Avg. Lagrange	-129.99	-131.32	-127.29	-157.94
Avg. # Samples	8.16	7.12	5.95	4.25
Avg. SOR	0.68	0.72	0.80	0.79
Avg. Est. Std. Dev.	15.97	15.78	14.25	12.06
Avg. Weight of Mean	0.25	0.24	0.22	0.21
Max. Neg. Weights (%)	13.00%	9.00%	4.00%	0.00%
% Blocks Populated	42.84%	38.05%	25.94%	8.54%

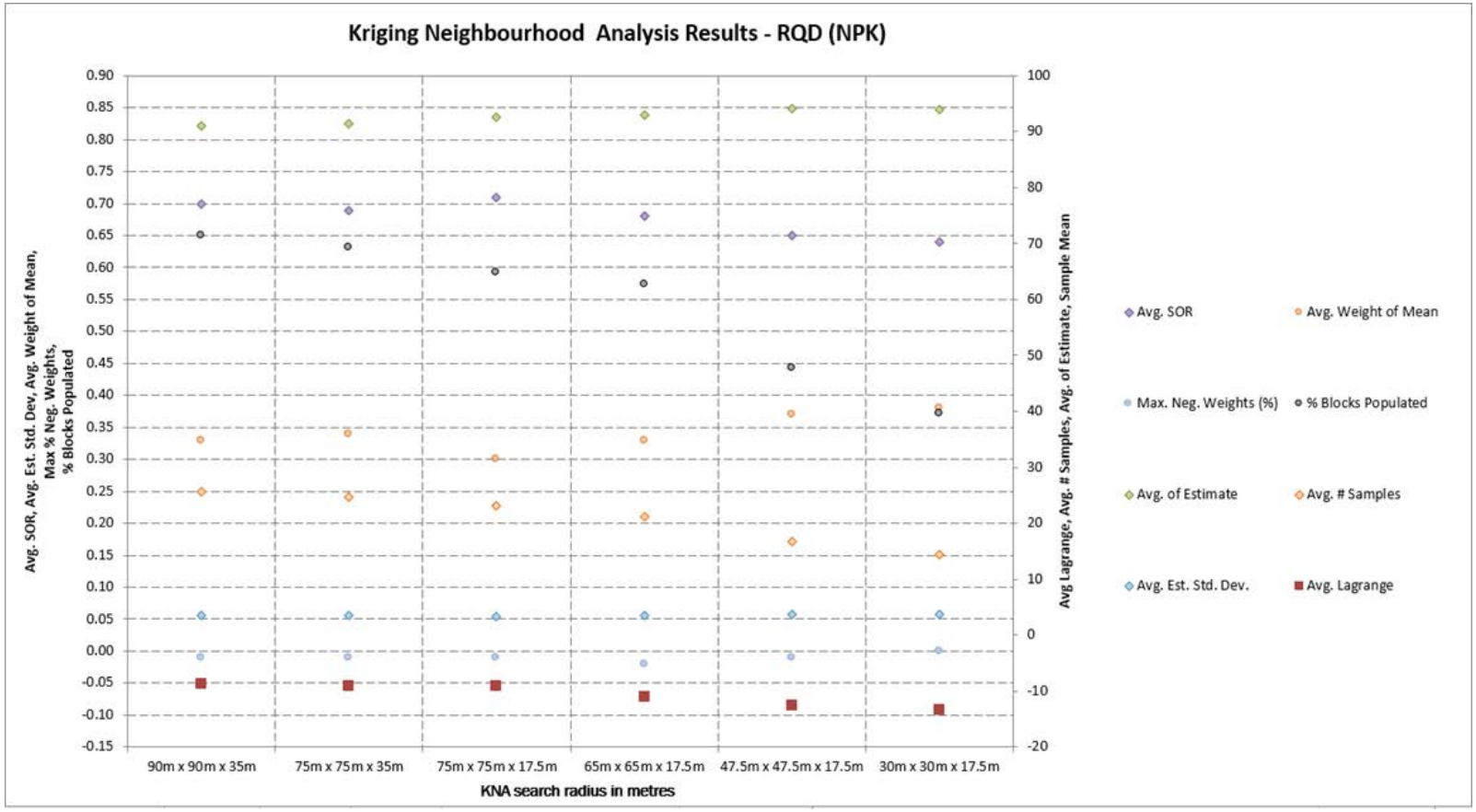


Figure 70 RQD Neighbourhood analysis results – NPK

Figure 70 shows a graphical presentation of KNA results for the RQD parameter in the NPK rocktype while Table 14 summarises the results numerically. P1_Est_NPK (30m x 30m x 17.5m) search radius has no negative weights, but reported a poor percentage of estimated blocks, the highest standard deviation and the lowest SOR. P2_Est_NPK (75m x 75m x 17.5m) gave the highest SOR, reasonably informed blocks, lowest standard deviation and 1% negative weights. The weight of the mean for this search radius is the lowest of all searches. These two search configurations have been selected as optimal and appropriate for the RQD parameter in the NPK rocktype compared to the rest of the search volumes considered.

Table 14 Summary RQD KNA results – NPK

Search Radius	90m x 90m x 35m	75m x 75m x 35m	75m x 75m x 17.5m	65m x 65m x 17.5m	47.5m x 47.5m x 17.5m	30m x 30m x 17.5m
Total # of Blocks	1,431	1,431	1,431	1,431	1,431	1,431
# Blocks Populated	930	903	848	822	635	533
Max Pos. Weights	1.01	1.01	1.01	1.02	1.01	1.00
Avg. of Estimate	91.11	91.46	92.51	92.99	94.07	93.86
Avg. Lagrange	-8.62	-9.17	-9.17	-10.97	-12.63	-13.42
Avg. # Samples	25.60	24.59	23.04	21.11	16.79	14.31
Avg. SOR	0.7	0.69	0.71	0.68	0.65	0.64
Avg. Est. Std. Dev.	3.50	3.57	3.34	3.54	3.68	3.73
Avg. Weight of Mean	0.33	0.34	0.30	0.33	0.37	0.38
Max (%) Neg. Weights	1.00%	1.00%	1.00%	2.00%	1.00%	0.00%
% Blocks Populated	64.99%	63.10%	59.26%	57.44%	44.37%	37.25%

9.2 Kriging of RMR parameters based on the KNA outcomes

The 1st Pass (P1_Est) and 2nd Pass (P2_Est) neighbourhood optimisation were applied to the different rocktypes so as to populate the blocks with estimates. Where applicable, a moving average (MA) was applied to populate the remaining blocks that had not been estimated.

Furthermore, for rocktypes that extend vertically, DHB, SDVK, MVK2, NPK and NPK_GG, a decision was made to populate the blocks that remained unpopulated after the MA was applied using a global estimation. This was achieved by using the zonal average of the final three benches of the sample data. Figures 71 and 72 illustrate examples of 1st Pass (P1_Est) and 2nd Pass (P2_Est) in the kriging neighbourhood optimisation process on the SDVK rocktype.

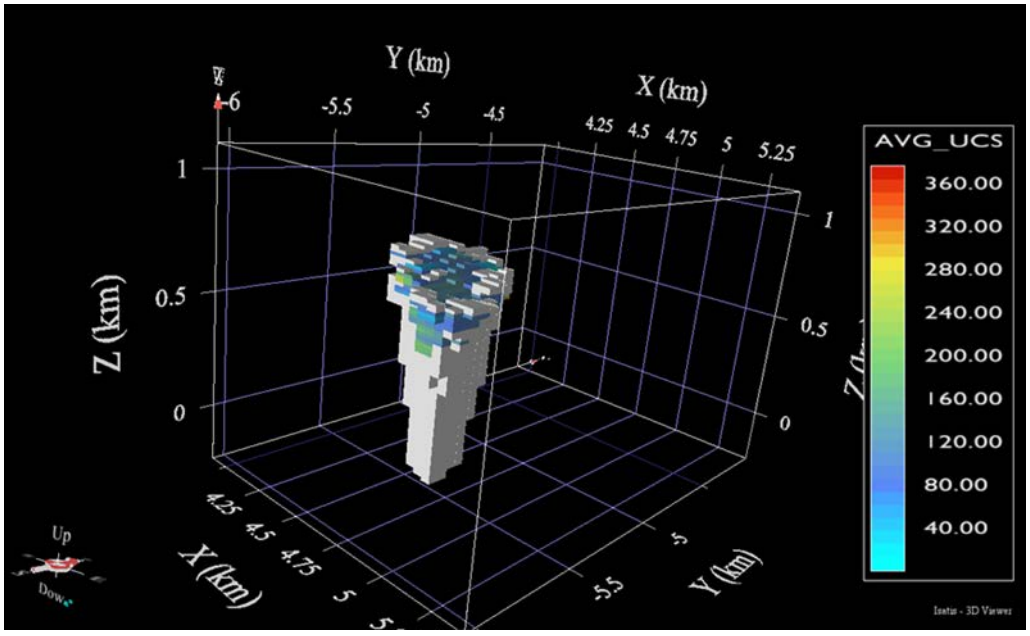


Figure 71 SDVK block model of UCS kriged blocks after the 1st pass

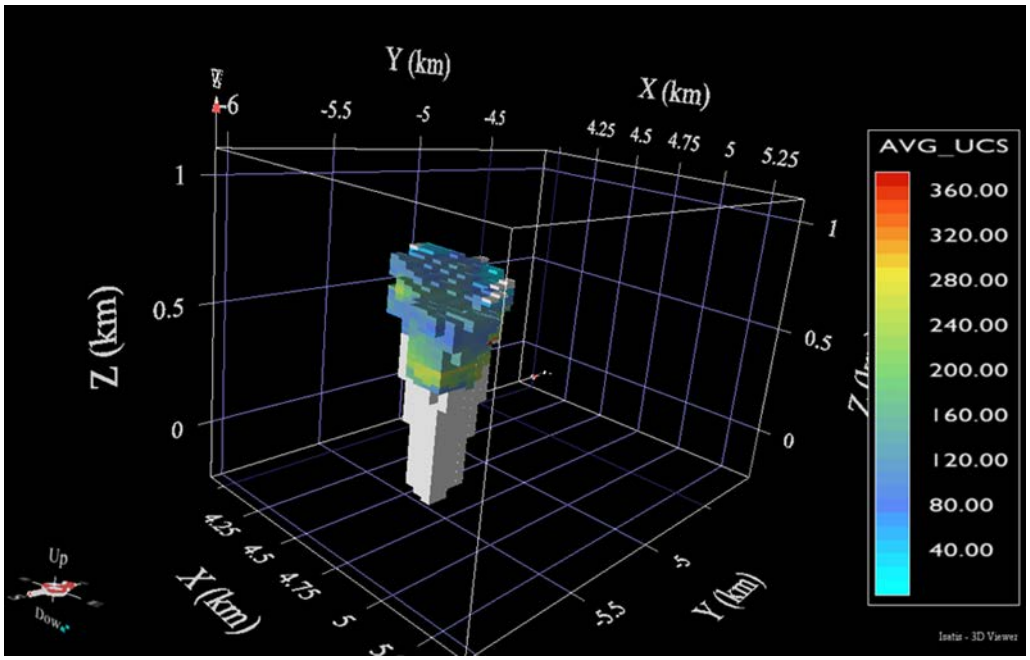


Figure 72 SDVK block model of UCS kriged blocks after the 2nd pass

9.3 Summary of Neighbourhood Optimisation Results

The optimised kriging neighbourhoods for RMR parameters within all the different rocktypes that were subjected to the estimation process are tabulated in Table 15.

It is clear from Table 15 that some rocktypes such as SPK, SVK_M, SVK_L, BBR, and NPKD are 100% populated using the MA methodology. These rocktypes are laterally extensive and constitute the upper sedimentary units of the AK1 kimberlite pipe. Where there were unpopulated blocks after applying the MA, a global estimate was applied, a feature which was applicable to geological units that extend vertically. Caution must be taken when interpreting these bench plots as this was mainly done for completeness of the estimation process, there was inadequate data at the lower benches hence the decision to use global extrapolation.

Table 15 UCS, FFPM, RQD & DD Kriging Neighbourhood optimisation results

UCS										
Rock Type	Ordinary Kriging Estimate								Moving Average Estimate	
	Min # Samples	Optimum # Sectors		No. of Blocks	1st Pass Neighbourhood	% Blocks Estimated	2nd Pass Neighbourhood	% Blocks Estimated	MA Neighbourhood	% Blocks Estimated
SDVK	3	10	4	2107	87.5x87.5x35	48.79%	157.5x157.5x47.5	63.41%	400x400x300	88.32%
SVK_M	3	10	4	1816	30x30x17.5	8.54%	55x55x17.5	25.94%	300x300x200	100%
SVK_L	3	10	4	614	75x75x17.5	42.35%	87.5x87.5x35	70.68%	200x200x100	100%
BBR	3	10	4	2736	87.5x87.5x17.5	12.24%	110x110x35	21.64%	450x450x300	100%
DHB	3	10	4	2998	60x60x17.5	12.58%	87.5x87.5x17.5	38.29%	400x400x350	87.46%
NPK	3	10	4	1431	30x30x17.5	11.95%	75x75x35	47.66%	400x400x300	95.81%
MVK2	3	10	4	3866	47.5x47.5x17.5	16.32%	110x110x35	55.10%	350x350x250	91.13%
FFPM										
A3T	3	10	4	2013	57.5x57.5x17.5	3.18%	105x105x35	10.68%	450x450x350	88.62%
SPK	3	10	4	239	47.5x47.5x17.5	59.83%	120x120x17.5	88.70%	150x150x50	100%
BBR	3	10	4	2736	75x75x17.5	32.05%	137.5x137.5x35	49.74%	450x450x300	100%
DHB	3	10	4	2998	30x30x17.5	19.31%	65x65x17.5	41.63%	400x400x300	89.29%
SDVK	3	10	4	2107	55x55x17.5	48.17%	110x110x47.5	62.65%	400x400x300	90.27%
SVK_U	3	10	4	2456	65x65x17.5	7.25%	127.5x127.5x17.5	19.14%	450x450x350	98.73%
SVK_M	3	10	4	1816	30x30x17.5	44.55%	75x75x17.5	71.04%	250x250x150	100%
SVK_L	3	10	4	614	55x55x17.5	73.45%	110x110x17.5	91.04%	200x200x100	100%
NPK	3	10	4	1431	47.5x47.5x17.5	43.40%	110x110x17.5	63.52%	400x400x300	96.65%
MVK2	3	10	4	3866	55x55x17.5	46.95%	137.5x137.5x17.5	61.48%	400x400x300	92.08%
MVK2_BBR	3	10	4	416	30x30x17.5	26.20%	87.5x87.5x17.5	62.98%	300x300x200	100%
NPK_GG	3	10	4	788	60x60x17.5	43.78%	87.5x87.5x35	63.32%	350x350x250	92.13%
RQD										
A3T	3	10	4	2013	65x65x17.5	4.62%	105x105x35	11.23%	450x450x350	87.38%
SPK	3	10	4	239	47.5x47.5x17.5	61.51%	120x120x17.5	88.70%	150x150x50	100%
BBR	3	10	4	2736	55x55x17.5	23.25%	110x110x17.5	38.08%	450x450x350	100%
DHB	3	10	4	2998	30x30x17.5	22.75%	75x75x17.5	46.66%	400x400x300	85.19%
SDVK	3	10	4	2107	75x75x17.5	57.43%	137.5x137.5x47.5	68.72%	400x400x300	91.98%
SVK_U	3	10	4	2456	55x55X17.5	7.33%	87.5x87.5x35	20.52%	450x450x350	98.21%
SVK_M	3	10	4	1816	30x30x17.5	48.13%	87.5x87.5x17.5	80.51%	300x300x200	100%
SVK_L	3	10	4	614	30x30x17.5	47.88%	87.5x87.5x17.5	87.46%	200x200x100	100%
NPKD	3	10	4	101	15x15x15	41.58%	37.5x37.5x35	68.32%	75x75x55	100%
NPK	3	10	4	1431	30x30x17.5	37.25%	75x75x17.5	59.26%	350x350x250	95.81%
MVK2	3	10	4	3866	47.5x47.5x17.5	16.32%	110x110x17.5	55.10%	350x350x250	92.45%
MVK2_BBR	3	10	4	416	17.5x17.5x17.5	22.36%	47.5x47.5x17.5	34.86%	250x250x150	89.18%
NPK_GG	3	10	4	788	30x30x17.5	19.92%	65x65x35	57.99%	300x300x200	89.97%
DRY DENSITY										
SPK	3	10	4	239	47.5x47.5x17.5	61.51%	120x120x17.5	88.70%	200x200x100	100%
BBR	3	10	4	2736	65x65x17.5	19.15%	110x110x35	35.16%	450x450x300	100%
DHB	3	10	4	2998	65x65x17.5	3.57%	137.5x137.5x17.5	11.64%	450x450x350	77.45%
SDVK	3	10	4	2107	30x30x17.5	23.45%	65x65x17.5	45.80%	400x400x300	89.27%
SVK_M	3	10	4	1816	47.5x47.5x17.5	35.74%	87.5x87.5x17.5	64.10%	300x300x200	100%
SVK_L	3	10	4	614	30x30x17.5	29.80%	110x110x17.5	84.04%	200x200x100	100%
NPK	3	10	4	1431	30x30x17.5	24.53%	65x65x17.5	45.49%	350x350x250	94.90%
MVK2	3	10	4	3866	47.5x47.5x17.5	36.50%	110x110x17.5	58.69%	350x350x250	92.16%
MVK2_BBR	3	10	4	416	47.5x47.5x17.5	23.08%	110x110x17.5	57.69%	350x350x250	100%
NPK_GG	3	10	4	788	55x55x17.5	24.37%	110x110x17.5	50.76%	300x300x200	89.21%
NPKD	3	10	4	101	17.5x17.5x17.5	30.69%	65x65x17.5	80.20%	100x100x55	100%

9.4 Estimation Validation

The RMR parameter estimates were validated by applying the following fundamental checks:

- Three-dimensional visualizing of the estimates 1st Pass & 2nd Pass) in the ISATIS^{TM} 2016.2 3D viewer. All samples assigned a particular rock code must appear inside the blocks of the same rock type.
- Tabulation of RMR sample classical statistics with mean block estimates for all the estimated rock types for evaluation of percent mean differences.
- Graphical presentation of de-clustered mean sample values with mean estimates of kriged 1st Pass, 2nd Pass, Moving Average (MA) and Final estimates (bench plots) where applicable were carried out.

9.4.1 Sample Averages versus Estimated Values

Comparisons of basic statistics of the input samples and block estimates for all the RMR parameters for the different rocktypes, were carried out using the tabulated summary statistics of the two to determine the confidence level on the estimation process. Where there were too few samples for local estimation, the average (global) values of the samples were considered more appropriate than kriging estimation.

9.4.2 Bench Plots

Bench plots were created by plotting the bench elevations against the de-clustered sample values and the mean block estimates (P1_Est, MA, and Final_Est) for all rocktypes. An example of a bench plot for the UCS variable for rocktype MVK2 is presented in Figure 73. The bench plots assisted in the determination of an estimate value of the RMR parameter at any given elevation within the AK1 pipe. Note that the mining bench height for Orapa Mine open pit are set at 15m, therefore the estimates are determined every 15m. Due to the vertical extent of some of the AK1 rocktypes, some of the bench plots have the x-axes crossing the y-axes at the lower values. Again, due to mining activities, there is no data for the upper benches hence the estimates extend beyond the sample data. The number labels on the graph represent the number of samples per bench. All the sample data and estimate values were exported from ISATIS^{TM} 2016.2 software to Microsoft Excel

spreadsheets using the application of pivot table functionality in Microsoft Excel. The sample data distributions for all the RMR parameters and resulting bench plots are attached at the end of this report, see APPENDICES.

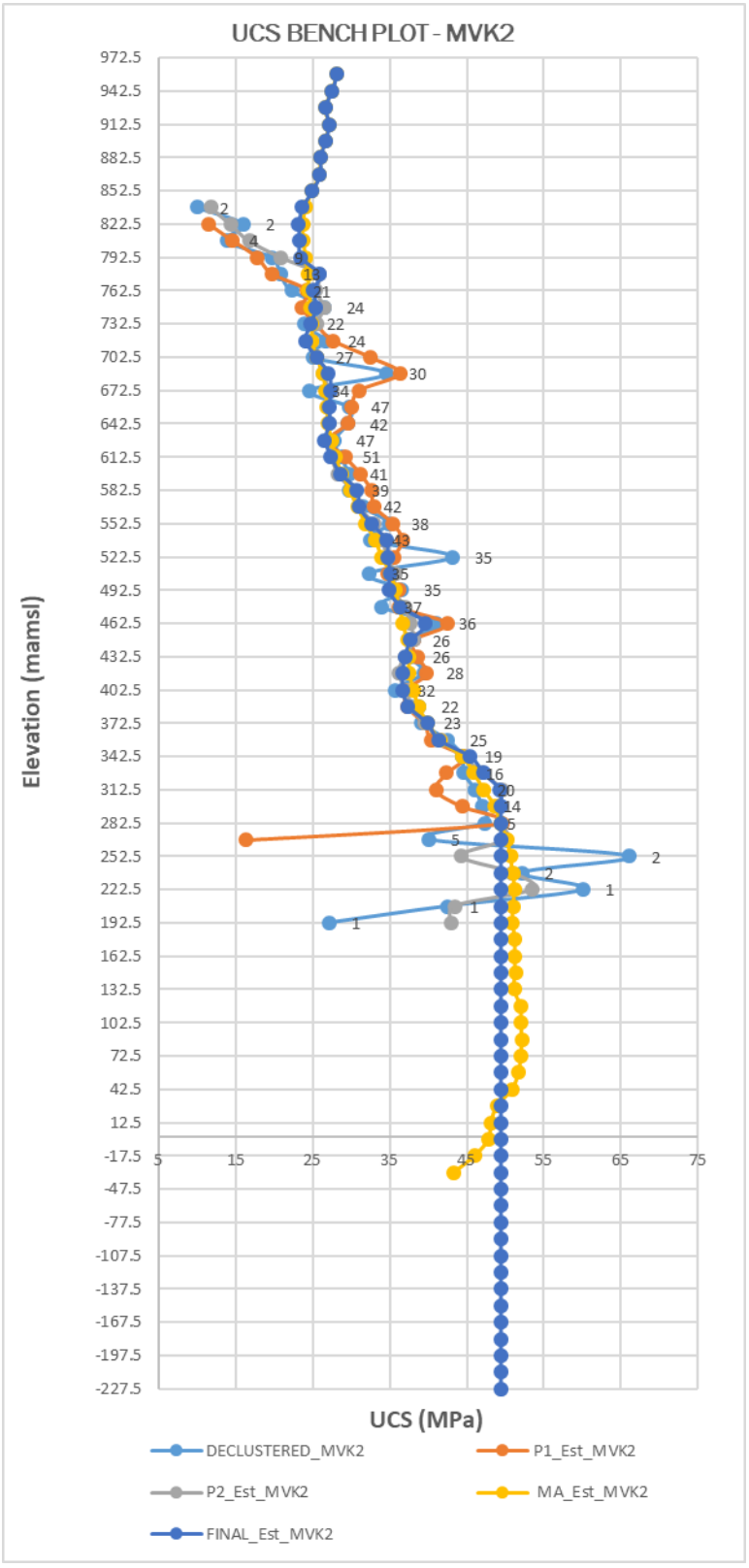


Figure 73 UCS Bench plot for – MVK2

This chapter focussed on the kriging neighbourhood optimisation methodology. The kriging neighbourhood analysis (KNA) and optimising methods were broadly discussed by referencing industry experts. Simulated KNA outcomes based on the RMR parameter variogram models within the AK1 rocktypes were used to identify the optimised search volumes to be used in the kriging process. The KNA results for each RMR parameter were presented in Tables 13 to 15. The RMR estimates were validated and compared with sample averages per bench to establish the accuracy and confidence of the estimates. Concluding this chapter, bench plots for each rocktype were generated by plotting de-clustered samples, 1st Pass estimate, 2nd Pass estimate, moving average (MA) and final estimate against bench elevations. The results on the bench plots are presented in the APPENDICES at the end of this research report.

10 DISCUSSION OF ESTIMATION RESULTS

In this research report the spatial characterisation and estimation of RMR input parameters was undertaken through the application of statistical and geostatistical techniques. The exploratory data analyses included, classical statistics, graphical presentation of the data (box plots, histograms and cumulative distributions plots), variography, kriging estimation and bench plots analysis. The application of the analytical tools outlined above has led to an enhanced level of understanding of the behaviour of the RMR parameters within the various Orapa AK1 (kimberlite) rock types in the mining value chain process.

It is this understanding that will be applied to reduce uncertainties associated with the RMR parameters in the various rock types within the AK1 kimberlite and associated inherent mining business risks. The objective of this research study was to develop an approach that would result in an estimation methodology that would populate each block for every RMR parameter with the final estimate (Final_Est). Figure 74 illustrates an unpopulated block model for the SDVK rocktype prior to local block estimation of the UCS variable.

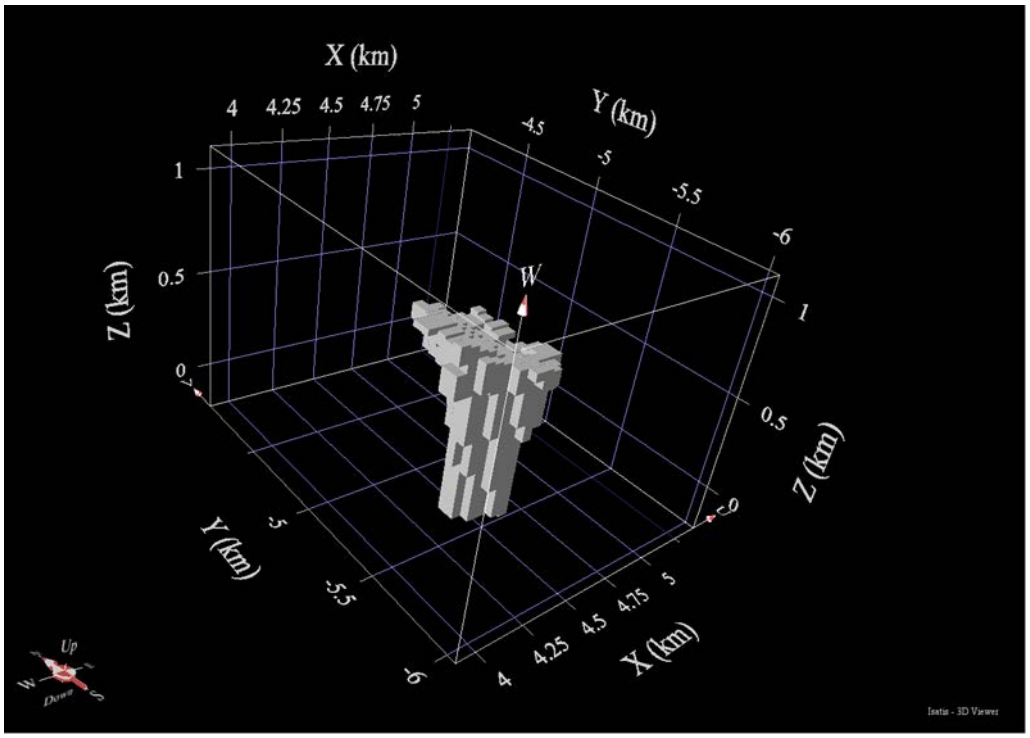


Figure 74 UCS unpopulated (0%) block model for SDVK

The local block estimation process entailed populating each rock type with the RMR input parameters, using firstly Ordinary Kriging (OK), secondly where blocks could not be estimated by OK, the moving average (MA) methodology was applied and thirdly in cases where the MA also ran out of data a global estimate was applied. This process resulted in local block estimates for the various Orapa AK1 kimberlite rocktypes. A view of 100% RMR (Final_Est_UCS) populated blocks for the rocktypes SDVK is illustrated below in Figure 75.

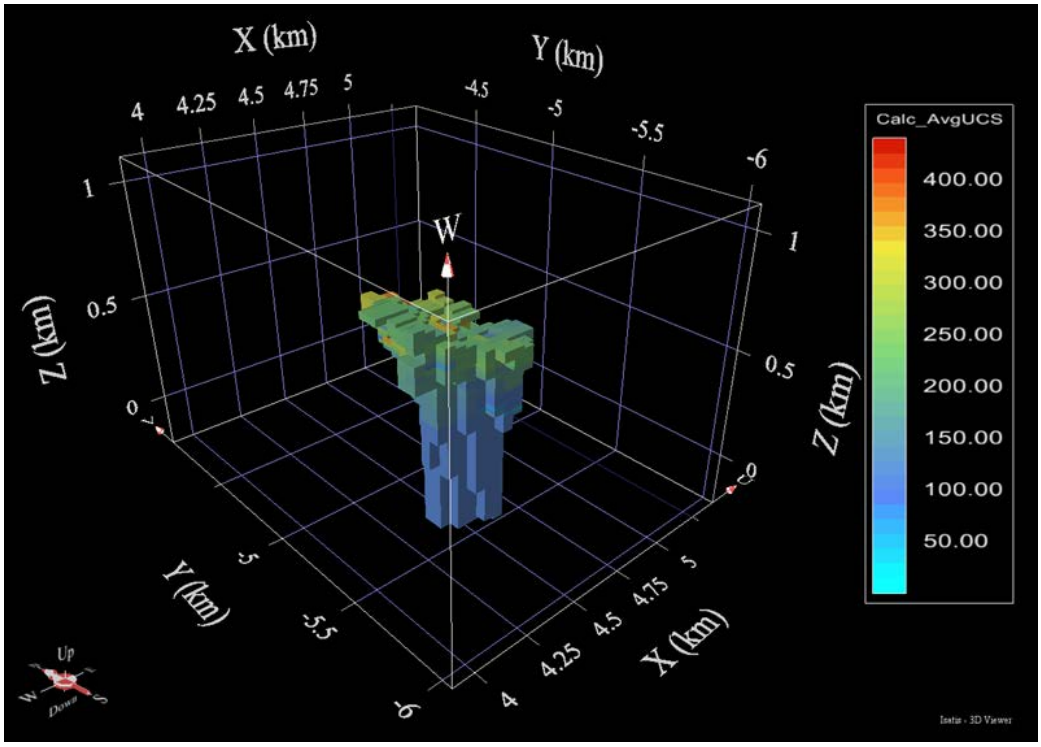


Figure 75 UCS 100% populated blocks – UCS estimates for SDVK

In this research report, a comparison of the RMR input variables (sample statistics) versus estimated (kriged) values was also undertaken. The results for each RMR input parameters are tabulated and discussed in the following subsections. Furthermore, the samples, estimates (P1_Est, P2_Est, MA & Final_Est) were plotted against bench elevations as a way of estimation validation in APPENDICES.

10.1 Sample Statistics versus Estimates – UCS

Statistics of all RMR input parameters for each AK1 rocktype were compared with block estimates. This step was undertaken to determine the accuracy of the estimation process and level of confidence on the results. The results are given in Table 16. It is worth noting that earlier on this report only seven (7)

rock types were subjected to histogram and variogram analysis on the UCS parameter (refer to section 7.12 and 7.13).

The results for the UCS parameter show that massive AK1 rocktypes (SDVK, NPK & MVK2) have low standard deviations and low percent mean variances (sample values versus estimates). The UCS parameter on the DHB rocktype has the highest standard deviation while on the MVK2 and SVK_L rocktypes, the UCS is characterized by the lowest percent mean difference, confirming the high accuracy of the estimates. This is in agreement with the histogram distributions and variogram models discussed in Chapter 7 of this report.

Table 16 UCS Sample versus block estimate statistics per rocktype

Rocktype		SVK_M	SVK_L	SDVK	BBR	DHB	NPK	MVK2
Sample Data	Count	626	176	561	186	372	564	1048
	Min	0.46	2.25	1.97	1.72	4.2	2.81	8.14
	Max	196.59	104.01	338.13	181.82	439.5	188.4	334.16
	Average	22.96	31.3	50.13	72.13	63.62	35.37	33.42
	Std Dev	29.92	26.03	31	33.32	66.12	19.13	19.11
	CoV	1.3	0.83	0.62	0.46	1.04	0.54	0.57
Combined Block Estimates	Count	1816	614	2107	2736	2998	1431	3866
	Min	5.48	6.37	15.36	17.53	6.85	13.79	10.29
	Max	108.08	83.8	116.28	121.05	129.33	119.27	122.54
	Average	21.24	28.03	52.63	58.23	79.75	33	35.31
	Std Dev	11.04	15.08	12.53	20.04	20.05	9.63	12.69
	CoV	0.1	0.18	0.11	0.17	0.16	0.08	0.1
% Mean Difference		-1.72	-3.27	2.5	-13.9	16.13	-2.37	1.89

10.2 Sample Statistics versus Estimates – FFPM

Statistics of sample values versus block (kriged) estimates were compared for the FFPM on the various AK1 rocktypes. The comparison on the FFPM variable was performed on twelve (12) AK1 rocktypes and the results are tabulated in Table 17.

The results for the FFPM parameter show that the SPK rocktype has the lowest percent mean difference followed by MVK2 and SVK_U in third. These rocktypes are a combination of massive and layered units of the AK1 kimberlite pipe. The brecciated rocktypes like the MVK2_BBR have the highest percent mean-difference. Generally the FFPM parameter for most rocktypes

have low standard deviations, with the A3T unit recording the lowest of them all.

Table 17 FFPM Sample versus block estimate statistics per rocktype

Lithology Code		A3T	SPK	SVK_U	SVK_M	SVK_L	SDVK
Sample Data	Count	101	580	208	5270	1436	3289
	Min	0	0	0	0	0	0
	Max	6.32	21.13	13.33	40	18.18	12.67
	Average	0.74	1.18	1.33	1.03	1.25	0.53
	Std Dev	1.02	1.66	1.68	1.46	1.65	0.86
	CoV	1.38	1.41	1.27	1.46	1.32	1.63
Final Block Estimates	Count	2013	239	2456	1816	614	2107
	Min	0.65	0.95	0.78	0.3	0.78	0.29
	Max	0.85	1.65	1.89	1.36	2.62	1.37
	Average	0.74	1.23	1.42	0.88	1.51	0.47
	Std Dev	0.06	0.22	0.27	0.27	0.57	0.24
	CoV	0.08	0.18	0.19	0.31	0.38	0.5
% Mean Difference		0	4.07	6.15	-17.47	17.36	-12.17
Lithology Code		**BBR**	**DHB**	**NPK**	**NPK_GG**	**MVK2**	**MVK2_BBR**
Sample Data	Count	1869	3487	3285	647	6872	572
	Min	0	0	0	0	0	0
	Max	44.73	38.57	7.33	5	10	6
	Average	1.55	1.79	0.26	0.47	0.34	0.92
	Std Dev	2.46	2.44	0.49	0.67	0.64	0.99
	CoV	1.6	1.36	1.93	1.42	1.89	1.08
Final Block Estimates	Count	2736	2998	1431	788	3866	416
	Min	0.8	1.37	0.13	0.35	0.11	0.48
	Max	3.48	2.31	0.53	0.74	0.98	2.19
	Average	1.31	1.67	0.25	0.44	0.35	1.36
	Std Dev	0.59	0.25	0.13	0.06	0.25	0.47
	CoV	0.45	0.15	0.5	0.13	0.71	0.35
% Mean Difference		-18.59	-7.38	-3.8	-6.55	3.82	32.27

10.3 Sample Statistics versus Estimates – RQD

The RQD sample values and estimates were again compared and the statistics are summarised in Table 18. A similar trend observed on the UCS and FFPM variables is seen the RQD variable.

The RQD for the SVK_L and NPKD rocktypes is characterized by the lowest percent mean difference (samples versus estimates), -0.49 and 0.85 respectively. On the SVK_U rocktype, RQD has the highest percent mean difference, surpassing the brecciated units. A point to note is that the RQD on the DHB rocktype (brecciated unit) has recorded the highest standard deviation compared to any other rocktype.

Table 18 RQD Sample versus block estimate statistics per rocktype

Lithology Code		A3T	SPK	SVK_U	SVK_M	SVK_L	SDVK	BBR
Sample Data	Count	108	616	275	626	1600	4273	2227
	Min	0	0	0	0	0	0	0
	Max	104.67	112.67	102.67	196.59	120	114.67	150
	Average	80.07	92.09	82.65	22.96	92.85	96.16	86.08
	Std Dev	26.36	14.92	24.82	29.92	13.46	10.52	23.36
	CoV	0.33	0.16	0.3	1.3	0.14	0.11	0.27
Final Block Estimates	Count	2013	239	2456	1816	614	2107	2736
	Min	72.58	79.57	67.82	5.48	86.35	88.32	79.66
	Max	91.49	93.45	88.02	108.08	96.28	97.3	102.38
	Average	82.82	86.36	74.45	21.24	92.23	92.48	90.14
	Std Dev	7.89	4.59	4.93	11.04	2.66	2.47	8.61
	CoV	0.1	0.05	0.07	0.1	0.03	0.03	0.1
% Mean Difference		3.43	-6.23	-9.92	-7.49	-0.67	-3.82	4.72

Lithology Code		DHB	NPK	NPKD	NPK_GG	MVK2	MVK2_BBR
Sample Data	Count	4529	4576	157	812	8387	596
	Min	0	0	0	0	0	0
	Max	119	120	110	110.67	120.49	115.56
	Average	88.26	96.12	97.71	90.51	96.96	93.51
	Std Dev	18.72	11.86	8.42	16.89	8.66	14.39
	CoV	0.21	0.12	0.09	0.19	0.09	0.15
Final Block Estimates	Count	2998	1431	106	788	3866	416
	Min	44.08	71.48	97.15	69.5	81.54	71
	Max	117.68	98.98	101.55	95.88	98.42	98.32
	Average	91.9	90.82	98.76	88.97	94.71	89.26
	Std Dev	25.7	6.54	1.12	4.05	4.35	6.62
	CoV	0.28	0.07	0.01	0.05	0.05	0.07
% Mean Difference		4.12	-5.51	1.07	-1.7	-2.32	-4.55

10.4 Sample Statistics versus Estimates – Dry Density (DD)

Lastly the dry density comparisons between sample values and the block estimates for various rocktypes of the AK1 pipe have also been completed. The basic statistics appear in Table 19 below, followed by a discussion of the results thereafter.

Table 19 DD Sample versus block estimate statistics per rocktype

Lithology Code		SPK	SVK_M	SVK_L	SDVK	BBR	DHB
Sample Data	Count	166	1888	579	1656	657	1270
	Min	1.98	1.99	1.98	1.98	1.92	1.56
	Max	2.83	2.91	2.87	3	2.88	2.88
	Average	2.37	2.31	2.4	2.43	2.56	2.31
	Std Dev	0.17	0.17	0.19	0.12	0.15	0.18
	CoV	0.07	0.07	0.08	0.05	0.06	0.08
Final Block Estimates	Count	239	1816	614	2107	2736	2998
	Min	2.33	2.25	2.3	2.27	2.48	2.55
	Max	2.42	2.42	2.62	2.56	2.67	2.6
	Average	2.36	2.3	2.44	2.5	2.56	2.56
	Std Dev	0.04	0.05	0.08	0.08	0.04	0.02
	CoV	0.02	0.02	0.03	0.03	0.01	0.01
% Mean Difference		-0.34	-0.37	1.63	2.94	0.2	10.75

Lithology Code		NPK	NPKD	NPK_GG	MVK2	MVK2_BBR
Sample Data	Count	1252	94	213	3864	94
	Min	2.04	2.3	2.01	2.1	2.3
	Max	2.81	2.64	2.89	2.91	2.64
	Average	2.29	2.46	2.21	2.45	2.46
	Std Dev	0.08	0.06	0.14	0.08	0.06
	CoV	0.03	0.02	0.07	0.03	0.02
Final Block Estimates	Count	1431	106	788	3866	416
	Min	2.22	2.424	2.15	2.35	2.42
	Max	2.39	2.565	2.32	2.54	2.57
	Average	2.34	2.49	2.28	2.47	2.49
	Std Dev	0.06	0.05	0.06	0.06	0.05
	CoV	0.03	0.02	0.03	0.03	0.02
% Mean Difference		2.01	1.26	3.09	0.72	1.26

The dry density variable in the BBR rocktype show the lowest percent mean difference followed by the SPK and SVK_M rocktypes. These rocktypes are mostly basaltic and homogeneous rocktypes with minor density differences. The SPK, SDVK and the MVK2 rocktypes are massive and consistent in terms of the dry density variable.

In summary, the dry density for massive and coherent rocktypes such as SDVK, MVK2, NPK and NPKD, and to some extent, the SPK and SVK_L rocktypes are characterized by block estimate values very close to sample values. For brecciated rocktypes such as the DHB, MVK2_BBR, NPK_GG and the BBR have high mean percent differences in RMR parameters such as the UCS and FFPM. These characteristics are easily detectable in the analysis of bench plots (de-clustered samples versus, P1_Est, MA & Final_Est) versus bench elevations. Basically this confirmed the robustness of the estimation process by kriging methodology.

10.5 Summary of Bench Plots Analysis

A summary of RMR bench plot illustrations are presented in the APPENDICES at the end of this research report. The bench plots for these parameters were generated by plotting bench elevation versus samples (de-clustered), 1st Pass estimate (P1_Est), Moving Average (MA) and Final estimate (Final_Est) for all the different rocktypes.

A closer look at the UCS parameter bench plots show an increase in rock strength with depth (Appendix 1) for the SDVK, MVK2 and the NPK to a certain extent. These are massive and coherent rocks of the AK1 kimberlite. Another point to note is the similarity (closeness) of the estimate to the de-clustered samples of these units confirming the robustness of the estimation process and the homogeneity of the rocktypes. Furthermore, the increase in UCS with depth can be associated with compaction within these large rocktypes. It is clear that the brecciated units (BBR, DHB and the SVK_M and SVK_L to some extent) have variable UCS values which is not directly linked to bench elevation or increase in depth. Another point to note, in Figure 76 the bench plots for all RMR parameters for the BBR unit have a break in between, due to two distinct occurrences of the BBR unit in 3D space as per the AK1 geological model.

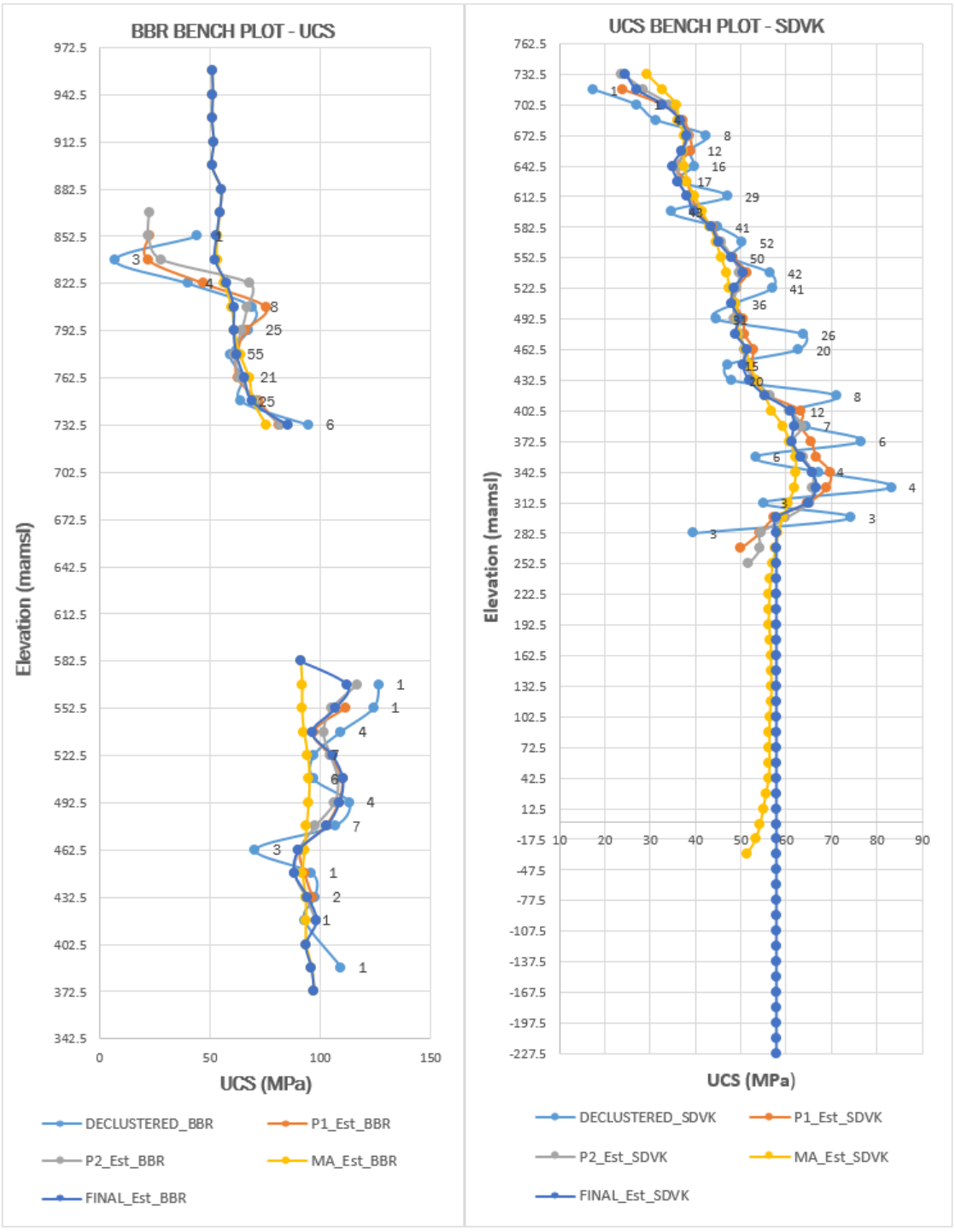


Figure 76 UCS bench plots – BBR & SDVK

Note the UCS increase with depth.

The general overview with FFPM parameter bench plots presented in Figure 77, show a decline in FFPM with depth for most rock types. This is entirely due to the increase in competency of the rock mass with depth, at near surfaces (higher elevations) the FFPM is higher which could be related to disturbances by mining activities and weathering processes. A striking feature with NPK_GG and SPK is the consistency on the FFPM from top to bottom. All the sample values are almost similar to estimated values, very small differences between samples and estimates due to global estimation at depth, see Appendix 3 at the end of the research report.

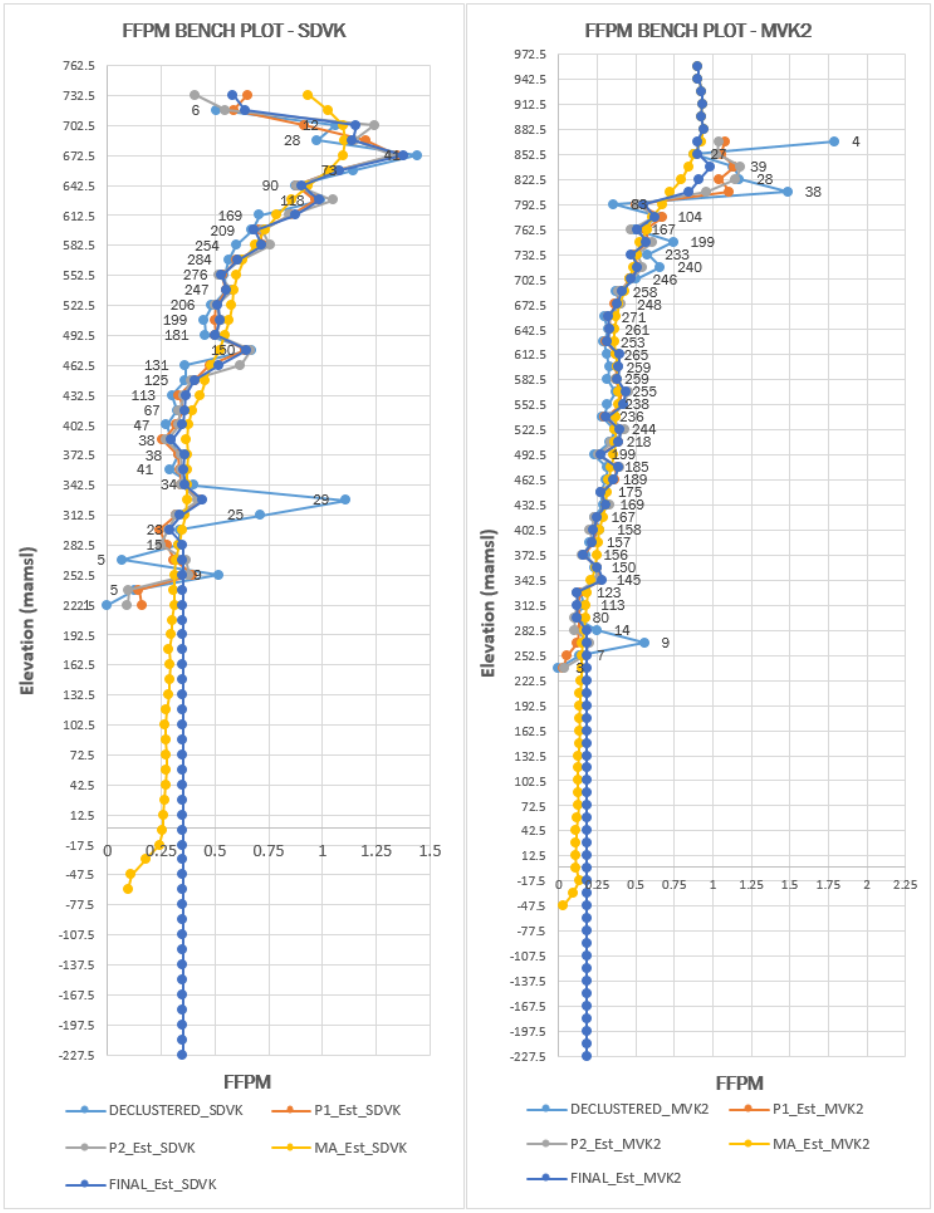


Figure 77 FFPM bench plots – SDVK and MVK2

Note the decrease in FFPM with Depth with depth.

The bench plots for the RQD parameter show consistent values with increase in depth (similar values with decrease in elevation) for massive AK1 rocktypes. These estimates are very close to the sample values confirming the high accuracy of the estimation process. The brecciated units show 'erratic' bench plots but generally following the same trend as massive units, illustrated in Figure 78.

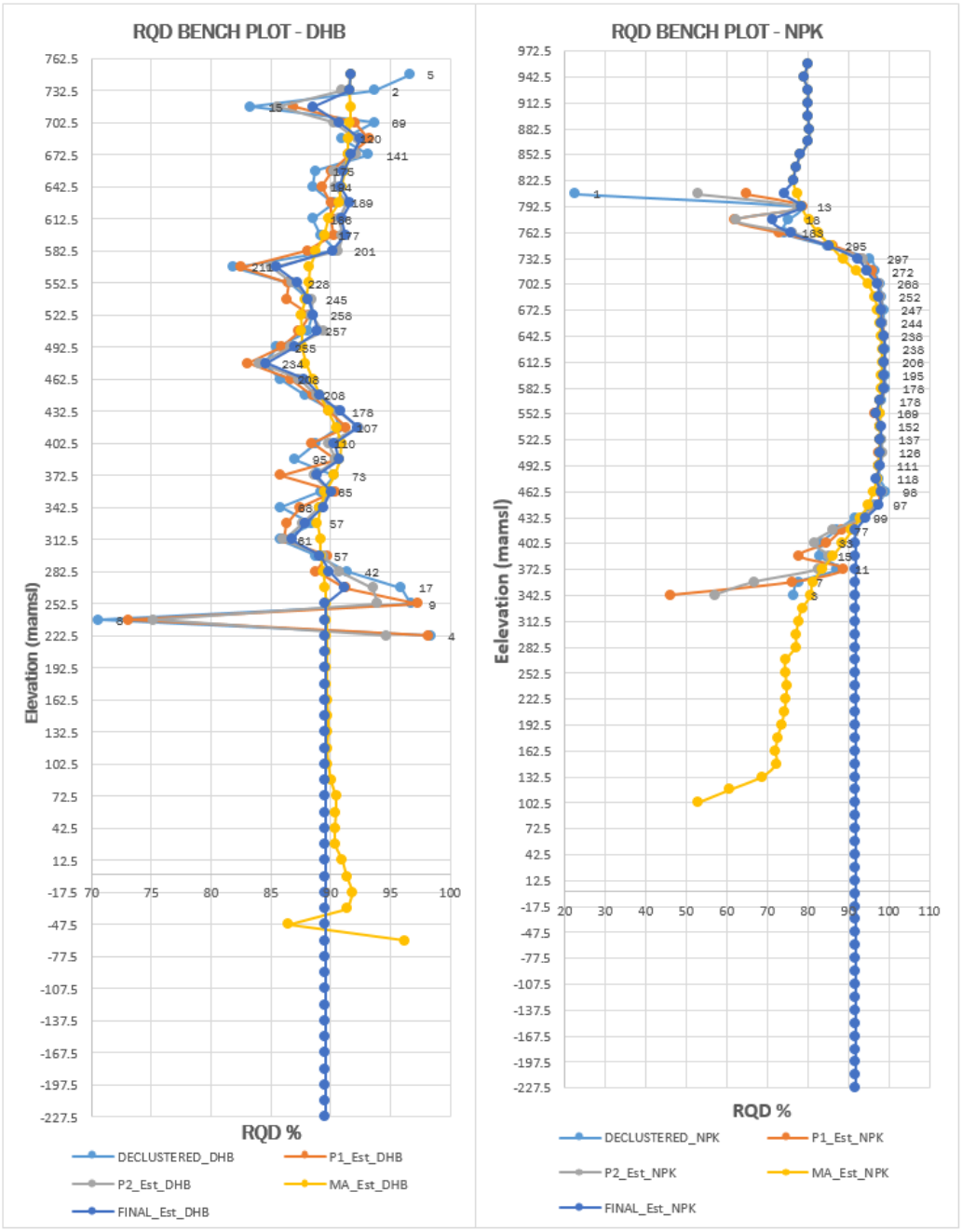


Figure 78 RQD bench plots – DHB and NPK

Note that there is no systematic change in RQD with depth, i.e. there is no trend.

The RQD parameter is not influenced by depth as for most of the rocktypes. Where the samples were insufficient the accuracy on the estimate was of low confidence and vice versa. The variability was more pronounced in brecciated units and where the samples were scarce. Therefore, where there was a lot of data the estimation was data driven where there was little information it was model driven and likely to have high errors.

The Dry Density parameter behaved slightly different from the other RMR parameters discussed in the previous paragraphs. Generally the dry density variable increase with depth for the SDVK, MVK2, NPK and the NPK_GG rocktypes, that is, the deeper the mining goes the denser the rock masses. These rocks are massive, homogeneous and cover large volumes of the AK1 pipe. The estimated values are very similar to the sample values, indicating a high accuracy in the estimate. The NPKD, SVK_M and SVK_L show this trend at around mid-areas but the accuracy on the estimate is less pronounced compared to the SDVK and MVK2 rocktypes.

The brecciated units such as the BBR, DHB and SVK_M were scarcely sampled for dry density parameter hence the estimates are low in confidence and variable. The trend on the dry density parameter identified in the massive rocktypes is not characteristic of the brecciated rocktypes. The dry density bench plots in the brecciated units are more variable as compared to smoother plots for the massive rocktypes, see Figure 79.

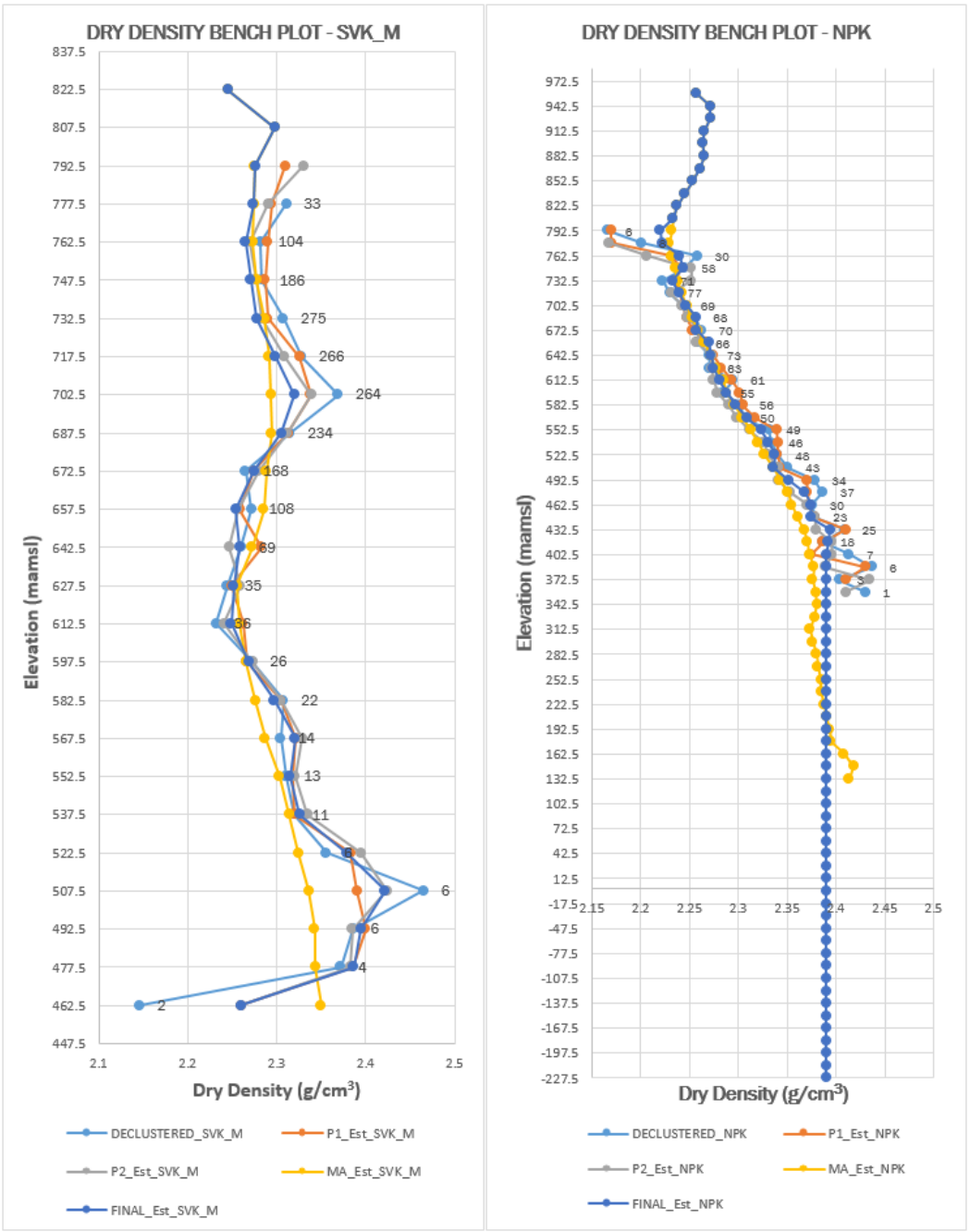


Figure 79 DD bench plots – SVK_M and NPK

Note the gradual changes in DD with depth on SVK_M in the above figure.

In summary, this penultimate chapter the kriging estimation results were discussed in detail. The chapter further focussed on establishing any observable patterns and trends in the estimates, including comments on estimation confidence. For example the comparison of sample values versus estimates for the UCS parameter showed that the massive AK1 rocktypes (SDVK, NPK & MVK2) have low standard deviations and low percent mean differences.

11 CONCLUSIONS AND RECOMMENDATIONS

In conclusion, geostatistical analysis have been successfully and confidently applied to investigate Rock Mass Rating (RMR) parameters for the various rocktypes of the Orapa AK1 kimberlite using Ordinary Kriging methodology. This research report has looked at the various aspects of statistics and geostatistics to analyse RMR parameters in an attempt to improve the author's understanding of the AK1 rocktypes and the spatial behaviour of the RMR parameters in three dimensions with the ultimate objective of enhancing Orapa plant performances and operational value generation.

This research applied relevant geostatistical techniques for RMR parameter estimation to almost all Orapa kimberlite rocktypes with a 95% success rate and where sample data was inadequate, appropriate statistical decisions were made to apply realistic estimates. These decisions were clearly motivated by using for example, the box plots and averages especially for limited numbers of samples in rocktypes either due to the size of rocktypes or the reality that these units have been mined out and are therefore without these data sets.

The analysis undertaken, and methodology applied have been illustrated and discussed in the various chapters of the report. In this research report, it has been demonstrated that it is possible to characterise RMR parameters using statistical and geostatistical techniques. Therefore, the objective of this research study has been completely and successfully achieved and learnings therefrom should be considered for future Debswana mining geoscience projects.

The AK1 RMR study has shown that massive and coherent rocktypes of the Orapa AK1 pipe such as NPK, SDVK, and MVK2 show an increase with depth of the UCS and Dry Density parameters. The brecciated rocktypes such as BBR, MVK2_BBR, SVK_M, and DHB have variable values for these two parameters due to the nature of these rocktypes. The FFPM parameter showed a decline with increase in depth for most rocktypes except for SPK and NPK_GG which were fairly consistent with increase in depth. RQD for most rocktypes is consistent with increase in depth and the estimates for this parameter was of high confidence (very close to the sample values).

The geostatistical approach provides a more reliable and accurate method (low kriging variance) by taking into account the spatial continuity of the

variable under study as compared to simple averaging of geotechnical parameters for a given rock mass. It is clear from this study that all the rocktypes of Orapa AK1 kimberlite pipe have different RMR characteristics which may suggest different approaches for mining extraction from the pit, crusher settings, plant feeding parameters and diamond liberation.

The recommendations following the experience of this research report are as follows:

- It is recommended that the evaluation of rock mass rating (RMR) parameters using geostatistics on future mining geoscience projects be one of the requirements for the data analysis and interpretation process. The geological and geotechnical data processing and interpretation should be augmented with geostatistical modelling at project pre-feasibility study phases to enhance the traditional methods used in geoscience mining projects.
- The need to confidently understand the rock masses is inevitable with deepening pits and increasing mining costs on the horizon. There is need for MRM/Geology section to proactively address all the challenges within its jurisdiction which directly or indirectly affect the diamond value chain. This may require collaboration with all stakeholders and prompt geoscience data dissemination to assist the business achieve its objectives.

REFERENCES

Anglo American PLC, 2016. Ore Reserves and Mineral Resources Report, 20 Carlton House Terrace, London, SW1Y5AN, England.

Ayalew L., Reik, G. and Busch, W., 2002. Characterizing weathered rock masses – A geostatistical approach, International Journal of Rock Mechanics and Mining Sciences, Volume 39, pp. 105 – 114.

Barton N., Lien R. and Lunde J., 1974. Engineering classification of rock masses for the design of tunnel support. Rock Mechanics, Volume 6, No. 4, pp. 189 - 236.

Basson I. J., 2006. 3-D Modelling of Country Rocks Hosting the Orapa A/KI Kimberlite, Prepared by TECT Geological Consulting for Orapa Mine, Botswana.

Bieniawski Z. T., 1989. Engineering Rock Mass Classifications: A Complete Manual for Engineers and Geologists in Mining, Civil and Petroleum Engineering, Wiley-Interscience, ISBN 0-471- 60172- 1, pp. 40 – 47.

Bohling G., 2005. Introduction to Geostatistics and Variogram Analysis, Kansas Geological Survey.

Brenning A., 2013. GEOSTATS, Geostatistics 1 course notes, University of Waterloo, Canada.

Broch E. and Franklin J. A., 1972. The Point-load Test Strength, International Journal of Rock Mechanics and Mining Sciences, Pergamon Press, Volume 9, pp 669 – 697.

Brook N., 1985. The Equivalent Core Diameter Method of Size and Shape Correction in Point Load Testing, International Journal of Rock Mechanics and Mining Sciences, Pergamon, Oxford, Volume 22, Number 2, pp. 51 – 60.

Clark M. and Barnett W., 2015. Conversion Factors for Orapa Mine Rock Units, SRK Consulting, Canada.

Dohm C. E., 2013a. Statistical Evaluation of Ore Reserves, Course notes for MINN7007, University of the Witwatersrand.

Dohm C. E., 2013b. Geostatistical Methods in Mineral Resource Evaluation, Course notes for MINN7006, University of the Witwatersrand.

Egana M. and Ortiz J. M., 2013. Assessment of RMR and its uncertainty by using Geostatistical Simulation in a Mining Project. Journal of GeoEngineering, Volume 8, No. 3, pp. 83-90.

Ferrari F., Apuani T. and Giani, G. P., 2014. Rock Mass Rating Spatial Estimation by Geostatistical Analysis. International Journal of Rock Mechanics and Mining Sciences, Volume 70, pp. 162 – 176.

Gibson J. G., 1984. Brief history of Discovery, Sampling and Mining of Orapa and Letlhakane Mines, Botswana.

Hoek E., 1994. The Strength of Rock and Rock Masses, International Society for Rock Mechanics, 35th U. S. Symposium on Rock Mechanics, Mackay School of Mines, University of Nevada, Reno. Volume 2, Number 2.

Isaaks E. H. and Srivastava R. M., 1989. An Introduction to Applied Geostatistics, Oxford University Press, New York, 592p.

Krige D. G., 1951. A statistical approach to some mine valuations and allied problems at the Witwatersrand, Master's thesis of the University of Witwatersrand, Johannesburg.

Laubscher D. H., 1990. A geomechanics classification system for the rating of rock mass in mine design, Journal for the South African Institute of Mining and Metallurgy, Volume 90, No. 10, pp. 257 – 273.

Letsatle B. M., Sejoe T., Maphane K., Gilika O., Kgomanyane J., Pelaelo L., Dintwe T. and Kruger K., 2015. Orapa Resource Extension Project (OREP) Phase II, Mineral Resource Management, Orapa Mine, Botswana.

Matheron G., 1963. Principles of Geostatistics, Economic Geology, Volume 58 (8), pp 1246 – 1266.

Matheron G. 1973. The intrinsic random functions and their applications, Adv. Appl. Prob., 5, pp. 439 – 468.

McCourt S., Kampunzu A. B., Bagai Z. and Armstrong R. A., 2004. The crustal architecture of Archaean terranes in North-eastern Botswana, South African Journal of Geology, Volume 107, pp 147 - 158.

McKillup S. and Dyar M. D., 2010. Geostatistics Explained: An Introductory Guide for Earth Scientists, Cambridge University Press, New York, USA.

Tait M., Letsatle B., Gaegopolwe P., Maphane M., Keakopa B. and Bonang B., 2009. Orapa 2125 A/K1 Resource Extension Project (OREP) Phase 1, Mineral Resource Management, Orapa Mine, Botswana.

Rivoirard J., 1987. Two key parameters when choosing the kriging neighbourhood, *Journal of Mathematical. Geology*, Volume 19, pp 851-856.

Sejoe T., 2014. 3- Dimensional Geological Model of A/KI Kimberlite Resource, Department of Mineral Resources, Orapa Mine, Botswana.

Ulusay R., 2014. The ISRM Suggested Methods for Rock Characterization, Testing and Monitoring, Department of Geological Engineering, Hacettepe University, Ankara, Turkey.

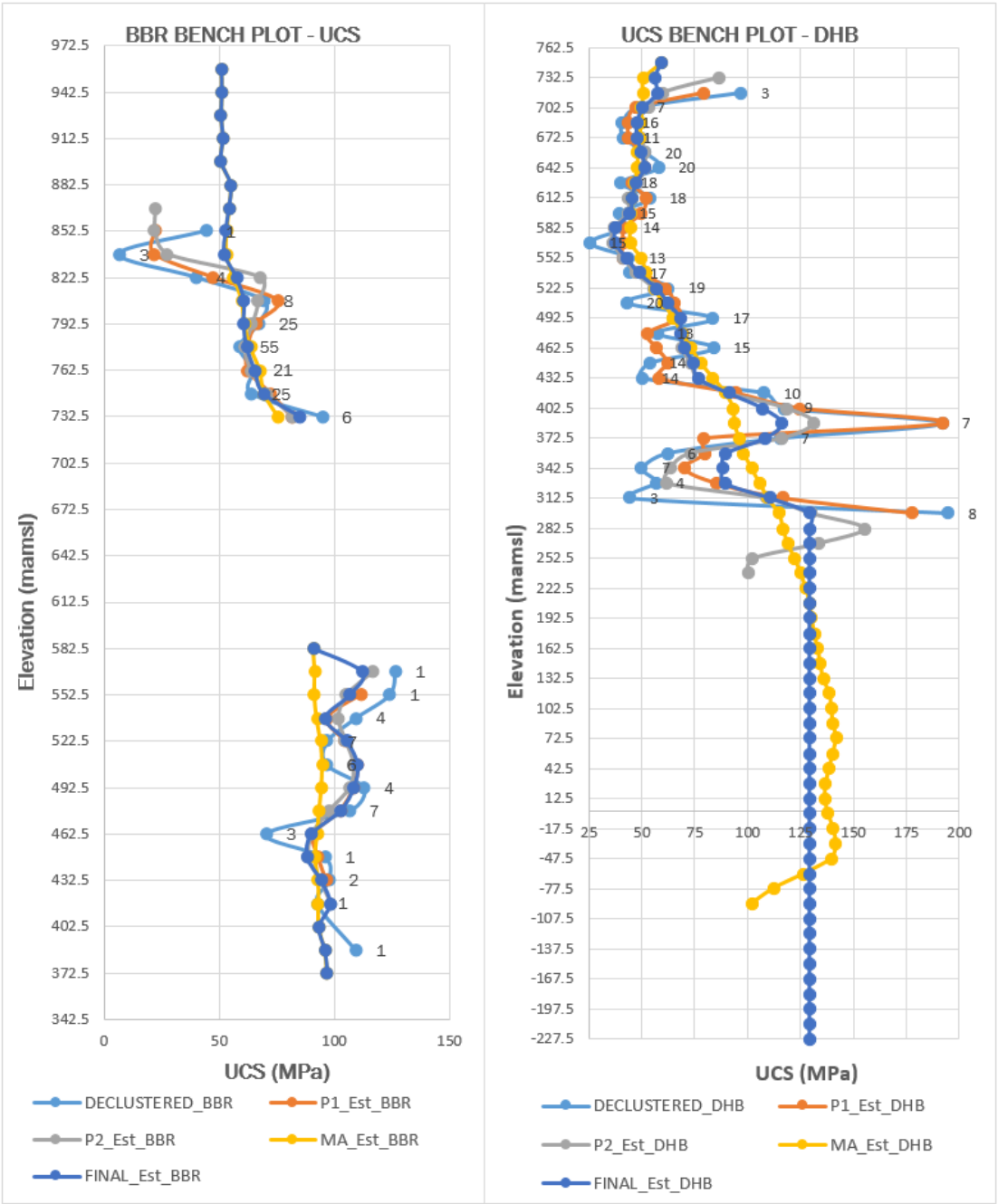
Van de Wall A. R. G. and Ajalu J. C., 1997. Characterization of the geotechnical properties of rock material for construction purposes, International Journal of Rock Mechanics and Mining Sciences, Volume 34, (3 – 4), p 319.

Vann J., Jackson S. and Bertoli O., 2003. Quantitative Kriging Neighbourhood Analysis for the Mining Geologist – A Description of the Method with Worked Case Examples, 5th International Mining Geology Conference, Bendigo, Vic.

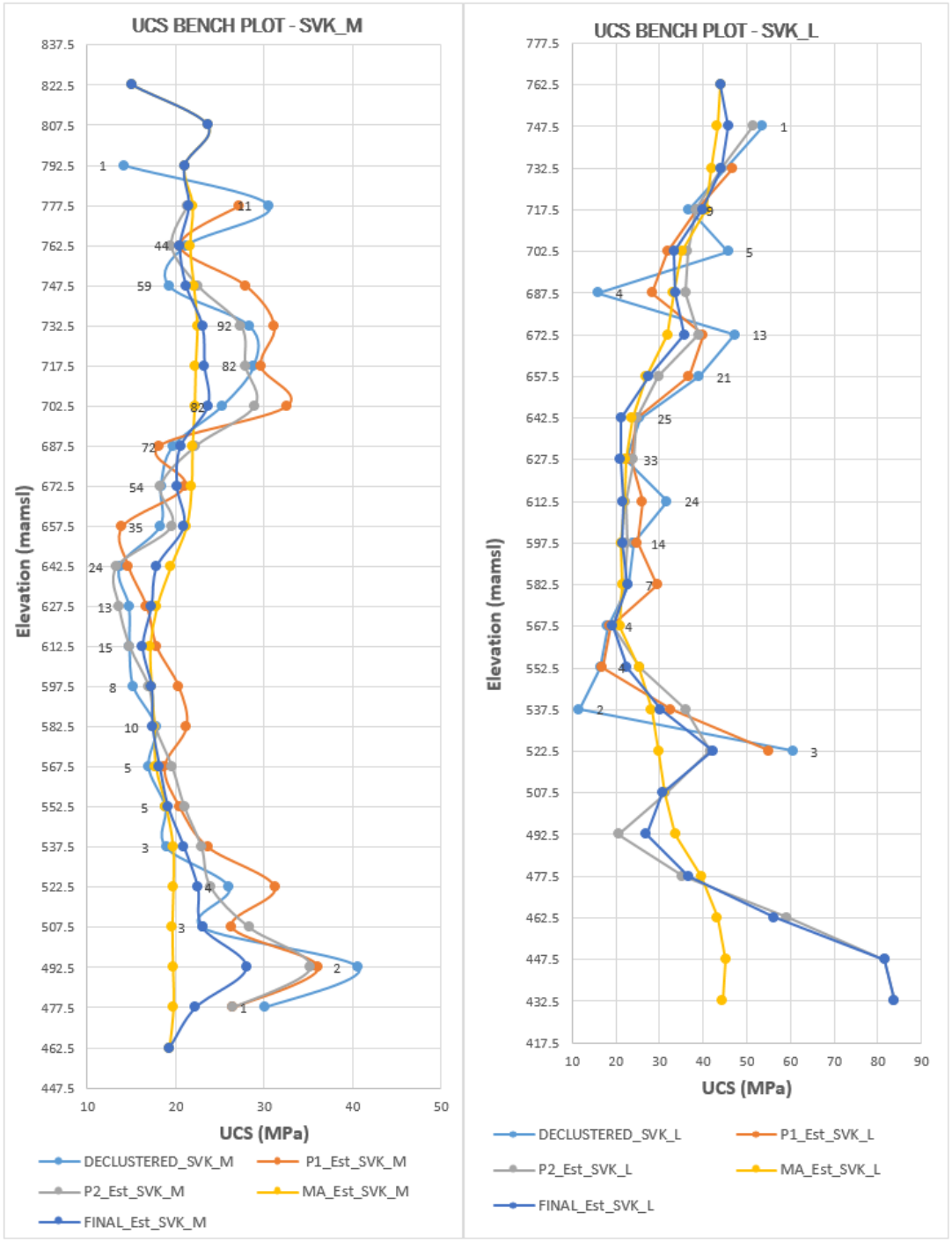
Zhang Y., 2011. Introduction to Geostatistics – Course Notes, Department of Geology and Geophysics, University of Wyoming, USA.

APPENDICES

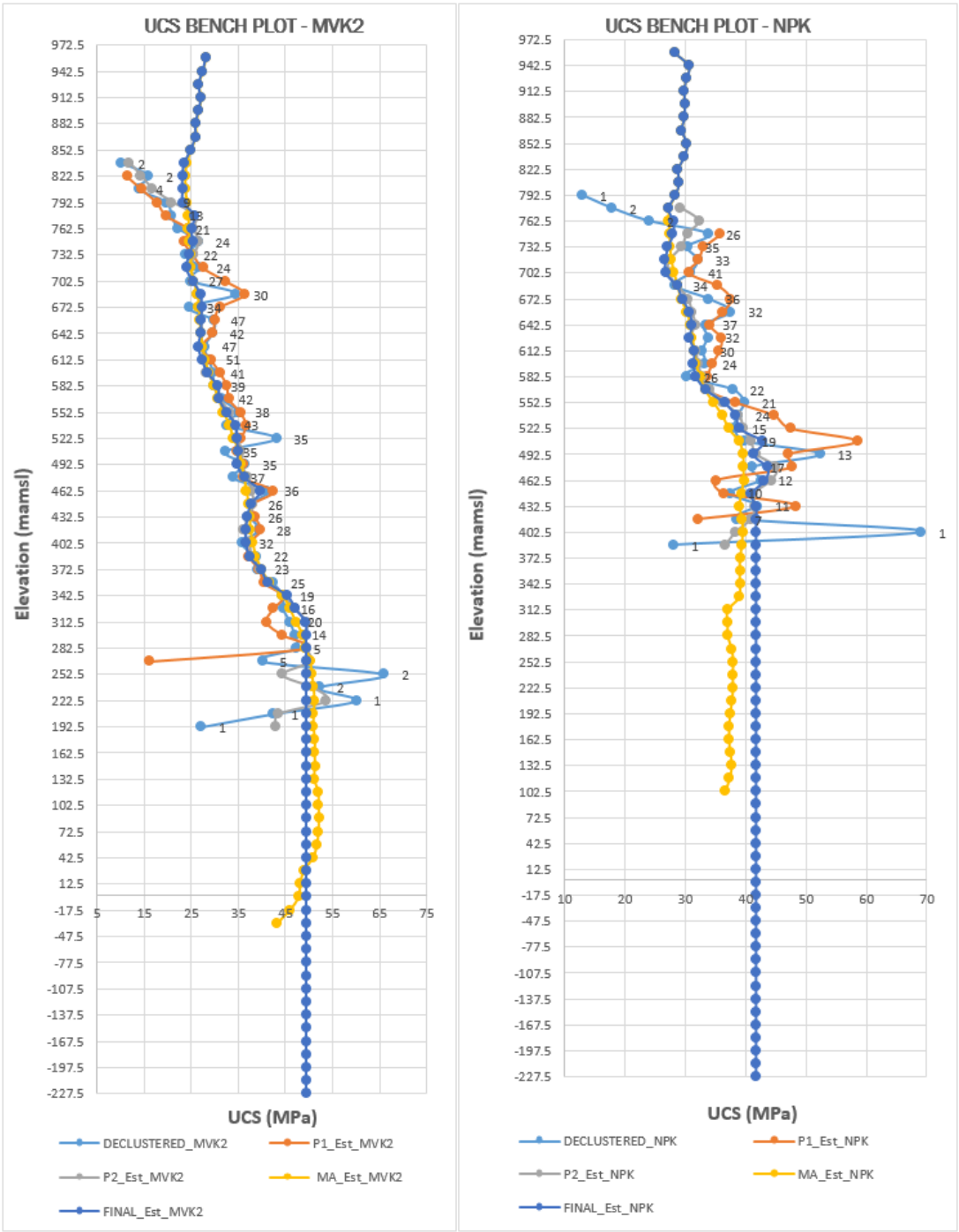
Appendix 1 UCS Bench plots within the AK1 rocktypes



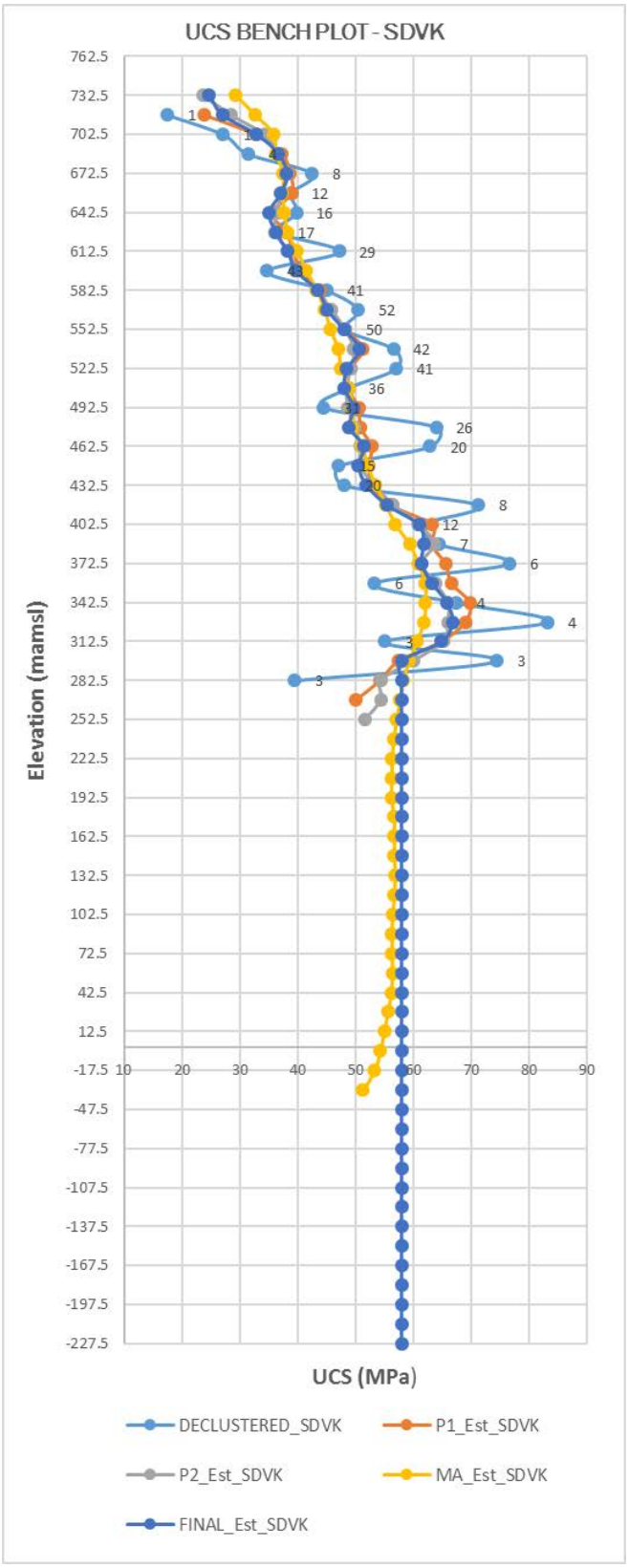
UCS Bench plots within the AK1 rocktypes continued



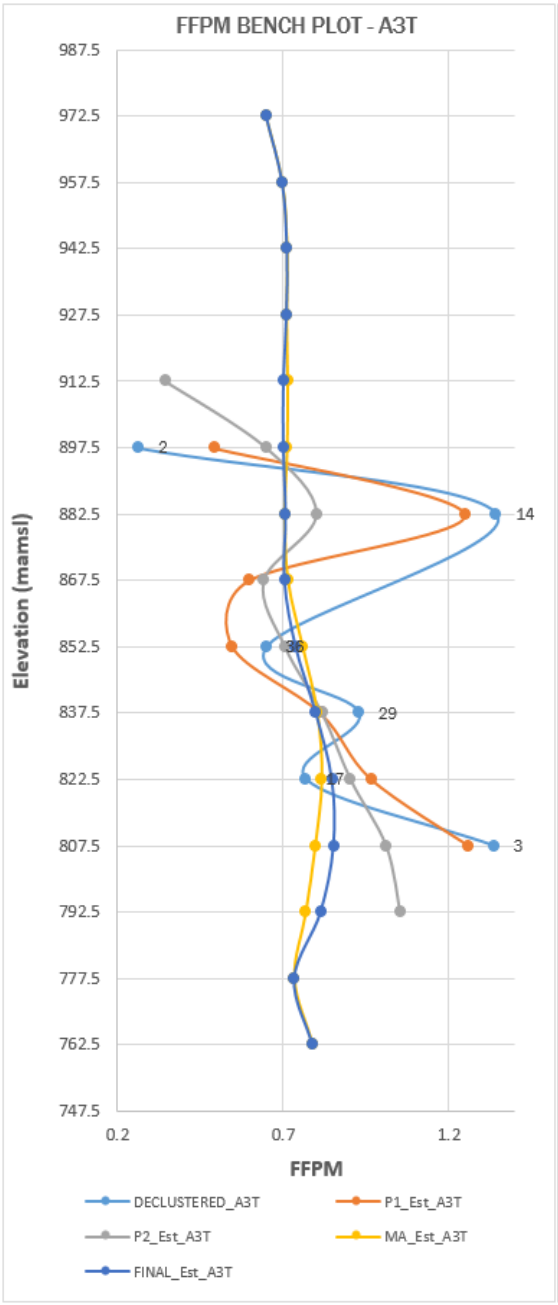
UCS Bench plots within the AK1 rocktypes continued

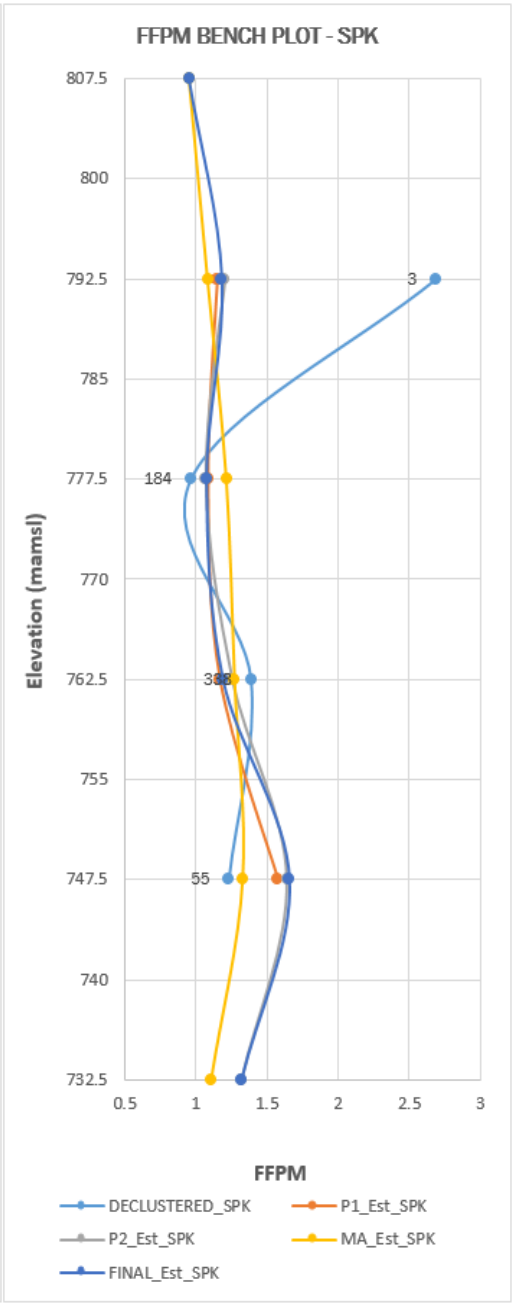


UCS Bench plots within the AK1 rocktypes continued

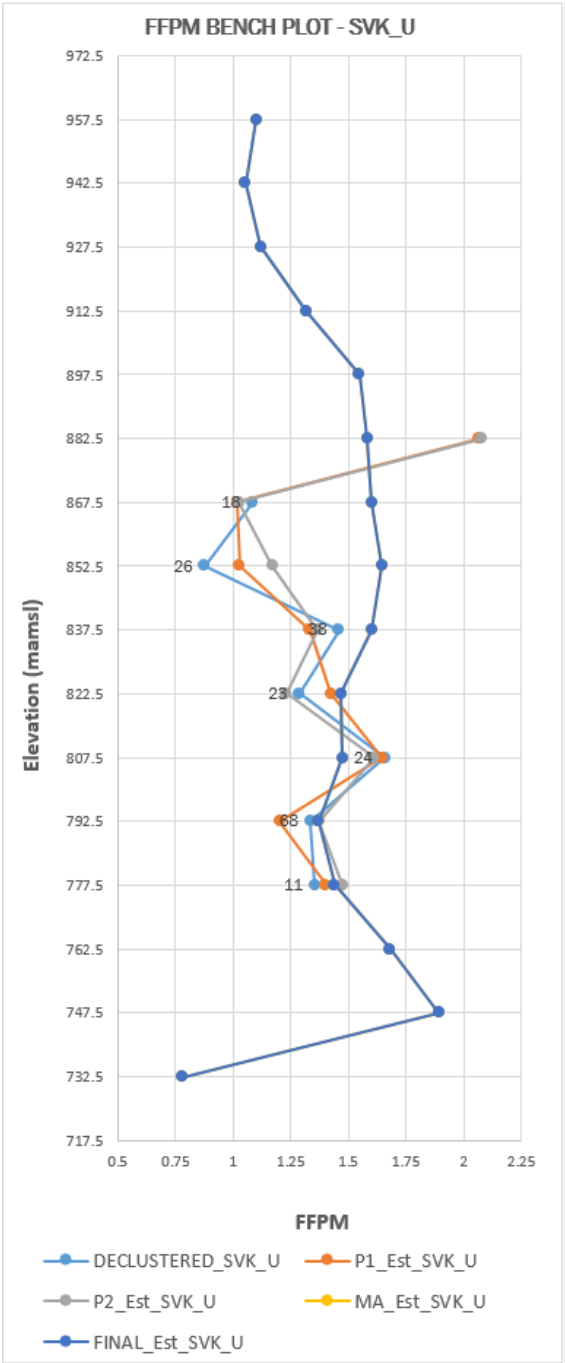


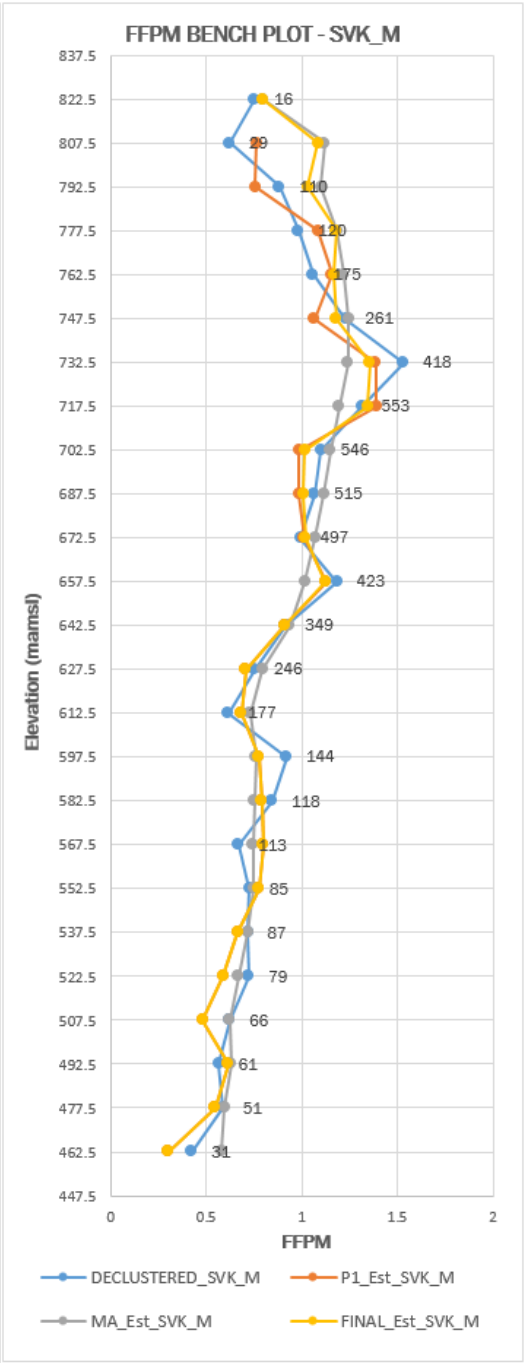
Appendix 2 FFPM Bench plots within AK1 rocktypes



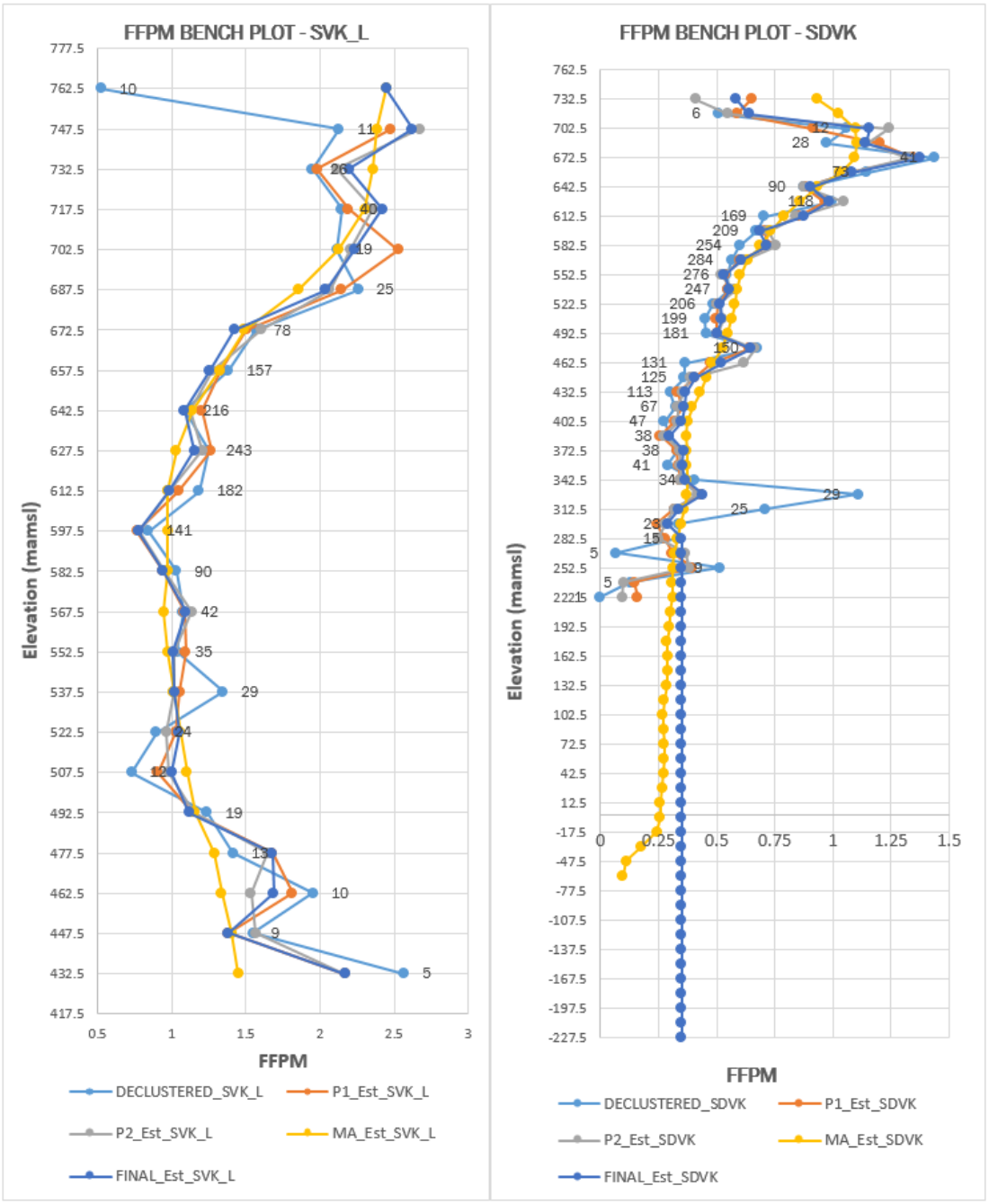


FFPM Bench plots within the AK1 rocktypes continued

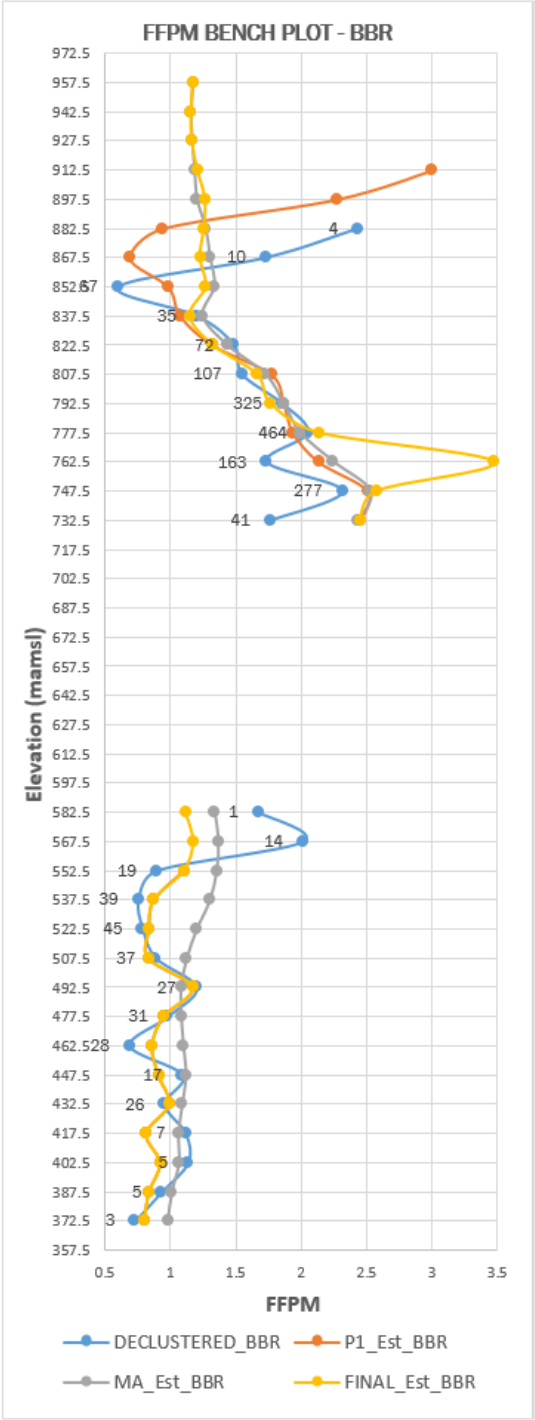


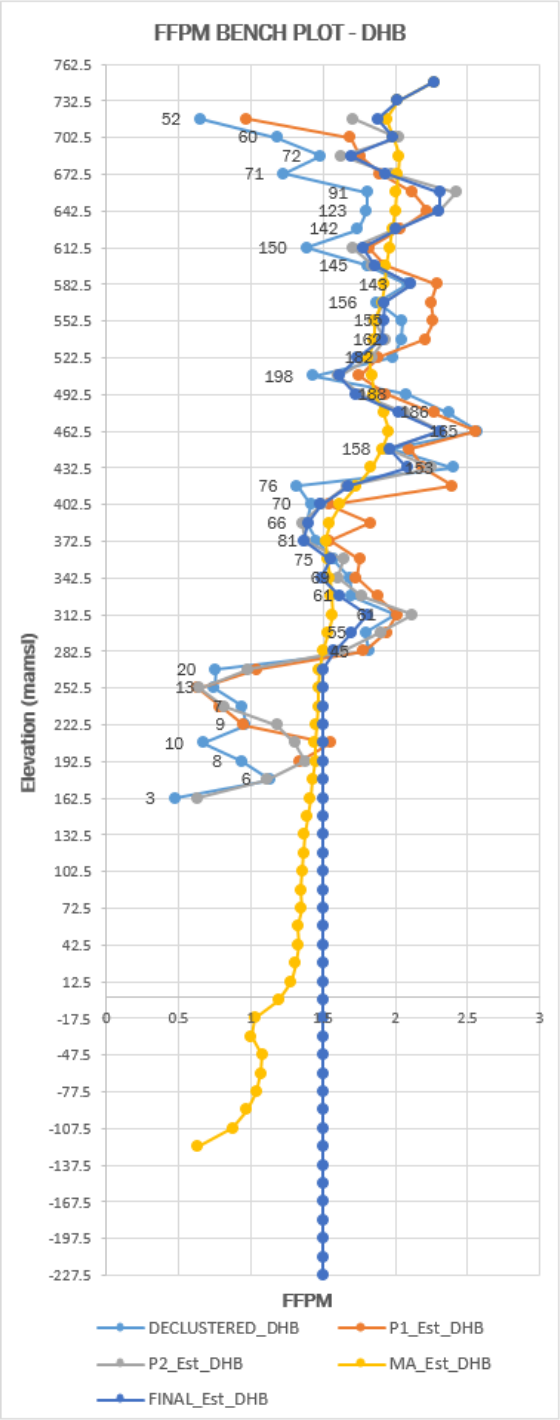


FFPM Bench plots within the AK1 rocktypes continued

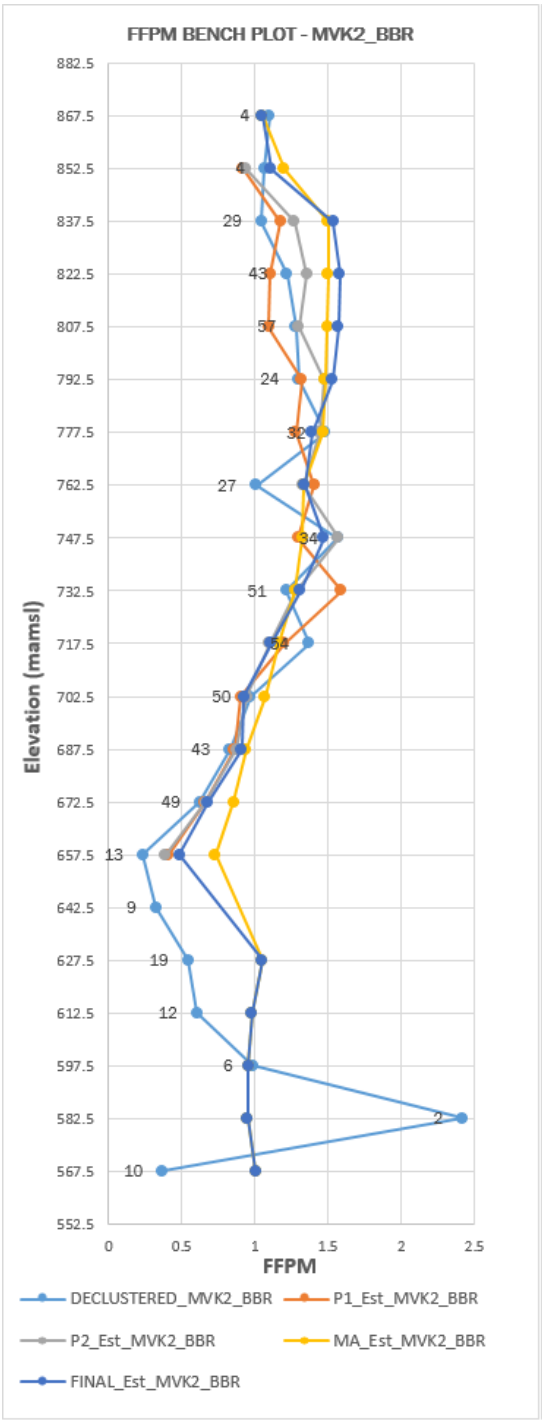


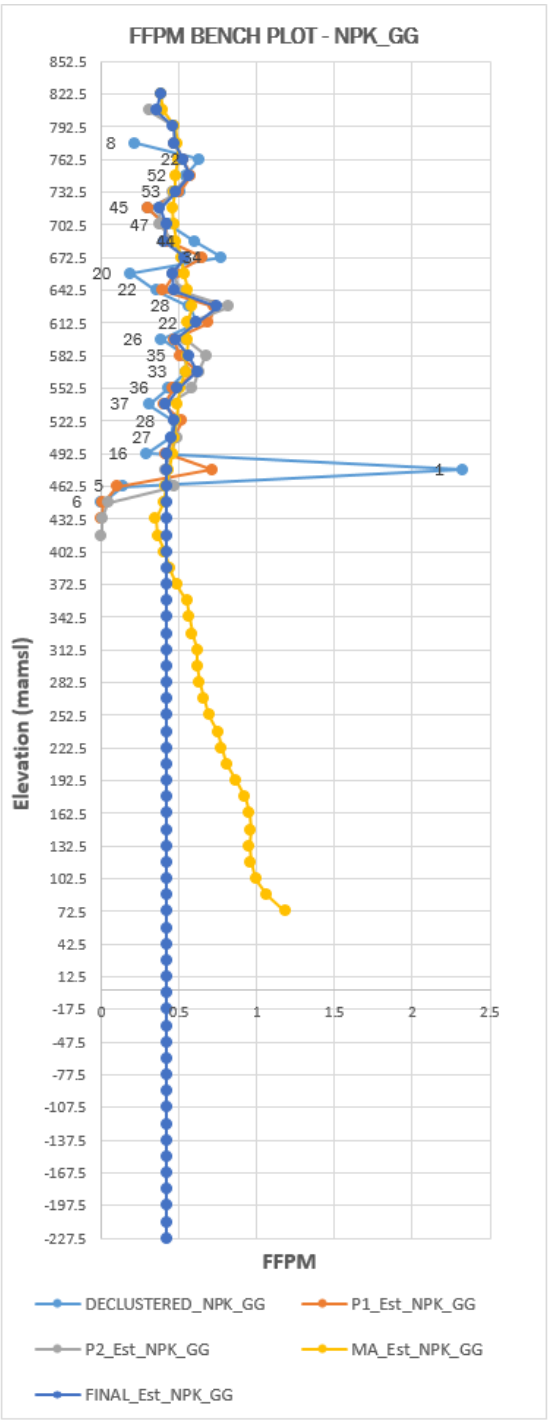
FFPM Bench plots within the AK1 rocktypes continued



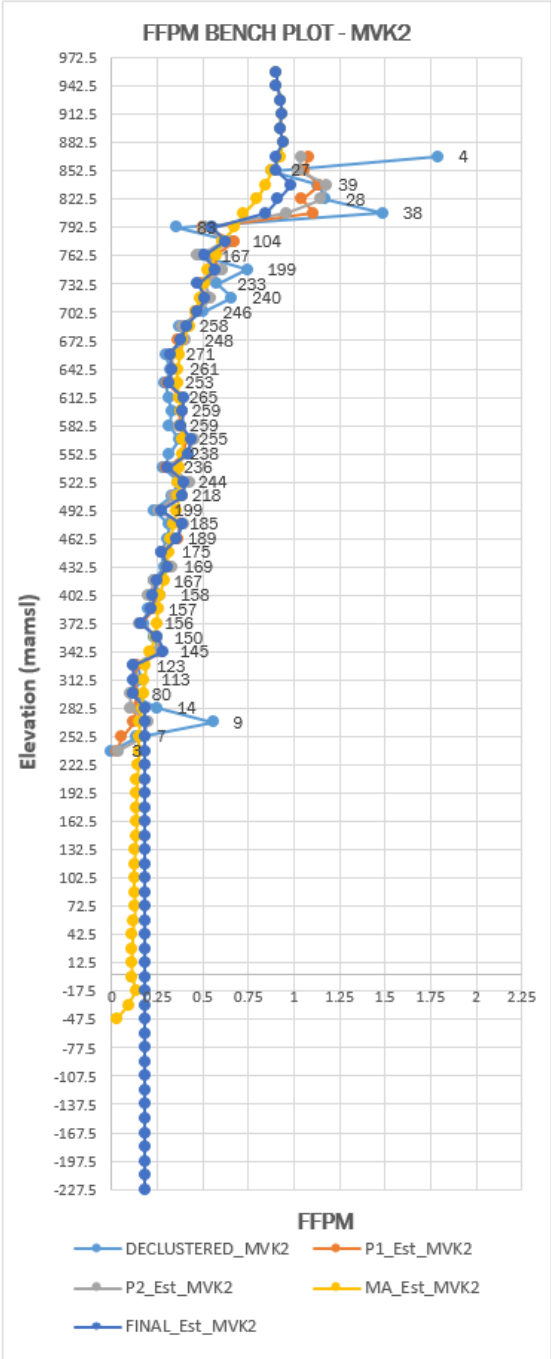


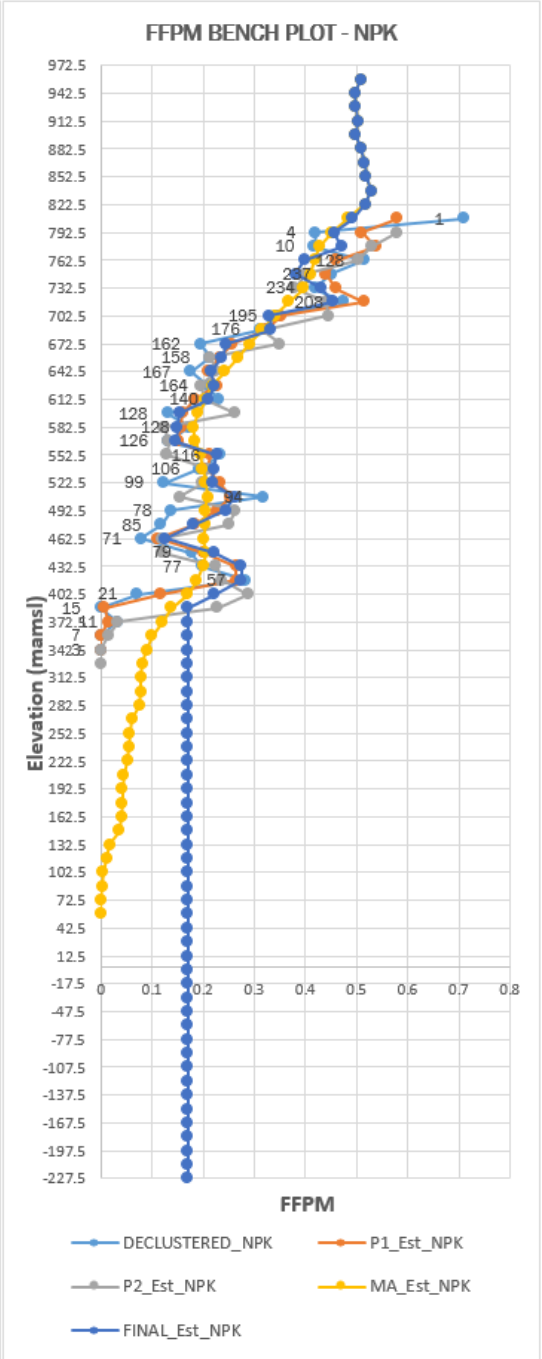
FFPM Bench plots within the AK1 rocktypes continued



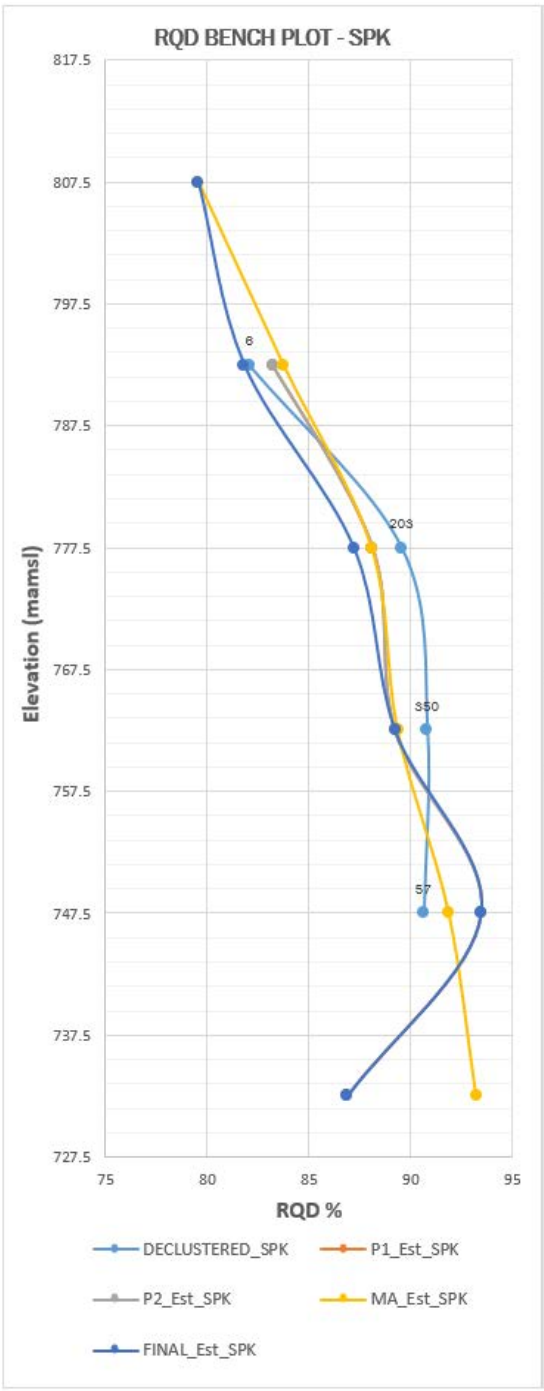


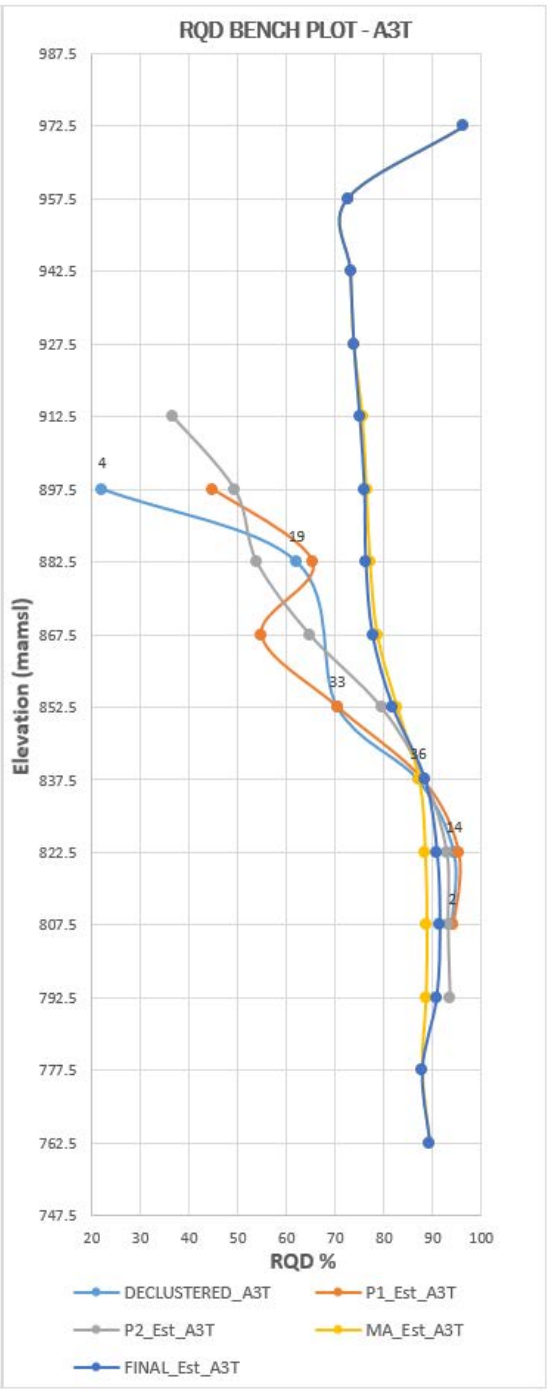
FFPM Bench plots within the AK1 rocktypes continued



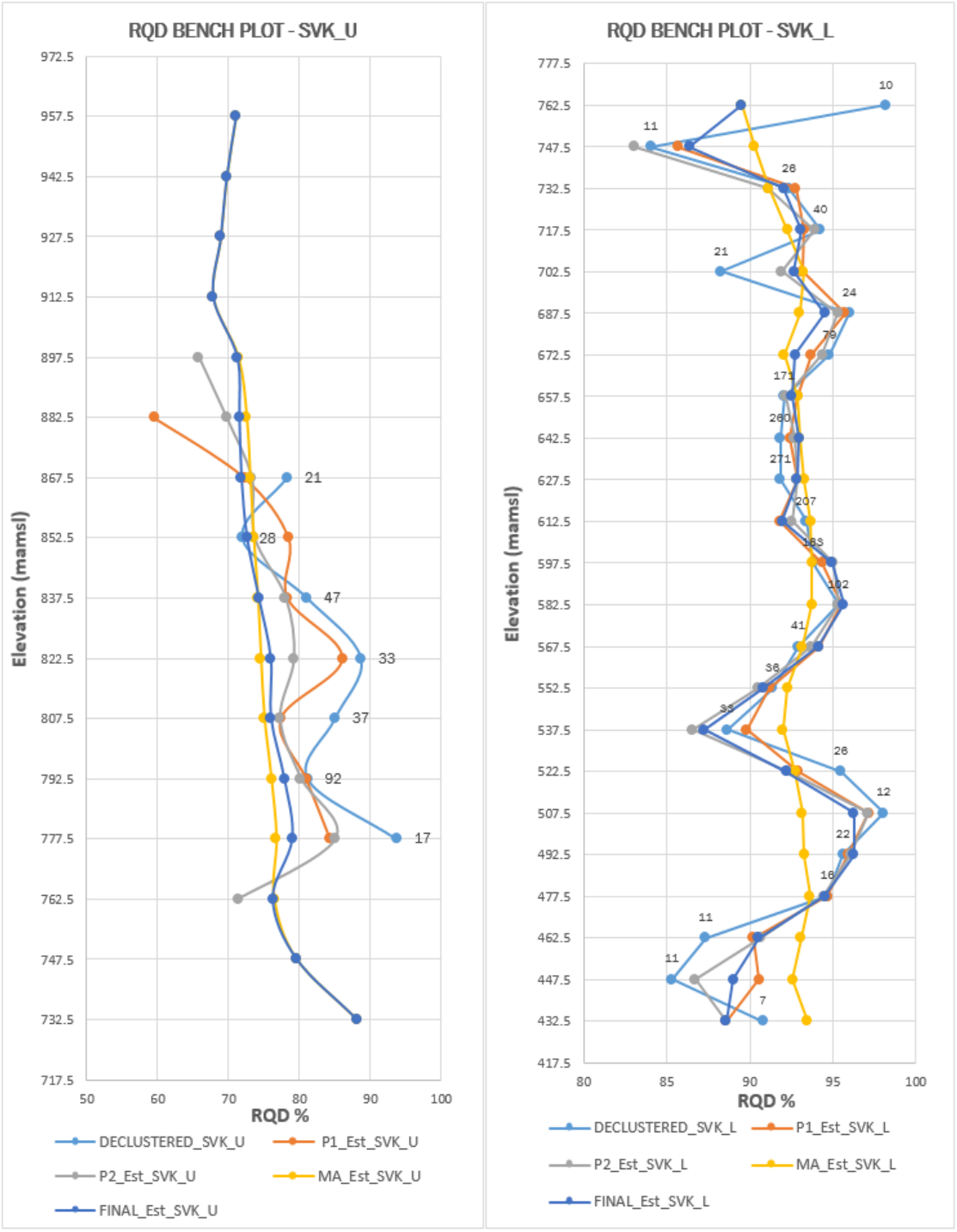


Appendix 3 RQD Bench plots within AK1 rocktypes

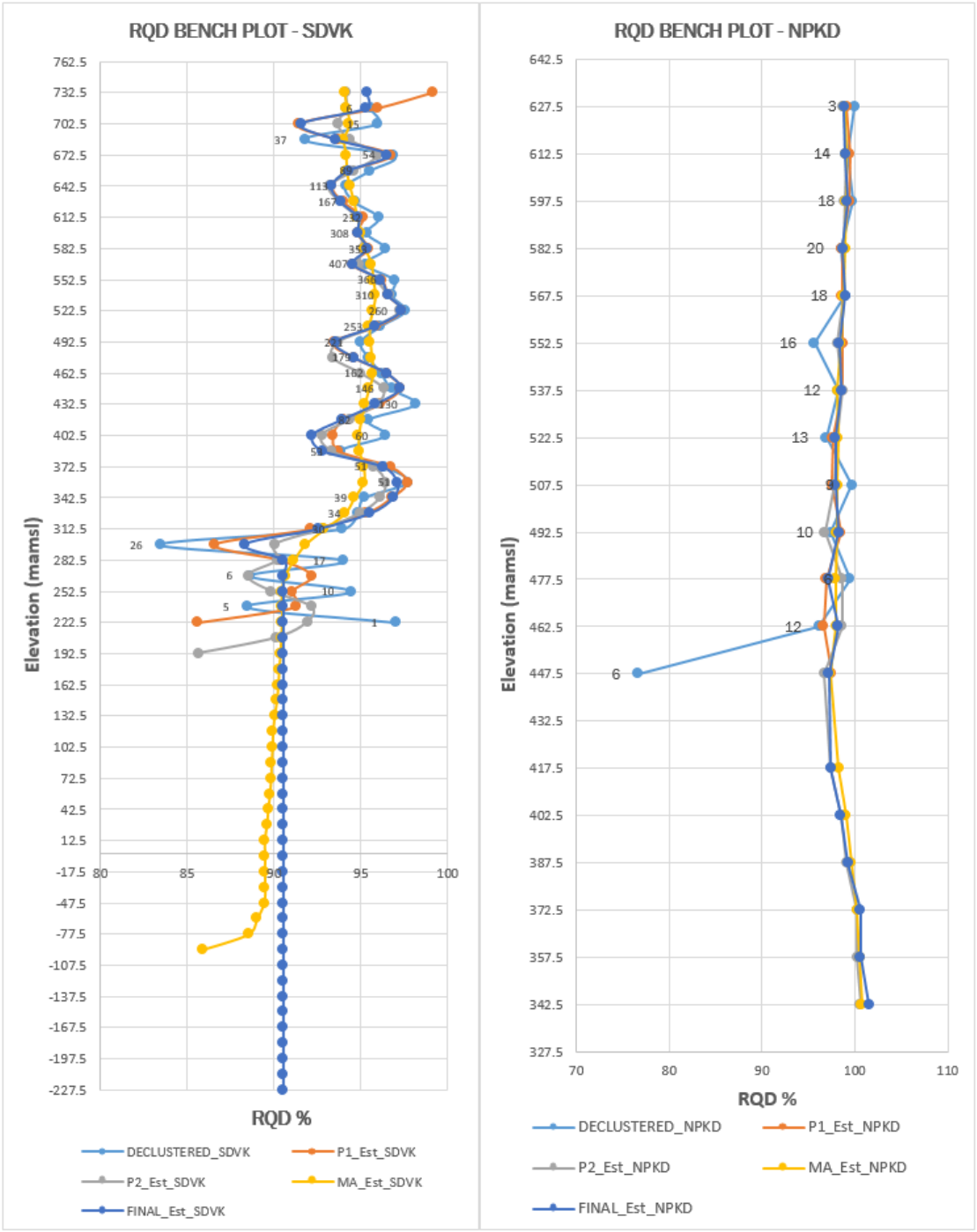




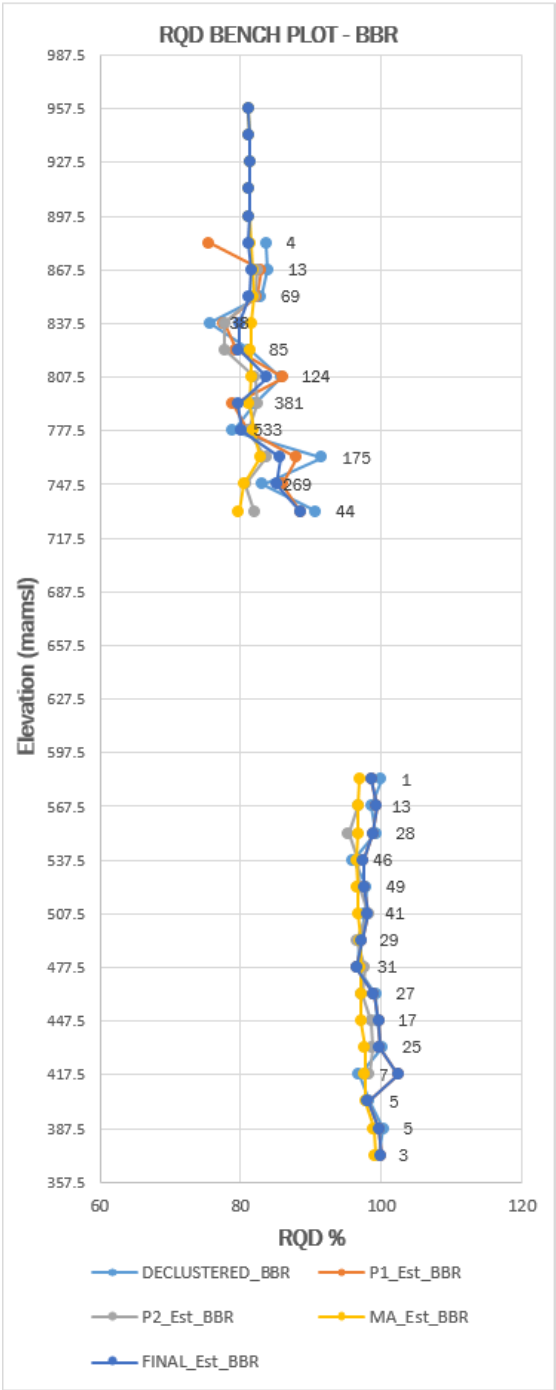
RQD Bench plots within the AK1 rocktypes continued

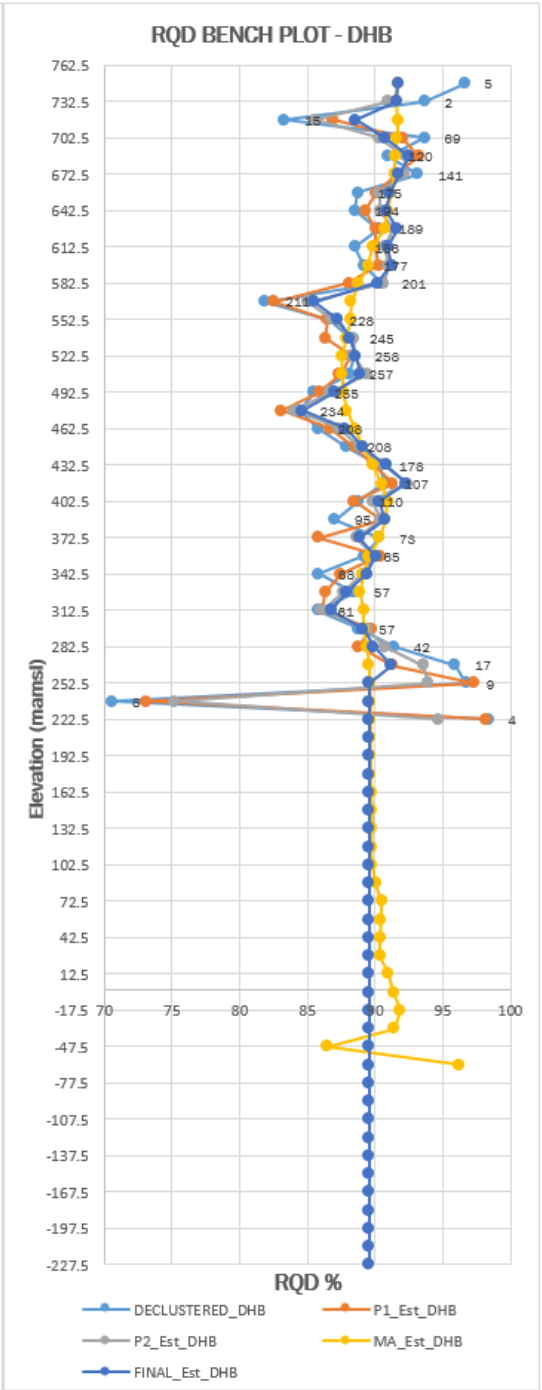


RQD Bench plots within the AK1 rocktypes continued

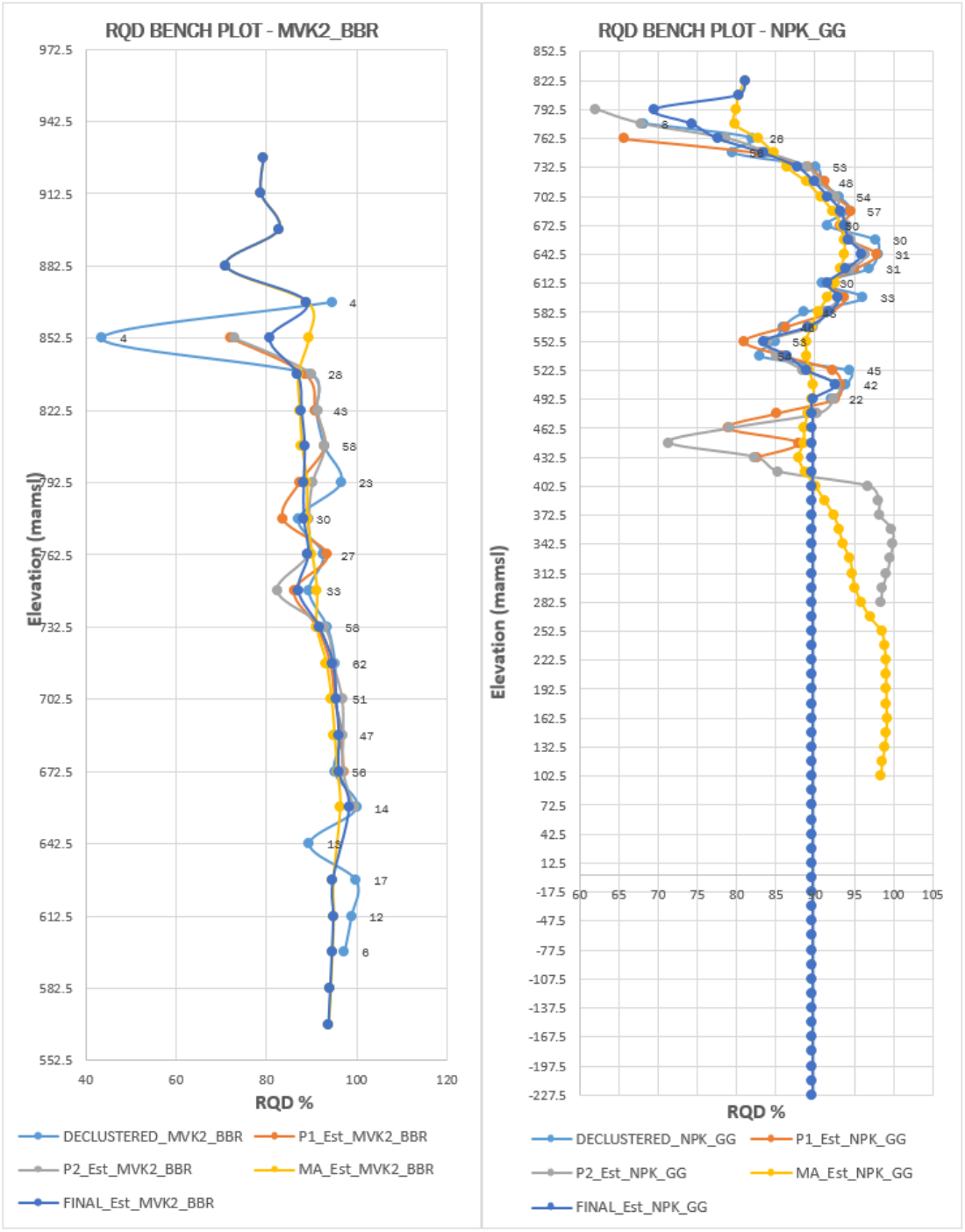


RQD Bench plots within the AK1 rocktypes continued

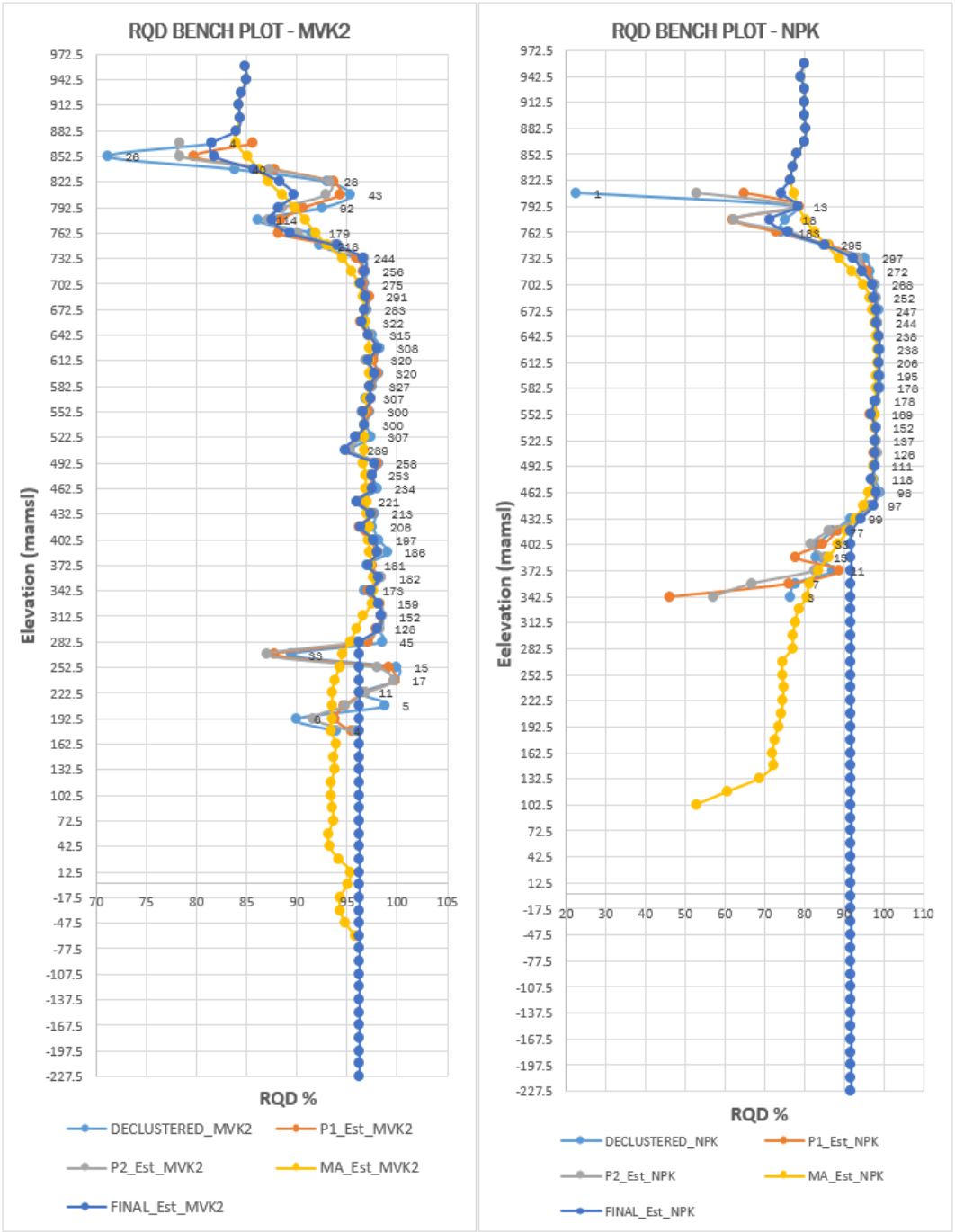




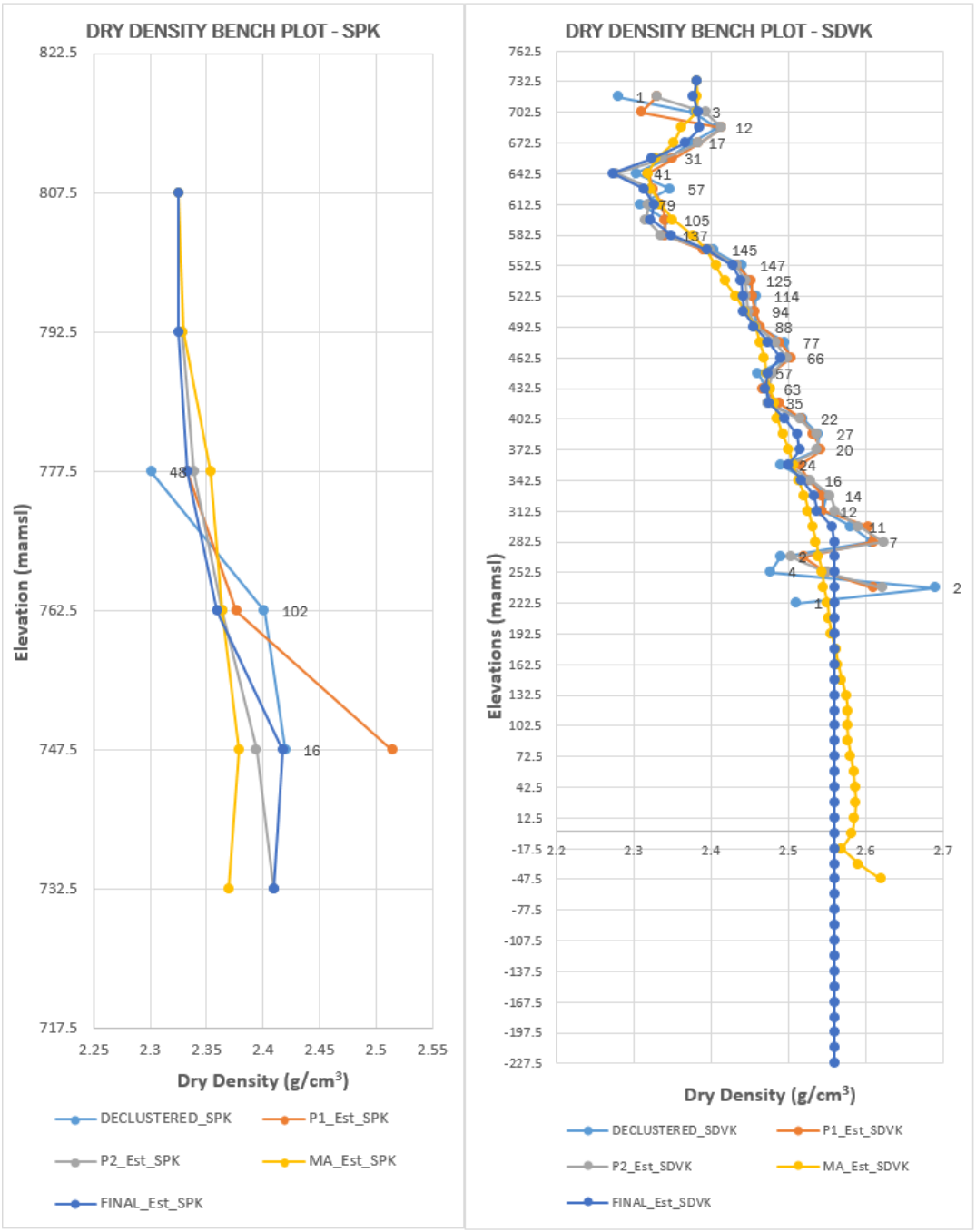
RQD Bench plots within the AK1 rocktypes continued



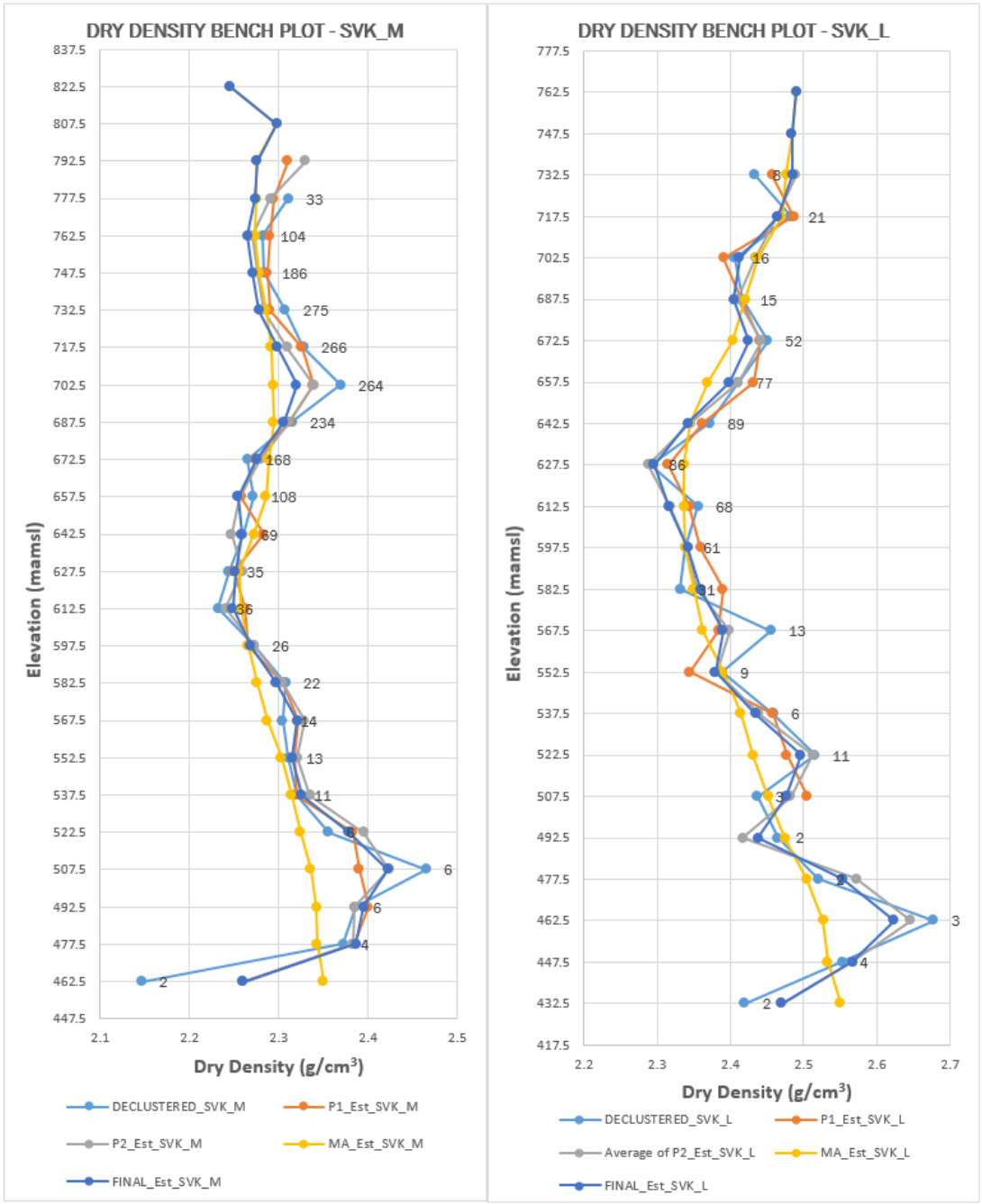
RQD Bench plots within the AK1 rocktypes continued



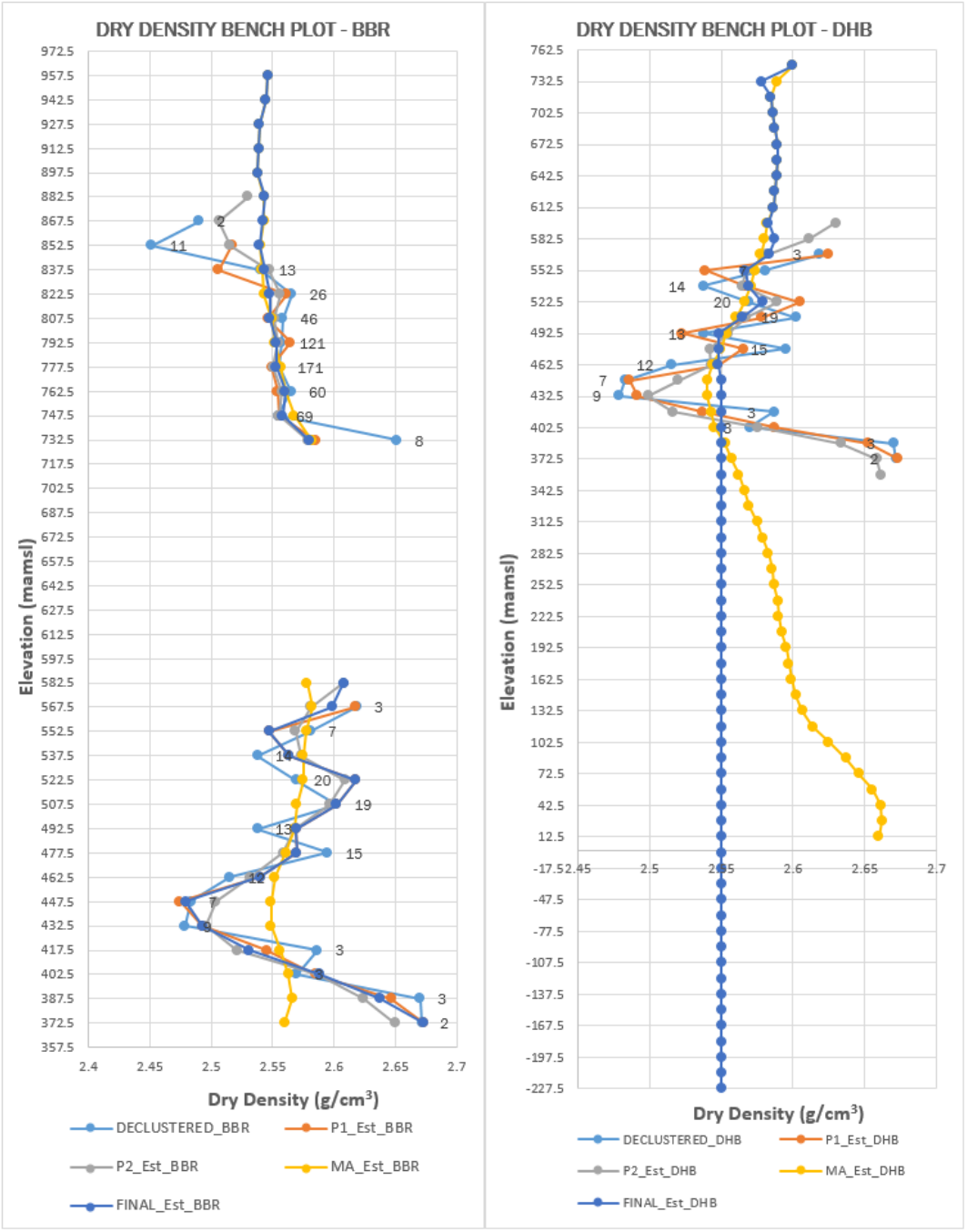
Appendix 4 Dry Density Bench plots within the AK1 rocktypes



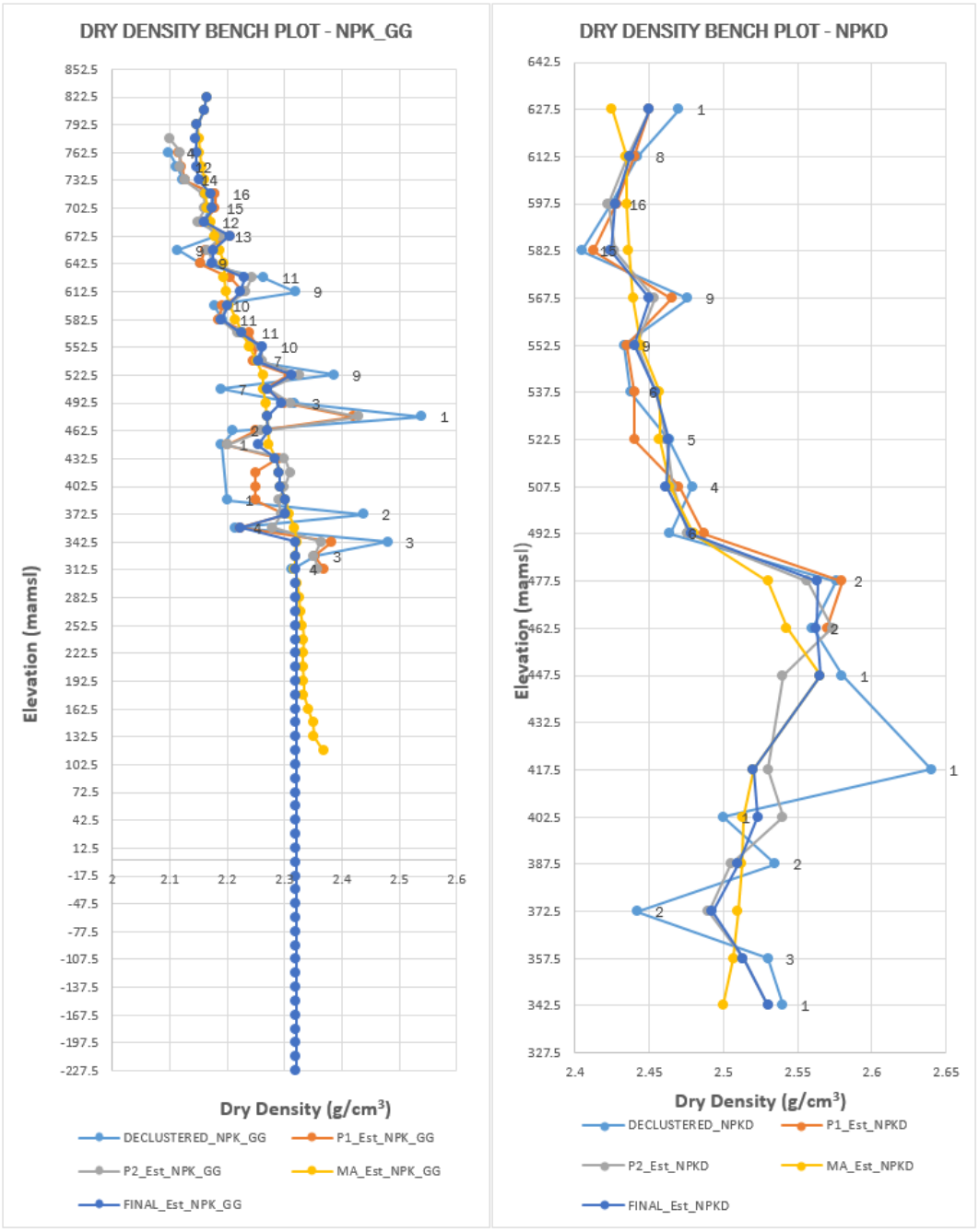
Dry Density Bench plots within the AK1 rocktypes continued



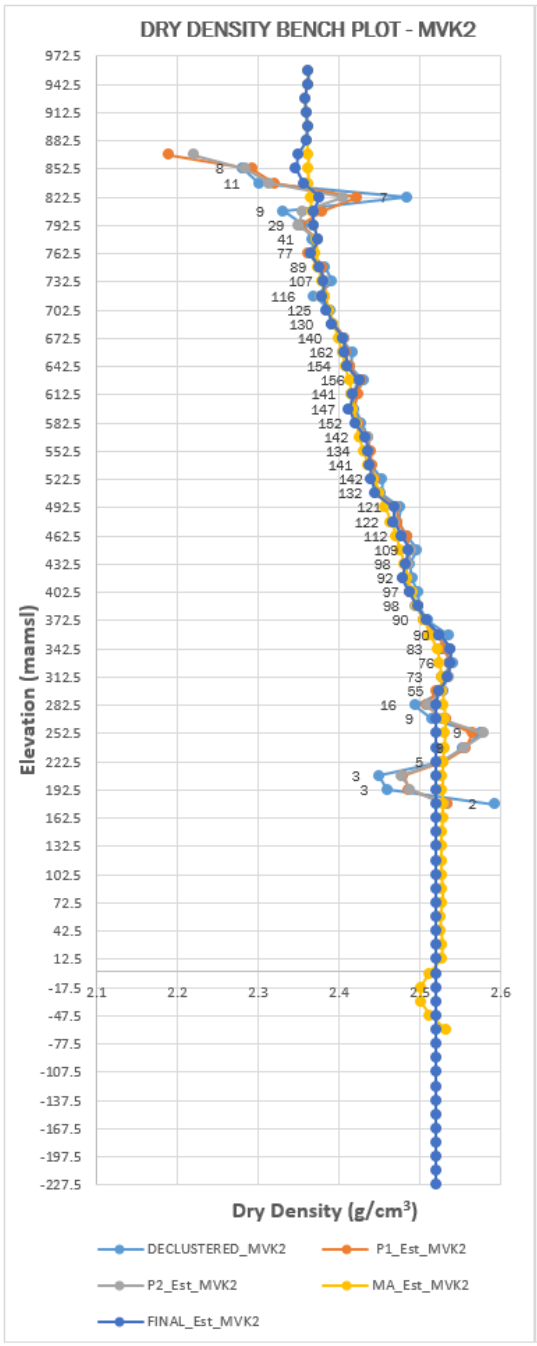
Dry Density Bench plots within the AK1 rocktypes continued

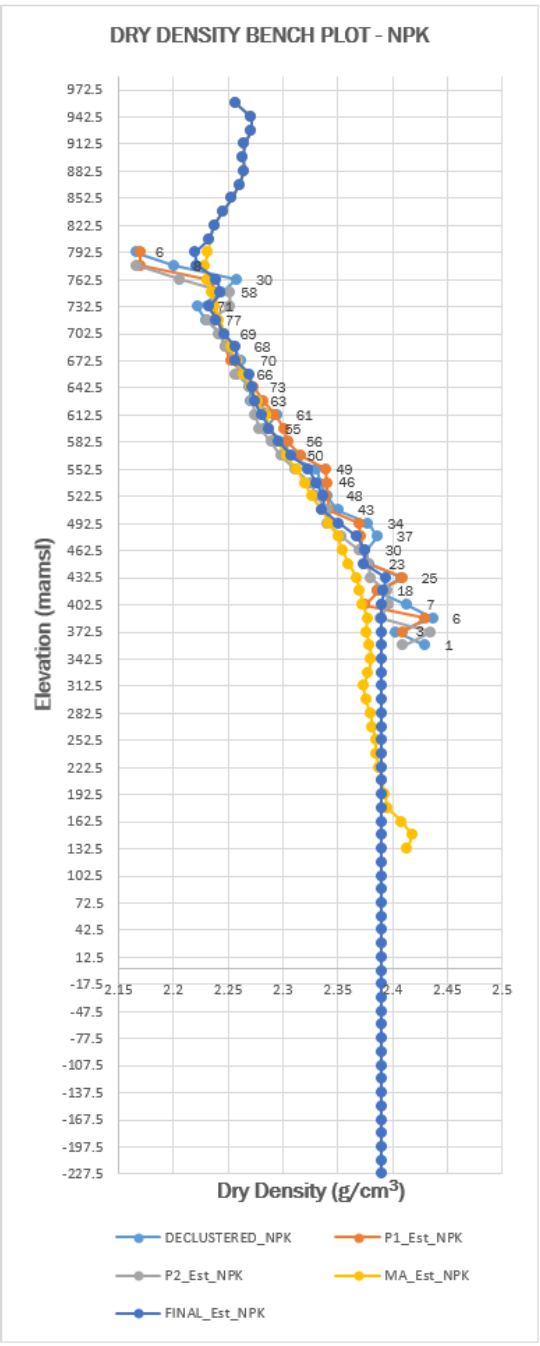


Dry Density Bench plots within the AK1 rocktypes continued

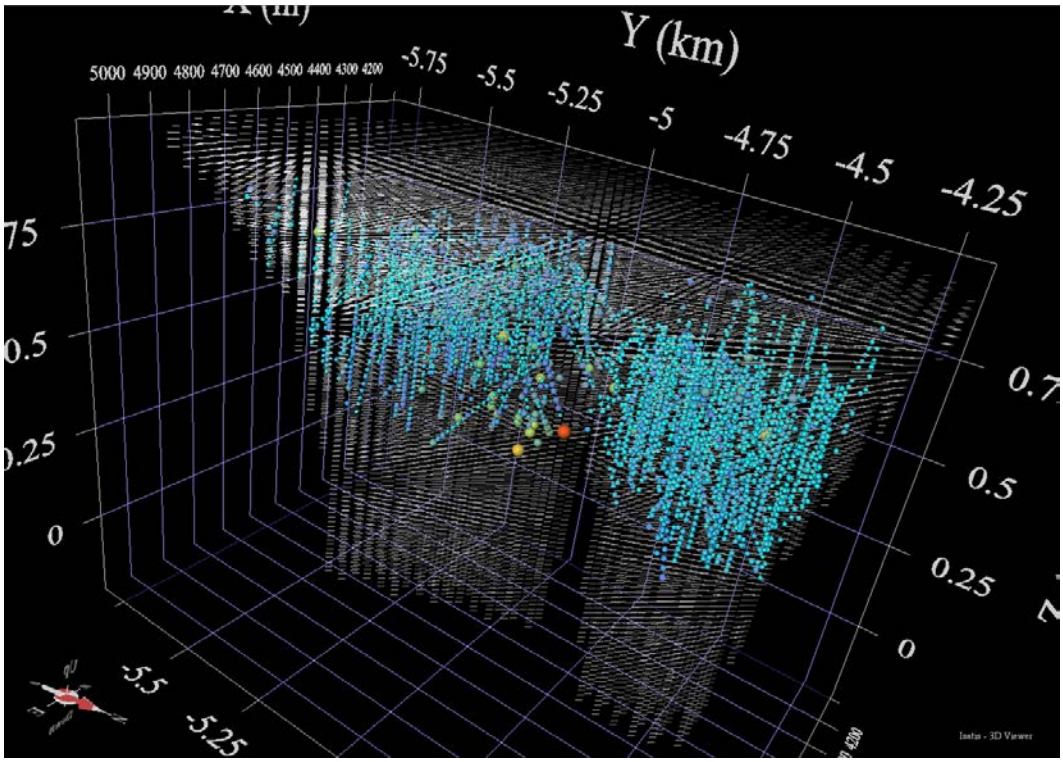


Dry Density Bench plots within the AK1 rocktypes continued

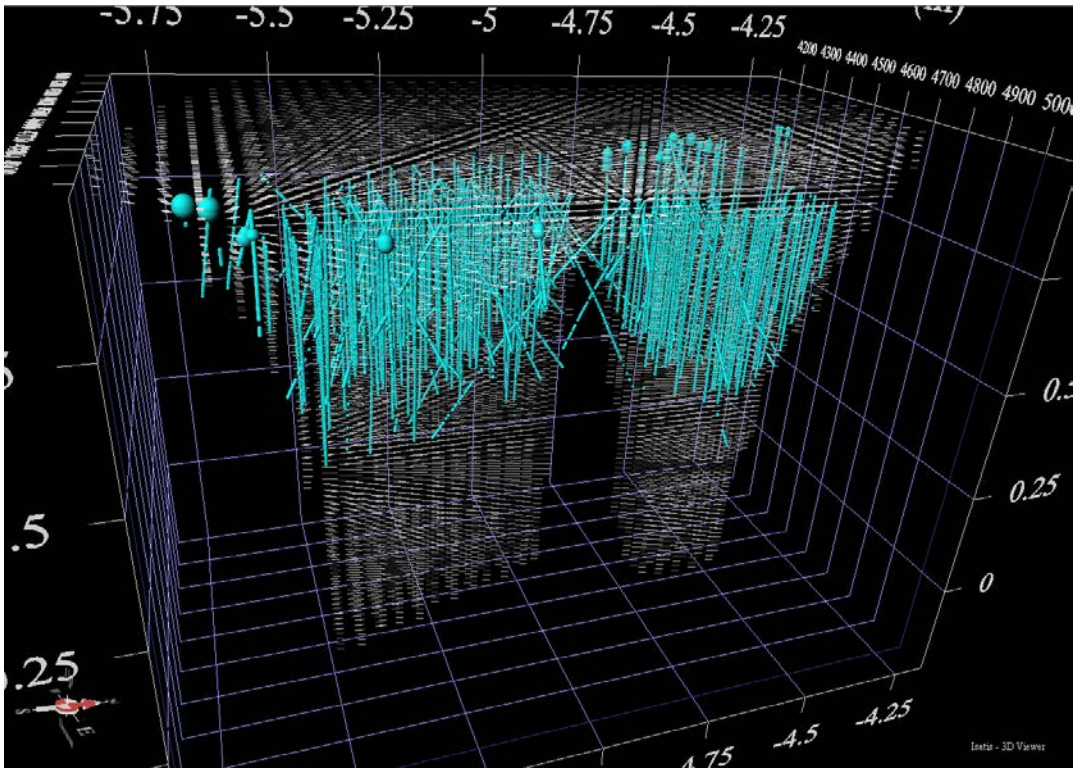




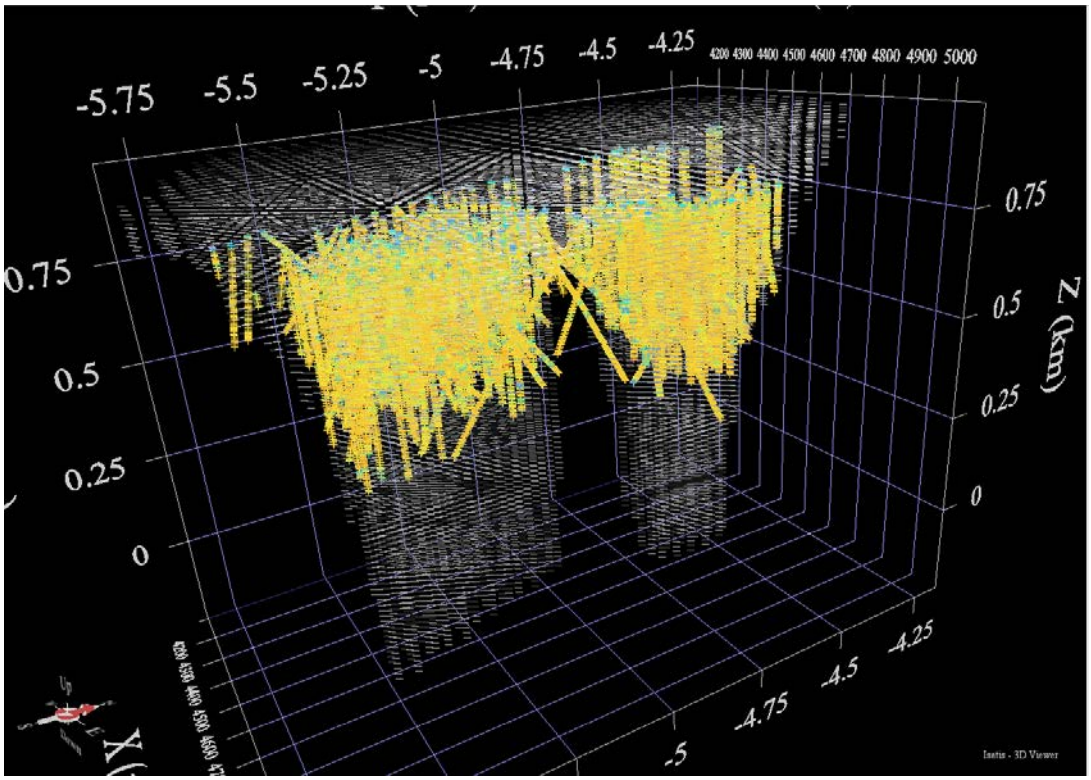
Appendix 5 AK1 UCS sample data distribution



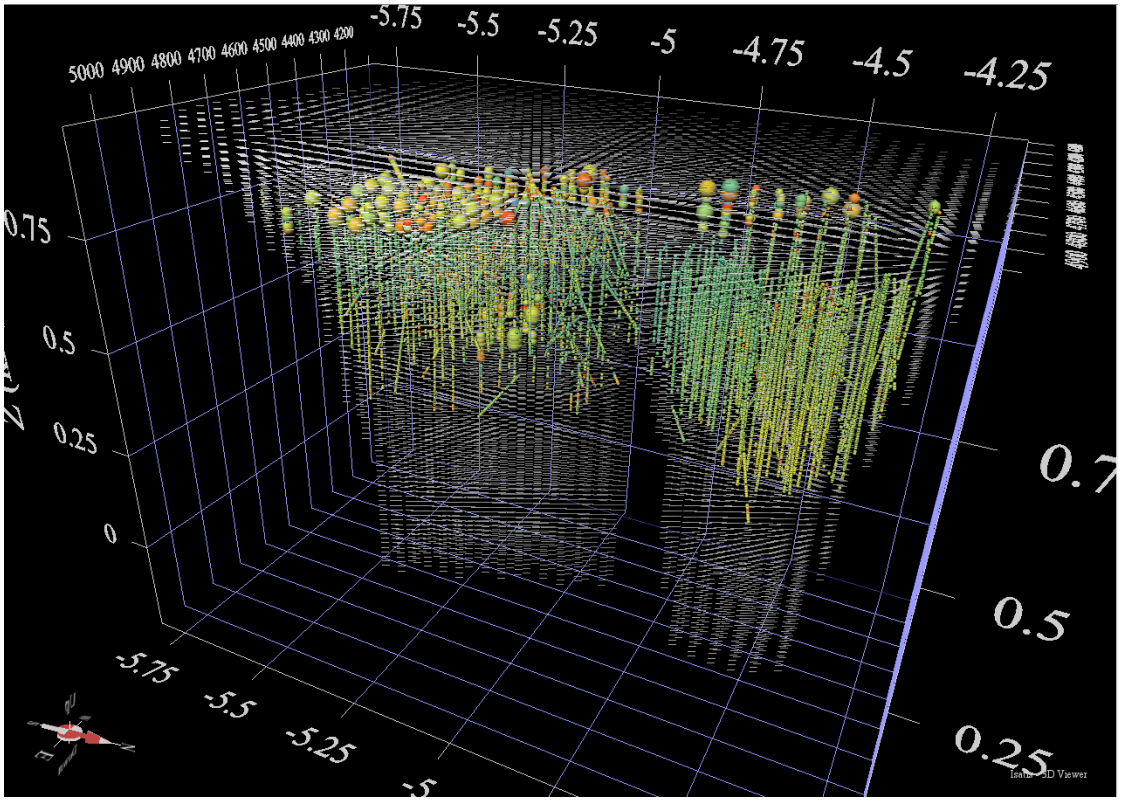
Appendix 6 AK1 FFPM sample data distribution



Appendix 7 AK1 RQD sample data distribution

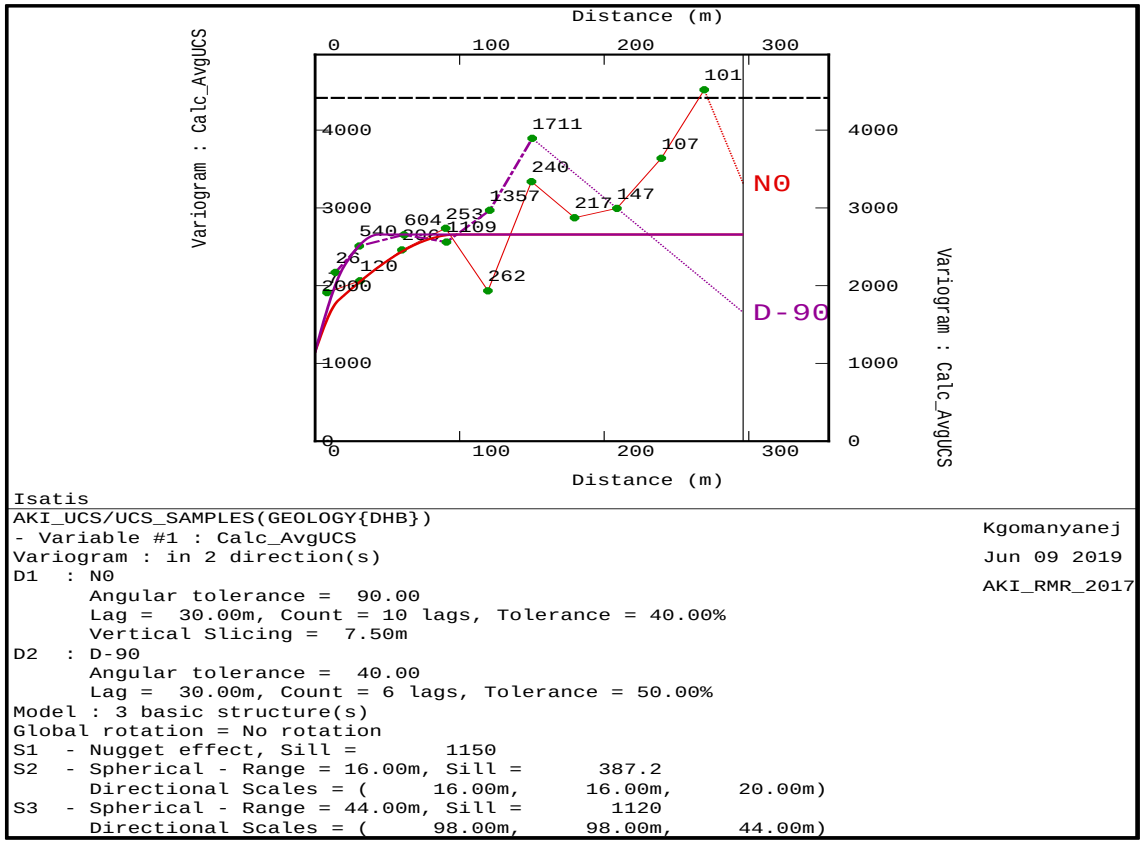


Appendix 8 AK1 Dry Density sample data distribution



Appendix 9 AK1 UCS variogram models

AK1 UCS variogram model – DHB



Isatis

AKI_UCS/UCS_SAMPLES(GEOLOGY{DHB})

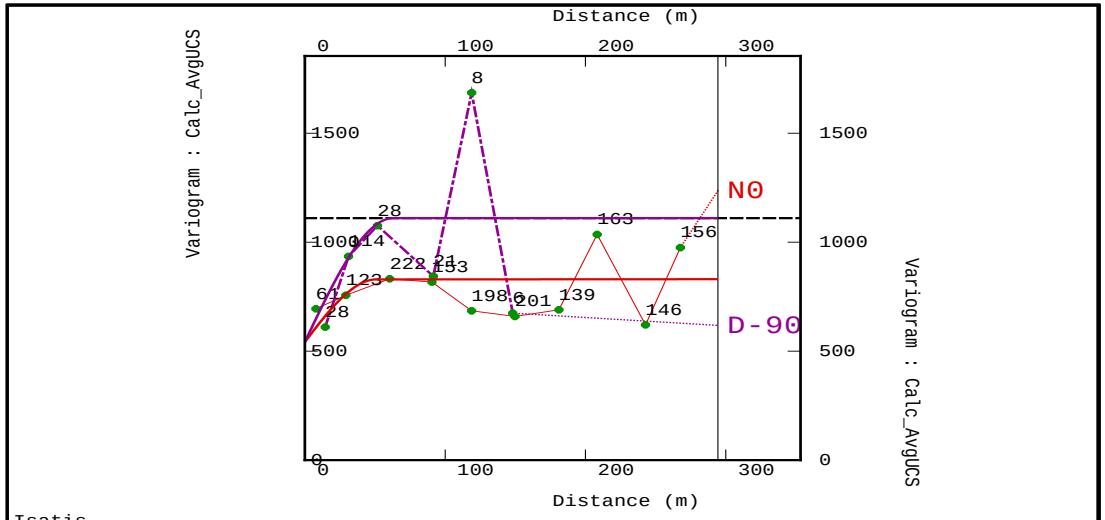
Kgomanyanej

Jun 09 2019

AKI_RMR_2017

- Variable #1 : Calc_AvgUCS
Variogram : in 2 direction(s)
D1 : N0
Angular tolerance = 90.00
Lag = 30.00m, Count = 10 lags, Tolerance = 40.00%
Vertical Slicing = 7.50m
D2 : D-90
Angular tolerance = 40.00
Lag = 30.00m, Count = 6 lags, Tolerance = 50.00%
Model : 3 basic structure(s)
Global rotation = No rotation
S1 - Nugget effect, Sill = 1150
S2 - Spherical - Range = 16.00m, Sill = 387.2
Directional Scales = (16.00m, 16.00m, 20.00m)
S3 - Spherical - Range = 44.00m, Sill = 1120
Directional Scales = (98.00m, 98.00m, 44.00m)

AK1 UCS variogram model – BBR

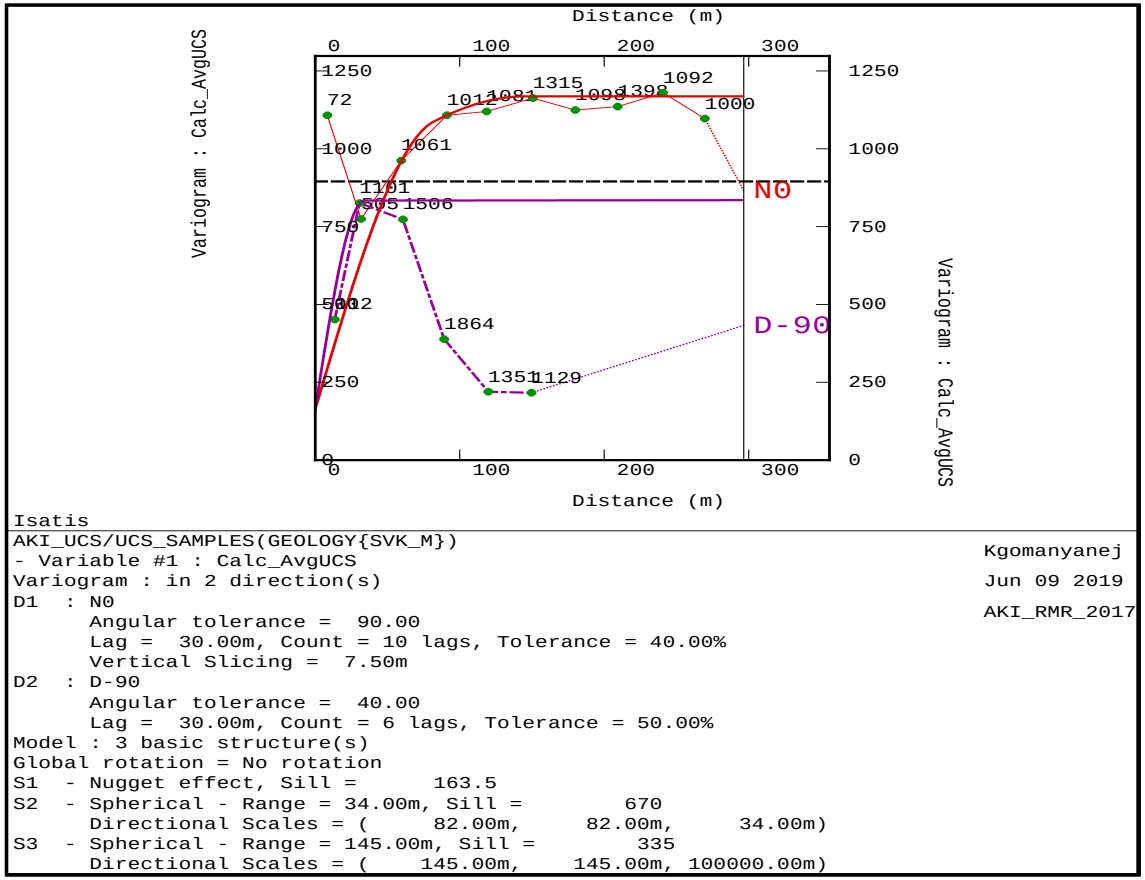


Isatis

AKI_UCS/UCS_SAMPLES(GEOLOGY{BBR})
- Variable #1 : Calc_AvgUCS
Variogram : in 2 direction(s)
D1 : N0
Angular tolerance = 90.00
Lag = 30.00m, Count = 10 lags, Tolerance = 40.00%
Vertical Slicing = 7.50m
D2 : D-90
Angular tolerance = 35.00
Lag = 30.00m, Count = 6 lags, Tolerance = 50.00%
Model : 3 basic structure(s)
Global rotation = No rotation
S1 - Nugget effect, Sill = 541.8
S2 - Spherical - Range = 51.00m, Sill = 287.2
Directional Scales = (51.00m, 51.00m, 63.00m)
S3 - Spherical - Range = 63.00m, Sill = 281.3
Directional Scales = (100000.00m, 100000.00m, 63.00m)

Kgomanyanej
Jun 09 2019
AKI_RMR_2017

AK1 UCS variogram model – SVK_M

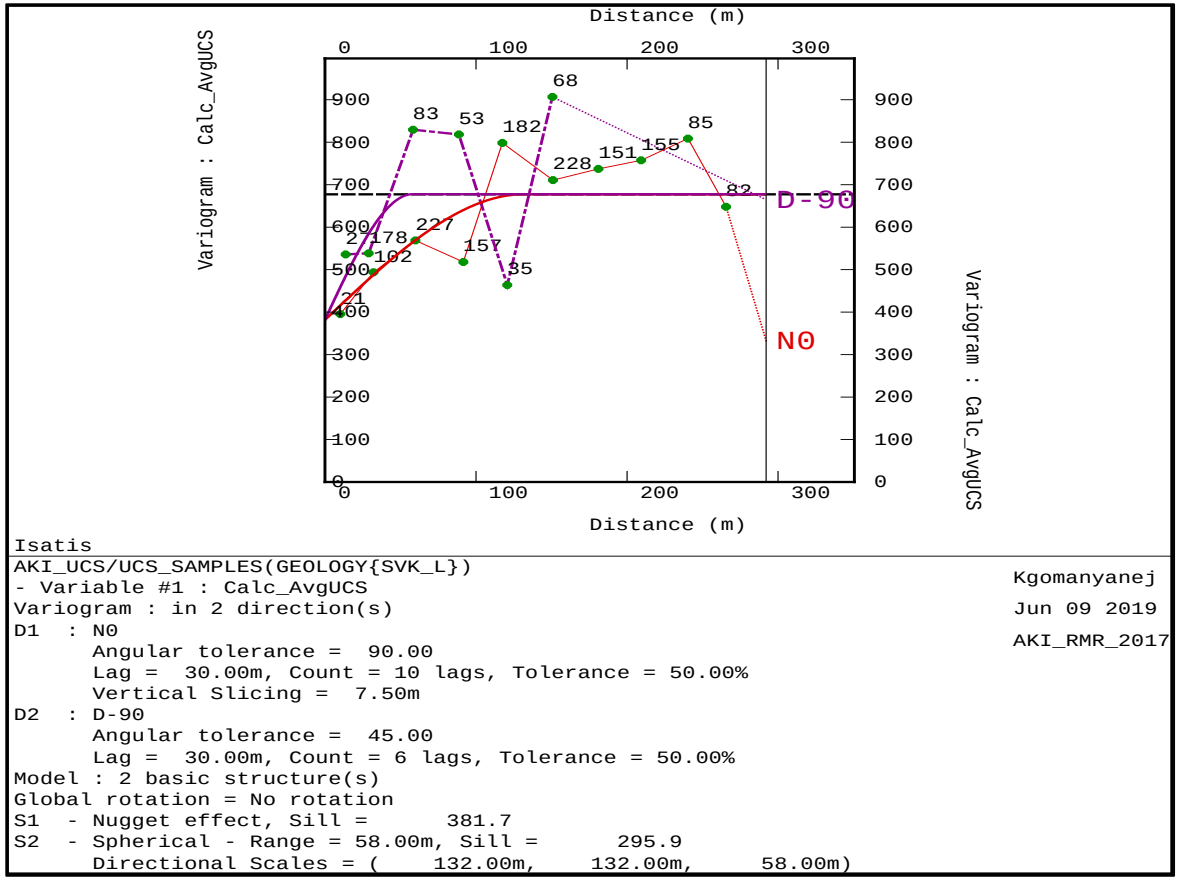


Isatis

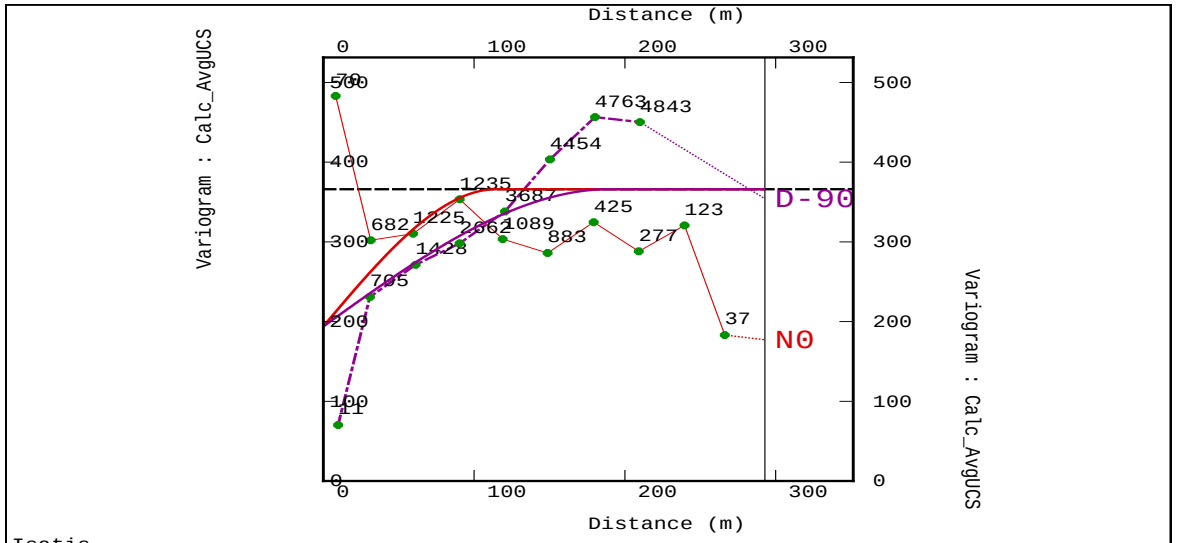
AKI_UCS/UCS_SAMPLES(GEOLOGY{SVK_M})
- Variable #1 : Calc_AvgUCS
Variogram : in 2 direction(s)
D1 : N0
Angular tolerance = 90.00
Lag = 30.00m, Count = 10 lags, Tolerance = 40.00%
Vertical Slicing = 7.50m
D2 : D-90
Angular tolerance = 40.00
Lag = 30.00m, Count = 6 lags, Tolerance = 50.00%
Model : 3 basic structure(s)
Global rotation = No rotation
S1 - Nugget effect, Sill = 163.5
S2 - Spherical - Range = 34.00m, Sill = 670
Directional Scales = (82.00m, 82.00m, 34.00m)
S3 - Spherical - Range = 145.00m, Sill = 335
Directional Scales = (145.00m, 145.00m, 100000.00m)

Kgomanyanej
Jun 09 2019
AKI_RMR_2017

AK1 UCS variogram model – SVK_L



AK1 UCS variogram model – NPK

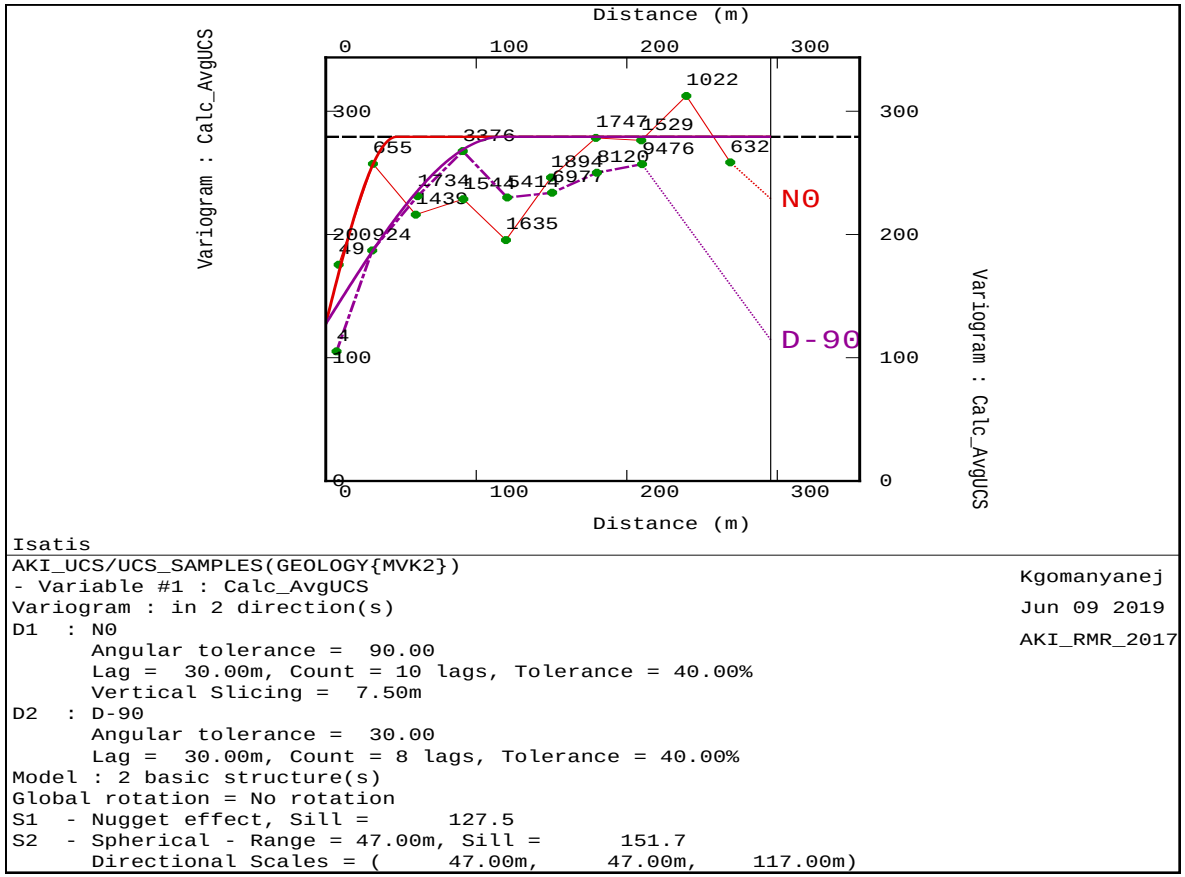


Isatis

AKI_UCS/UCS_SAMPLES(GEOLOGY{NPK})
- Variable #1 : Calc_AvgUCS
Variogram : in 2 direction(s)
D1 : N0
Angular tolerance = 90.00
Lag = 30.00m, Count = 10 lags, Tolerance = 40.00%
Vertical Slicing = 7.50m
D2 : D-90
Angular tolerance = 30.00
Lag = 30.00m, Count = 8 lags, Tolerance = 40.00%
Model : 2 basic structure(s)
Global rotation = No rotation
S1 - Nugget effect, Sill = 193.9
S2 - Spherical - Range = 115.00m, Sill = 172.2
Directional Scales = (115.00m, 115.00m, 190.00m)

Kgomanyanej
Jun 09 2019
AKI_RMR_2017

AK1 UCS variogram model – MVK2

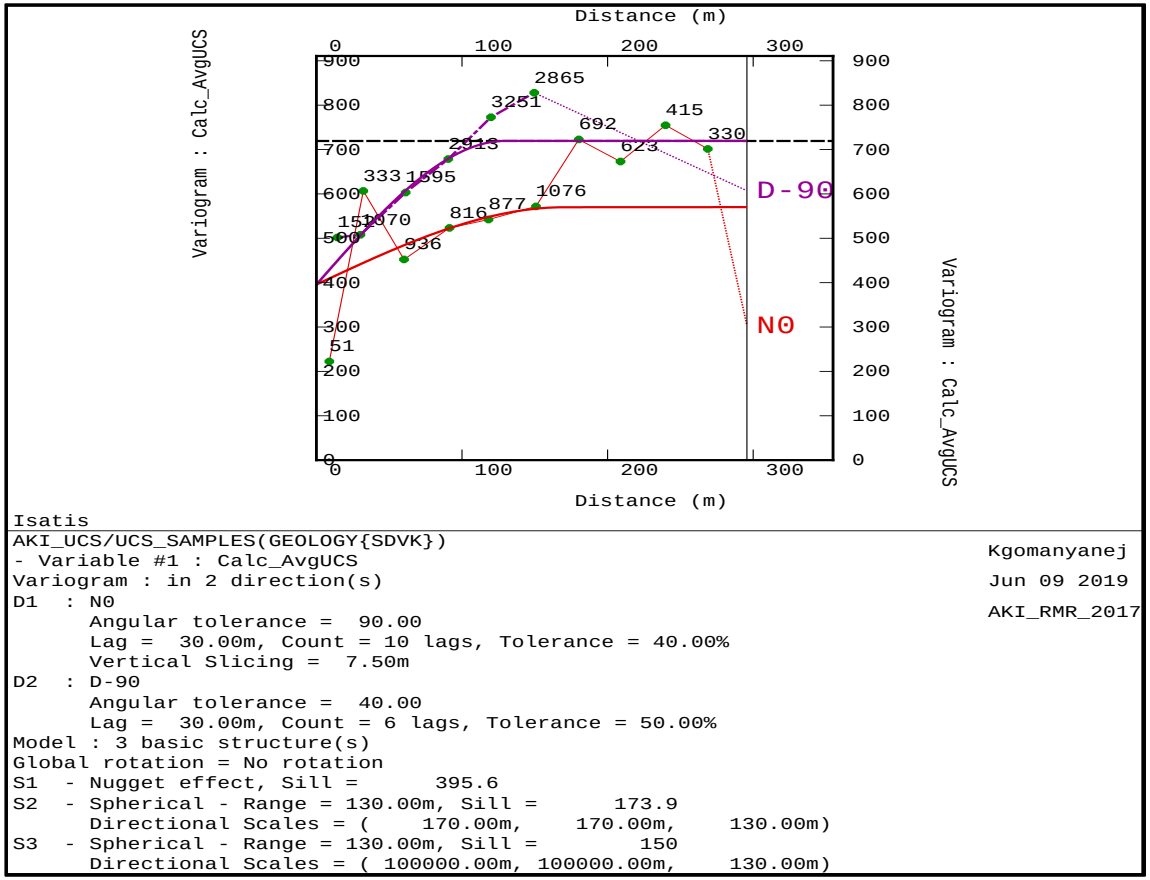


Isatis

AKI_UCS/UCS_SAMPLES(GEOLOGY{MVK2})
- Variable #1 : Calc_AvgUCS
Variogram : in 2 direction(s)
D1 : N0
Angular tolerance = 90.00
Lag = 30.00m, Count = 10 lags, Tolerance = 40.00%
Vertical Slicing = 7.50m
D2 : D-90
Angular tolerance = 30.00
Lag = 30.00m, Count = 8 lags, Tolerance = 40.00%
Model : 2 basic structure(s)
Global rotation = No rotation
S1 - Nugget effect, Sill = 127.5
S2 - Spherical - Range = 47.00m, Sill = 151.7
Directional Scales = (47.00m, 47.00m, 117.00m)

Kgomanyanej
Jun 09 2019
AKI_RMR_2017

AK1 UCS variogram model – SDVK



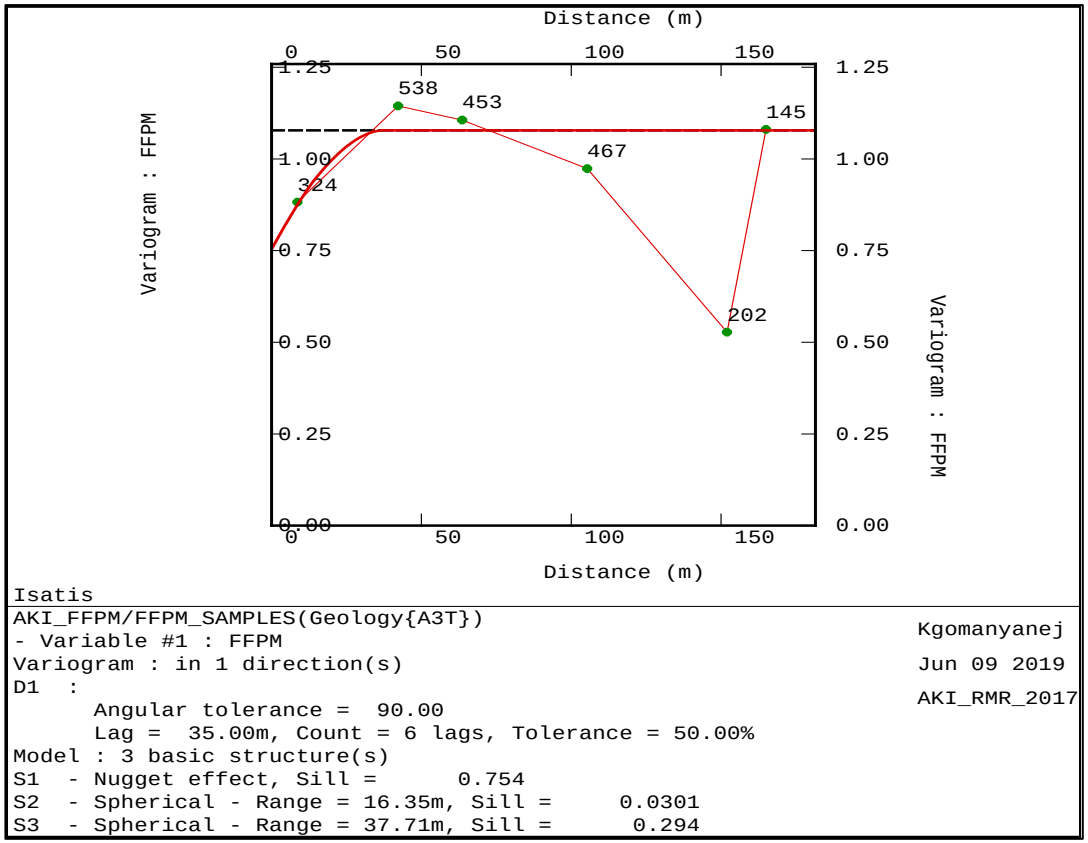
Isatis

AKI_UCS/UCS_SAMPLES(GEOLOGY{SDVK})
- Variable #1 : Calc_AvgUCS
Variogram : in 2 direction(s)
D1 : N0
Angular tolerance = 90.00
Lag = 30.00m, Count = 10 lags, Tolerance = 40.00%
Vertical Slicing = 7.50m
D2 : D-90
Angular tolerance = 40.00
Lag = 30.00m, Count = 6 lags, Tolerance = 50.00%
Model : 3 basic structure(s)
Global rotation = No rotation
S1 - Nugget effect, Sill = 395.6
S2 - Spherical - Range = 130.00m, Sill = 173.9
Directional Scales = (170.00m, 170.00m, 130.00m)
S3 - Spherical - Range = 130.00m, Sill = 150
Directional Scales = (100000.00m, 100000.00m, 130.00m)

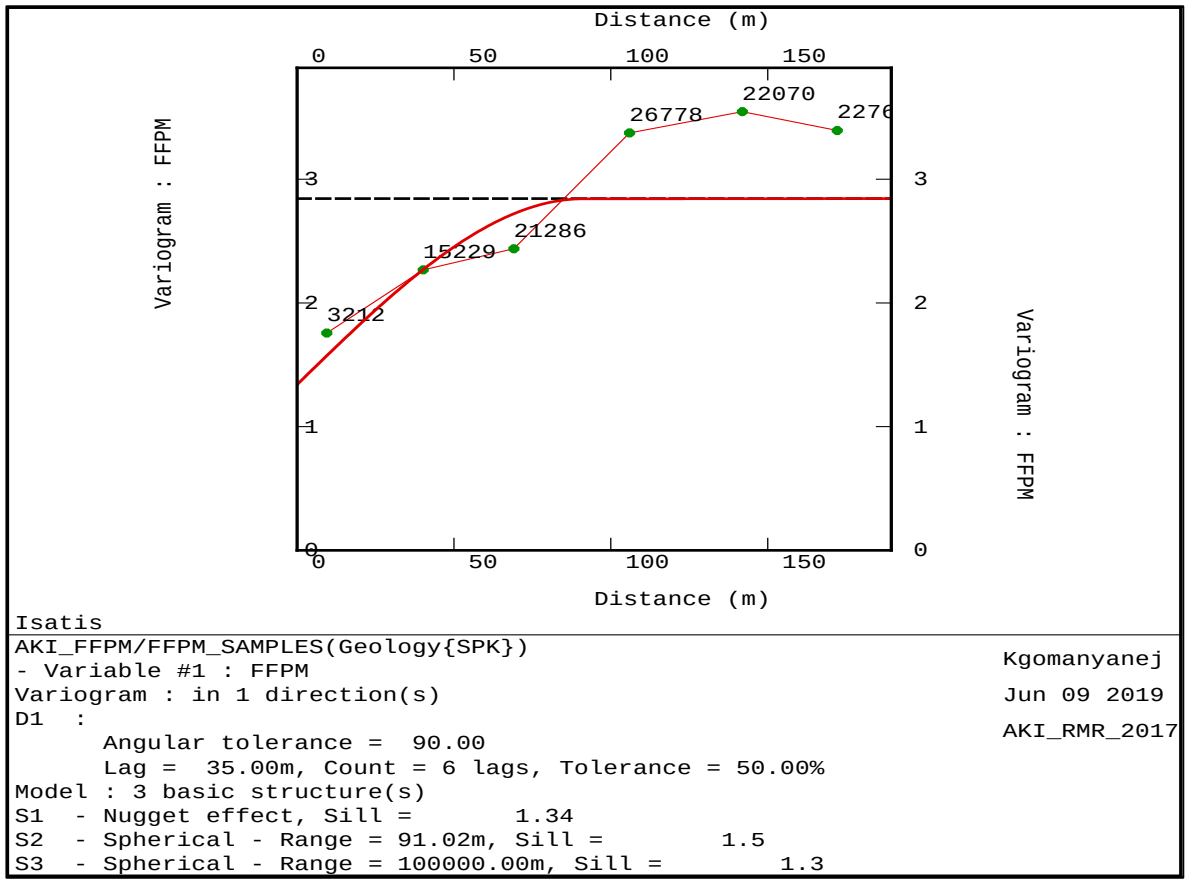
Kgomanyanej
Jun 09 2019
AKI_RMR_2017

Appendix 10 AK1 FFPM variogram models

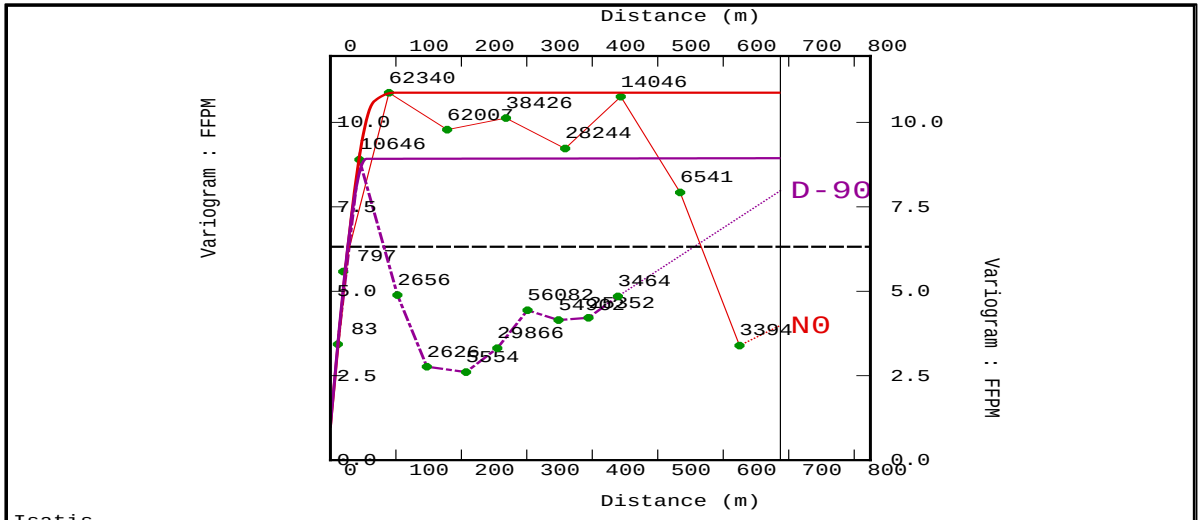
AK1 FFPM variogram model – AT3



AK1 FFPM variogram model – SPK



AK1 FFPM variogram model – BBR

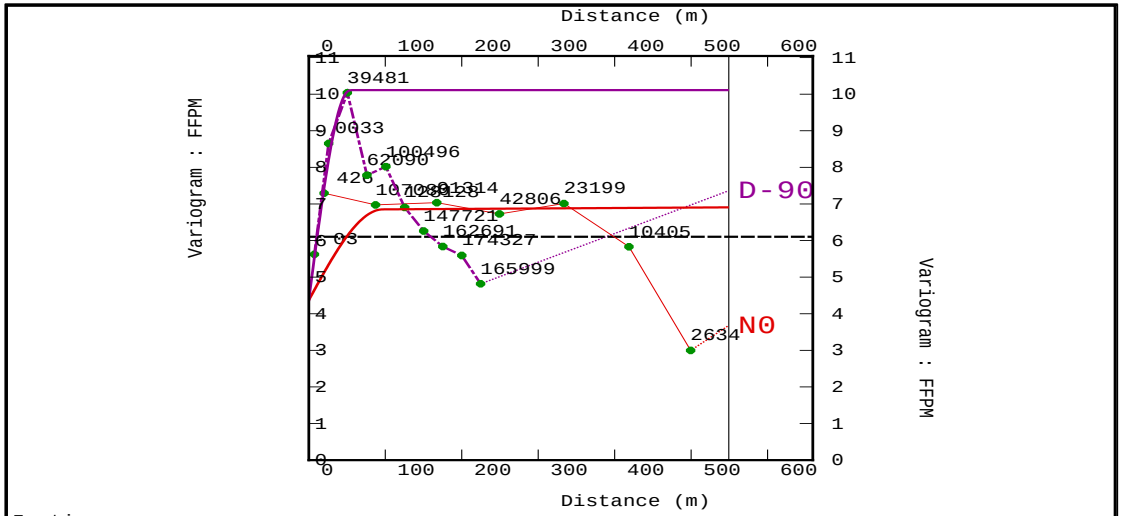


Isatis

AKI_FFPM/FFPM_SAMPLES(Geology{BBR})
- Variable #1 : FFPM
Variogram : in 2 direction(s)
D1 : N0
Angular tolerance = 90.00
Lag = 90.00m, Count = 8 lags, Tolerance = 50.00%
Vertical Slicing = 7.50m
D2 : D-90
Angular tolerance = 30.00
Lag = 50.00m, Count = 10 lags, Tolerance = 50.00%
Model : 3 basic structure(s)
Global rotation = No rotation
S1 - Nugget effect, Sill = 1
S2 - Spherical - Range = 54.76m, Sill = 7.92
Directional Scales = (66.58m, 66.58m, 54.76m)
S3 - Spherical - Range = 97.11m, Sill = 1.96
Directional Scales = (97.11m, 97.11m, 100000.00m)

Kgomanyanej
Jun 09 2019
AKI_RMR_2017

AK1 FFPM variogram model – DHB

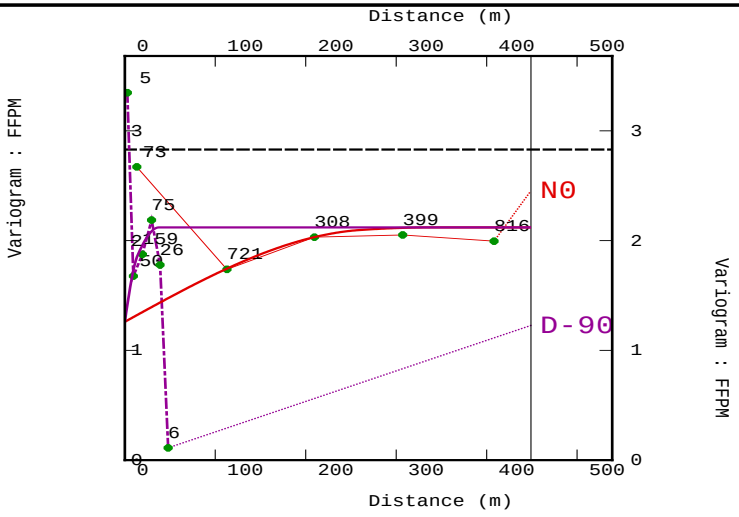


Isatis

AKI_FFPM/FFPM_SAMPLES(Geology{DHB})
- Variable #1 : FFPM
Variogram : in 2 direction(s)
D1 : N0
Angular tolerance = 90.00
Lag = 85.00m, Count = 7 lags, Tolerance = 50.00%
Vertical Slicing = 7.50m
D2 : D-90
Angular tolerance = 35.00
Lag = 25.00m, Count = 10 lags, Tolerance = 50.00%
Model : 3 basic structure(s)
Global rotation = No rotation
S1 - Nugget effect, Sill = 4.37
S2 - Spherical - Range = 51.33m, Sill = 2.47
Directional Scales = (96.77m, 96.77m, 51.33m)
S3 - Spherical - Range = 55.33m, Sill = 3.27
Directional Scales = (40000.00m, 40000.00m, 55.33m)

Kgomanyanej
Jun 09 2019
AKI_RMR_2017

AK1 FFPM variogram model – SVK_U

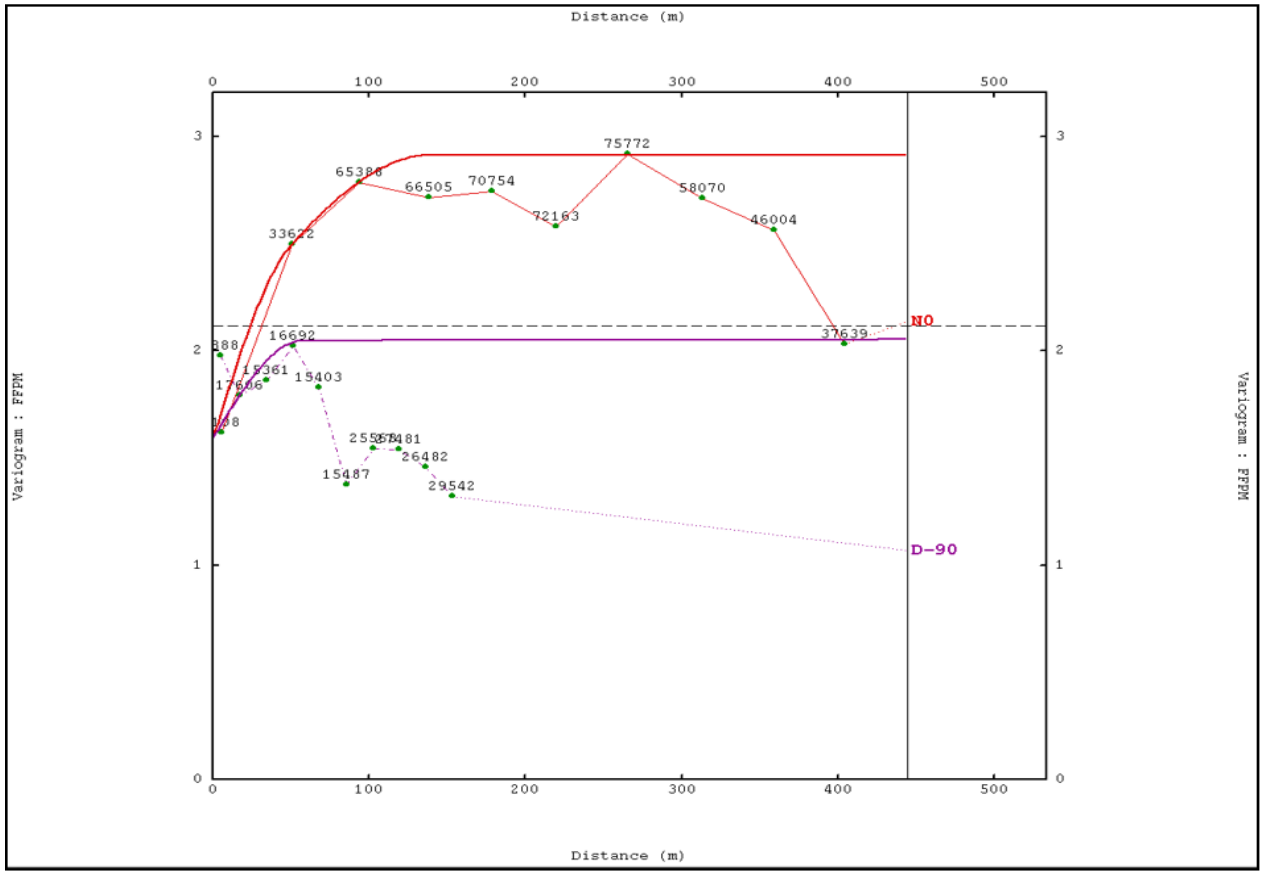


Isatis

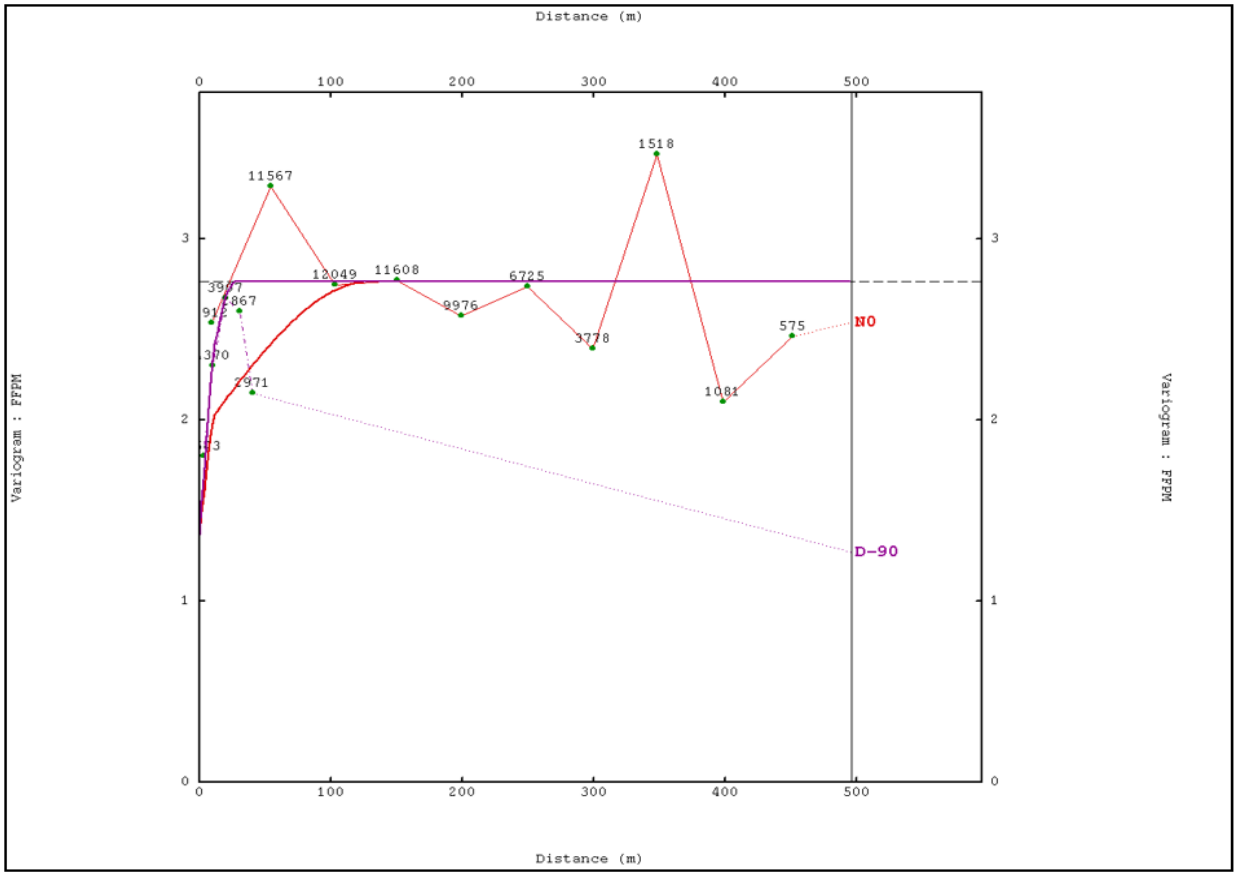
AKI_FFPM/FFPM_SAMPLES(Geology{SVK_U})
- Variable #1 : FFPM
Variogram : in 2 direction(s)
D1 : N0
Angular tolerance = 90.00
Lag = 100.00m, Count = 5 lags, Tolerance = 50.00%
Vertical Slicing = 7.50m
D2 : D-90
Angular tolerance = 25.00
Lag = 10.00m, Count = 10 lags, Tolerance = 50.00%
Model : 3 basic structure(s)
Global rotation = No rotation
S1 - Nugget effect, Sill = 1.26
S2 - Spherical - Range = 37.69m, Sill = 0.55
Directional Scales = (260.00m, 260.00m, 37.69m)
S3 - Spherical - Range = 13.83m, Sill = 0.31
Directional Scales = (340.00m, 340.00m, 13.83m)

Kgomanyanej
Jun 10 2019
AKI_RMR_2017

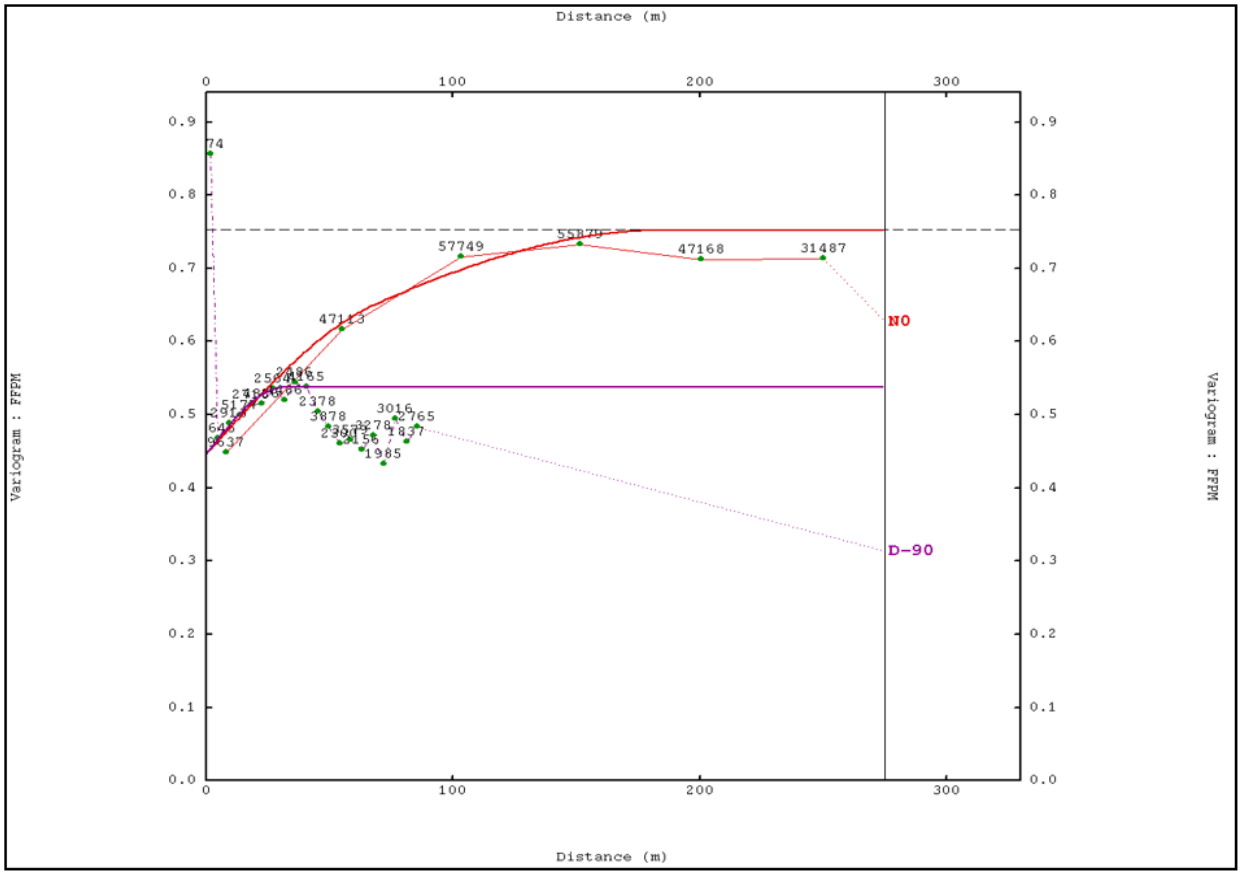
AK1 FFPM variogram model – SVK_M



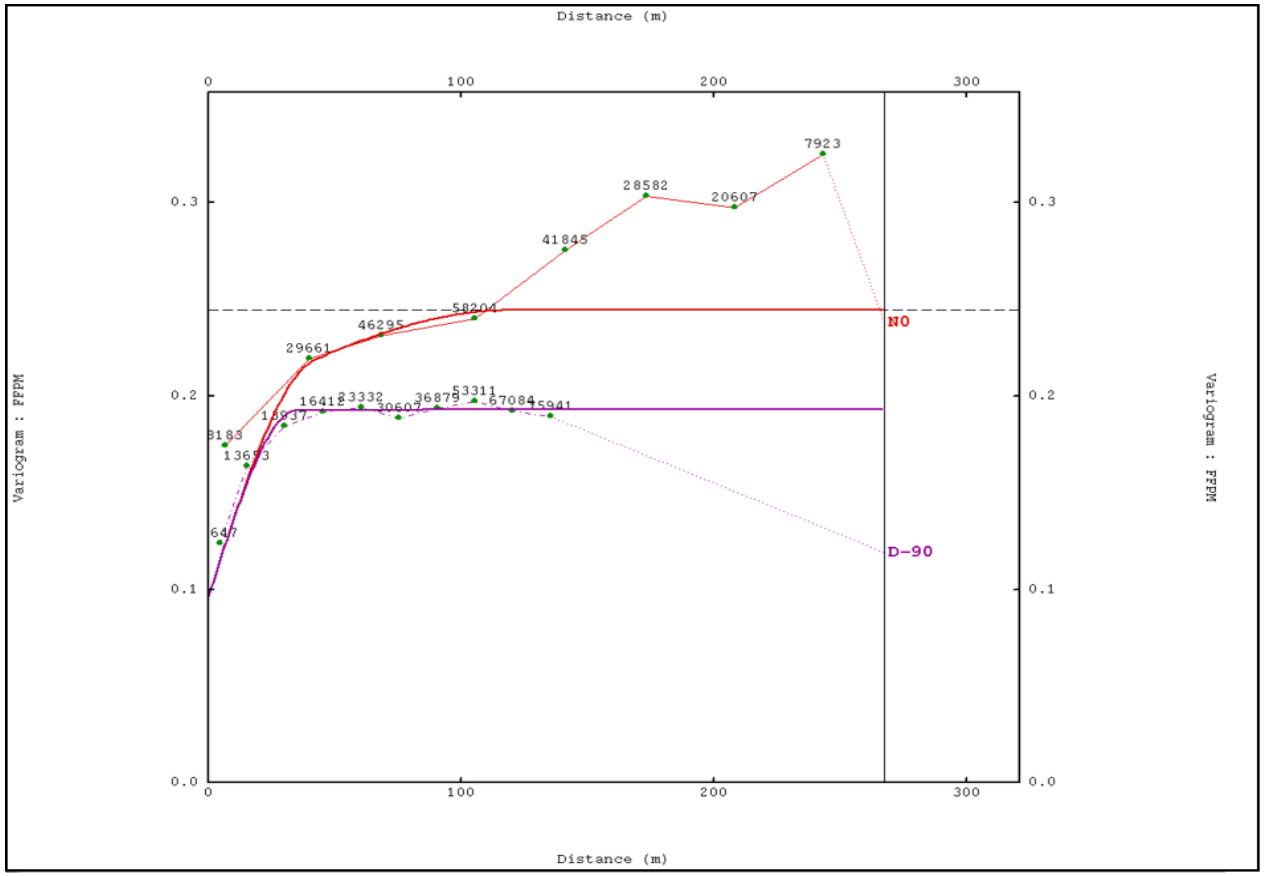
AK1 FFPM variogram model – SVK_L



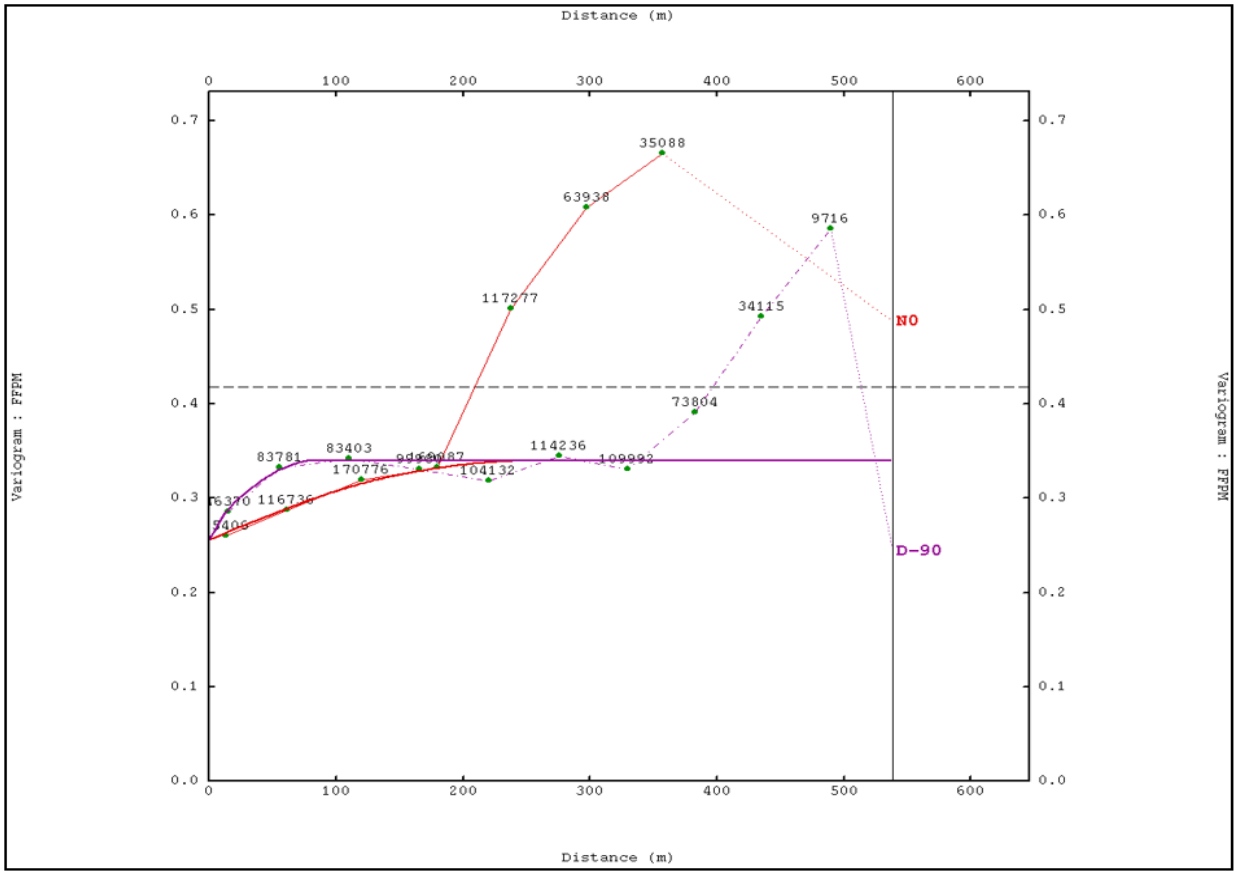
AK1 FFPM variogram model – SDVK



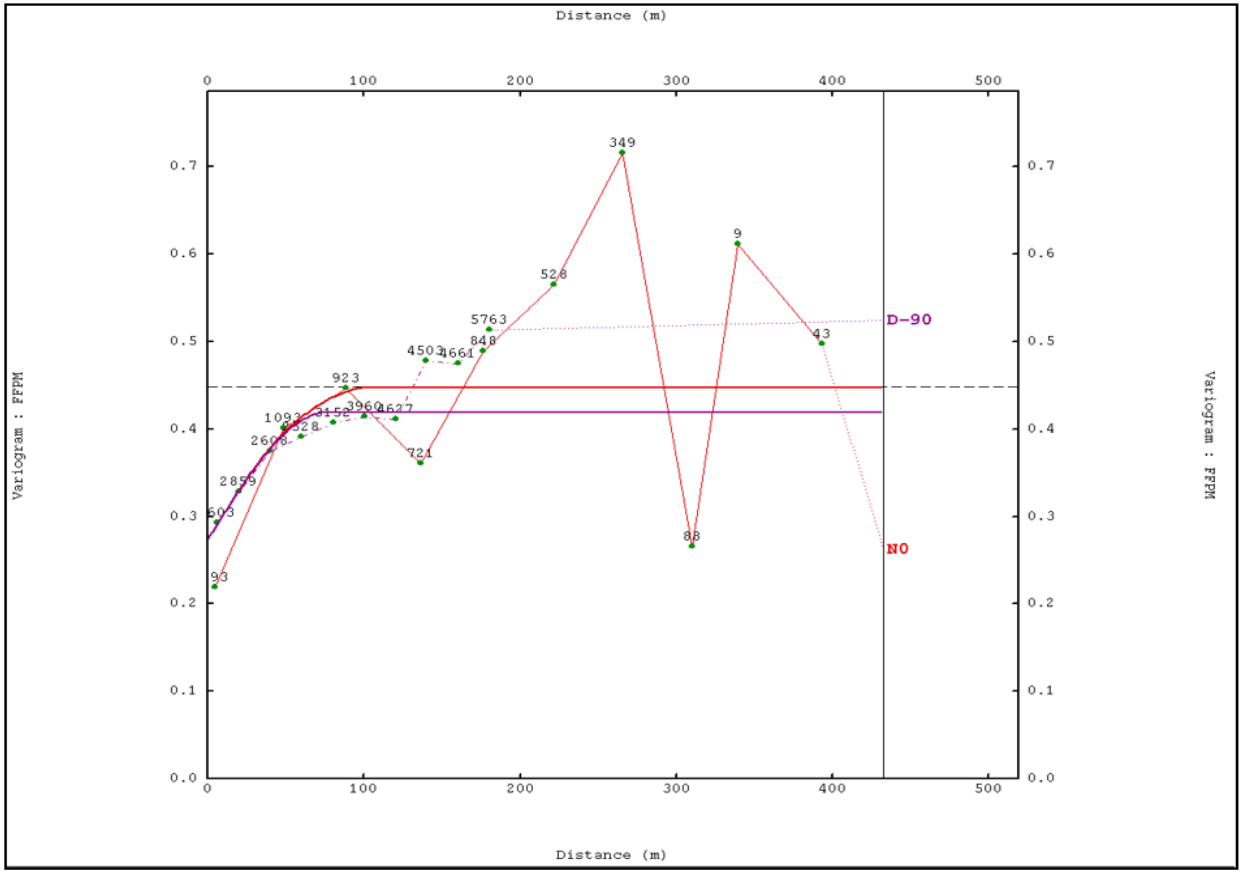
AK1 FFPM variogram model – NPK



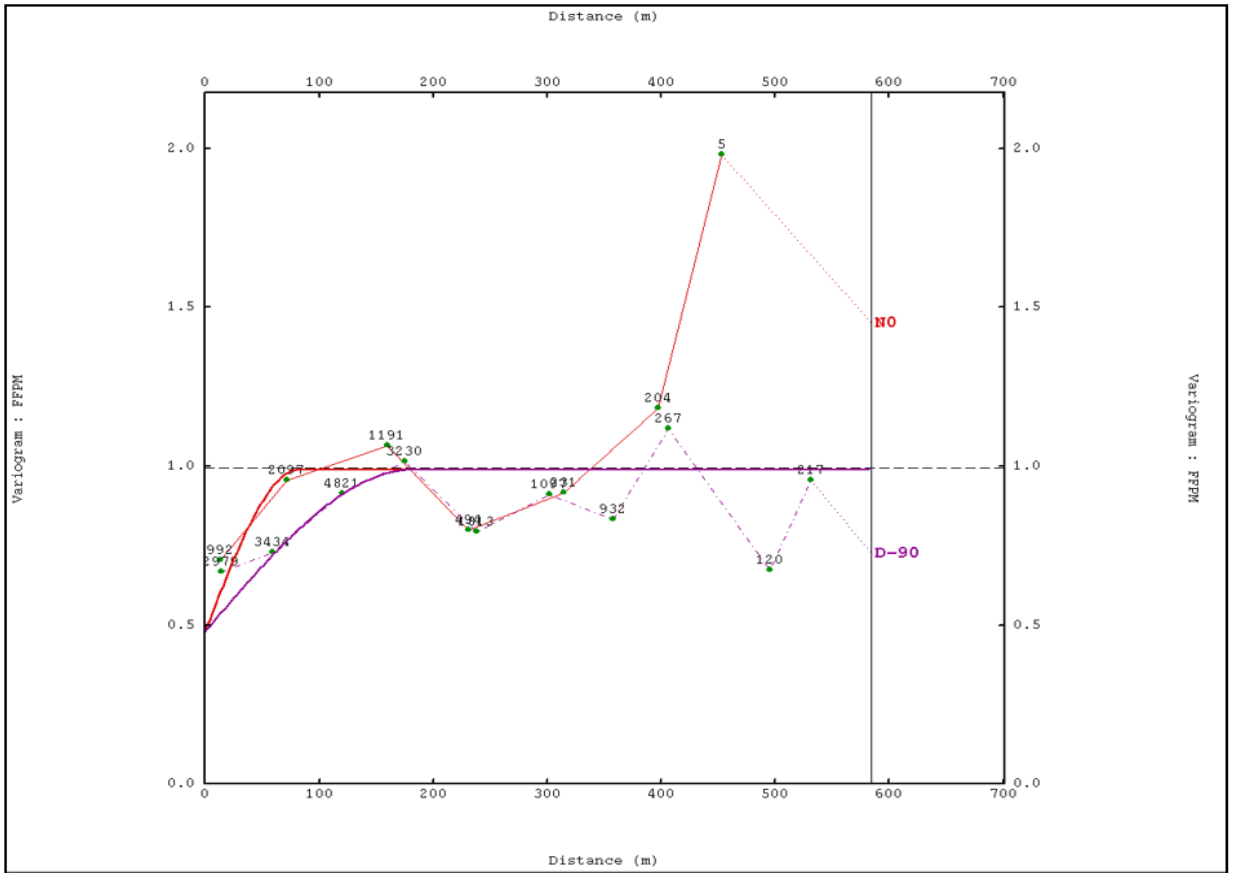
AK1 FFPM variogram model – MVK2



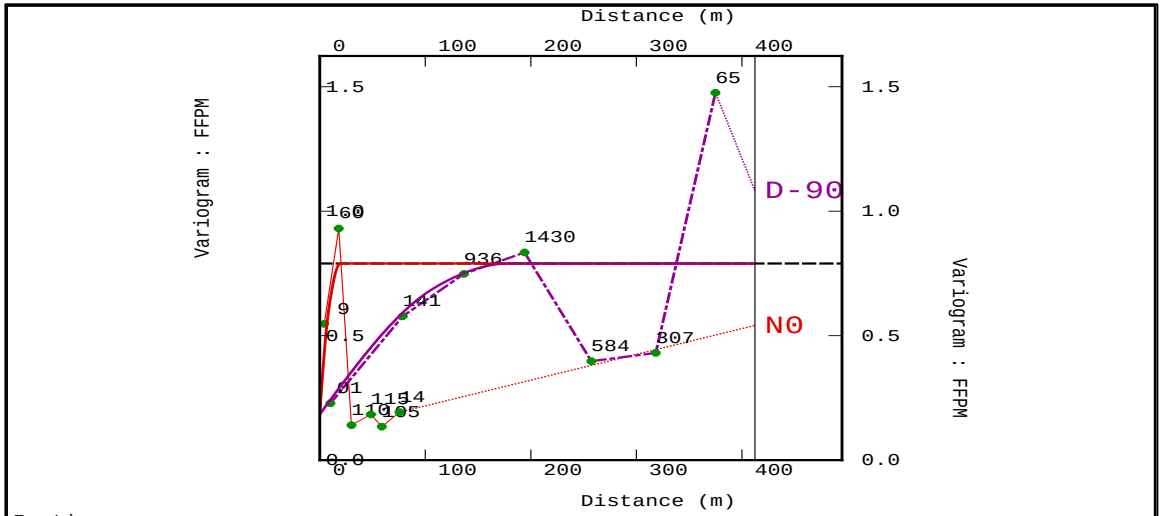
AK1 FFPM variogram model – NPK_GG



AK1 FFPM variogram model – MVK2_BBR



AK1 FFPM variogram model – NPKD



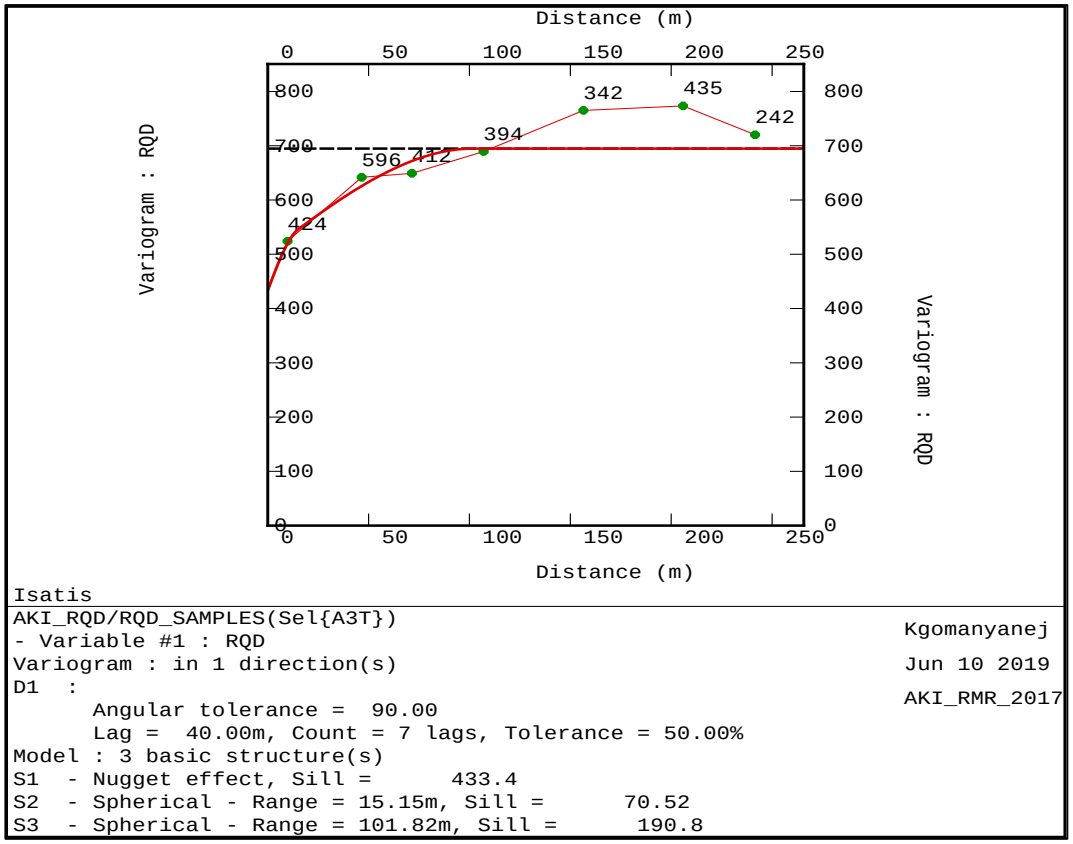
Isatis

AKI_FFPM/FFPM_SAMPLES(Geology{NPKD})
- Variable #1 : FFPM
Variogram : in 2 direction(s)
D1 : N0
Angular tolerance = 90.00
Lag = 15.00m, Count = 6 lags, Tolerance = 50.00%
Vertical Slicing = 7.50m
D2 : D-90
Angular tolerance = 25.00
Lag = 65.00m, Count = 10 lags, Tolerance = 50.00%
Model : 3 basic structure(s)
Global rotation = No rotation
S1 - Nugget effect, Sill = 0.184
S2 - Spherical - Range = 8.06m, Sill = 0.129
Directional Scales = (8.06m, 8.06m, 107.91m)
S3 - Spherical - Range = 19.57m, Sill = 0.477
Directional Scales = (19.57m, 19.57m, 180.26m)

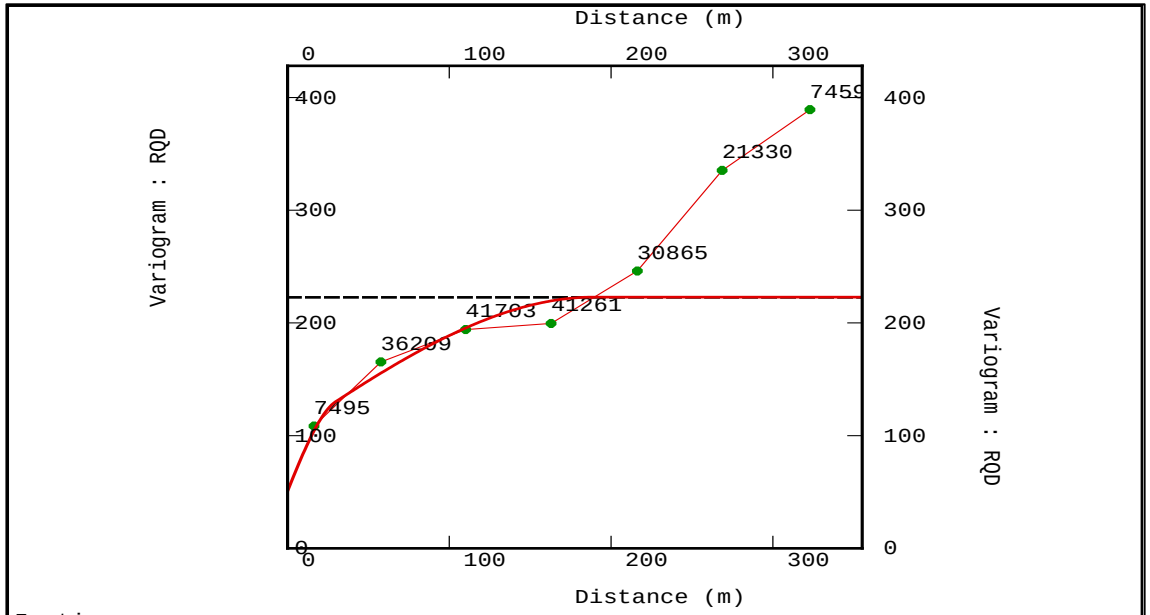
Kgomanyanej
Jun 10 2019
AKI_RMR_2017

Appendix 11 AK1 RQD variogram models

AK1 RQD variogram model – A3T



AK1 RQD variogram model – SPK

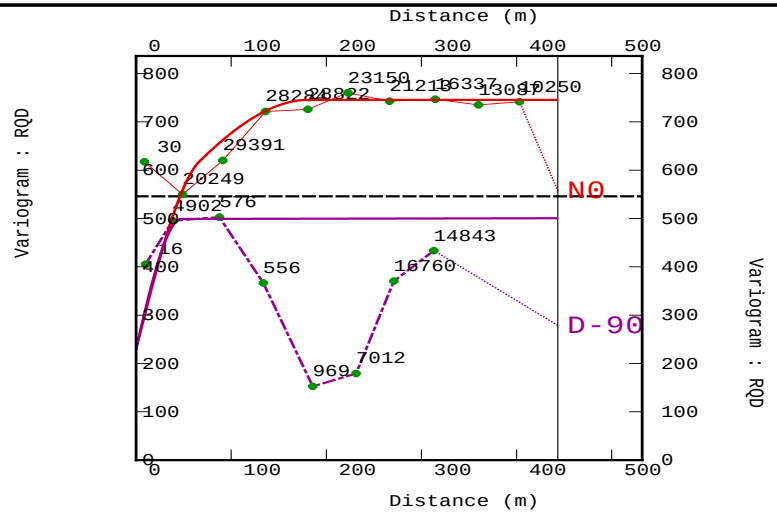


Isatis

AKI_RQD/RQD_SAMPLES(Sel{SPK})
- Variable #1 : RQD
Variogram : in 1 direction(s)
D1 :
Angular tolerance = 90.00
Lag = 55.00m, Count = 7 lags, Tolerance = 50.00%
Model : 3 basic structure(s)
S1 - Nugget effect, Sill = 50.81
S2 - Spherical - Range = 29.76m, Sill = 51.02
S3 - Spherical - Range = 189.42m, Sill = 121.1

Kgomanyanej
Jun 10 2019
AKI_RMR_2017

AK1 RQD variogram model – BBR

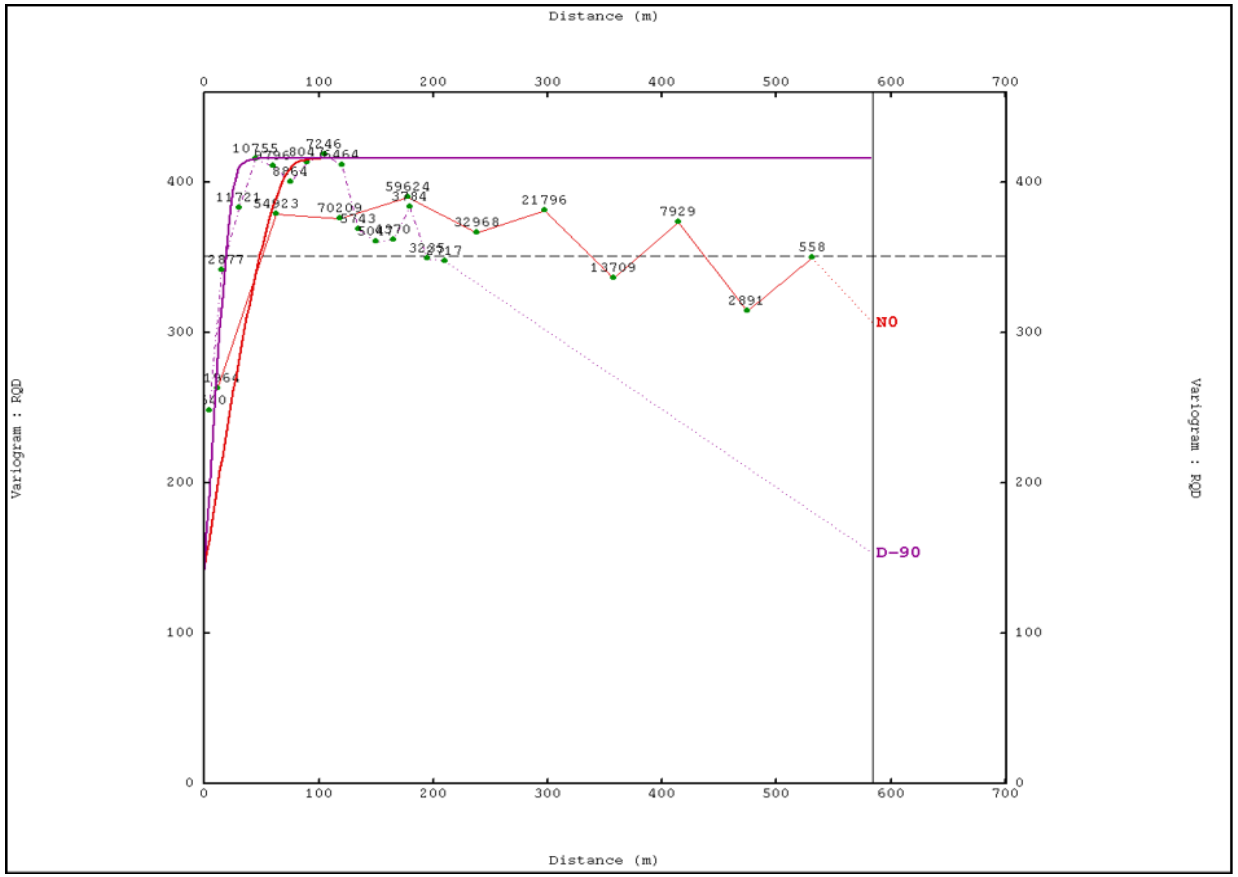


Isatis

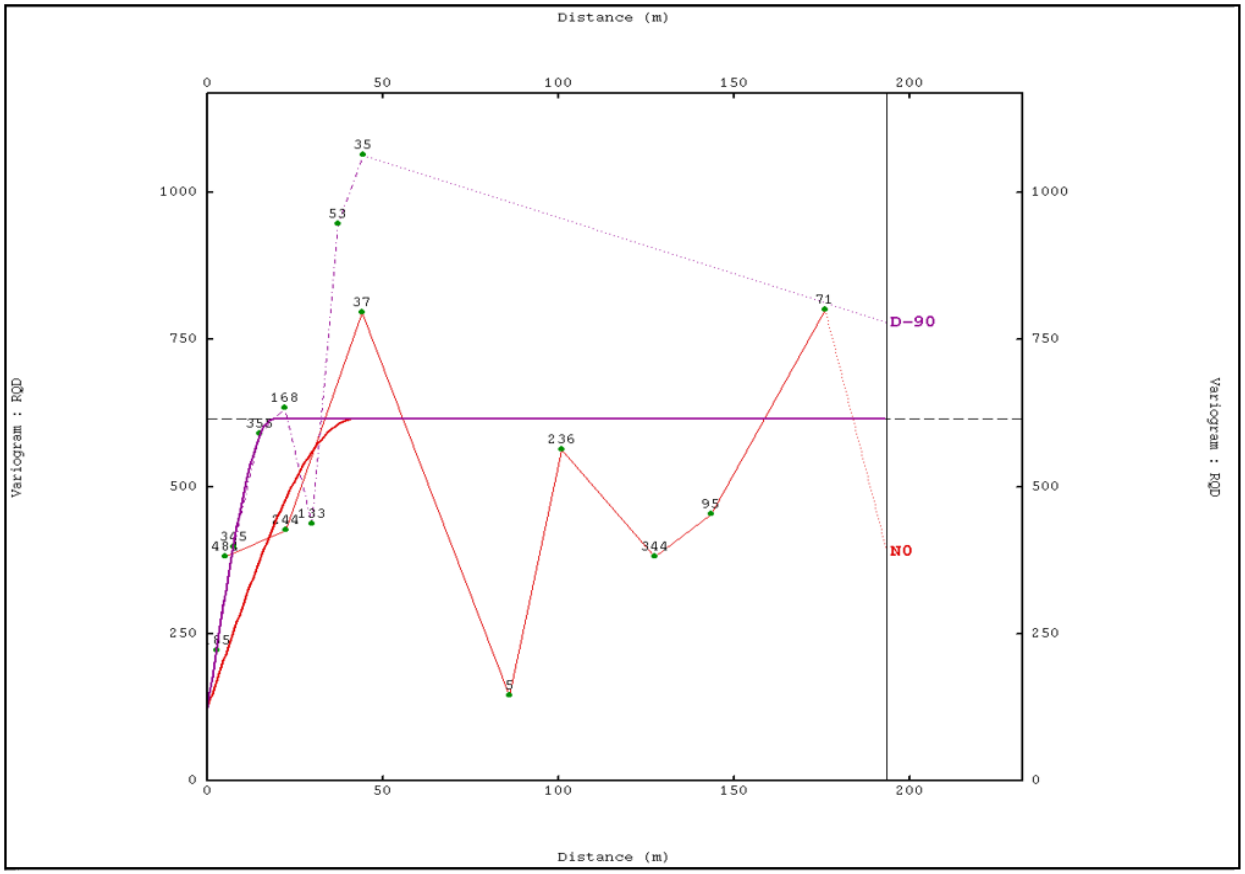
DUPLICATES/RQD_DUP(Geology{BBR})
- Variable #1 : RQD
Variogram : in 2 direction(s)
D1 : N0
Angular tolerance = 90.00
Lag = 45.00m, Count = 10 lags, Tolerance = 50.00%
Vertical Slicing = 5.50m
D2 : D-90
Angular tolerance = 15.00
Lag = 45.00m, Count = 8 lags, Tolerance = 50.00%
Model : 3 basic structure(s)
Global rotation = No rotation
S1 - Nugget effect, Sill = 229.9
S2 - Spherical - Range = 66.71m, Sill = 246.6
Directional Scales = (66.71m, 66.71m, 100000.00m)
S3 - Spherical - Range = 47.89m, Sill = 269
Directional Scales = (181.25m, 181.25m, 47.89m)

Kgomanyanej
Jun 10 2019
AKI_RMR_2017

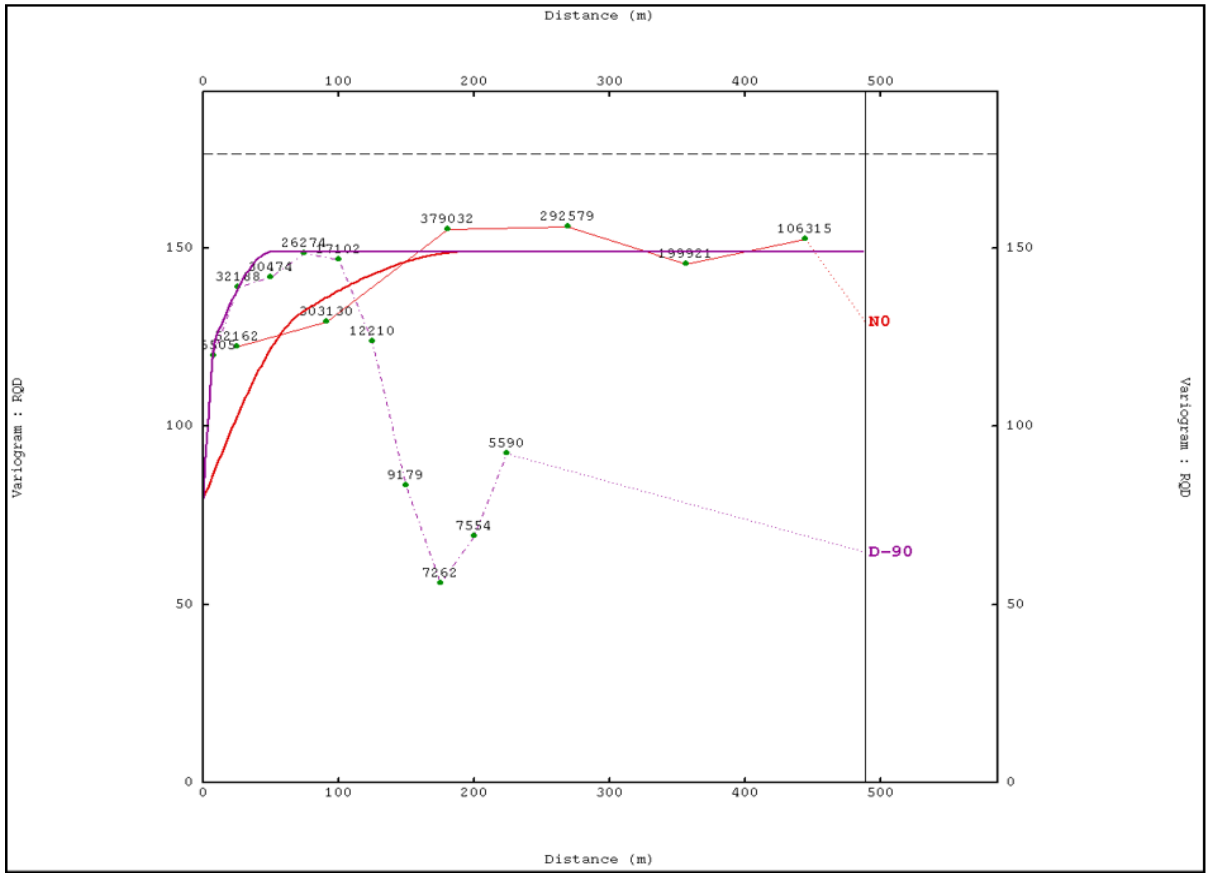
AK1 RQD variogram model – DHB



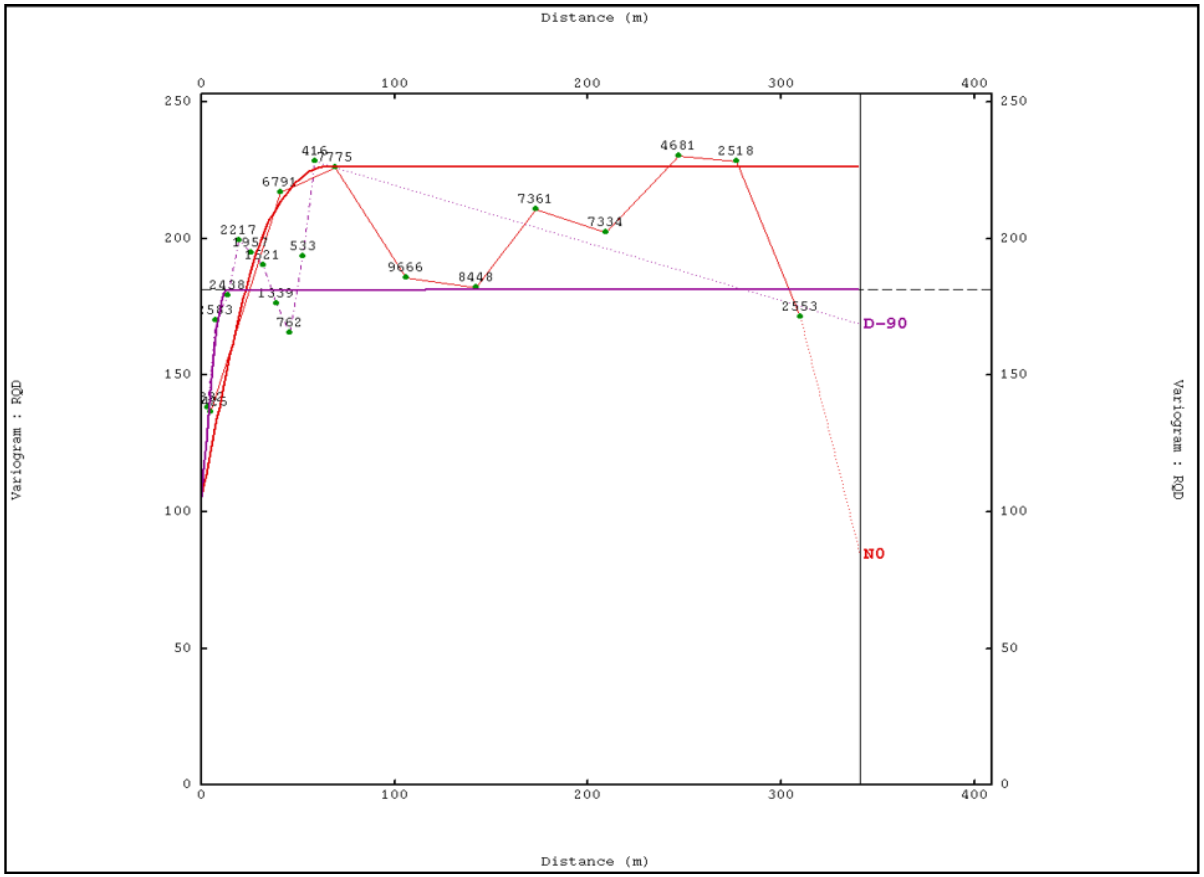
AK1 RQD variogram model – SVK_U



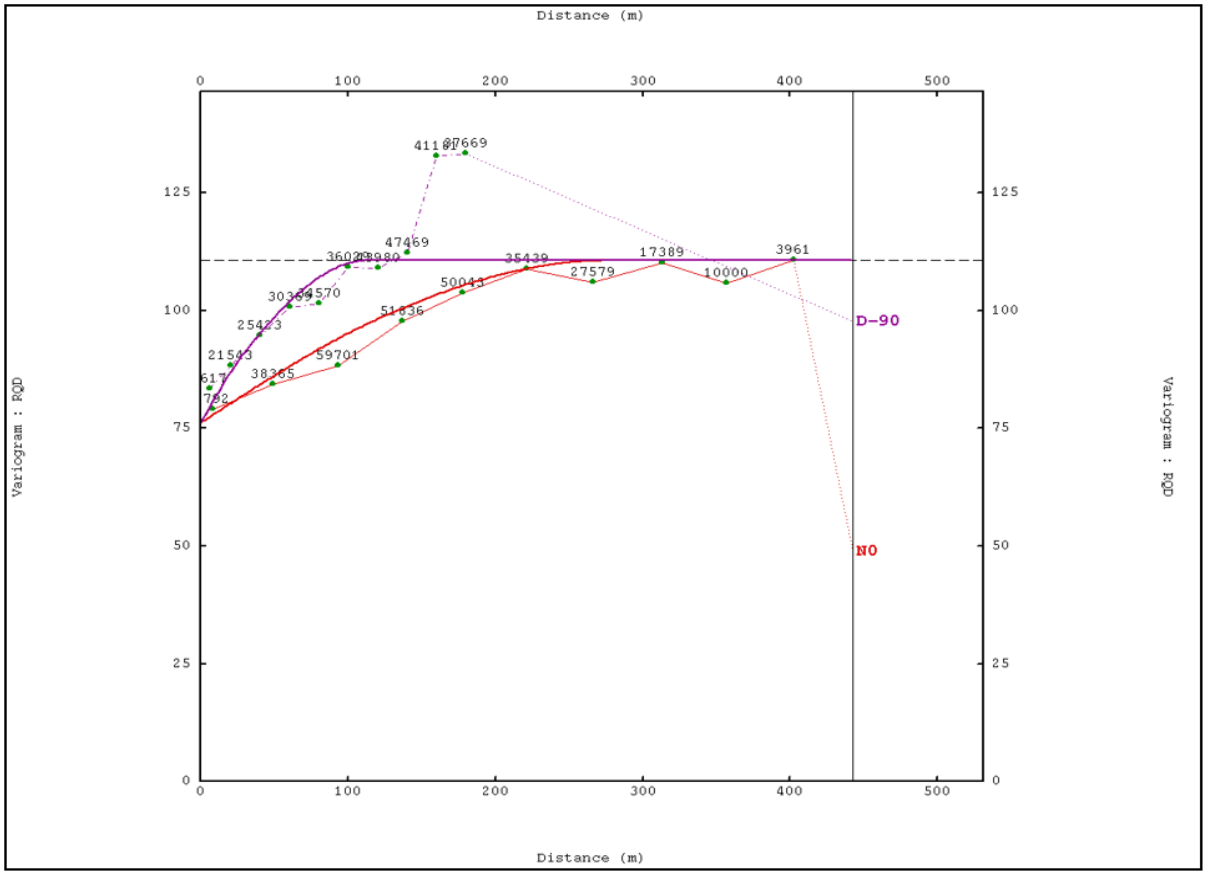
AK1 RQD variogram model – SVK_M



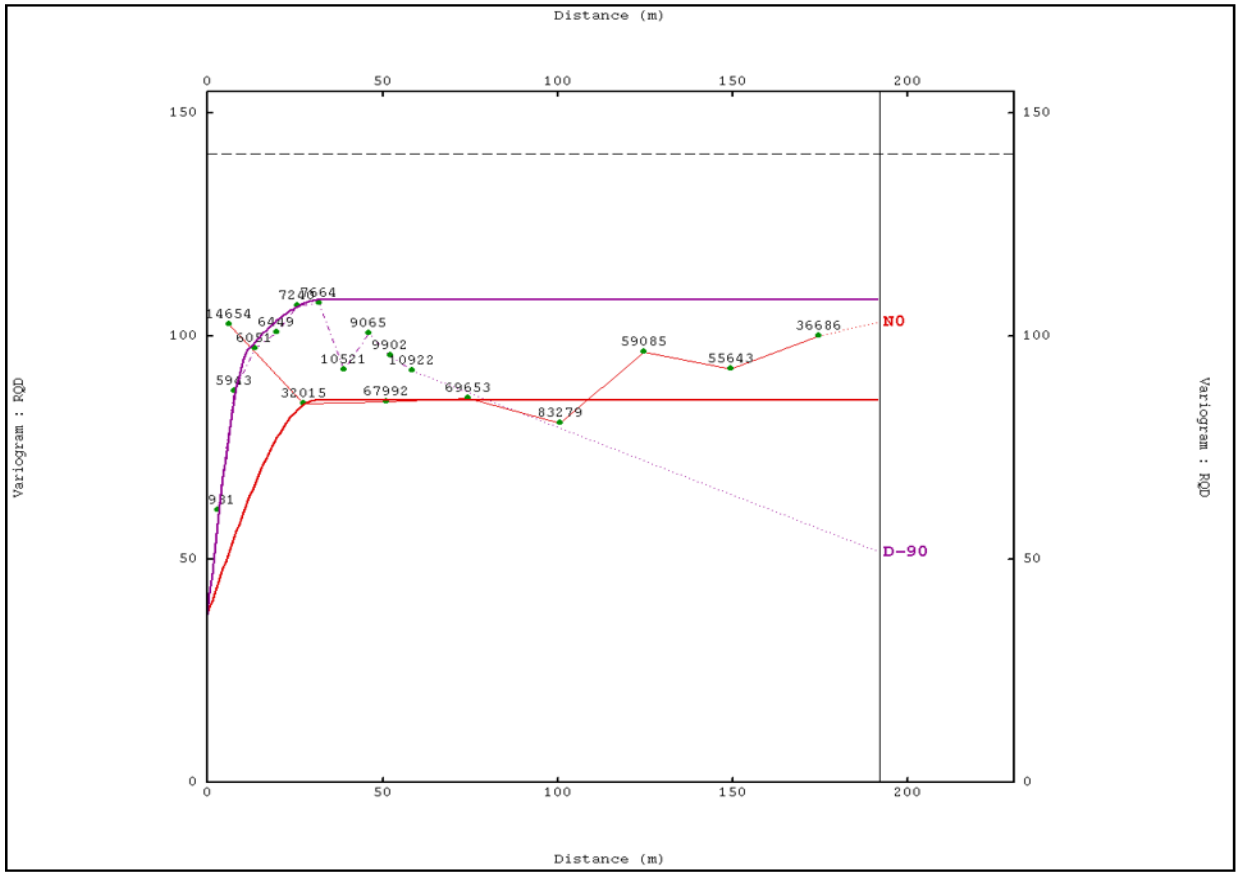
AK1 RQD variogram model – SVK_L



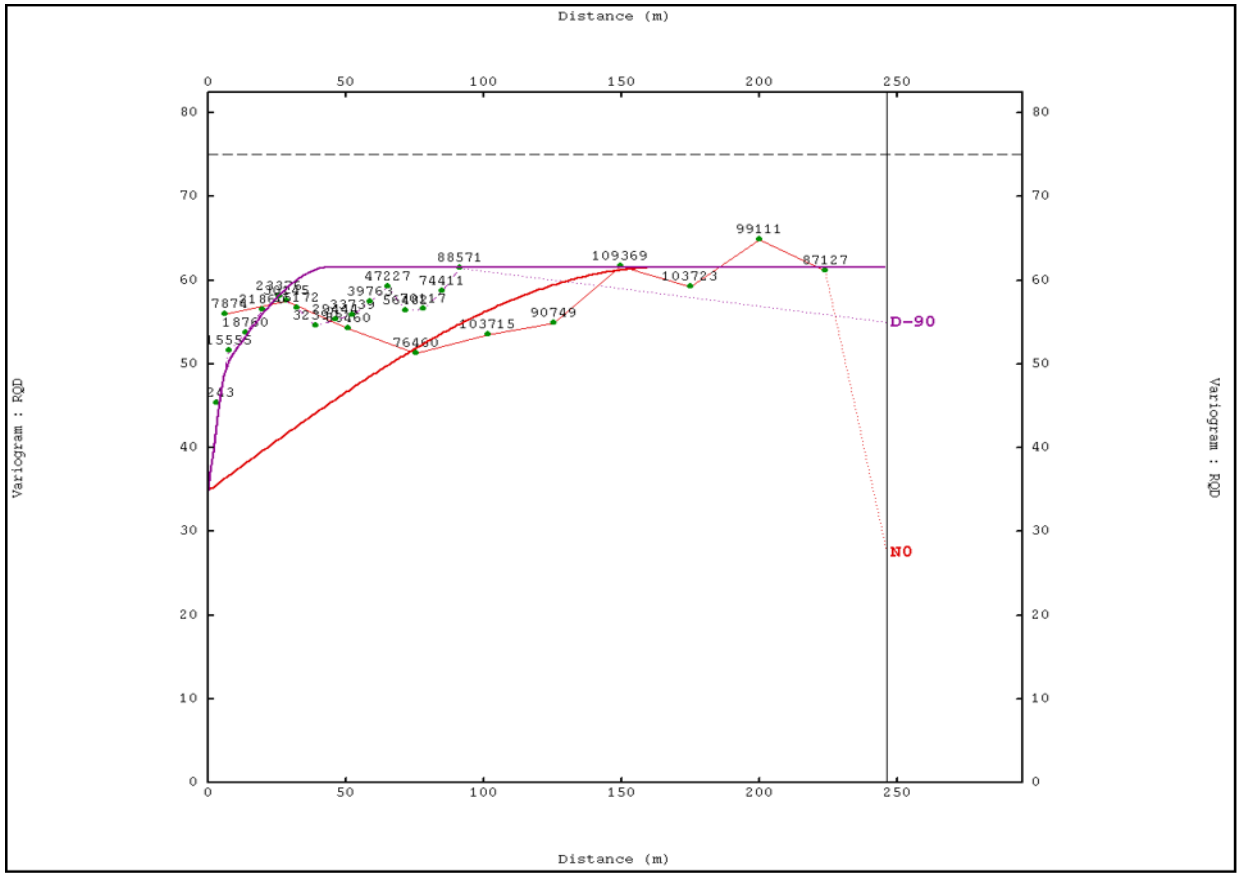
AK1 RQD variogram model – SDVK



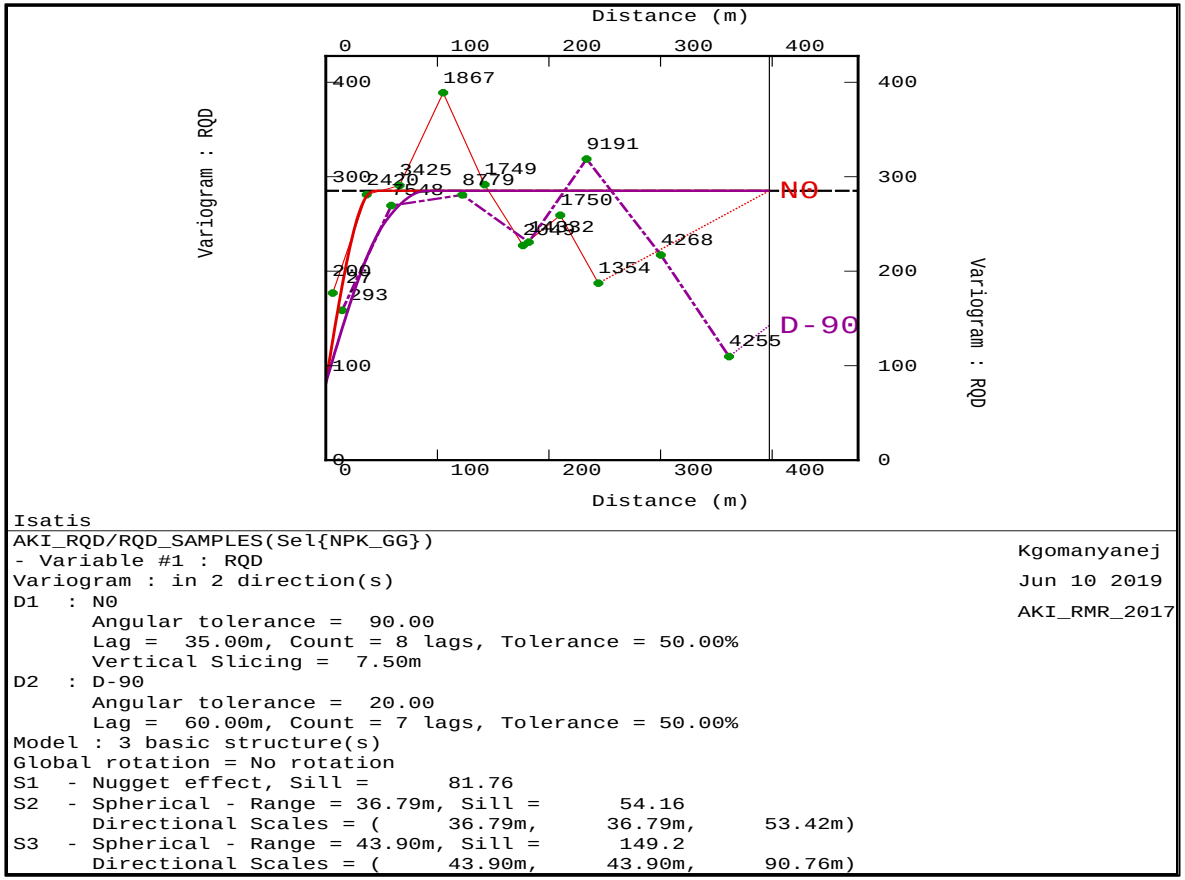
AK1 RQD variogram model – NPK



AK1 RQD variogram model – MVK2



AK1 RQD variogram model – NPK_GG

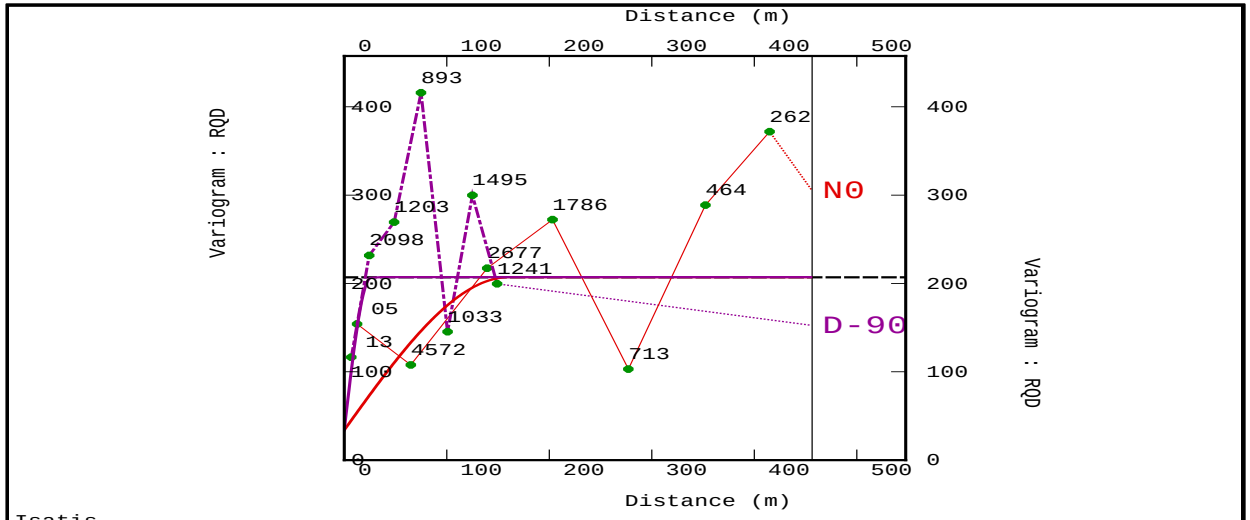


Isatis

AKI_RQD/RQD_SAMPLES(Sel{NPK_GG})
- Variable #1 : RQD
Variogram : in 2 direction(s)
D1 : N0
Angular tolerance = 90.00
Lag = 35.00m, Count = 8 lags, Tolerance = 50.00%
Vertical Slicing = 7.50m
D2 : D-90
Angular tolerance = 20.00
Lag = 60.00m, Count = 7 lags, Tolerance = 50.00%
Model : 3 basic structure(s)
Global rotation = No rotation
S1 - Nugget effect, Sill = 81.76
S2 - Spherical - Range = 36.79m, Sill = 54.16
Directional Scales = (36.79m, 36.79m, 53.42m)
S3 - Spherical - Range = 43.90m, Sill = 149.2
Directional Scales = (43.90m, 43.90m, 90.76m)

Kgomanyanej
Jun 10 2019
AKI_RMR_2017

AK1 RQD variogram model – MVK2_BBR

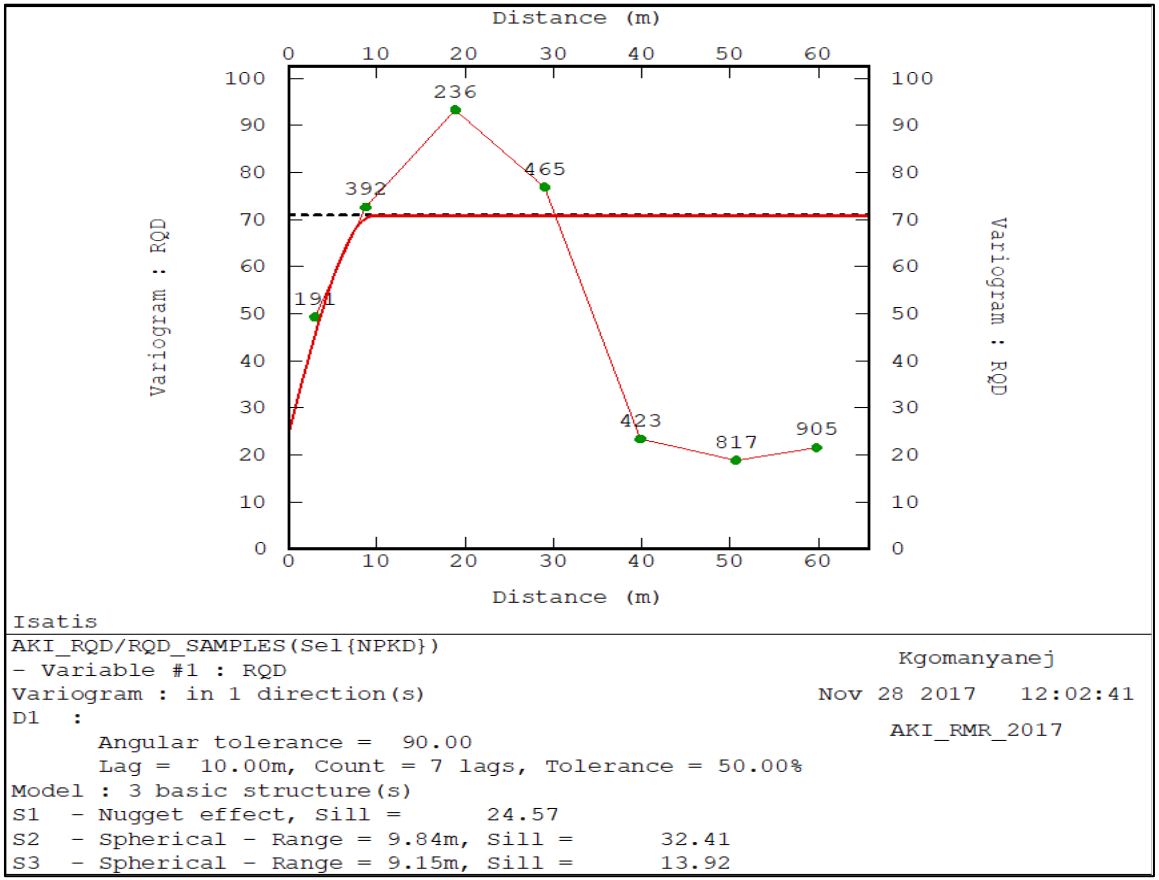


Isatis

AKI_RQD/RQD_SAMPLES(Sel{MVK2_BBR})
- Variable #1 : RQD
Variogram : in 2 direction(s)
D1 : N0
Angular tolerance = 90.00
Lag = 70.00m, Count = 7 lags, Tolerance = 50.00%
Vertical Slicing = 7.50m
D2 : D-90
Angular tolerance = 25.00
Lag = 25.00m, Count = 7 lags, Tolerance = 50.00%
Model : 3 basic structure(s)
Global rotation = No rotation
S1 - Nugget effect, Sill = 33.97
S2 - Spherical - Range = 39.28m, Sill = 5.38
Directional Scales = (152.23m, 152.23m, 39.28m)
S3 - Spherical - Range = 25.61m, Sill = 167.8
Directional Scales = (161.08m, 161.08m, 25.61m)

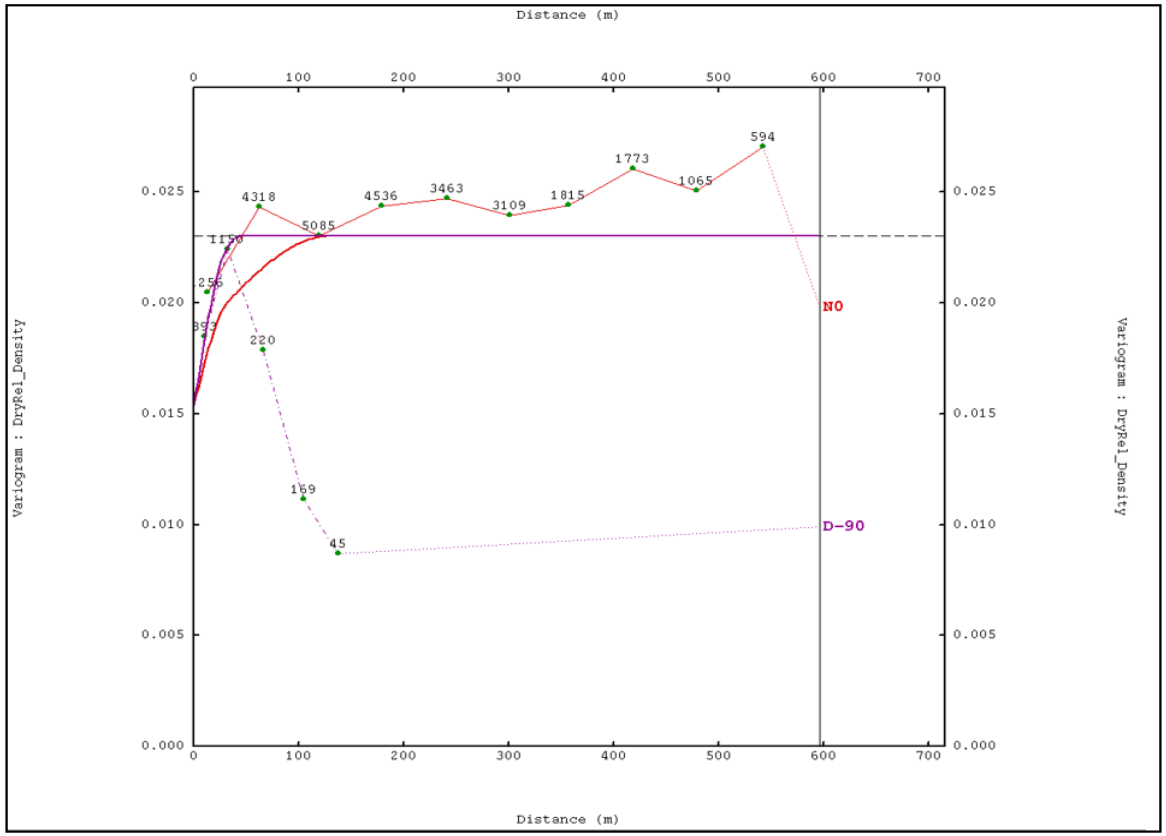
Kgomanyanej
Jun 10 2019
AKI_RMR_2017

AK1 RQD variogram model – NPKD

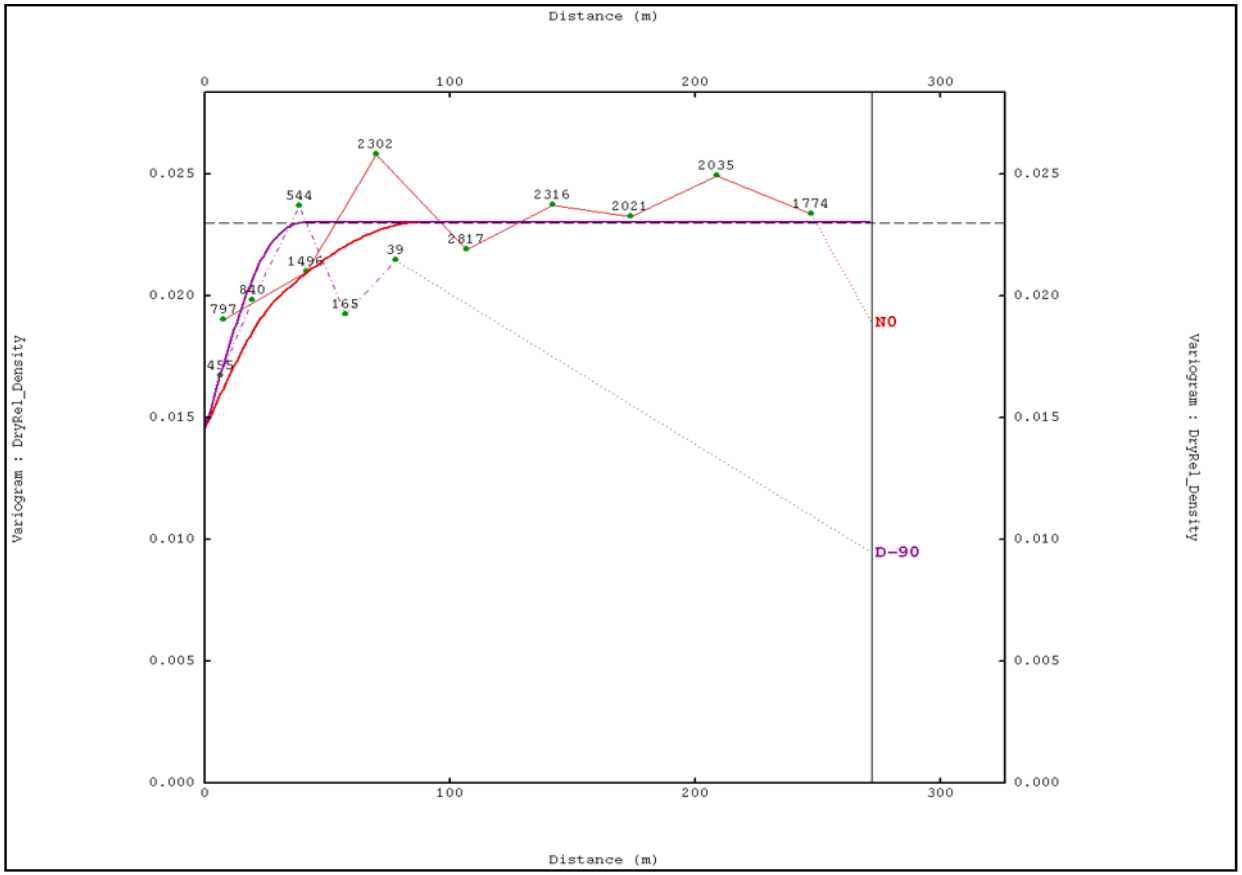


Appendix 12 AK1 Dry Density variogram models

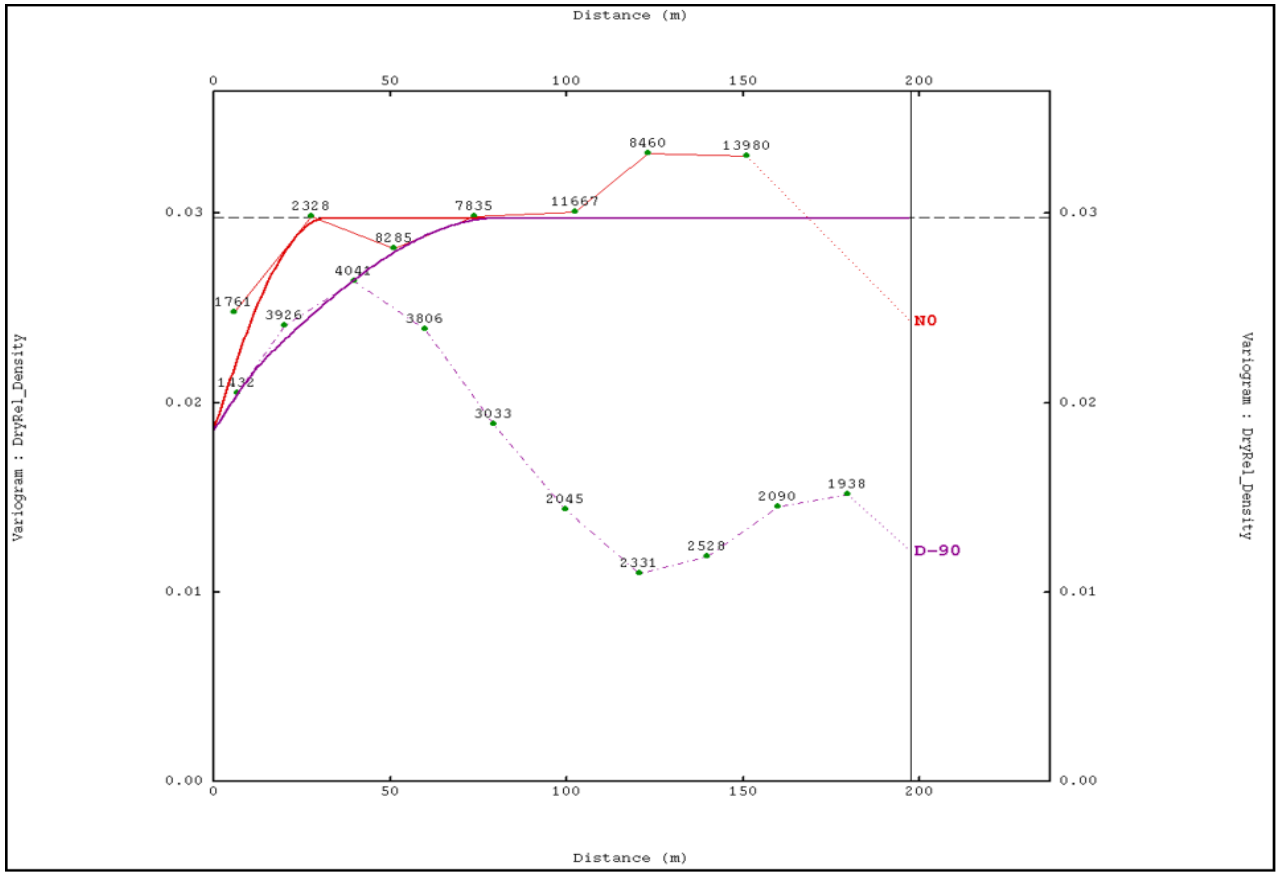
AK1 Dry Density variogram model – BBR



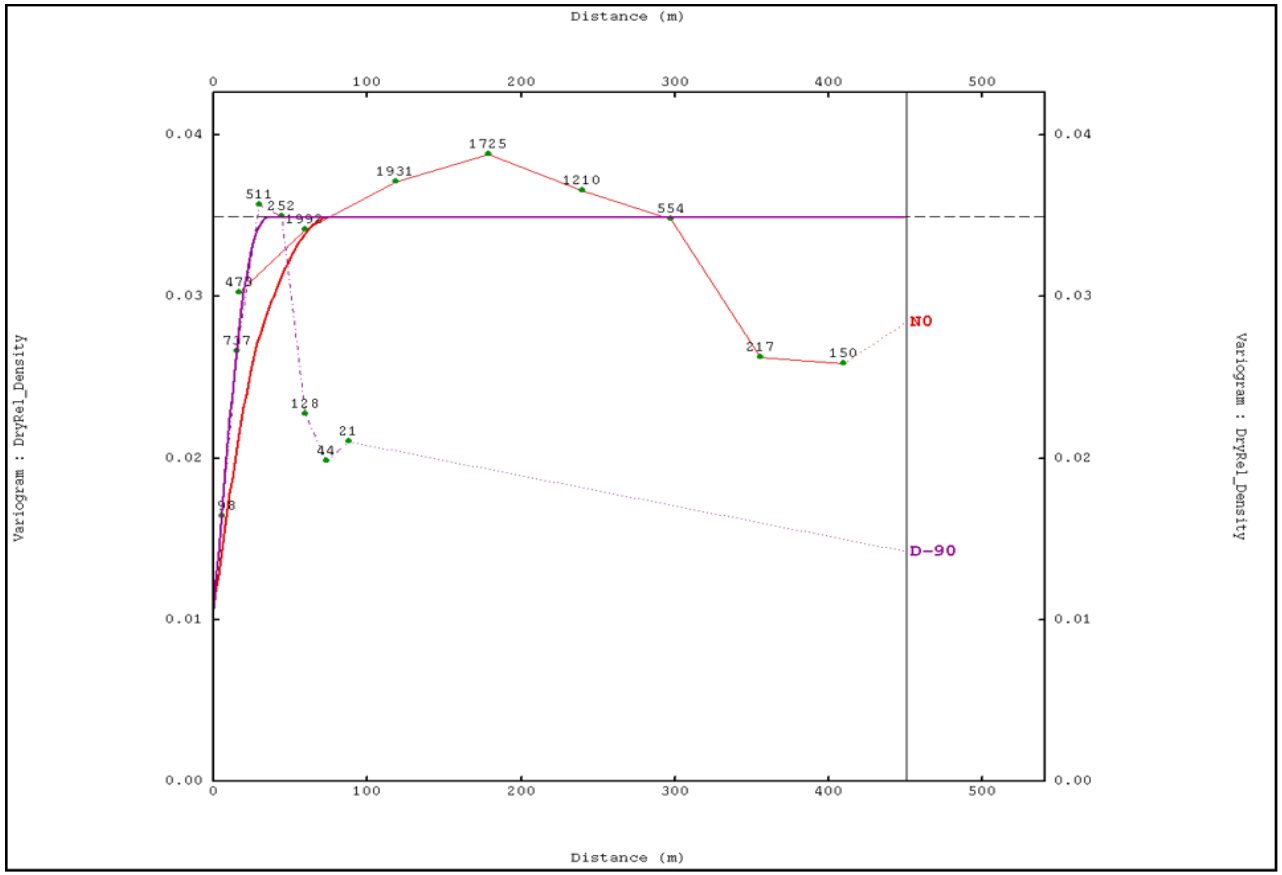
AK1 Dry Density variogram model – DHB



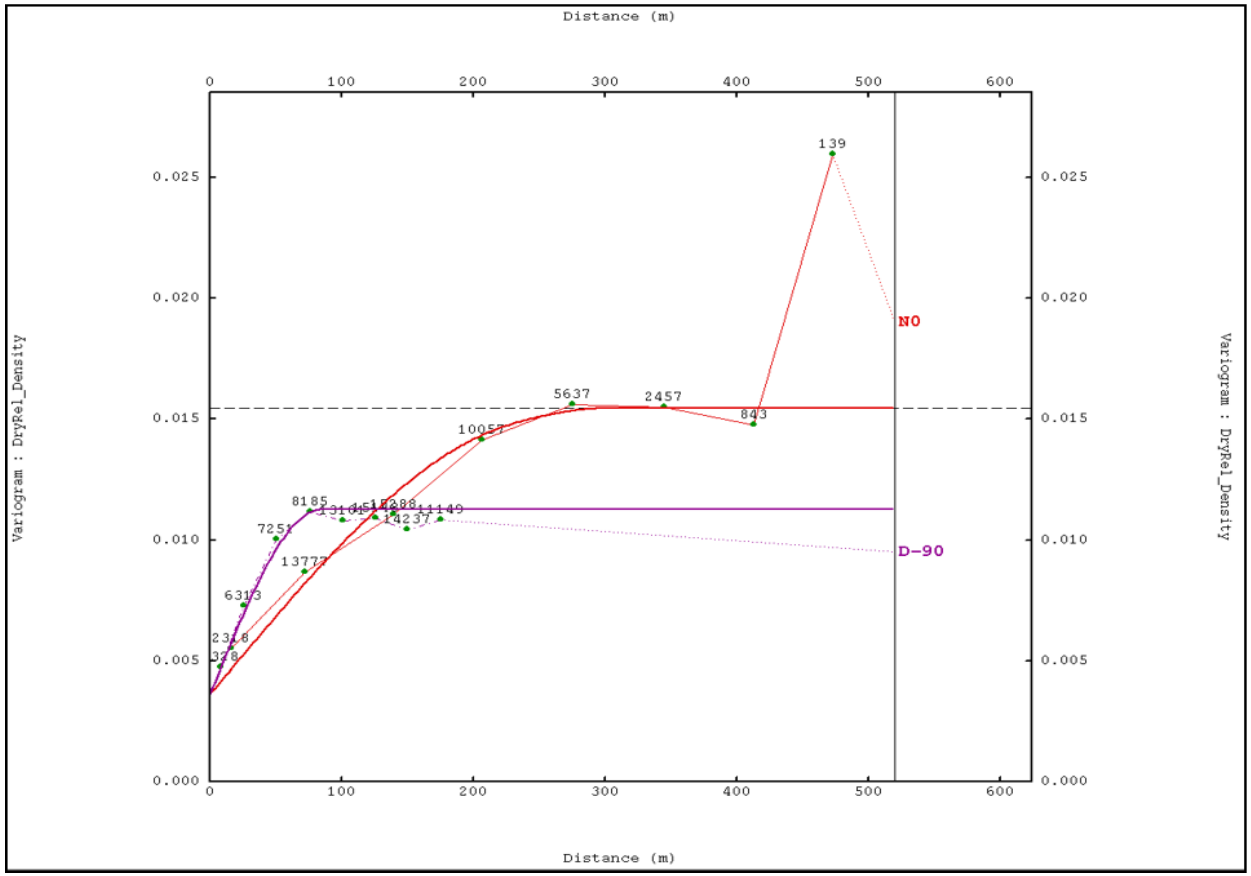
AK1 Dry Density variogram model – SVK_M



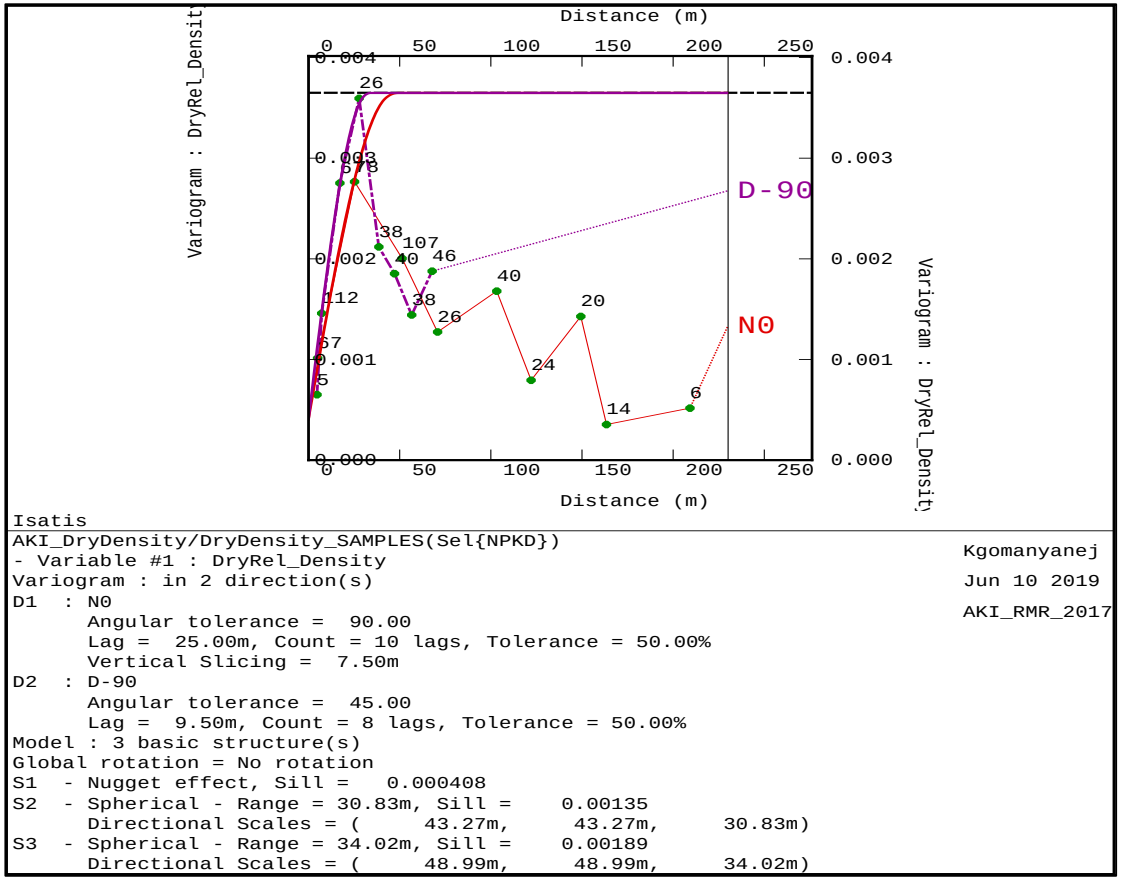
AK1 Dry Density variogram model – SVK_L



AK1 Dry Density variogram model – SDVK



AK1 Dry Density variogram model – NPKD

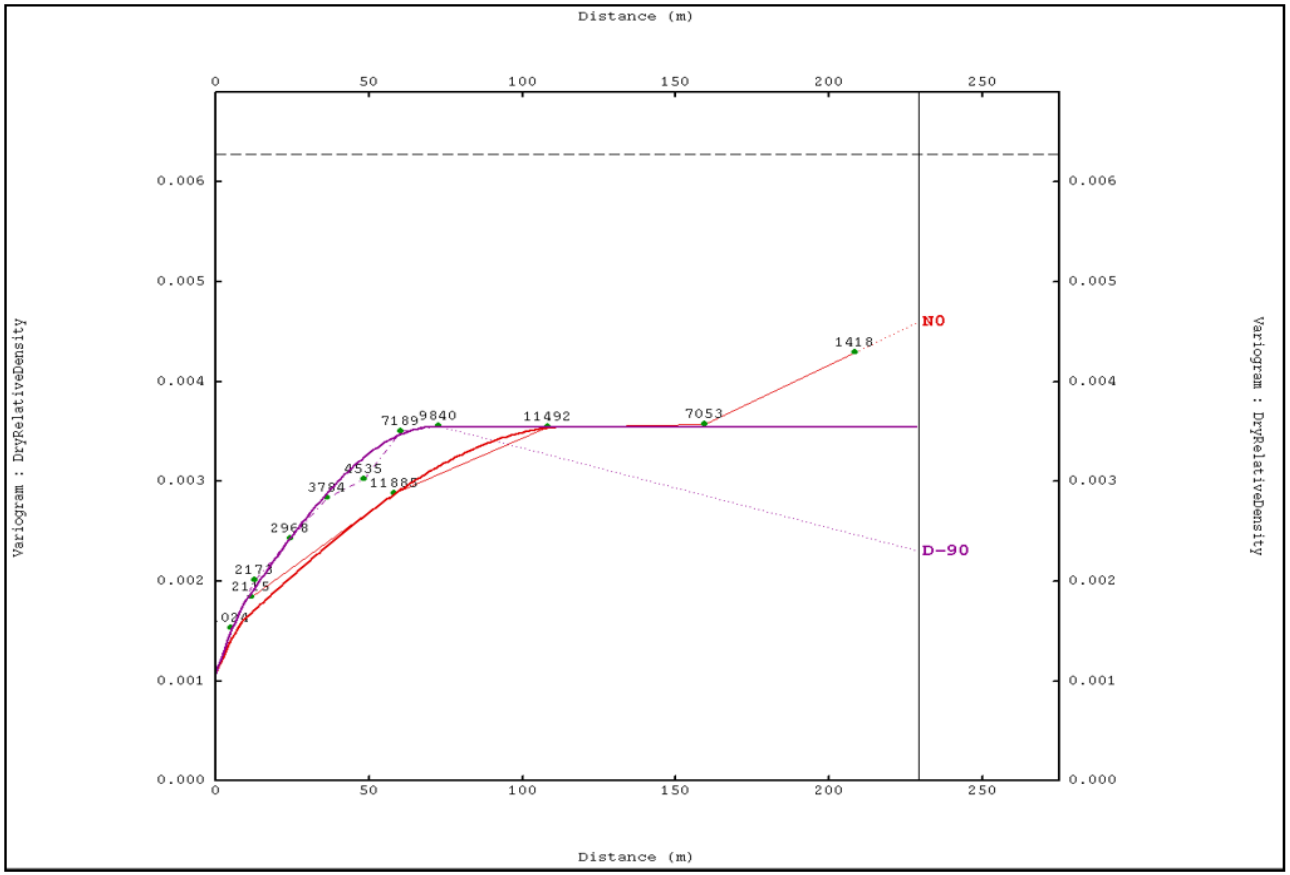


Isatis

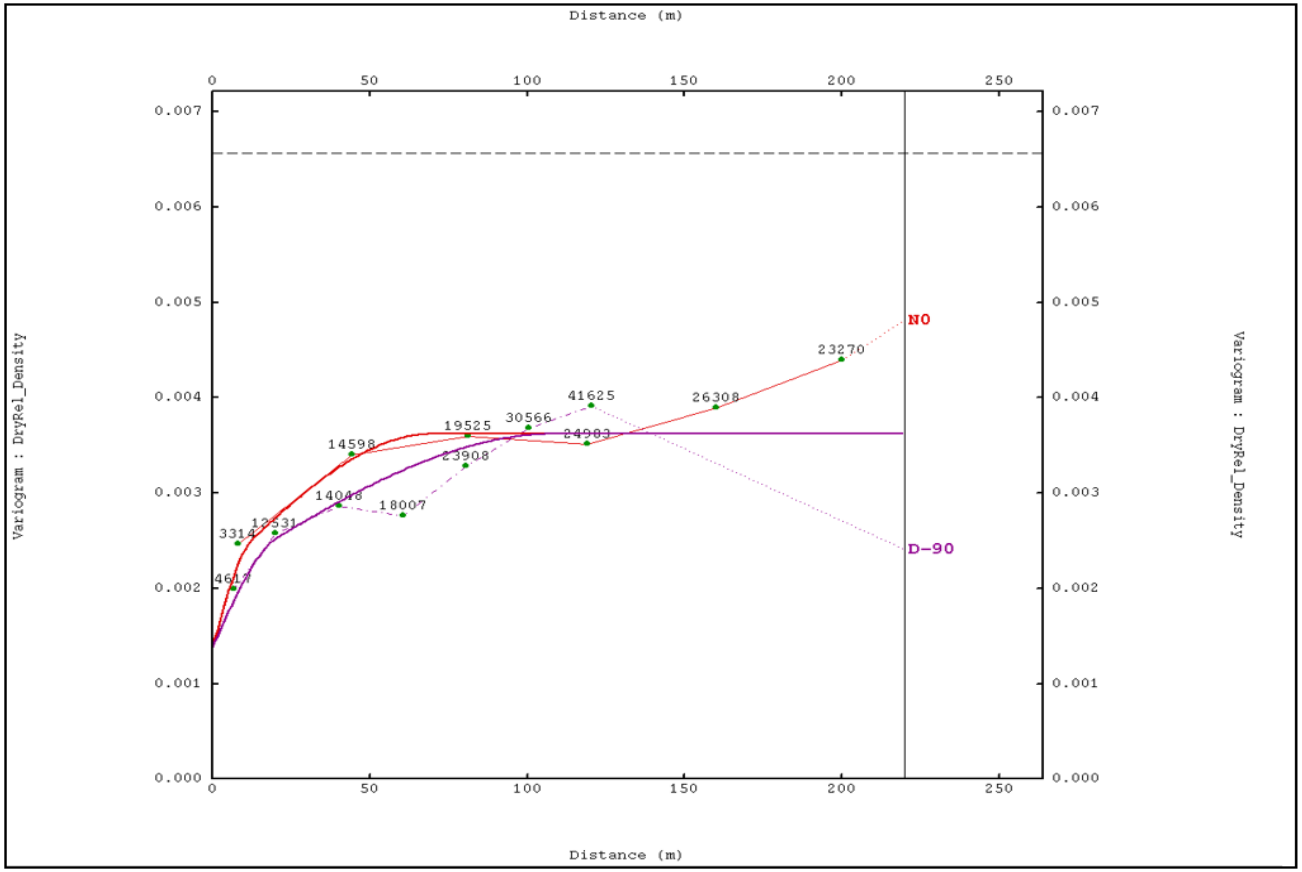
AKI_DryDensity/DryDensity_SAMPLES(Sel{NPKD})
- Variable #1 : DryRel_Density
Variogram : in 2 direction(s)
D1 : N0
Angular tolerance = 90.00
Lag = 25.00m, Count = 10 lags, Tolerance = 50.00%
Vertical Slicing = 7.50m
D2 : D-90
Angular tolerance = 45.00
Lag = 9.50m, Count = 8 lags, Tolerance = 50.00%
Model : 3 basic structure(s)
Global rotation = No rotation
S1 - Nugget effect, Sill = 0.000408
S2 - Spherical - Range = 30.83m, Sill = 0.00135
Directional Scales = (43.27m, 43.27m, 30.83m)
S3 - Spherical - Range = 34.02m, Sill = 0.00189
Directional Scales = (48.99m, 48.99m, 34.02m)

Kgomanyanej
Jun 10 2019
AKI_RMR_2017

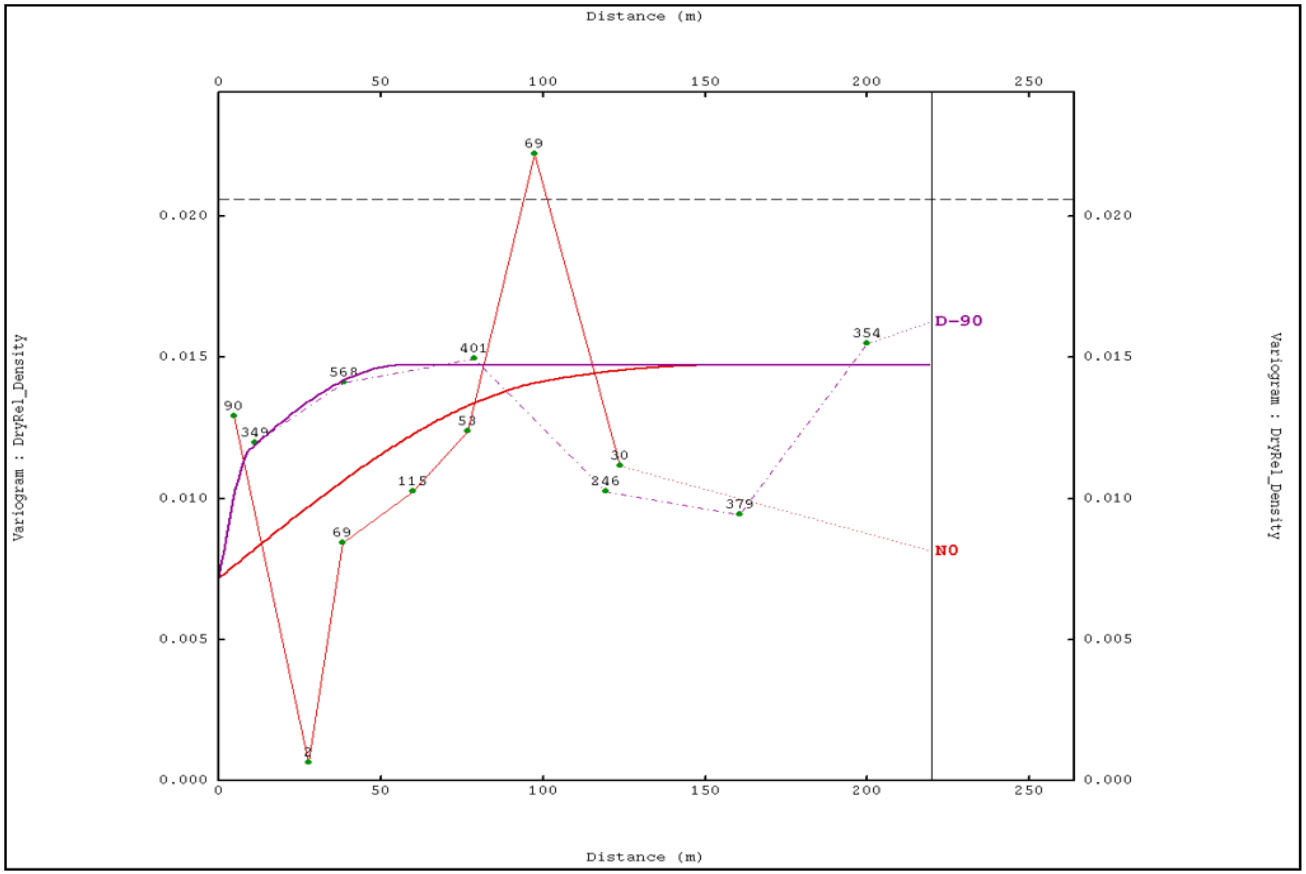
AK1 Dry Density variogram model – NPK



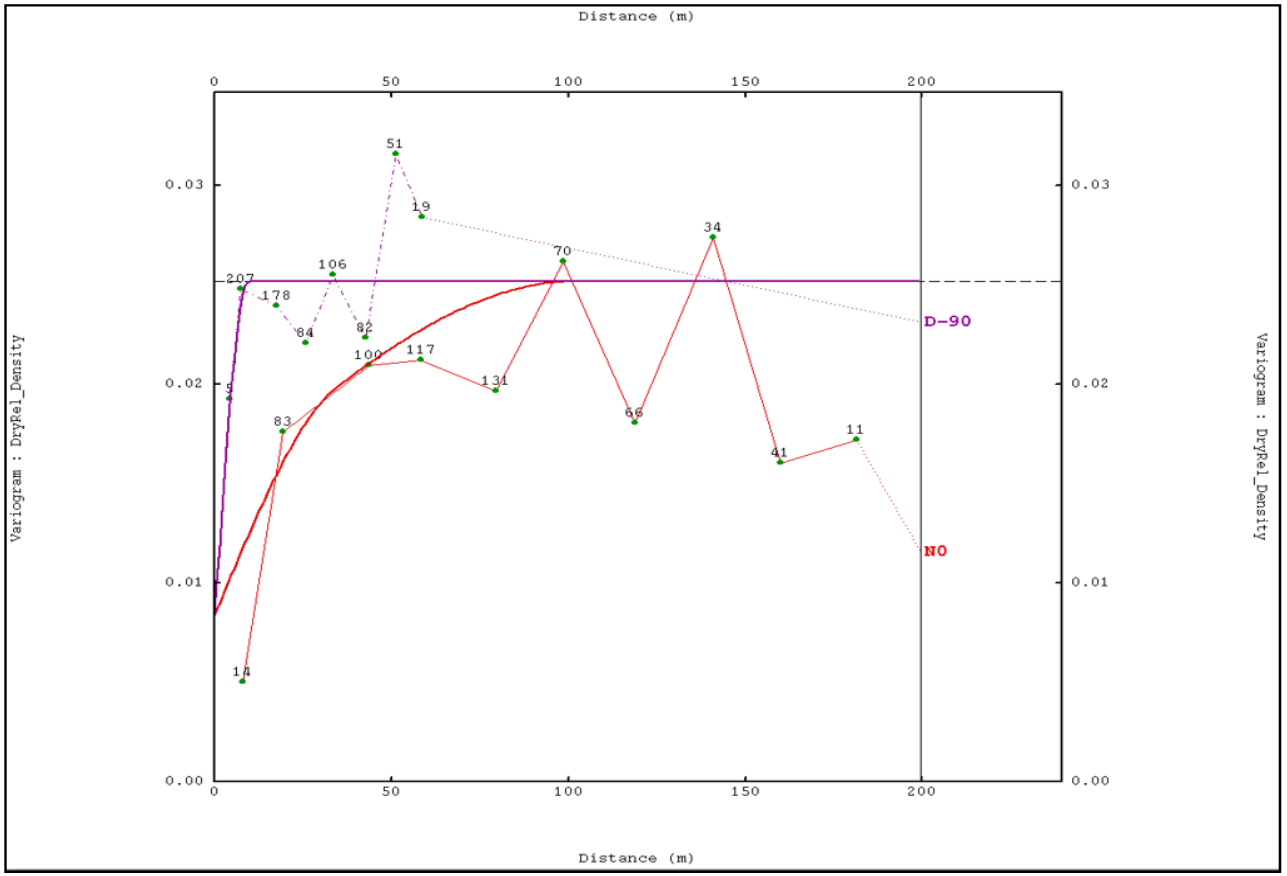
AK1 Dry Density variogram model – MVK2



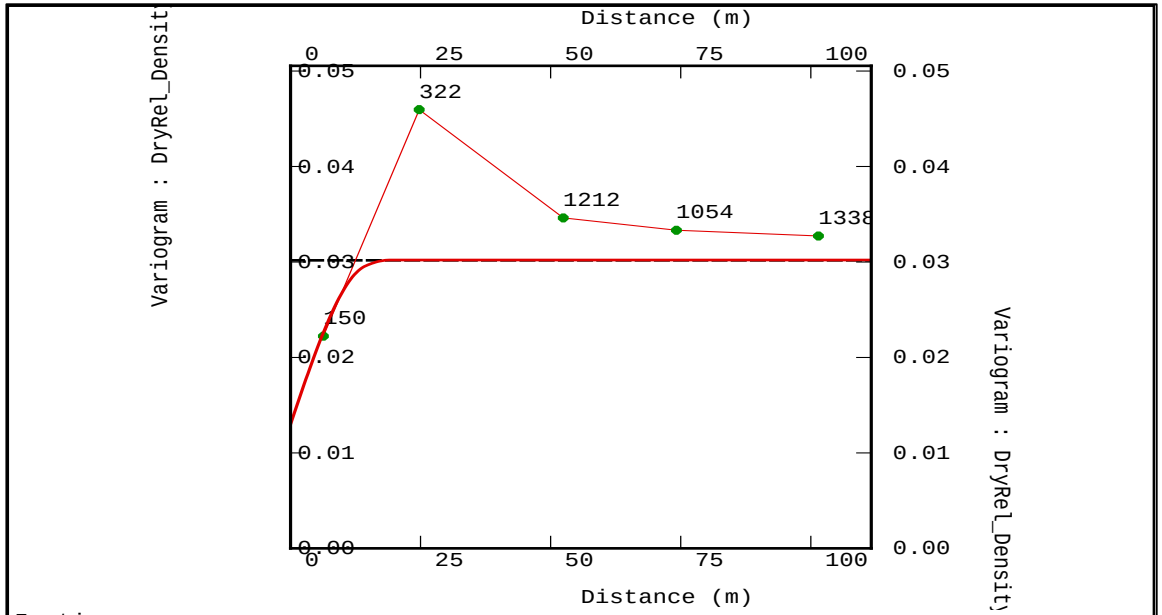
AK1 Dry Density variogram model – NPK_GG



AK1 Dry Density variogram model – MVK2_BBR



AK1 Dry Density variogram model – SPK



Isatis

AKI_DryDensity/DryDensity_SAMPLES(Sel{SPK})
- Variable #1 : DryRel_Density
Variogram : in 1 direction(s)
D1 :
Angular tolerance = 90.00
Lag = 25.00m, Count = 5 lags, Tolerance = 40.00%
Model : 3 basic structure(s)
S1 - Nugget effect, Sill = 0.013
S2 - Spherical - Range = 14.33m, Sill = 0.01
S3 - Spherical - Range = 19.25m, Sill = 0.00721

Kgomanyanej
Jun 11 2019
AKI_RMR_2017